Intelligent precast construction systems: Project, realization, maintenance technology for the optimization of the environment

(Article begins on next page)

26 April 2024

POLITECNICO DI BARI

D. R. R. S.

UNIVERSIDAD DE CANTABRIA

D.R.P.R.

Silvia Martiradonna

INTELLIGENT PRECAST CONSTRUCTION SYSTEMS: Project, realization, maintenance technology for the optimization of the environment and economic sustainability

Prof. Fabio Fatiguso
DICATECh
Politecnico di Bari

Prof. Ignacio Lombillo Vozmediano
ETSICCP
Universidad de Cantabria

POLITECNICO DI BARI

D.R.R.S

PhD Program in Environmental and Building Risk and Development

Coordinator: Prof. Michele Mossa

XXXIII CYCLE
ICAR/10 – Building Design

DICATECh

Department of Civil, Environmental, Building Engineering and Chemistry

UC UNIVERSIDAD
UNIVERSIDAD DE CANTABRIA **DE CANTABRIA**

D.R.P.R.

Doctor en Patrimonio Arquitectónico, Civil, Urbanístico y Rehabilitación de Construcciones Existentes

Coordinator: Prof. Maria del Mar Marcos Sánchez

ETSICCP
Department of Structural Engineering and Mechanics

PhD Thesis "En Co-tutelle"

05
2020
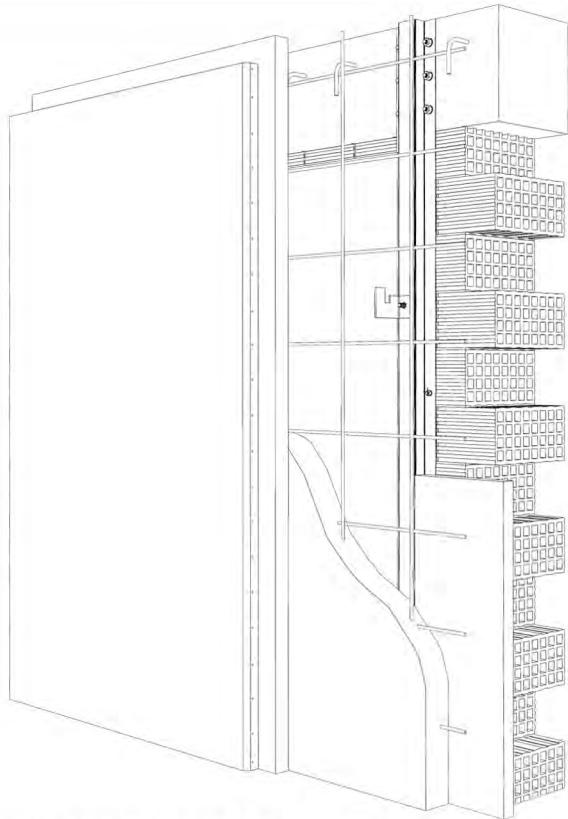
INTELLIGENT PRECAST CONSTRUCTION SYSTEMS: Project, realization, maintenance technology for the optimization of the environment and economic sustainability

Prof. Fabio Fatiguso
DICATECh
Politecnico di Bari

Prof. Ignacio Lombillo Vozmediano
ETSICCP
Universidad de Cantabria

Silvia Martiradonna

POLITECNICO DI BARI

D.R.R.S

Dottorato di Ricerca in Rischio e Sviluppo ambientale, territoriale ed edilizio

Coordinatore: Prof. Michele Mossa

XXXIII CICLO
ICAR/10 – Architettura Tecnica

DICATECh

Dipartimento di Ingegneria Civile, Ambientale, del Territorio, Edile e di Chimica

UC UNIVERSIDAD DE CANTABRIA
UNIVERSIDAD DE CANTABRIA

D.R.P. R.

Doctor en Patrimonio Arquitectónico, Civil, Urbanístico y Rehabilitación de Construcciones Existentes

Coordinador: Prof. Maria del Mar Marcos Sánchez

ETSICCP
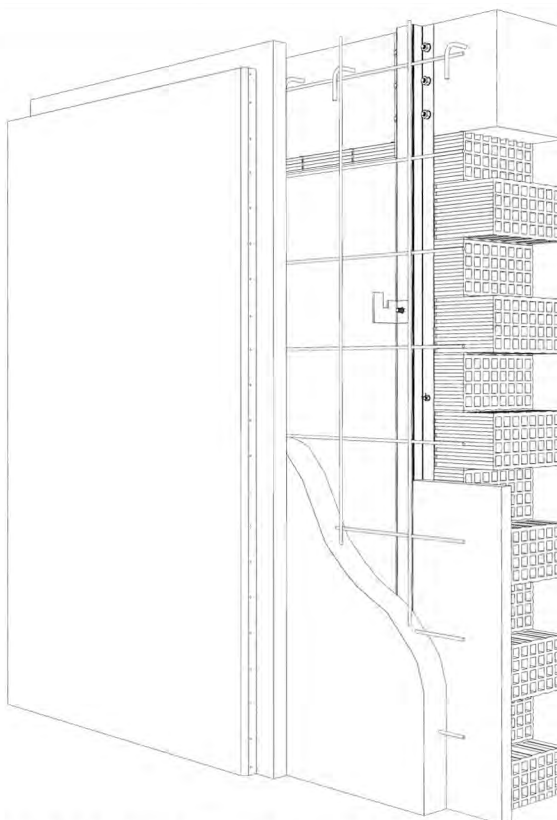Departamento de Ingeniería Estructural y Mecánica

Tesi di dottorato "En Co-tutelle"

05
2020

SISTEMI COSTRUTTIVI PREFABBRICATI INTELLIGENTI:
Progettazione, realizzazione, tecnologia di manutenzione per l'ottimizzazione della sostenibilità ambientale ed economica

Prof. Fabio Fatiguso
DICATECh
Politecnico di Bari

Prof. Ignacio Lombillo Vozmediano
ETSICCP
Universidad de Cantabria

Silvia Martiradonna

EXTENDED ABSTRACT (eng)

Climate change and recent seismic activity have underlined the inadequacy of the existing RC building stock to protect people from damages that may occur during the building's life cycle. More than 50% of the existing buildings, constructed in the second post-War World, does not present suitable technical and constructive features due to the haste of rebuilding the cities. They present criticalities regarding performance and durability related to many issues: insufficient structural capacity due to bad designed technical details, obsoleted, inadequate, and deteriorated materials, incorrect execution methods and lack of maintenance.

The renovation of these buildings has become a primary long-term strategy in the European scenario. The energy retrofit have the aim to transform the existing buildings into nearly zero-energy buildings, reduce the greenhouse gas emissions and the energy costs related to the need for winter heating and summer cooling. It brings benefits to the internal environment and to the people health and safety. On the other hand, the purpose to adapt the existing structures to the anti-seismic building codes, is mitigating the damage caused by the earthquakes to property and people.

Nowadays, there are many traditional interventions which aim to renovate the buildings, though they are expensive, involve long, difficult, and not prompt procedures, but above all, they are separated according to work categories.

This doctoral thesis proposes an innovative building renovation system of novel precast concrete (PC) modules devoted to the optimization of the energy and structural performance of the existing RC buildings. It consists in covering the façade with the PC modules with high thermal performance, by means steel elements directly installed on the building. The structural strengthening is assured by a cast-onsite lightweight concrete in

the resulting cavity between the novel and the existing wall. Moreover, the system project takes into account the possibility to insert into the stratigraphy, performance monitoring devises for the diagnosis and building automation already during the construction phases and inspect them anytime in case of maintenance. The aim is decreasing time and costs of maintenance, monitoring the building performance, and preventing the damages in case of bad functioning or structural uncertainty.

The analysis of the existing building typologies has led to the choice of the less performed façade for which the system stratigraphy has been designed. It has been assumed that if the system improves the performance of the worst building façade for complying with the national codes, it is verified also for the other typologies for which a specific project is necessary.

In compliance with the principles of environmental and economic sustainability, the PC panels contain materials from industrial wastes. In detail, an innovative lightweight mortar with recycled Extruded Sintered Polystyrene (rEPS) has been designed and tested in order to get a performed insulating material with high thermal properties. Initial simulated analyses have been performed to understand the system characteristics of thermal insulation, structural strengthening, thus, to apport improvements on technical details. Finite-element-method models (FEM-models) have been realized with COMSOL Multiphysics software for thermal investigation and SAP2000 for structural assessment.

An Italian meaningful case study has been considered in order to simulate the application of the system and estimate the benefits it provides in terms of thermal performance and structural strengthening. The results show deep improvements in thermal performance and stiffness of the building, although a reduction of ductile capacity occurs. Six prototypes of the PC panel have been realized in compliance with the project partner enterprise with the aim to comprehend the production procedure of the building component. The panels have been distinguished in two dimensional categories in function of the height to better understand the ease of transport and installation. A RC frame with brick infill wall has been constructed with features similar to which of the existing building typology selected to design the technology. The wall dimensions have been chosen for applying the six panels in two rows and three columns. Finally, the theoretical procedure for the

technological system installation has been really applied to the sample in order to verify the suitability of the phases and the coupling of the panels along vertical and horizontal direction. The positive result of the installation test validated the procedure and the design details.

key words

Precast Concrete Module, recycled Sintered Expanded Polystyrene EPS (rEPS), Existing buildings, Energetic and Structural Retrofit, Technological design.

EXTENDED ABSTRACT (ita)

Il cambiamento climatico e l'intensa attività sismica sottolineano l'inadeguatezza del patrimonio edilizio esistente a proteggere la vita dei cittadini dai danni che possono verificarsi durante il ciclo di vita di un edificio. Più della metà degli edifici esistenti è stata costruita a partire dal 1950 senza adeguate caratteristiche tecniche e costruttive a causa della fretta di ricostruire le città danneggiate dalla guerra. Le criticità prestazionali che caratterizzano tali organismi sono legate a diversi fattori, quali l'insufficiente capacità strutturale dovuta alla cattiva progettazione dei dettagli tecnici, la presenza di materiali inadeguati e deteriorati, metodologie di esecuzione errate e mancanza di manutenzione. Negli ultimi anni, la politica di recupero attuata dagli Stati Membri dell'Unione Europea, è diventata la strategia a lungo termine principale per ridurre le emissioni di gas serra ed i costi energetici legati alla necessità di riscaldamento invernale e di raffrescamento estivo degli edifici. Il recupero energetico mira a trasformare le strutture esistenti in edifici a energia quasi zero (nZEB) al fine di migliorare il comfort indoor e proteggere la salute degli utenti. D'altra parte, adattare le strutture esistenti agli standard dei nuovi codici edilizi antisismici, ha lo scopo di mitigare le conseguenze legate all'intensa azione sismica.

Attualmente, gli interventi tradizionali che mirano a limitare tali problematiche richiedono tempi e procedure di esecuzione lunghe, costose, talvolta pericolose ma soprattutto suddivise per categorie di lavoro ovvero a seconda del campo di applicazione per il quale sono richiesti.

Questa tesi di dottorato, dunque, propone un'innovativa tecnologia di recupero basata su un sistema di pannelli prefabbricati innovativi dedicati all'ottimizzazione energetica e strutturale delle prestazioni degli edifici esistenti in cemento armato. Essa consiste nel rivestire l'edificio con moduli prefabbricati ad alte prestazioni termiche per mezzo di

elementi metallici direttamente installati sulla facciata. La funzione di irrigidimento è garantita da un getto di calcestruzzo alleggerito nella cavità risultante tra la nuova facciata e l'edificio esistente, conferendo maggiore portanza e solidità alla struttura.

La nuova tecnologia permette di integrare, già durante le fasi di installazione del sistema, dei sensori di monitoraggio atti a garantire il controllo delle prestazioni dell'edificio durante il suo ciclo di vita. Esso ha lo scopo di ridurre i tempi ed i costi di manutenzione e prevenire possibili danni irreversibili dell'edificio.

Grazie ad un'attenta analisi dello stato dell'arte, all'osservazione delle procedure di prefabbricazione presso l'azienda partner del progetto, è stato possibile definire le condizioni e gli specifici obiettivi sul quale fondare il progetto del nuovo sistema tecnologico. In aggiunta, lo studio delle tipologie edilizie più diffuse all'interno del territorio Europeo e Nazionale ha condotto alla scelta del tipo di facciata meno performante dal punto di vista energetico per la quale approfondire la progettazione del sistema.

Procedendo per scale di dettaglio a partire dalla caratterizzazione del materiale di isolamento del modulo prefabbricato, concepito con utilizzo di materiale proveniente dagli scarti industriali, si è giunti allo studio della configurazione dimensionale del pannello e della tecnologia di connessione con la facciata esistente, fornendo indicazioni sull'approccio di calcolo da utilizzare. Inoltre, grazie all'utilizzo di software di analisi agli elementi finiti, è stata fornita la metodologia preliminare per la verifica termo-igrometrica della stratigrafia in aggiunta all'approccio numerico di verifica del comportamento strutturale sotto l'azione sismica.

Con la finalità di verificare preliminarmente il comportamento simulato del sistema applicato ad un edificio esistente, è stato selezionato un idoneo caso di studio italiano avente caratteristiche coerenti con la tipologia edilizia scelta per la progettazione del sistema tecnologico. Dai primi risultati è emerso che l'innovativo sistema di pannelli prefabbricati conferisce benefici in termini di riduzione delle dispersioni termiche, protezione dal rischio di formazione di ponti termici e irrigidimento strutturale a scapito però della duttilità dell'apparato portante.

In seguito alla fase di progettazione e alla verifica preliminare delle prestazioni dell'innovativo sistema tecnologico si è passati alla validazione industriale dei componenti

prefabbricati, delle procedure di fabbricazione e delle fasi di installazione del sistema, presso l'azienda partner del progetto. Pertanto, a partire dalla riproduzione su grande scala della nuova malta alleggerita, sono stati realizzati sei moduli prefabbricati, distinti secondo due categorie dimensionali al fine di comprendere le questioni legate alla loro movimentazione ed installazione.

La simulazione di intervento di recupero è stata effettuata su un campione di muro costruito con le caratteristiche dell'edificio del secondo dopoguerra considerato nella fase di progettazione. L'esito positivo della prova di installazione e completamento dell'intervento, ha validato la procedura, i calcoli ed i dettagli costruttivi dell'innovativo sistema tecnologico.

EXTENDED ABSTRACT (esp)

El cambio climático, unido a la intensa actividad sísmica, pone de manifiesto la falta de adecuación del patrimonio construido existente para proteger la vida de los ciudadanos ante los daños que pueden producirse durante el ciclo de vida de un edificio. Debido a la premura por reconstruir las ciudades tras la II Guerra Mundial, más de la mitad de los edificios existentes se construyeron a partir del 1950 sin las características técnicas adecuadas. Habitualmente, los problemas que caracterizan a estas construcciones se relacionan con su insuficiente capacidad estructural debido a detalles técnicos incorrectos, la presencia de materiales inadecuados y su progresivo deterioro, métodos de ejecución inapropiados, y la falta de mantenimiento. Además, en los últimos años, en materia de Edificación, las políticas de de la Unión Europea, y por ende de los Estados Miembros, se han focalizado en la reducción de las emisiones de gases del efecto invernadero de los edificios y de los costes energéticos relacionados con las necesidades de calefacción en invierno y refrigeración en verano. Estas estrategias energéticas tienen por objeto transformar las estructuras existentes en edificios de consumo casi nulo (nZEB), con el fin de mejorar el confort interior y proteger la salud de los usuarios. Por otra parte, adaptar las estructuras existentes a las normas de los nuevos códigos de construcción antisísmica persigue mitigar las consecuencias de eventos sísmicos.

En la actualidad, las intervenciones tradicionales dirigidas a limitar estos problemas requieren plazos y procedimientos de ejecución largos, costosos, a veces peligrosos, pero sobre todo clasificados en base a los diferentes categorías de trabajo o según el ámbito de aplicación.

Esta tesis doctoral propone una tecnología de intervención racionalizada basada en un sistema de paneles prefabricados innovadores orientados a la optimización de las prestaciones tanto energéticas como estructurales de edificios existentes con entramado resistente de hormigón armado. La metodología consiste en revestir el edificio con módulos prefabricados de altas prestaciones térmicas, referidos a la fachada mediante elementos metálicos directamente instalados sobre esta. La optimización de su desempeño estructural, a base de crear un comportamiento tipo caja, se materializa por el vertido in situ de un hormigón aligerado en la cavidad resultante entre la nueva fachada (paneles prefabricados) y la del edificio existente. Además, la nueva tecnología permite integrar, desde la fase de instalación del sistema, sensores para monitorizar el rendimiento del edificio durante su ciclo de vida. Con este nuevo sistema se pretende reducir el tiempo de materialización de la intervención, los costes de mantenimiento y prevenir posibles daños irreversibles al edificio.

Gracias a un exhaustivo análisis del estado del arte y a la observación de los procedimientos de prefabricación en la empresa colaboradora del proyecto, ha sido posible definir las condiciones y los objetivos específicos en los cuales se fundamenta el proyecto del nuevo sistema tecnológico. Además, tras realizar un estudio detenido de los tipos edilicios más comunes existentes en Europa, especialmente en Italia y España, se ha escogido la tipología de fachada menos favorable desde el punto de vista energético con la finalidad de valorar la optimización obtenida por sistema diseñado.Mediante el empleo de software de análisis de elementos finitos se ha realizado tanto una verificación termo-higrométrica preliminar del sistema, como su comportamiento estructural bajo acción sísmica. Igualmente, se simuló el sistema propuesto aplicado a un edificio real localizado en Italia, con estructura de entramado resistente de hormigón armado y fachada de bajo rendimiento energético. De los resultados obtenidos se desprende que el sistema a base de paneles prefabricados aporta beneficios en términos de reducción de las dispersiones térmicas, protección contra el riesgo de formación de puentes térmicos y rigidez estructural, en detrimento de la ductilidad del sistema portante.

Finalmente, tras la fase de diseño y la verificación previa de las prestaciones del sistema tecnológico, se describe la fase de prototipo en la que se realizó, en las instalaciones de la empresa asociada con el proyecto, la validación industrial de los componentes prefabricados, de los procedimientos de fabricación y de las fases de instalación del sistema en obra. Así, se han realizado seis módulos prefabricados distintos según dos categorías dimensionales, con el fin de comprender aspectos relacionados con su manipulación e instalación. La simulación de la instalación se llevó a cabo sobre una muestra de fachada recercada por una retícula de hormigón armado (haciendo las veces de vigas y pilares de una estructura de entramado resistente), construida con las características propias de un edificio de la posguerra. El resultado de la prueba de instalación fue satisfactorio, permitiendo validar el procedimiento y los detalles constructivos del innovador sistema tecnológico propuesto.

key words

Módulos prefabricados en hormigón armado, Poliestireno Extruido Sinterizado reciclado (rEPS), Edificios existentes, Recuperación energética y estructural, Diseño tecnológico.

INDEX

INTRODUCTION

Reduction of greenhouse gas emissions, improvement of energy efficiency, citizens' safety and sustainability have become the most ambitious challenges for Europe to mitigate the consequences of the recent environmental events. The climate change and the earthquakes have led to the definition of new European policies for a global safer sustainable development. The construction sector bears a huge responsibility in relation of man life defence, environmental and economic impacts in terms of structural instability, CO_2 emissions and final energy consumption for heating, cooling, and domestic use. The heterogeneousness of existing building stock in which more than 35% of buildings is over 50 years old, emphasizes the risk to suffer significant consequences due to the inefficiency in terms of structural and energy performance. In particular, the buildings in reinforced concrete (RC), constructed in the post-World-War II (post-WW2) which are in bad conditions due to inadequate technical properties, constructive technologies, and deteriorated materials, do not comply with the current standards, increasing the structural and energetic vulnerability. Under European directives, the National long-term strategy to support the building improvement and safety, involves the refurbishment of the elements belonging to the building envelope that have a significant impact in terms of performance. The use of innovative approaches, technics and recycled materials are incentivized to modernize the construction processes and reduce waste, under the circular economy criterion. Moreover, the strategy includes the definition of monitoring approaches with the aim to prevent failures, facilitate the maintenance operations, ensure the good service, and increase the building life cycle.

In the last twenty years, the role of the prefabricated modules has been fundamental in building refurbishment for the advantages that provide in terms of speed, quality certifi-

cation, safety, standardization, performance control, times, and costs optimization. Several international research groups have investigated prefab solutions with the aim to improve the building performance, minimizing the occupant disturbance, costs and environmental impacts. However, the two application fields have always been treated separately due to the several variables to consider in the project. The difficulties are related to the adaptability on the existing facades, that makes it hard the design of prefabricated elements that intent simultaneously mitigate the structural and thermal deficiencies of the buildings.

Therefore, accepting the challenge, the goal of this doctoral thesis is proposing an innovative technological system which, based on precast concrete (PC) modules integrating recycled materials, aims to improve the building thermal insulation, stiffen the existing frame structure, and provide the building for the integration of automatic devices for performance monitoring.

An in-depth critical literature review has been carried out regarding to precast concrete (PC) modules, cement-based material with recycled aggregates, existing building typologies and facades, as well as the prefabricated processes and products by the project partner company (chapter 3). It aimed to individuate the criticalities in using PC modules on existing buildings and recycled material in cement compounds, classify the buildings by typologies and facades, as well as comprehend the prefabrication processes and the company's innovation needs. After fixing the project criteria and its specific goals, a strategical method has been proposed (chapter 4) for designing the technological system of building retrofitting at three different scales of detail (*Material, Component* and *System scales*) with the perspective of preliminarily assess the thermal and seismic behaviour on a building type (chapter 5) and realize a first prototype (chapter 6) for validating the execution phases in safety.

INDUSTRIAL PHD THESIS

This PhD project belongs to the Italian "National Operative Program of Research and Innovation 2014-2020" which promotes the innovation in research, believing in the synergic collaboration among European Universities and Italian industrial companies. It may achieve reciprocal advantages in information, production, commercial and products that can have very significant results. This collaboration aims to increase the capacity to produce innovation by a quality research to trigger smart, sustainable and inclusive development.

The project called "*INTELLIGENT PRECAST CONSTRUCTION SYSTEMS: Project, realization, maintenance technology for the optimization of the environment and economic sustainability*" has been developed in double agreement with the University of Cantabria, in Santander (Spain) and in collaboration with the Italian company of prefabricated elements Ferramati International s.r.l. Starting from the benchmark by Ferramati, the overall objective of this thesis was proposing an advanced constructive technology to be inserted in the producing chain of the company, promoting the automation and innovation in industry for a sustainable development of the building sector and in particular of prefabrication.

The investigation activities were carried out in three different places: at the University of Cantabria for a duration of 6 months, at the production site of Ferramati Int. for other 6 months, and at the Polytechnic University of Bari for 26 months.

Depending on the state of research, the activities have been segmented in such a way as to acquire the knowledge necessary for the strategic development of the project.

1 THE PROBLEMS OF THE EXISTING RC BUILDINGS

1.1. Thermal insulation issues

The second half of the 20th century, better identified as post-WW2, was characterized from the haste to rebuild the cities after the damages due to the bombardments. The purpose of the first emergency plans for reconstruction was to speed up and simplify the building interventions to receive the displaced not paying attention to the building technological aspects (Pagliai, 2018). The constructive technology widely used was the reinforced concrete with infill walls in brick, for the advantages of ease and speed that provided. No consideration was given to thermal protection. Only after the energy crisis of the 70s, the first law on energy saving was enacted, taking into account the aspects related to thermal insulation, quality of materials and microclimatic well-being inside the buildings. Nowadays, this great portion of the building stock represents a risk to the health and well-being of the inhabitants due to great energy consumption and heat dispersions which affect the indoor microclimatic aspects, burdening the economic aspect. The deterioration of materials, the lack of maintenance and the inappropriate insulation system are the most diffused problems which are translated in low capacity in thermal resistance and weak thermal inertia of the building components, in particular, of external walls. In fact, the different thermal behaviour of their components and the non-uniform composition generate so-called thermal bridges. They are defined by the EN ISO 10211:2008 as a «part of the building envelope where the otherwise uniform thermal resistance is significantly changed by full or partial penetration of the building envelope by materials with a different thermal conductivity, and/or a change in thickness of the fabric, and/or a difference between internal and external areas» (EN ISO 10211, 2018). The building portions most exposed are the pil-

lars-infill walls joints and walls-floor junctions, especially in the rooms on the upper floors and those in contact with the ground. The temperature gradient between the indoor and outdoor environments and the different capacity of the wall components materials in heat absorbing, leads to the formation of condensation in absence of adequate insulation (Martiradonna, Fatiguso and Lombillo, 2020b). It is noticeable scanning the building surface by infrared cameras as in Figure 1.1-1a or in worst cases, at naked eye due to the formation of black spots on the surface as in Figure 1.1-1b.

a) b)
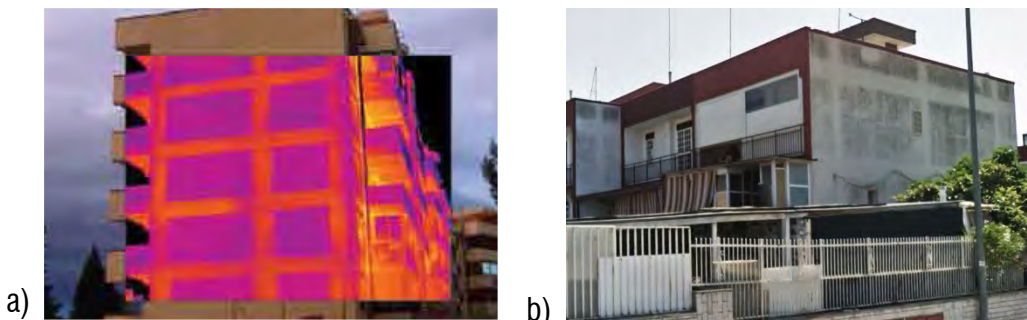
Fig. 1.1-1 – Observation of thermal bridges in building wall by a) infrared camera; b) naked eyes. Source: Zanchini *et al.*, (2014); Martiradonna, Fatiguso and Lombillo, (2020a).

The behaviour of the walls in winter and in summer is the same during the night: they exchange heat with the colder environment. However, during the summer daily hours, the heat produced by solar radiation warms up the room to reach high temperatures. The dispersing surfaces begin to progressively transfer heat to the interior, reaching, in few hours, inner temperatures very similar to the external ones creating thermal discomfort (Zanchini *et al.*, 2014). This phenomenon is due to the insufficient thermal inertia of the walls, defined by EN ISO 13786:2013 as the capacity of a building component to accumulate and release heat after several hours as well as to mitigate the temperature fluxes in the inner environment due to the thermal loads variation throughout the day (EN ISO 13788, 2013).

1.2. Structural safety

The observations of the damages due to recent seismic events occurred in the Mediterranean area, have suggested several vulnerability sources, with the necessity to investigate the role of all structural and non-structural elements in the seismic response of buildings, especially for that designed with any anti-seismic details. In particular, many seismic collapses are due to failures of the masonry panels which are usually considered as non-structural elements. Although the possible interaction with the structural skeleton under horizontal actions can cause extensive damages with high economic and human losses, masonry infills can induce some benefit in existing RC buildings, overall, in terms of energy dissipation increment, as well as for stiffness and strength (Negro and Colombo, 1997), with reduction of horizontal displacement caused by seismic actions. On the other hand, infill panels provoke the increment of seismic demand on the surrounding frame, with consequent premature local collapse, induced also in the structural elements (without forgetting the possible degradation of the bond-friction in the frame-infill contact length). In addition, in some cases, they can provide variation of global structural behaviour, such as the introduction of additional torsional actions of soft-storey mechanism in the cases of pilotis or short-column (Dolšek and Fajfar, 2001). Of course, the structural behaviour of RC buildings can be strongly influenced by brittle failures of panels, which change the equilibria of the loads in the building elements.

The studies about linear and nonlinear of infilled RC frames subjected to seismic actions, which proposes a vast panorama of numerical and experimental results (for instance, Furtado and De Risi (2020) and references therein), can be subdivided in two main categories: In-Plane (IP) and Out-of-Plane (OOP) behaviour.

Regarding the IP behaviour, the possible collapse mechanisms of masonry panels can be subdivided in shear, flexural and compression failures, while for the reinforced concrete frames, in flexural, axial, shear failures, besides to beam-column joints failures. In details, to consider the coupling of masonry panel and surrounding frame, as reported in El-Dakhakhni, Elgaaly and Hamid (2003), or in Asteris *et al.* (2011), the possible

failure mechanisms due to horizontal actions can be summarized as shown in Figure 1.2-1 and reported below:

a) Diagonal compression failure, which is given by diagonal cracks in the centre of infill. This kind of failure is usually due to the geometric infill properties, e.g. the slender;

b) Diagonal cracking failure, which is identifiable through some cracks, along to the infill panel compression diagonal. It is usually due to weak frame or strong frame with weak infill or strong frame with strong infill and weak joints;

c) Sliding shear failure, which is given by a horizontal sliding along the bed joints of infill. This type of collapse is due to the poor mechanical features of mortar presents in the joints;

d) Corner crushing failure, which exhibits crushing at the infill corners. It is usually due to weak infill panel and joints with strong frame elements;

e) Frame failure crushing, which is given by the plastic hinges in the surrounding frame due to weak frame or frame with weak joints.
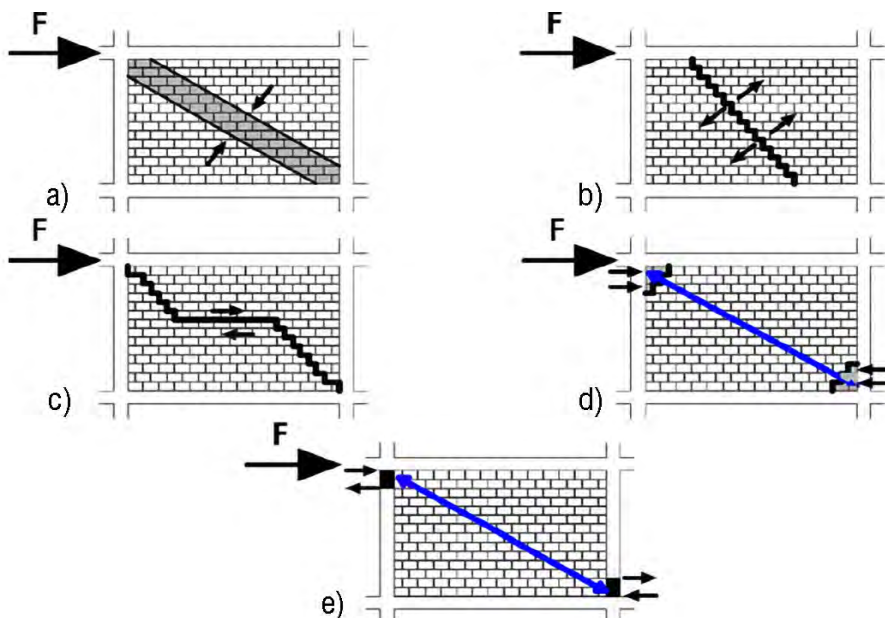
Fig. 1.2-1 – Possible failure mechanisms of infilled frames under IP seismic actions (F): a) diagonal compression failure; b) diagonal cracking failure; c) sliding shear failure; d) corner crushing failure; e) frame failure crushing. Source: (Ruggieri, 2018)

As concern the OOP behaviour, the possible failures are due to different reasons i.e. the presence or not of any kind of connections between the masonry and the surrounding RC frame, panel support type and width, the presence of single or double leaf, besides to consider other boundary conditions, as well as panel slenderness (height/thickness) or the features of the upper bed joint. The possible failure path, occurring for OOP actions, can be observed as the sequence of four steps, proposed by Pasca and Liberatore (2015): a linear elastic stage; cracks propagation and development of a yield-line failure; masonry disposed following an arch shape; crush of the masonry and total collapse. Still, in a view of OOP damages, failures could be schematized by defining the possible kinematic mechanisms due to the occurrence of one or more yield-lines. Figure 1.2-2 reports three of the failure possibilities, among which:

a) Rigid overturning of the masonry without arch effect;
b) Rigid overturning of the masonry with arch effect and one yield-line;
c) Rigid overturning of the masonry with arch effect and two or more yield-lines.
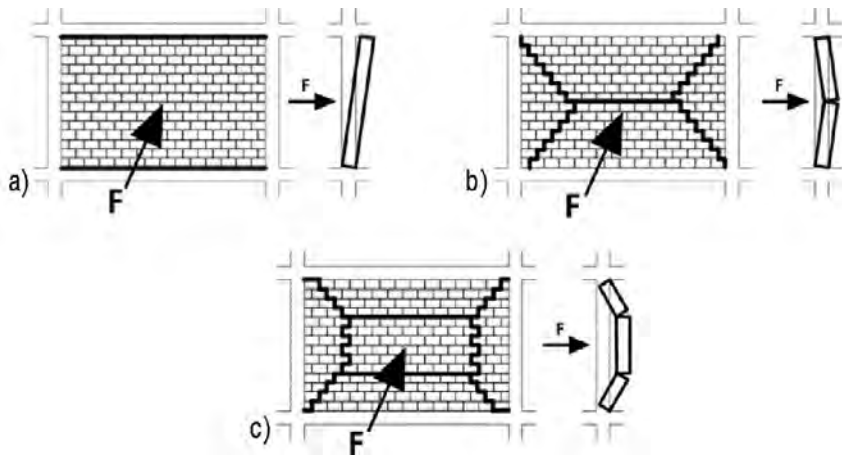

Fig. 1.2-2 – Possible failure mechanisms of infilled frames under OOP seismic actions (F): a) rigid overturning of the masonry without arch effect; b) rigid overturning of the masonry with arch effect with one and c) two yield-lines. Source: Ruggieri, (2018).

2 THE INNOVATIVE SOLUTION FOR THE RC BUILDING RETROFIT

In the field of building retrofit, many traditional techniques exist aiming at mitigating the thermal-insulation and structural deficiencies of the existing RC buildings. For instance, external-internal thermal coating or aerated walls for the energy improvements, plating of structural elements with steel or composite materials for structural protection. Nevertheless, they involve several supplies and professionals to be coordinated other than being expensive in term of costs and time of realization. Moreover, they cause a great discomfort of the occupants for the presence of numerous workers inside and outside the building, scaffolding and props or, in severe cases, the evacuation from the building for the dangerousness of the intervention.

The aesthetic aspect of the building is not to be neglected. Since it may vary according to the type of intervention, it is possible that it does not integrate with the context and it does not restore dignity to the building.

Therefore, the purpose of this doctoral thesis is the technological design for the industrial production of an Intelligent PC panels system based on prefabricated modules for the thermal and structural retrofit of a building typology chosen from the existing RC building stock. In particular, it aims to reduce thermal losses, improving the thermal resistance and inertia of the wall and stiffen the whole structure to mitigate the damages due to IP and OOP failures related to the infill walls in bricks. It intends also integrating monitoring devices for the building performance control over time, in order to facilitate maintenance and prevent preliminary failures.

Hence, the innovation stands in solving two important problems in the field of existing buildings, through a single intervention that, thanks to its technological configuration,

gives high thermal and structural performance, controllable over time to protect the inhabitants and extend the life cycle of the building.

According to the principles of sustainability and circular economy, the system shall incorporate materials coming from the industrial wastes and propose sustainable processes of prefabrication and installation. Developed with the Italian company Ferramati International, the PC panels shall adapt to the existing buildings, however maintaining the properties and material of the already started chain of manufactured products, i.e. concrete, expanded polystyrene sintered (EPS) and lattices girders.

In the light of the problems related to the typical retrofitting interventions, the system intends not to burden the existing structure and not alter the daily activities of the building occupants, assuming that the use of props is only permitted at openings.

The preliminary analyses of thermal and seismic behaviour seek to comprehend the advantages the system provides and the optimization that are necessary to improve the technology. In addition, the industrial production of the several panel prototypes, aiming at being installed on a sample of building wall, has the purpose of validating the execution phases, verify the speed of installation in safety and individuate the improvements to apport to the proposal.

2.1. Investigation Methodology

The ambitious challenge is achieved by dividing the investigation into three methodological macro-phases, aiming at providing the basis for the development of the next one: *Research Stage*, *Design Stage* and *Prototyping Stage*.

The ***Research Stage*** focuses on the synergy analysis of the state-of-the-art about prefabricated elements used in construction for new buildings, energy renovations and structural enhancement. It aims to understand and compare the characteristics of real market products with those investigated in the scientific scenario, identifying potential and deficiencies. At the same time, the analysis by climate, seismic hazard, building typologies and facades widely diffused in Europe, focusing on the case of Italy and Spain in accordance with the census by the European project EPISCOPE (Corrado,

Ballarini and Corgnati, 2014; EPISCOPE, 2016; García-Prieto Ruiz, Serrano Lanzarote and Ortega Madrigal, 2016) frame the study area in which the project shall develop.

In parallel, the observation and study of the Ferramati's production processes as well as the machinery and materials employed to produce the PC elements and EPS manufactures aim to understand the standardized methodology, the sequences of work, the production times and the corporate structure. In addition, the comprehension of the company's needs and prospects, individuates the limits of the actual products laying the foundations for the preliminary design idea, downstream of the general objectives set by the project.

From the general frame provided by the research auditing, it is possible to initiate the **Design Phase** by fixing the boundary conditions and the design criteria, e.g. geographic area, climate, and building location, in order to determine the characteristics the proposal should own in terms of thermo-hygrometric and seismic protection, according to the standards fixed by legislations. Hence, it is possible to develop the general concept of the proposal which needs the approval by the company in terms of feasibility and compatibility with the industrial plants and supplies. It proceeds with the design of the technology for scales of detail in compliance with the specific goals of the project. Three definition levels are specified: *Material, Component,* and *System*. Each next level inherits the characteristics of the previous one, incorporating it in its own design process. Basing on different methodological procedures, each level has its own approach for the definition of properties and performance.

The *Material scale* corresponds to the hub experimental design of an innovative light-weight base-cement mortar with aggregates in recycled EPS, which methodology and application is focused on section 4.4. At the *Component scale*, the prefabricated panel is considered. For it, three different approaches are used: quantitative and qualitative approaches based on the European and National standards for comprehending aspects related to the layers and junction between the panels. It is deepened in section 4.5. The *System scale* is referred to the whole building scale for which the design of the connection elements and completing technology follow the quantitative method founded on the application of the standards and the scientific approaches by the literature (section

4.6). In this phase, the preliminary thermal and structural behaviours of a building type are also assessed by simulations performed in accordance with qualitative approaches and numerical attempts. Moreover, a qualitative evaluation of the aesthetic impact and a preliminary monitoring technology draft is proposed.

The design results of each scale of detail allow initiate the industrial experimental phase of **Prototyping Stage** in which the studied material, components and system are realized with the intent of validating the merely technological aspects under safety requirements and verify the industrial reproducibility as assumed in the design phase.

Figure 2.1-1 illustrates the methodological process of the investigation. It has been developed and managed with the creative approach of the "Design thinking" in particular, according to the model of the "Sprint Execution", the objectives of the project and the type of company involved (Dell'era, 2018). The Figure 2.1-2 reinterprets the investigation methodology agreeing with the Sprint Execution paradigm of the Design Thinking.
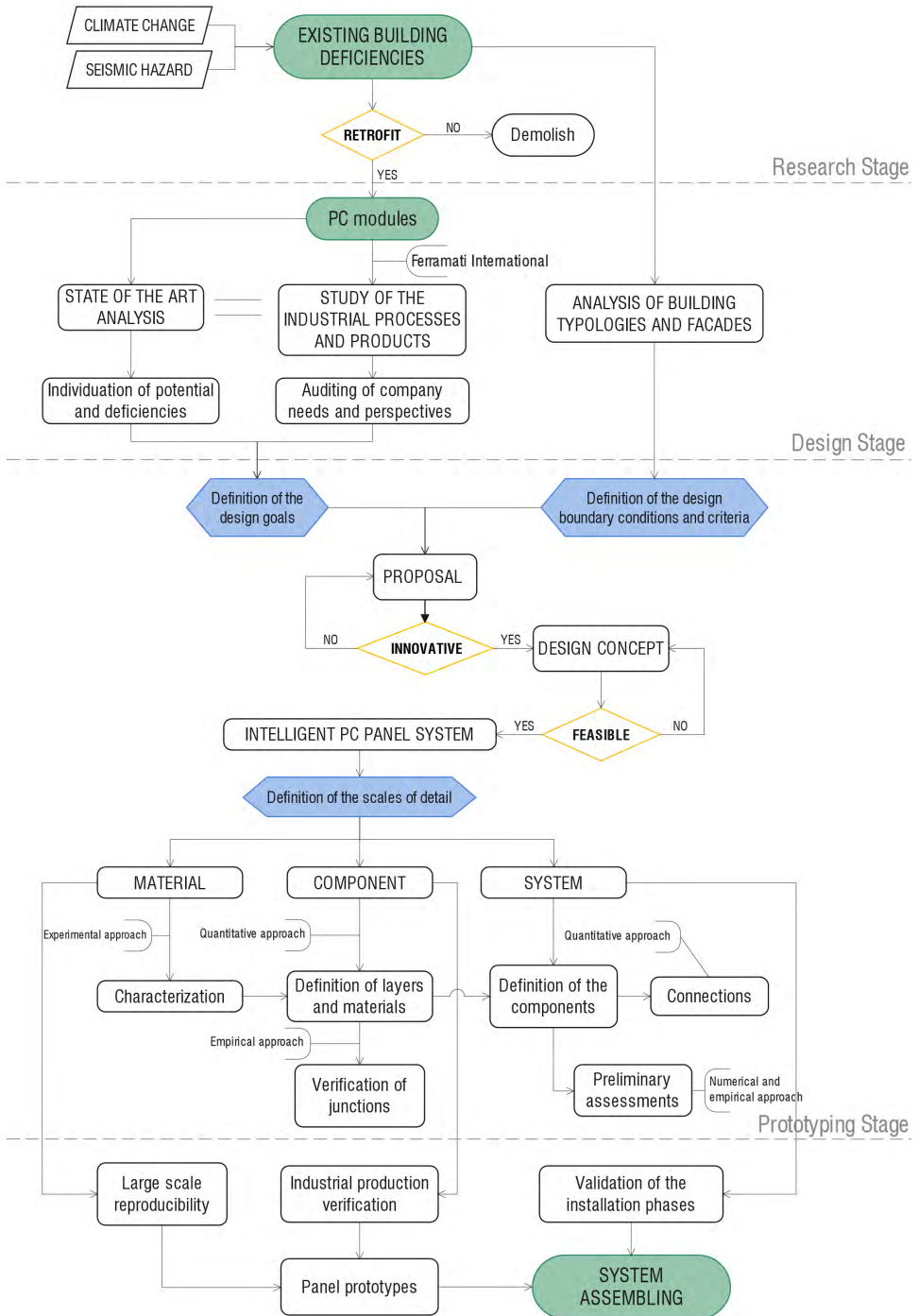
Fig. 2.1-1 - The investigation methodological process. Source: Author

RESEARCH STAGE
- Prefabricated modules
- Recycled materials
- Climate
- Seismic hazard
- Existing building typologies
- Façades
- Prefabrication Processes

DESIGN STAGE
- Definitions
- Technological Idea
- Preliminary project
- Feasibility
- Reduced 3D models
- Preliminary assessment

PROTOTYPE STAGE
- Composition
- 3D models
- Detail design and calculation
- Material supplying forming/assembling
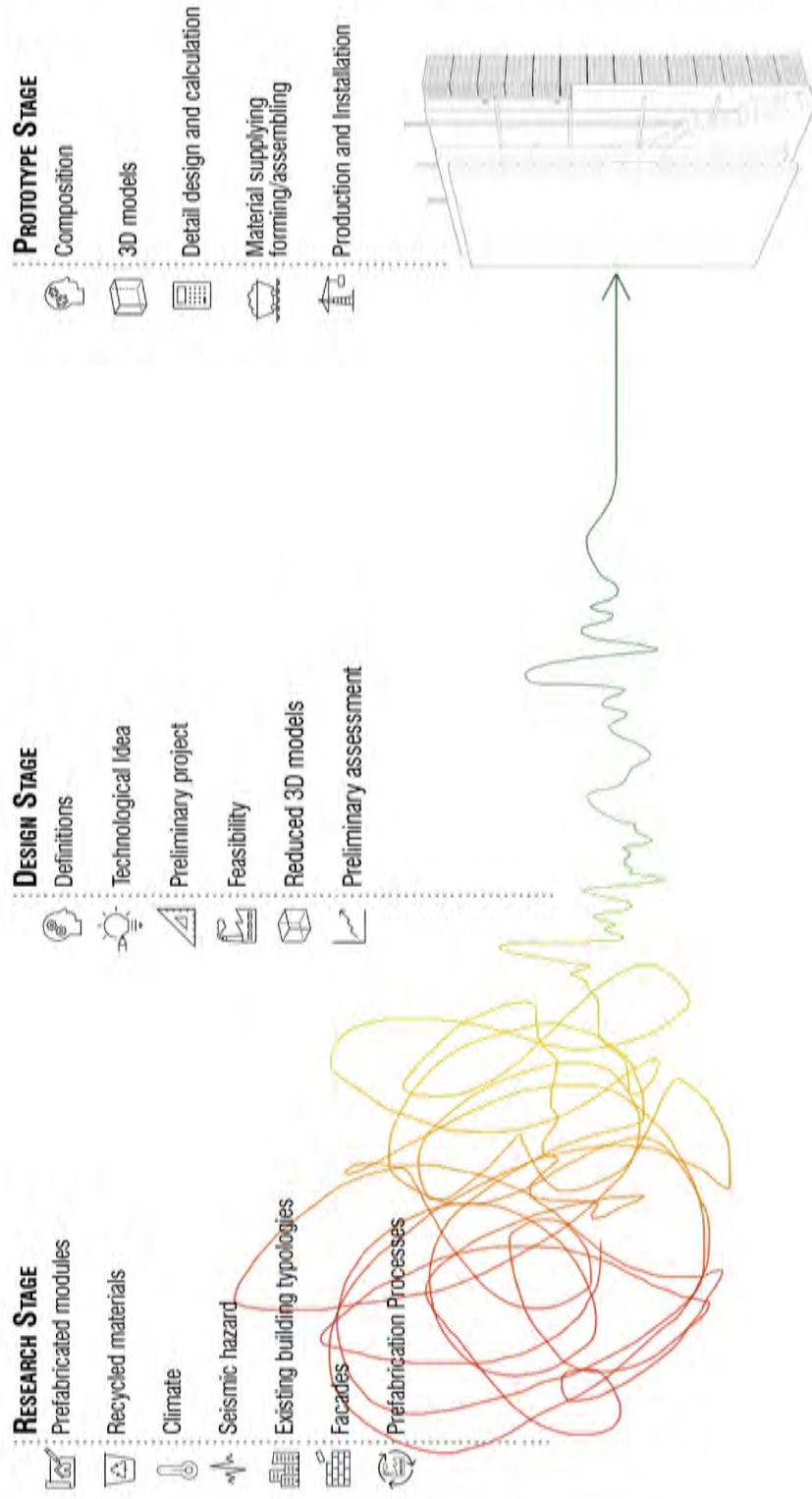- Production and Installation

Fig. 2.1-2 – Design Thinking: Sprint execution. Source: Author

2.2. Regulatory framework

The study of current legislation, both at European and National level, is essential for the design and preliminarily assess the retrofitting system proposal. The analysis of the European directives helps to understand the general issues, goals, and strategies the EU wants to achieve within next years. Instead, Eurocodes and National legislations give theoretical and practical indications to design and assess the performance of the proposal. Therefore, this section aims to provide the regulatory framework which is useful to develop every phase of the project. Table 2.2-1 aims to show the principal European Green Deals with related directives and codes from European 2030 Agenda which intends reaching the Sustainable Development Goals (SDGs), in particular, SDG 11 "Sustainable cities and communities" (Figure 2.2-1a) and SDG 12 "Responsible consumption and production" (Figure 2.2-1b) (European Union, 2020).

Table 2.2-1. Mean European Green Deals for efficient buildings toward SDGs 11, 12

| EU's GREEN DEALS	DIRECTIVE CODE	MEAN GOALS	APPLICATION SECTOR
GREENHOUSE GAS (GHG) EMISSIONS	2009/406/EC	- GHG emissions reduction of 20% by 2020 compared to 1990, or to 2005 in base of the GDP per capita criteria - GHG global emissions reduction of 50% by 2050 compared to 1990	- European Member States
	2018/842/EU	- GHG emissions reduction of 40% by 2030 compared to 2005 for every economy sector - GHG emissions reduction of 30% by 2030 compared to 2005 for industrial processes and product use	
ENERGY PERFORMANCE OF BUILDINGS	EPBD 2010/31/EU EPBD 2018/844/EU EPB standards	- Strong long-term renovation strategies - National energy and climate plans - Optimal minimum energy performance requirements - Energy performance certificate	- New buildings - Existing buildings (major renovation)
ENERGY EFFICIENCY	EED 2012/27/EU		- Existing buildings (replacement or retrofit of elements)
RENOVATION WAVE	COM/2020/662	- Double annual energy renovation rates - Enhance life quality of people living in and using buildings - Reduce Europe's greenhouse gas emissions - Create new green jobs in the construction sector	- Existing buildings
SAFETY IN CONSTRUCTION	EN EUROCODES 1990-1998	- Provide common technical rules to design buildings, civil engineering works and construction products - Structural risk reduction in construction	- New buildings - Existing buildings
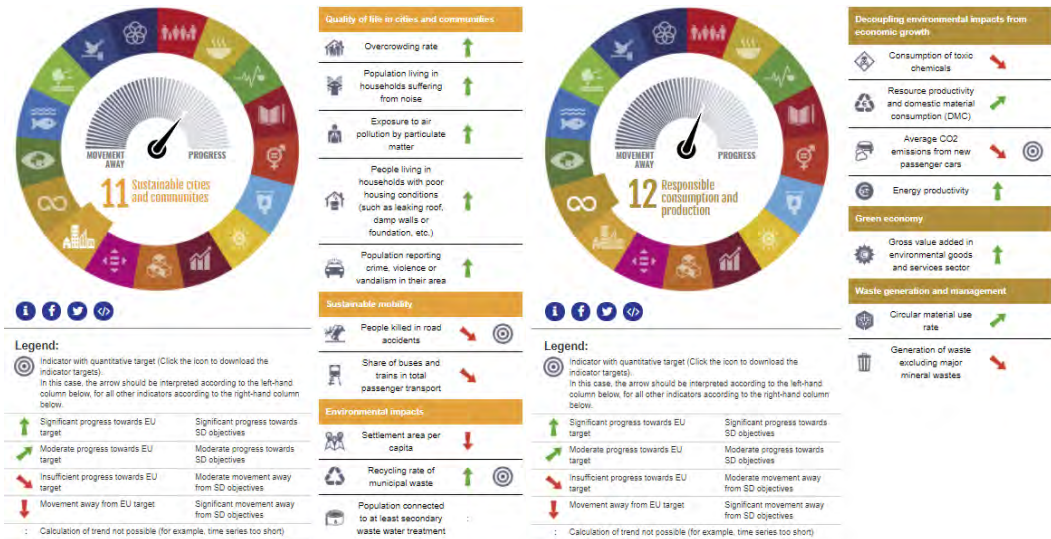
Fig. 2.2-1– 2020 progress about Sustainable Development Goals (SDGs) from 2030 Agenda: a) SDG 11: "Sustainable cities and communities"; b) SDG 12: "Responsible consumption and production". Source: https://ec.europa.eu/eurostat/web/sdi/key-findings

The regulatory framework underlying the design and performance verification of the innovative technology is schematically outlined in the table 3.4-2. It is referred at the macro phase *Design Stage* by the three scales of detail defined in the investigation methodology: "Material level", "Component level", and "System level".

Table 2.2-2. Reference regulatory framework for the proposal design

DESIGN STAGE			
MATERIAL SCALE			
INNOVATIVE LWM	AGGREGATES CHARACTERIZATION	- BULK DENSITY	- EN 16025-1:2013 - EN 10667-12:2006
		- PARTICLE SIZE GROUP OF EPS AGGREGATE	- EN 16025-1:2013 - EN 13163:2017 - EN 933-1 - EN 933-2
	MIX DESIGN, SAMPLINGS AND MECHANICAL STRENGTH ANALYSES		- EN 196-1:2016
	WORKABILITY: FLOW TEST		- EN 7044:1972
	THERMO-HYGROMETRIC ANALYSES		- EN 16025-1:2013 - EN 12667 - EN 12086:2013
COMPONENT SCALE			
SLAB CONCRETE	MATERIAL CHARACTERISTICS		- EN 206:2013 + A1:2016

18

STEEL REBAR	MATERIAL CHARACTERISTICS		- EN 13369:2018 - Eurocode 2 - Italian technical code for construction (NTC18)
	MINIMUM REINFORCEMENT		- Italian Regulation 12/03/1987
	REBAR COVER		- Eurocode 2 - EN 13369:2018 Annex A

SYSTEM SCALE

MULLIONS AND ANCHORS	MATERIAL CHARACTERISTICS		- NTC18 - Eurocode 3 - EN 10025:2019 - EN 10027-1:2016 - EN 15048-2:2016
	ANCHORAGES	- MASONRY	- ETAG 029 - ETA-12/1036 - ETA-19/0160
		- CONCRETE	- Eurocode 8 - ETAG 001 - ETA-07/0260
	POST-INSTALLED STEEL REBAR		- Eurocode 2 - Eurocode 8 - EOTA TR23
WEAKLY REINFORCED CONCRETE	MINIMUM REINFORCEMENT		- Italian Regulation 117/2011
	CONCRETE HYDROSTATIC PRESSURE		- DIN 18213:2008

PRELIMINARY ASSESSMENT: THERMO-HYGROMETRIC BEHAVIOUR

MINIMUM REQUIREMENTS	ITALY		- Ministerial Decree of 06/26/2015 + ANNEXES 1/2 and APPENDICES A/B - Legislative Decree n.48/2020
	SPAIN		- Código Técnico de la Edificación (CTE) n.732/2019 - Documento Básico-HE 2019 + DA-HE/1-3
THERMAL PARAMETERS	THERMAL RESISTANCE AND TRANSMITTANCE		- UNI/TS 11300-1:2014 - EN ISO 6946:2018
	THERMAL INERTIA		- EN ISO 13786:2018 - EN 10375:2011
	THERMAL BRIDGES		- EN ISO 10211:2008
HYGROTHERMAL PERFORMANCE	VERIFICATION OF INTERSTITIAL CONDENSATION FORMATION		- EN ISO 13788:2013

PRELIMINARY ASSESSMENT: SEISMIC BEHAVIOUR

	SEISMIC EVALUATION		- Eurocode 8 - NTC18

3 STATE OF THE ART

In this context, this revision of the state-of-the-art is drawn up for the following purposes: 1) having a clear frame of the actual prefabricated elements in the market scenario to understand the most diffused typologies; 2) analysing criticalities and potentialities of the prefabricated solutions for the energy and structural retrofit of the existing buildings in the scientific scenario; 3) understanding and comparing the characteristics of the lightweight cement-based compounds with aggregates in EPS, both virgin and recycled; 4) studying the processes of the industrial production and the context in which the system is inserted. The projection is the development of a system able to give an answer to the problems that affect the existing buildings toward the standardization of the retrofit too.

According to the methodology proposed in the chapter 2, the state of the art belongs to the macro phase "Research stage" in which three parallel spheres of the analysis are taken in account. Each one having the purpose to lay the foundations for the definition of the specific goals that the system intends to achieve, the conditions and criteria of the project development. Starting from a brief history of the prefabricates used for new construction, between which the most significant patents are also analysed, the comparison of the market products aims to individuate what type of prefab systems are developed to play both the insulating and structural functions and to study the technology of the most performant ones. It proceeds entering the field of retrofit of the post-WW2 existing buildings. Several studies are critically analysed with the purpose of individuating advantages and disadvantages as well as the technology used to ensure the connection with the existing buildings. As regard the prefab modules employed for structural improvements, the study is concentrated to the solutions aiming at mitigating the damages due to the

action of the filling wall under seismic activity, deepening the connection aspects and the results obtained. The analyses of the approaches employed allow identifying the methods to follow, in the design phase, for the preliminary assessment of the proposal system behaviour under thermal and seismic conditions.

Since one of the objectives of the project is the use of material coming from the industrial wastes, section 3.3 deepens the aspects related to the compounds with light aggregates in recycled EPS. Although, a comparison with those that employ the virgin polystyrene is necessary to understand the advantages and limitations in using recycled aggregates and identify the starting point for the investigation of a new mortar with enhanced performance.

After analysing the international sphere, in section 3.4 the study focuses on the local area, in particular on industrial products and processes from the partner company of the project: Ferramati International. The audit of the prefabrication methods as well as the machineries and materials employed, aims to comprehend the needs and future perspectives of the company for exalting the strengths.

The analysis of these two different study areas provides the basis for the definition of the specific design goals at the start of the design phase.

The third focusing area concentrates on the analysis of the building typologies widely diffused in Europe and in particular in Italy and Spain, the two partner countries of the project, starting from the climatic and seismic hazard conditions. It aims to understand the context in which the system has to be developed and start the design phase. This study allows to define the design criteria and choose the building typology and façade for which initiate the project.

3.1   Precast concrete modules in building constructions

The prefabrication conception transformed over the time, starting from the invention of modern reinforced concrete in the 19th century. Precast concrete elements have rarely been used as a building façade due to the lack of attention at materials, considered unworthy and unsightly, the unwanted presence of junctions between the modules and the limited versatility. However, the advantages in terms of economic affordability, speed,

ease of installation, higher quality fabrication in controlled factory environments and re-duced construction times, have made them popular all over the world. Starting from the post-war period, precast concrete modules were widely applied in the façades of housing buildings, as large loadbearing wall panels, as attached elements to frame structures, or as insulated panels (Van de Voorde, Bertels and Wouters, 2015).

Two macro-categories of precast systems were developed differing each other for the use of materials characterized by various density: massive and light technologies (Figure 3.1-1).
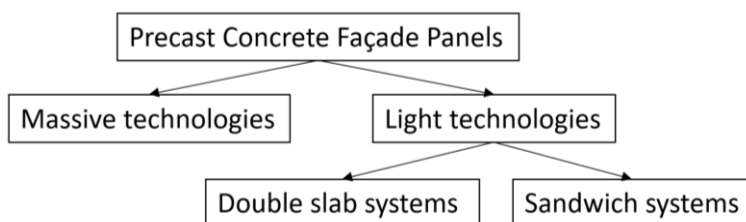

Fig. 3.1-1 – Categories of Precast Concrete Façade Systems. Source: Author

The firsts were composed by heavy materials, the seconds, i.e. double slab systems and sandwich walls, widely used, by more layers, also insulating, that gave the advantages in terms of lightness, thermal inertia and insulation, acoustic isolation, ease of transport and installation. More in detail, a double slab system consists of two parallel walls, made in factory, generally about 5 cm thick, maintained at a mutual distance varying between 20 and 40 cm and connected each by steel reinforcing. They contain the reinforcement necessary to ensure the stability of the wall. The space between the two slabs is filled with an in situ concrete casting which creates a monolithic wall in reinforced concrete.

A sandwich wall with insulating layers consists of two precast concrete elements con-nected each other with internal structures of hot galvanized steel metal profiles. One or more layers of insulation are placed into the cavity between the two concrete elements. The profiles, drowned in each panel, ensure the fixing to special brackets previously ar-ranged in the floors or pillars, and allow to anchor the system to the load-bearing struc-ture of the building (Scioti, 2015).

These two typologies of precast concrete walls have transformed over the time to satisfy the structural and thermal requirements of buildings. Different materials, in particular the insulating ones, were combined with concrete to optimize its performance. Many patents have been released over the years. In 1988, Hans-Ulrich Terkl invented a prefabricated wall panel made by a lightweight concrete and polystyrene, regularly spaced from parallel semi-circular cavities along the width and length directions, filled with structural concrete casted on site (Terkl, 1988) (Figure 3.1-2a). In 1991, Philippe Durand introduced a typology of double slab wall composed by two parallel panels in insulating material linked each by horizontal stiffeners and shores in order to define a cavity filled on site with concrete (Durand, 1991) (Figure 3.1-2b). Chin T. Kim, in 1995, patented a double-wall structure which included outer and inner sheets, coupled by mechanic links directly on site. The reinforcement was added in the region between the walls, then filled with concrete (Kim, 1995) (Figure 3.1-2b).
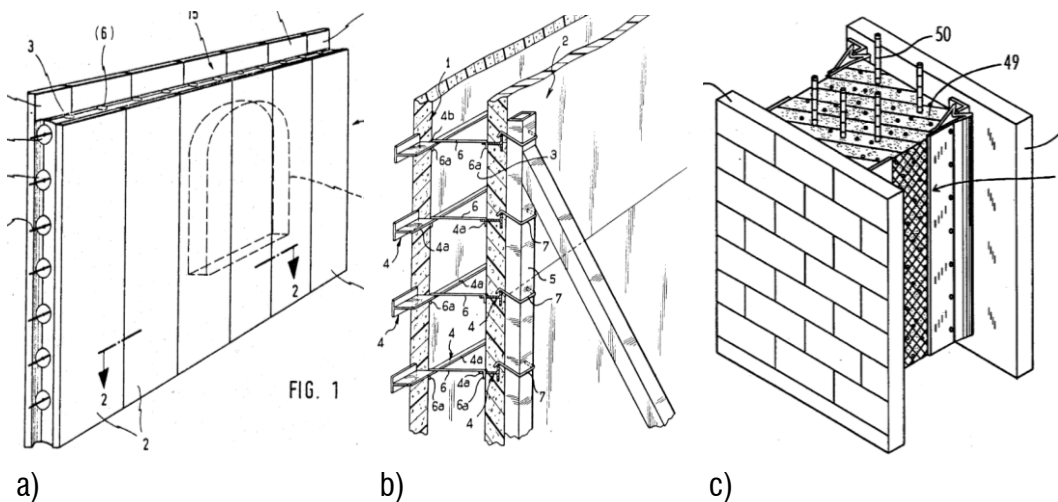

a)   b)   c)

Fig. 3.1-2 – Examples of patents of prefabricated panels: a) Terkl, 1988; b) Durand, 1991; c) Kim, 1995.

Other patents were: US04706429A (Young, 1987), US05528876A (Lu, 1995), US05491947A (Kim, 1996), US005927032A (Record, 1999), US007073300B1 (Sohns, 2006), US006167671B1 (Wilson, 2001), US006301851B1 (Matsubara, 2001), US006443666B1 (Smith, 2002), US007124547B2 (Bravinski, 2006), US007162845B2

(Messiqua, 2007), US007516589B2 (Messiqua and Messiqua, 2009), WO2010040183A1 (Sharpe and Sharpe, 2010), WO2011123082A2 (Kargin, 2011), US20110265412A1 (Sharpe and Sharpe, 2011).

The newest needs of structural and thermal protection of buildings, defined by the latest international codes (*ACI 318-14* 2005, *Eurocode 2* 2004), the increase of materials knowledge and construction issues, have led the scientific and technological community to develop even more innovating solutions devoted to minimize the structure vulnerability and optimize the energy performance. Gara *et al.*, (2012) carried out an experimental investigation on structural sandwich walls with non-shear connectors, inner layer in polystyrene and reinforced concrete beams under in-plane vertical and horizontal axial and eccentric loads. The strength of panels decreased with the slender ratios increasing. Kang, (2015) investigated the structural performance of foam-insulated concrete sandwich panels under axial compression. The FEM method was adopted, considering non-linear behaviour of concrete, foam and rebar components to predict the resistance of the shear ties. Abramski, (2017) studied three different precast panels in lightweight aggregate concrete with open structure and compared their load-carrying capacity and stiffness with traditional wall components. Qun, Shuai and Chun, (2018) examined the structural behaviour of a precast concrete sandwich panel under axial loads and observed that no substantial cracks generated on the panel surface and no out-of-plane deflections occurred. On the other hand, the inner ununiform components of the panel generated thermal bridges that invalidated the wall thermal performance.

One of the hardest challenges in designing precast concrete panels has always been the searching of internal connections among the layers. Their shape, material and position into the layers usually are the major responsible of an appropriate/unsuitable structural and thermal performance of the wall. Previous studies have investigated the structural properties that single or coupled connectors conferred to the precast concrete panels, leaving the thermal performance not rigorously evaluated (O'Hegarty and Kinnane, 2020). Many recent investigations, instead, have focused on evaluating different typologies of connectors with the aim to achieve the structural efficiency, minimising the thermal bridging effect. Therefore, connection devices made by steel alternative materials such
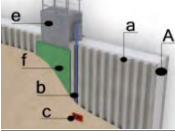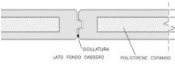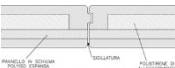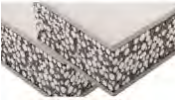
as fiber-reinforced polymer (FRP) (Norris and Chen, 2016), carbon-FRP (Frankl *et al.*, 2011; Hodicky *et al.*, 2015), basalt-FRP (BFRP) (Teixeira, Tomlinson and Fam, 2016; Al-Rubaye *et al.*, 2018), glass-FRP (GFRP) (Frankl *et al.*, 2011; Woltman, Tomlinson and Fam, 2011; Williams Portal *et al.*, 2017) have been studied.
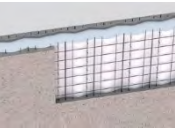
However, some undesirable effects occurred on the panels for structural applications such as bond slip, brittleness and low shear strength (Bida *et al.*, 2018). From the thermal point of view, the results obtained have demonstrated that, despite the internal insu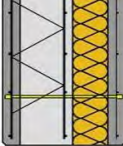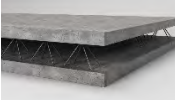lating layers, the joints affected the overall thermal behaviour of the building envelope (Al-Rubaye *et al.*, 2018; Klõšeiko *et al.*, 2020). On the other hand, the analyses carried out on panels containing well designed steel ties, have revealed satisfying under thermal and structural profile (Kinnane, West and Hegarty, 2020).

3.1.1   Precast concrete wall panels market

The market of the precast concrete has grown in concomitance with the advance of the industrialization, urbanization and infrastructural improvements. Customer's tendency to prefer eco-friendly, economical and modern buildings has opened growth opportunities to the prefabricated market. As concern the precast concrete walls, in particular thermal walls, the market is segmented into structural and non-structural components (*Precast Concrete Market Size, Share, Global Industry Forecast Till 2023*, no date). In the market scenario, it is possible to find various typologies of panels for the wall composition, although the most diffused systems, over the world, are almost the same. Every Nation has adapted the design process (dimensions, materials, supplies, methods, etc.) to comply with the own requirements, standards and regulations. The most interesting typology of the panels emerged from the market analysis are essentially three: the sandwich panels, the double slab panels and saad system. The following table (3.1-1) describes and compares some market products, classified in accordance with the typologies below.

Table 3.1-1. Market products

IMAGE	PANEL TYPE	DESCRIPTION	LOAD-BEARING WALL	FILLING WALL	THERMAL INSULATION	NEED TO BE COMPLETED AT WORK
	Sandwich panel	Two outer sheets in fiber-reinforced concrete lightened with polystyrene beads and inner layer of EPS insulation. Connection to pillar through a cast-in-place concrete. Source: http://www.lacasaprefabbricata.it/documenti/klimasismico.pdf		X	partially	partially
	Sandwich panel	Sandwich panel in vibrated reinforced concrete, 20 cm thick, with an insulated core in polystyrene. Source: http://www.premacweb.com/pannelli.html		X	partially	
	Sandwich panel	Sandwich panel in vibrated reinforced concrete, 28 cm thick, internally insulated by a polystyrene layer and a continuous thermal cut section in expanded foam. Source: http://www.premacweb.com/pannelli.html		X	X	
	Sandwich panel	Two exterior boards, 5mm thick, in calcium silicate and lightweight core in polystyrene beads and cement or ceramsite. Source: https://zjteps.en.made-in-china.com/product/LsBJPgdYZpWK/China-Sandwich-Panel-Insulation-EPS-Fiber-Cement-Internal-External-Wall-Board.html		X	X	
	Double slab panel	Two external layers of structural concrete of different thickness sizes and internal core of extruded polystyrene. Plastic connectors are used to link the concrete layers. No thermal bridges occur. Source: https://www.yourhome.gov.au/materials/precast-concrete	X		X	
	Double slab panel	Two external concrete shells connected by means plastic and glass fibres links and reinforced by lattice girder. Inner insulation layer in polystyrene. Internal resulting cavity filled through a cast-in-place concrete Source: https://www.progress.cc/it/costruire-con-prefabbricati-cls-con-isolamento-termico-interno	X		X	X
	Double slab panel	Cast-in-place concrete jet inside two panels in mineralized fiber-wood and concrete arranged in parallel and held by appropriate elements. Source: https://www.celenit.com/en-UK/isolamento-involucro.php	X		X	X
	Double slab panel	Two parallel slabs, 5-6 cm thick, reinforced with electro-welded mesh and with interposed lattice girders. Completed in situ with concrete casting. Source: http://www.ferramati.it/web/prodotti/doppia-lastra/	X			X
	Double slab panel	Two external EPS panels joined to a precast double slab wall. The connections between the walls is ensured by horizontal pylons. The resulting cavity is filled with a cast-in-place concrete. Source: http://www.ferramati.it/web/prodotti/doppia-lastra/	X		X	X

	Double slab panel	Two external concrete layers, connected by internal joists embedded along the underside into a layer in polystyrene, internally fixed to one of the two concrete slabs. The resulting cavity is filled with a cast in-place concrete Source: https://www.esseteam.it/la-gamma-prodotti/esse-therm-system/termobilastra/	X	X	X
	Double slab panel	Two outer concrete slabs connected by steel pylons and inner insulated layer in polyurethane foam. The remaining place is casted in-place with concrete. Source: https://www.coce-prefabbricati.it/index.php/component/content/article/9-prefabbricati/26-doppia-lastra-coibentata	X	X	X
	Double slab panel	Double slab panel connected to a further concrete sheet by means a insulated layer. The inner space is casted in place with structural concrete. Source: https://www.brandellerosolai.com/murature-prefabbricate-bi-lastra/	X	X	X
	Saad system (Step system)	Two polystyrene "to lose" formworks inner connected by means plastic ties and brackets that sustained the rebars. After the EPS blocks assembling, the cavity is filled with structural concrete. Source: http://www.ferramati.it/web/prodotti/sistema-step/	X	X	X
	Saad system	Electro-welded jail containing a polystyrene sheet. It is completed in situ with two outer layers of sprayed concrete. Source: https://www.baupanel.com/en/download-brochures-and-technical-specifications/		X	X	X
	Saad system	Two polystyrene or ceramic sheets with attached electro-welded galvanized steel meshes, connected each through steel connectors. The inner resulting gap is filled with a concrete conglomerate casted in place. Source: https://www.ecosism.com/moduli/modulo-getto-singolo/	X	X	X
	Saad system (Plastbau)	Two panels of high density expanded polystyrene joined and spaced by metal lattices that make the rebar of the concrete casting. Source: https://www.poliespanso.it/prodotti/muro-plastbau-3/	X	X	X

3.2   The existing building retrofit

In the latest years, some important factors (i.e. economic crisis, climate change and seismic activities), have considerably influenced the construction sector. The increasing demand of existing building stock renovation encouraged the scientific and technological community to develop new solutions devoted to convert the existing buildings into nearly zero energy buildings (NZEB) and structurally safe. In particular, the study has focused on reinforced concrete (RC) buildings of post-WW2 which are in worst conditions due

to the deterioration of materials, the lack of maintenance, the unsatisfactory insulation systems and the inadequate technical properties.

3.2.1   Prefabricated modules towards the building energy renovation

From the analysis of the scientific literature regarding the strategies of the building energy performance improvement, it has emerged that the restoration of the building facades which have significant impacts on energy efficiency, has become the new challenge. The goal is to overcome the problem related to the typical retrofit in terms of aesthetic dignity, low performance (reduction of thermal losses only up to 60% (Borodinecs *et al.*, 2017)), too high construction times and costs (Miloni *et al.*, 2011).

Off-site prefabrication can be the innovative and advantageous answer to these issues. In addition to the benefits associated with prefabrication itself (e.g. speed, quality, safety, standardization, control, reduction of production and execution times and costs, etc.), it can minimize the discomfort of tenants, the risk of condensation, internal surface losses as well as ensuring architectural flexibility especially for finishes. With the use of prefab modules, conventional formworks and props are eliminated or reduced, the production of wastage and various other environmental hazards are greatly dropped and consequently, a safer working site for the workers is provided (Seghezzi and Masera, 2015).

In the document of European Union about recommendations on building renovation, the use of prefabricated solutions is highly suggested. It cites so «Industrialised retrofitting by way of serial prefabrication off-site of insulating facade and roof elements including cabling, tubing and glazing can result in more cost-effective renovation and low-disturbance of residents during the renovation» (The European Commission, 2019). The document indicates as pilot project in the use of prefabricated modules for building renovation, the 2ndskin project by Woningbouw et al. (Figure 3.2-1). They have demonstrated that the application of prefabricated modules on the existing building facades maximized building energy performance, reducing the disturbance for tenants during the works. Although, the too high starting investment made the retrofit not viable and financeable (Woningbouw *et al.*, 2016; Azcarate-aguerre, Guerra-santin and Silvester, 2017; Konstantinou *et al.*, 2017).
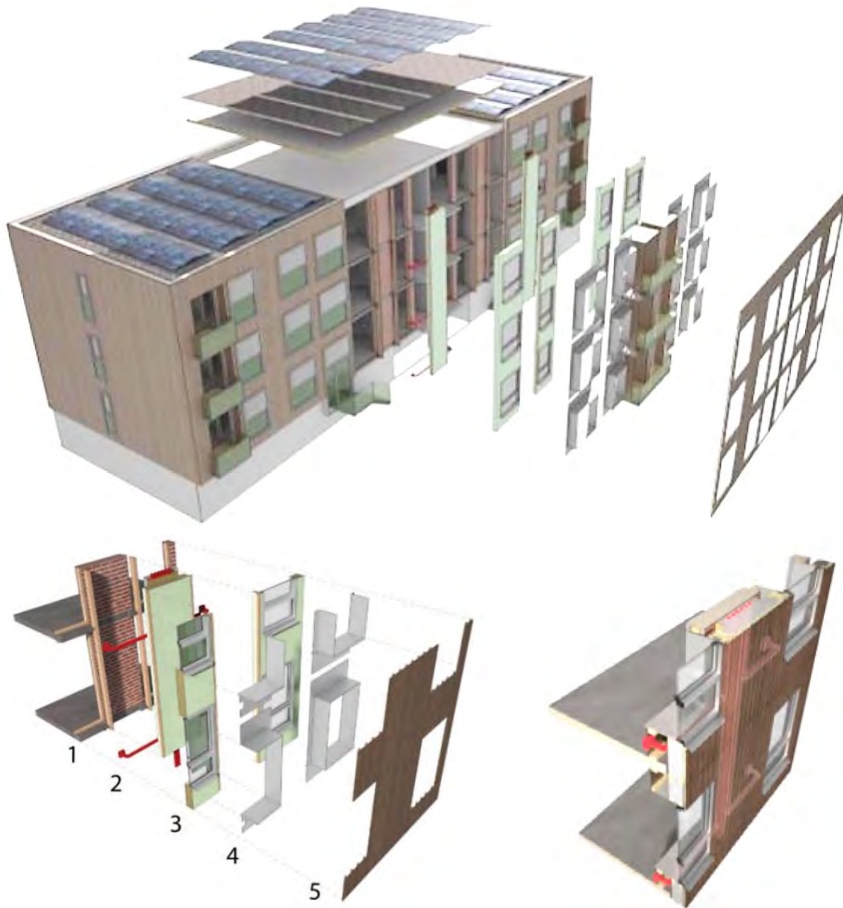
Fig. 3.2-1 – Details of the 2ndskin project for the optimization of the energy performance of the existing buildings. Source: Woningbouw et al., (2016); Azcarate-aguerre, Guerra-santin and Silvester, (2017).

Earlier projects, involving building renovations with prefabricated panels, have been developed by research teams across the world for the general project by the International Energy Agency (IEA) called Energy Conservation in Buildings and Community Systems (ECBCS). The participating countries were Australia, Austria, Belgium, France, Germany, Italy, Poland, Portugal, Spain, and many others. The ECBCS Annex 50 contained a collection of design guides, case studies and technical reports, mainly focusing on residential building renovation. In particular, the retrofit strategies design guide defined the approach to employ, the parameters and instruments to take into account for starting an

advanced retrofit with prefabricated panels (Schwehr, Fischer and Geier, 2011). The retrofit module design guide identified the factors that influenced the prefabricated module project i.e. the design, fabrication, transport and mounting requirements but also the way of assembling the modules on different typologies of facades (Kobler *et al.*, 2011). The case studies have demonstrated that the retrofitted buildings by prefabricated modules achieved high values of energy saving for heating, gaining aesthetic and architectural quality (Miloni *et al.*, 2011; Zimmermann, 2012). Therefore, the IEA ECBCS Annex 50 can be considered as a guide model for every retrofitting projects.

Many other researchers have investigated different prefabricated solutions devoted to improving the façade performance of the RC buildings. Masera *et al.*, (2017) have applied an innovative sandwich panel as a second skin of an existing residential building in Italy, achieving a total reduction of the primary energy consumption for heating of 82%. In Portugal, the application on two size type of buildings of a panel containing recycled materials has involved reducing the overall energy needs (Silva *et al.*, 2013). Garay, Arregi and Elguezabal, (2017) have investigated the performance of a prefabricated module composed by a polyisocyanurate insulating layer and a photocatalytic concrete finish, applied to a Spanish residential building. From the analyses results, the overall thermal performance of the building was improved, even though thermal bridges occurred on the intermediate floor where the panels were anchored. In Figure 3.2-2 shows the images of the panels of the contributions above.

Fig. 3.2-2 – Some examples of prefabricated solutions for thermal improvements of the existing buildings: a) Masera et al., (2017); b) Silva et al., (2013); c) Garay, Arregi and Elguezabal, (2017).

Among the problems associated with the retrofit through prefabricated modules, dimensional adaptability and anchoring systems have been the most studied. As existing buildings have their geometric and dimensional characteristics, the notion of standardisation is lacking. A prefabricated module that adapts to an existing building, cannot fit to another. For this reason, the concept of custom prefabrication was born.

Several researchers have employed the 3D laser scanning technique on RC existing buildings in order to acquire correct data on dimensions and geometrical features, with the aim to decrease human error during the traditional measurements and to start an accurate module design process (Dobelis, Kalinka and Borodinecs, 2016; Borodinecs *et al.*, 2017, 2018; Pihelo, Kalamees and Kuusk, 2017).

Nevertheless, the anchoring system project is a hard challenge to face due to the materials compatibility, the fixing technology, the air tightness of the system and the thermal bridges that might occur along the edges of the panels. It is also related to the panel dimensions, weight and to the design of the joints that should allow an easy assembly of the modules and absorb the thermal expansion. Silva et al. have investigated a prefabricated retrofit module equipped with two steel U-profiles placed on each side of the modules and with a set of pins and holes to fit into a metal support structure already fixed to the existing wall. From the thermal bridges analysis, they observed that a significant heat flux occurred on the coupling area between the modules. Thus, they proposed some corrective measures on the layers distribution that drastically reduced the thermal losses (Silva *et al.*, 2013). Kobler et al. have employed some metal flats with one slotted hole and one or more round holes to suspend the modules. The metal flats were through-bolted to the panels (Kobler *et al.*, 2011).

As the theme is being developed, the academic community is seeking to deepen these problematic aspects and give importance to compatibility and adaptability with existing facades to standardize production. Indeed, since each project has its own particularities related to the environmental conditions and context in which it is born, the challenge consists in the development of a prefabricated system that could mitigate geometric differences and thus adapt to multiple conditions.

3.2.2 Prefabricated modules for structural strengthening

Recent intense seismic activities have highlighted the vulnerability of the existing RC buildings to the damage and collapse associated to the structural insecurity and the lack of prevention. A significant problem related to these buildings is the inadequate or absent joining between the infill walls and the structural frame, specifically along the upper and lateral edges. In the latest years, in-plane (Cavaleri and Di Trapani, 2014) and out-of-plane tests (Ricci, Di Domenico and Verderame, 2018; Furtado *et al.*, 2020) have been carried out to better understand the behaviour of masonry infill panels during the earthquakes and the interaction with the bordering RC frame (Porco *et al.*, 2015).

It has emerged that the frame-infill interface should not be ignored since the masonry infills considerably influence the building dynamic response. They provoke the shear stresses concentration on the higher part of the pillars as consequence of the lack of transfer of the forces along the upper beam. Hence, the damages are the ruinous collapse of the wall panels out of the plane and the increase in shear stresses in the most stressed sections (Dolce and Manfredi, 2011).

In the scientific scenario many solutions have been investigated with the aim to mitigate the infill walls influence, improve the whole structural response of the building, and perform the work safely in the shortest time possible (Kaplan and Ylmaz, 2012). Entire or partial cast-in-place RC infill walls to be integrated to the existing ones have been studied. These solutions increased the lateral stiffness and discharged the existing frame from large lateral forces. Though, the application was expensive and required heavy construction work which made necessary the evacuation of the building (Emin and Altin, 2006; Turk, Ersoy and Ozcebe, 2006; Altin, Anil and Kara, 2008).

In the latest years, a series of researches oriented towards novel techniques have been carried out to convert the hollow bricks/blocks into strong and rigid infills. For this research, among all, the most interesting methods have been the application of sheets or strips of fiber-reinforced polymer (Binici and Ozcebe, 2006; Valluzzi *et al.*, 2014), textile reinforced mortar (da Porto *et al.*, 2015; Akhoundi, Vasconcelos and Lourenço, 2018; De Risi *et al.*, 2020), wire mesh reinforced shotcrete (Kamanli *et al.*, 2015), and precast

concrete (PC) panels. They were cheap, structurally effective, and easily applicable techniques of strengthening without the need of building evacuation.

In what follows, the state of the art concentrated on the PC panels solutions is analysed more in detail. Ha, Yu and Kim, (2018) have proposed an L-type PC panel inserted into the infill wall and anchored to the RC frame by means bolts, using the dowel-connection technique. They tested the specimens under reverse cyclic loading and compared the results with a brick wall of the same dimensions. They demonstrated that the seismic behaviour of the RC frame was greatly improved unlike the traditional wall. Baran and Tankut, (2011) have investigated the initial advantages of their reinforced PC panels bonded to the interior infill walls and RC frame of the building with epoxy mortar. The panels were designed to be practically applied and ease connected to each other. The test results revealed that both strength and stiffness of the specimens were improved. Nevertheless, the authors observed some troubles to deeper investigate, in particular, about the number and orientation of the anchors among the panels. Another interesting research about the RC frame strengthening by precast wall panels was carried out by Choi *et al.*, (2020). Such panels were designed to be applied on the external face of the building, hence, to ensure the occupants carrying out their daily activities and reduce their disturbance. The specimens were tested under cyclic loading and the results exhibited improvements in strength, stiffness and capacity of energy dissipation in comparison with the RC frame structures without seismic details. In Figure 3.2-3 shows the images of the panels of these contributions.
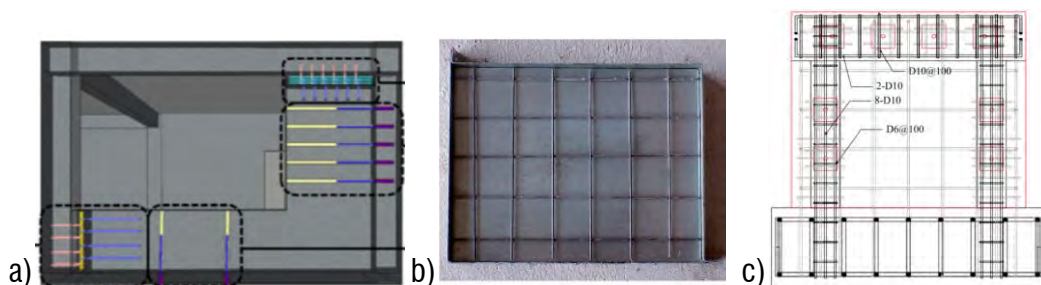

Fig. 3.2-3 – Prefabricated solution for the existing building strengthening: a) Ha, Yu and Kim, (2018) b) Baran and Tankut, (2011); c) Choi et al., (2020).

The panel weight is an important feature to consider since it influences the structural performance as well as the work phases in terms of ease of transport, installation and manpower required. Thus, both geometry and dimensions of the panels should be designed properly.

The literature provides many examples of panels projected to satisfy this requirement. Akin and Sezer, (2016) have investigated five different types of PC panels with the aim of detecting the effect of the panel shape on the strengthening procedure. The models proposed have been square, striped, hexagonal, double T and irregularly shaped (Figure 3.2-4). The results demonstrated that the RC frames strengthening against lateral loads was more effective with smooth or recessed panels.
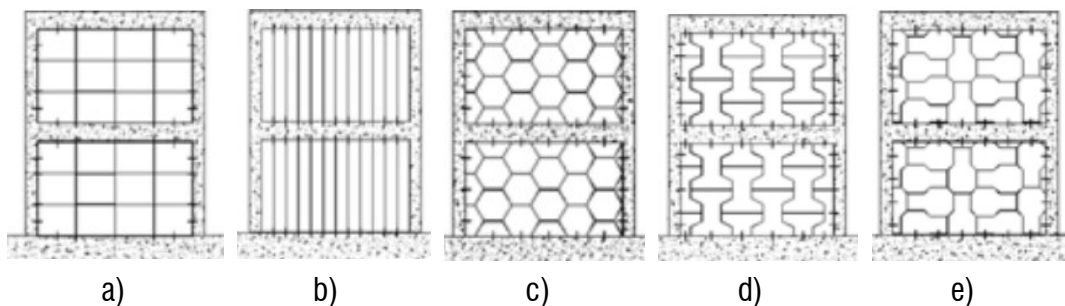

| a) | b) | c) | d) | e) |

Fig. 3.2-4 – The five different types of PC panels for the building strengthening by Akin and Sezer, (2016): a) Square type; b) Striped type; c) Hexagonal type; d) Double T type; e) Irregular shape type.

Aksoylu and Sezer, (2018) and Aksoylu and Kara, (2020) have proposed a series of PC panels combined to each other to be placed only along the cross directions of the infill walls during the earthquakes. The results demonstrated that the technique increased the capacity of the elements to energy dissipation and improved the earthquake behaviour of the whole structure.

As a result of the analysis of the scientific literature, it could be concluded that the structural protection of the existing RC buildings through PC panels is a current and developing topic. Many tests are necessary to individuate the optimum solution to be effectively applied to a real case study. The difficulty consists to assume possible scenarios and preview problems which may occur case by case, since every existing building has its own peculiarities and history.

3.3 Recycled EPS as concrete lightweight aggregate for environmentally-friendly industrial production

In recent years, the advancement of a green economy promoted by the European Commission has encouraged the industrial sectors to develop environmentally-friendly technologies and products towards innovated strategy. The attention has been paid on the re-use of the resources and lower consumption of raw materials that may lead to both environmental, social and economic benefits (Tamborelli and Furno, 2014). The Extruded Sintered Polystyrene (EPS) is an industrial material used in many fields, e.g. in building construction, packaging, food preservation, decorations, and many others. In construction, it is widely used in panels as thermal insulating layers or in beads as lightweight concrete aggregates (Ramli Sulong, Mustapa and Abdul Rashid, 2019). It replaces a volume percentage of sand in the mortar and concrete mix design to increase the volume, create voids, improve thermal and acoustic performance of the compound, reducing the self-weight loads of the structures.

To better understand the differences and advantages on using recycled EPS (rEPS) instead of virgin beads (vEPS), in what follows a brief literature review of the scientific studies about vEPS is presented. Several authors have investigated vEPS beads as lightweight aggregates of cement compound in terms of physical features (Maaroufi *et al.*, 2018; Wang, Hu and Soon, 2019), thermal insulation properties (Gomes *et al.*, 2018), concrete compressive strength, drying shrinkage, water absorption (Li, Liu and Chen, 2015), porosity (Dixit *et al.*, 2019), workability (Madandoust, Ranjbar and Yasin Mousavi, 2011), and fire resistance (Sayadi *et al.*, 2016). The hydrophobicity of the vEPS beads makes the mixture design of lightweight concretes and mortars more difficult than plain compounds due to the occurring of segregation. In the scientific literature some methods to prevent this phenomenon are provided. The use of superplasticiser additives which make the pearl surface hydrophilic and improve the cohesiveness of the mixture (Babu and Babu, 2003). Avoiding the vibratory compaction of the mixture with self-compacting concrete (You *et al.*, 2019) and the addition of further insulating or lightweight aggregates e.g. silica aerogel, silica fume, silica sand, fly ash, paper sludge ash,

magnesia phosphate, quartz powder, polycarboxylate based, and others. These also improve the other characteristics.

From these studies, it is evident that the usage of virgin expanded polymeric particles in cements and mortars decreases the concrete dry density and the capacity of mechanic resistance due to the relatively high water-binder ratio. Although the properties of thermal-acoustic insulation improve due to the closely linking between dry density and thermal conductivity coefficient.

The calculation of the amount of vEPS beads in the mixture, then the dry density, depends on the intended uses: structural or non-structural. They are distinguished in accordance with the American Concrete Institute which establishes 800 kg/m^3 as a density threshold value for structural and non-structural use (American Concrete Institute, 2013). The results of scientific research provide dry density values of structural lightweight concrete and mortars varying from 1000 kg/m^3 to 2045 kg/m^3 corresponding to thermal conductivity and compressive strength values of 0.38 – 1.69W/mK and 3 - 94 MPa. For non-structural compounds, the dry density supplied is 200 - 800 kg/m^3 with thermal conductivity values of 0.06 – 0.28 W/mK and compressive strength capacity of 0.69 – 2.5 MPa. Table 3.3-1 summarizes these data.

Table 3.3-1. Types of compound with lightweight aggregates in virgin EPS

COMPOUND USE	DENSITY	THERMAL CONDUCTIVITY	COMPRESSIVE STRENGTH
	kg/m^3	W/mK	MPa
Structural	1000 - 2045	0.38 – 1.69	3 - 94
Non-structural	200 - 800	0.06 – 0.28	0.69 – 2.5

The disproportionate consumption of virgin EPS in many fields, involves the production of large quantities of waste that are often not regularly disposed, then released in nature. It remains many years without disappearing due to its characteristic of being non-biodegradable. However, if well treated, EPS has the advantage to be entirely recycled and used to realize new product without the final environmentally performance being penalised. It apports benefits in terms of economic and environmental sustainability. Indeed, from the comparison of costs between vEPS and rEPS, Tittarelli et al. have deduced that a cubic meter cost of vEPS is four times greater than the same quantity of rEPS (Tittarelli

et al., 2016). The energy directly used by the companies to transform the raw material into EPS manufactures has a high percentage on the main environmental impact indicators: Gross Energy Requirement (GER) and Global Warming Potential (GWP). The use of rEPS progressively decreases these values thanks to the reduction of virgin raw material requirements (Tamborelli and Furno, 2014).

In the latest years, rEPS has been employed as lightweight aggregate of cement mortars or concretes, though, the literature does not report many contributes about this developing theme. Nevertheless, many advantages on using rEPS have emerged. From the microstructure study of mortars with variable dimensions of rEPS beads, several authors have conveyed that at the increasing of EPS percentage, the porosity was much higher than the traditional mortar. Images from scanning electronic microscope (SEM) analysis have confirmed it and showed the porous composition of the beads (Ferrándiz, Huesca and García, 2011). This property has allowed to obtain excellent performance in terms of thermal insulation and sound absorption due to the presence of numerous air voids. Kekanović et al. have observed that the pearls had open pores surface as result of recycling process, hence, cement paste was able to close voids, prevent the particles floating and segregation. However, more water was needed in order to reach a plastic mixture with good workability (Kekanović *et al.*, 2014). It is a high advantage compared with vEPS beads. Many other researches have investigated the mortar mixing process without additional treatment of the rEPS, gaining the same benefit (Bedeković *et al.*, 2019; Petrella, Di Mundo and Notarnicola, 2020).

However, the use of air-entraining agent, water retainer and superplasticizer additives have been investigated with the aim to prove the effect on the mortars. Many researchers have observed that these products promoted the bond between the light aggregate and the cement matrix, improved the mortar durability and permitted using more quantity of rEPS.

Nevertheless, the overuse of lightweight beads provoked the reduction of mechanical resistance (Bedeković *et al.*, 2019). Only in additivated mortars a minimal improvement percentage of flexural strength have been detected.

Further studies have deepened the compressive strength capacity of mortars in ordinary conditions (Petrella *et al.*, 2014) and also subjected to heat and freeze–thaw cycles. Mortars subjected to heat cycles have showed a slight capacity increase (Sancho *et al.*, 2014); those subjected to freeze–thaw cycles, likely improves have been reported thanks to the capacity of the expanded polystyrene particles to absorb part of the pressure of ice crystallization (Ferrándiz-Mas and García-Alcocel, 2012, 2013). Other advantages emerged from the stress–strain curves evaluation performed by Chen and Liu, in which EPS foamed concrete appeared ductile and capable of retaining the load after ultimate stress. Furthermore, high energy absorption capacity under compressive load have been measured (Chen and Liu, 2013).

Several authors have investigated lightweight mortars with rEPS as thermal point of view. From the comparison of the same dosage of vEPS, Tittarelli et al. have observed that thermal insulation performance of the mortars with rEPS decreased. However, the addition of hydrophobic admixtures, recovered this penalization due to the increasing in cement porosity (Tittarelli *et al.*, 2016). In order to improve this property, many researchers have investigated other materials to be added to the mix design e.g. lime (Aciu *et al.*, 2015), ceramic shell fragments (G. de Moraes *et al.*, 2019), mineral fill material (Bedeković *et al.*, 2019), brick rubble (Mercader-Moyano, Yajnes and Caruso, 2016), paper sludge ash (Ferrándiz-Mas *et al.*, 2014).

In the table 3.3-2 main literature studies on mortars with rEPS beads are compared. From it emerged that the mortars with high dry density values, designed for structural use, reached good compressive strength performance at the expense of thermal insulation capacity. The mortars for non-structural use, with dry density up to 300 kg/m^3, achieved thermal conductivity values no less than 0.06 W/mK.

Table 3.3-2. Lightweight concretes and mortars with rEPS in the literature

References	%vol REPS	Other Materials	Additives	Water/Binder Ratio	Dry Density [Kg/m³]	Thermal Conductivity [W/mK]	Compressive Strength [MPa]
(Ferrándiz-Mas and García-Alcocel, 2012, 2013)	0÷70	- CEM I 52,5R - Silica sand	- Air entraining - Water retainer - Superplasticizer	n/d	n/d	n/d	26.8÷13.9
(Ferrándiz-Mas et al., 2014)	60	- CEM II/A-L 32.5R - Silica sand - Paper sludge ash	- Air entraining - Water retainer - Superplasticizer	0.60÷1.30	1210÷880	0.65÷0.4	4÷0.2
(Kekanović et al., 2014)	66	- CEM II/B-M 32.5R - Sand Moravac - Polypropylene fibers	n/a	0.65	1090	n/d	5.67
(Sancho et al., 2014)	10-30	- CEM II/B-M 32.5N - River sand	n/d	0.43	1824.5-1640	n/d	17.53÷3.46
(Aciu et al., 2015)	50	- Portland cement 42.5 - Lime - Sand	n/d	0.65÷0.75	1291÷217.5	0.32÷0.064	13.35÷0.19
(Tittarelli et al., 2016)	33÷100	- CEM II/A-L 42.5R - Calcareous sand	- Air entraining - Water retainer	0.55	1900÷600	1.18÷0.1	21÷0.8
(Mercader-Moyano, Yajnes and Caruso, 2016)	n/d	- Portland cement - Sand - Rubble	Superplasticizer	0.50÷0.60	1300÷300	0.35÷0.09	n/d
(Maaroufi et al., 2018)	n/d	- Portland cement	n/d	0.32	n/d	0.142	4
(Pavlu et al., 2019)	0÷100	- CEM I 42.5R - Recycled masonry	n/d	0.50	2305÷1561	n/d	47.99÷12.65
(G. de Moraes et al., 2019)	10÷70	- Ceramic shell fragments	Sodium silicate solution	n/d	n/d	0.061	5.4
(Bedeković et al., 2019)	n/d	- CEM II/A-M 42.5N - Sand	n/a	0.55	915÷360	n/d	2.53÷0.38
(Mohammed and Aayeel, 2020)	15÷60	- CEM I - River sand - Natural coarse	Superplasticizer	0.32÷0.43	2129÷1732	n/d	n/d
(Petrella, Di Mundo and Notarnicola, 2020)	25-50	- CEM II/A-LL 42.5R - Sand	n/a	0.50	1320÷1850	0.80÷0.29	33÷8

3.4 Prefabrication process by Ferramati International s.r.l.

Ferramati International s.r.l., the Italian partner enterprise of this PhD project, is specialized in supplying and installing of materials for civil and industrial constructions, especially in the production of PC elements in RC, virgin and recycled EPS beads and artifacts, in processing and assembling steel rebars for concrete works.

It is located in Fasano (BR), in Apulia region in the south of Italy. Its facilities covers an area of almost 25000 m^2 and it is divided into seven industrial establishments and hubs, each aimed at the production, storing and testing of individual manufacture.

In the hypothesis of following the Ferramati production chain, consolidated for years, the analysis of its products, especially the PC slabs, is necessary to understand the novel project parents and fix the starting point.

3.4.1 Precast concrete products

Ferramati produces essentially four typologies of PC slabs that may be employed as load-bearing walls, floor components and retaining walls: single RC slab for floors (Figure 3.4-1 a, b), single RC slab for wall (Figure 3.4-1 c), double layered RC slab for walls (Figure 3.4-2 a), double layered RC slab HPwalls (high performance wall system, Figure 3.4-2 b), and double layered RC slab for retaining walls (Figure 3.4-2 c). The RC slabs generally contain an electro-welded mesh and lattices, placed at mutual distance of 60 cm for floors and 40 cm for walls. At the customer's request, the RC slabs used for floors may include EPS blocks as lightweight elements, placed on fresh concrete during the production. It is completed on site with the top reinforcement net and concrete casting, as for the double RC walls.

The latest Ferramati's product, born in collaboration with the Polytechnic University of Bari, is HPwalls, a double RC slab wall which integrates two external insulating layers in EPS. It has very high thermo-hygrometric, acoustic, and structural characteristics.
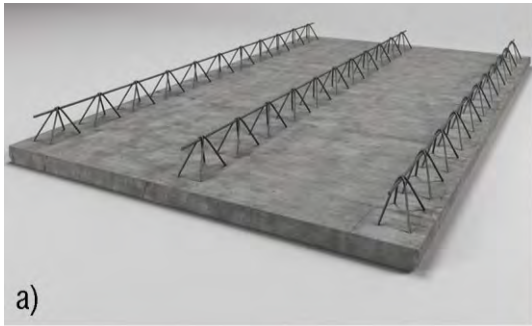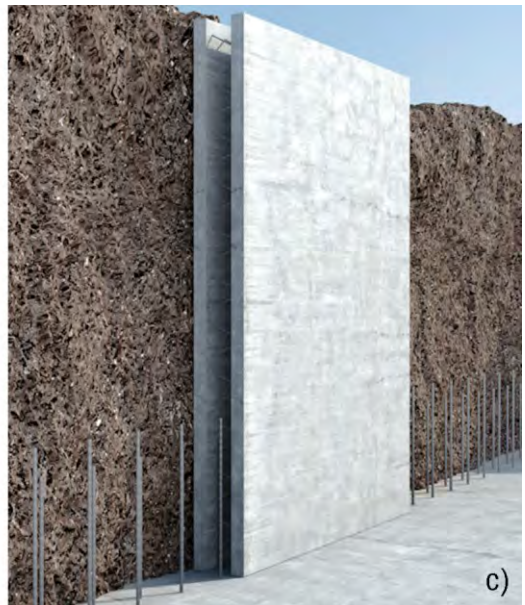
Fig. 3.4-1 - Single RC slab: a) for floors; b) for floors with lightened blocks; c) for walls. Source: http://www.ferramati.it/web/en/prodotti/single-layered/ (Accessed November 10, 2020)

Fig. 3.4-2 - Double layered RC slab: a) for walls; b) HPwalls (with two external layers in EPS); c) for retaining walls. Source: http://www.ferramati.it/web/en/prodotti/double-layered/ (Accessed November 10, 2020)

The first phase of the production process is the analysis of the structural, morphological, and geometric characteristics of the project commissioned to the technical study. In particular, the client provides the structural carpentry scheme of the building and the numerical data by the designer. Ferramati implements a prefabrication tailored to the customer's dimensional needs. Hence, it can realize elements of any shape and size. Thanks to the software "Allplan Prefabricated" which CAD interface allows visualizing design scheme on 2D and 3D views, the design and production phases are easily managed. It permits selecting the PC element to be applied to the building and design the arrangement scheme to be sent into production.

The detailed tables of the designed products and those to be assigned to the production workers, are drawn. The data for the numerical control of the plant in the production establishment are defined and the disposition of the elements on the production trays are planned. The modules are arranged according to the storage and transport order.

The plant used for the production the PC modules is the automated carousel system in Figure 3.4-3. It is composed of 37 metal formworks with a useful size of 13.50 x 2.50 m that translate in series according to a continuous circle, occupying the different locations on which the subsequent processing on the artifacts are carried out.

Fig. 3.4-3 - The prefabrication plant: the automated carousel system. Source: Ferramati International s.r.l.

The production phase begins with the cleaning of metal formwork through the brushing machine and the spreading of the disarming liquid through the atomizing oil machine. Then, the formwork moves to the next location where the plotter-robot traces the bulk of the panels and places the banks stop jet magnet. If the design scheme requires particular holes or shapes, the operator inserts additional jet stops manually, also with EPS blocks. At this stage, the electro-welded wire mesh and lattices, the slab steel reinforcement, are disposed in the framework (Figure 3.4-4 a). The lattice position on the plate, thus the size of the steel cover, varies according to the design exposition class to external agents and fire class (Figure 3.4-4 b). The operator performs the concrete casting by means the dosing machine that allows to spread the concrete in a homogeneous and measured way up to the required thickness (Figure 3.4-4 c). The concrete dosing machine is directly connected to the batching plant, which produce continuously the concrete based on the materials amount the project requires. The area of the dosing machine is integrated by equipment for the automatic vibration of the formworks with the aim of filling all the voids within the section and distributing the dough homogeneously in the formwork.
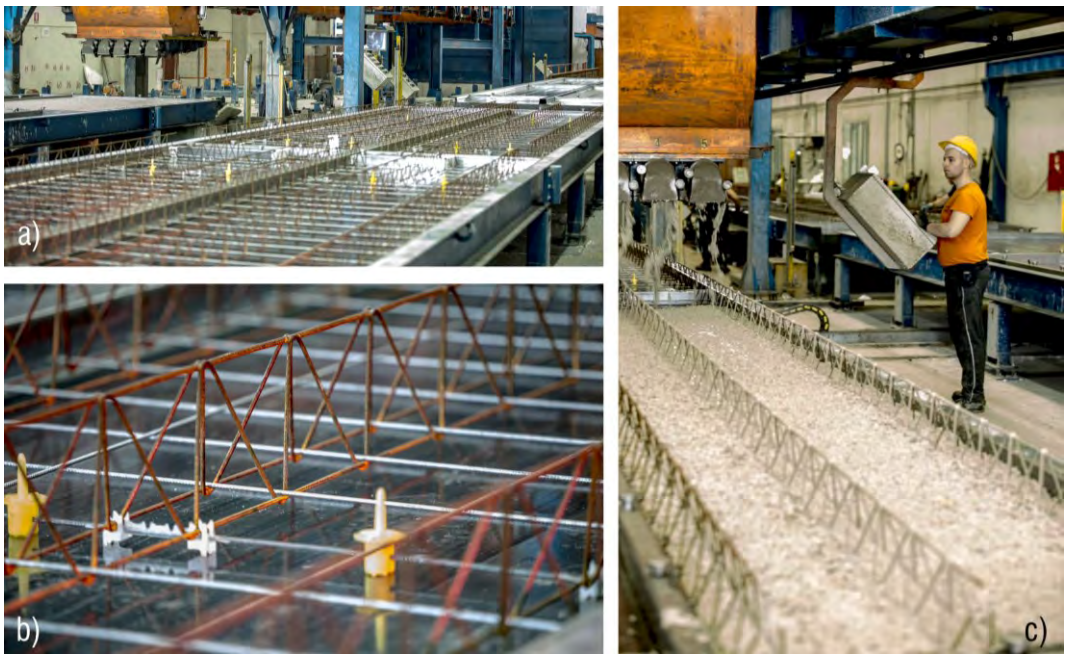

Fig. 3.4-4 - The production phases: a) steel reinforcement disposition; b) steel cover control; c) concrete casting. Source: Ferramati International s.r.l.

The plant transports the formwork to the storage tower for the maturation of the artifacts. The tower is composed by three contiguous compartments divided into ten levels and maintained at a constant temperature of 15° C. The next day, if the tray contains single slabs, it goes from the tower to the area where the slabs are moved off the framework by means of pliers connected to a crane and transported to the storage area using fork-lifts. On the other hand, if the formwork contains double slabs, it leaves the maturation tower backwards to reach the area destined to the overturning on the formwork in which the casting of the second slab has already been carried out. After aligned the two opposite PC modules, the entire system is vibrated to ensure that the lattices are evenly immersed in the fresh concrete of the second RC slab. Then, the formwork goes again in the storage tower for the second maturation day.

3.4.2   Expanded Polystyrene Sintered

Ferramati is also specialized in production of building components in EPS deriving from the raw material processing, stamping and block shaping, performed directly in its EPS establishment. It includes all the machineries devoted to the production stages of pre-exposure, maturation, moulding and cutting.

Briefly, the growth of the EPS production process is reported to understand the differences and the characteristics of the EPS products with different densities, according to the Italian association of expanded polystyrene (AIPE).

It starts from the arrival of the raw material in Polystyrene (PS) in the factory in the form of glass-looking beads, with a particle size ranging from 0.2 mm for high density products and 3.6 mm for low density. Pre-addicted with pentane, a hydrocarbon used as an expanding agent, the PS beads are loaded into the pre-expander machine. The pentane vaporizes by means of water vapour at temperatures between 80°C and 110°C, allowing the pearls to swell up to 50 times the initial volume. The expansion time depends on the required density for the specific uses. The physical structure of the EPS beads, at all densities, is at closed cells. The next step is decanting or maturing in aerated silos that allow the cooling of the expanded structure, mechanically unstable due to the presence of expansive and condensate residues. The conveyance from the pre-expander to the

silos is carried out by ducting pipes. After the maturing time, the spheres undergo sintering or the transformation of the loose material into blocks (AIPE, 2017). In Figure 3.4-5 the Ferramati's EPS production plant is illustrated.

Fig. 3.4-5 - Ferramati's EPS production plant. Source: Ferramati International s.r.l.

All products comply with the regulations EN 13163:2017. EPS products have density varying from 10 to 30 kg/m^3 (EPS30 – EPS200) from which depend the physical and thermal insulation characteristics. Low density EPS panels have lower performance than the high density ones. They contain large beads due to the longer expansion time. The amount of them is less than in high density products that contain smaller and thickened spheres. In the Figure 3.4-6 the declared characteristics of EPS products by Ferramati technical sheet is reported.

CARATTERISTICHE	CODICE UNI EN 13163	U.M.	EPS 30 (CE)	EPS 80 (CE)	EPS 100 (CE)	EPS 120 (CE)	EPS 150 (CE)	EPS 200 (CE)	Norma di prova
Conducibilità Termica Dichiarata	λ_d	W/m k	0,040	0,036	0,036	0,034	0,033	0,033	EN 12667
Resistenza Termica Dichiarata	R_d								
Spessore mm 30	R_d	m^{2}K/W	0,75	0,83	0,83	0,88	0,91	0,91	EN 12667
Spessore mm 40	R_d	m^{2}K/W	1,00	1,11	1,11	1,18	1,21	1,21	EN 12667
Spessore mm 50	R_d	m^{2}K/W	1,25	1,39	1,39	1,47	1,52	1,52	EN 12667
Spessore mm 60	R_d	m^{2}K/W	1,50	1,67	1,67	1,76	1,82	1,82	EN 12667
Spessore mm 70	R_d	m^{2}K/W	1,75	1,94	1,94	2,06	2,12	2,12	EN 12667
Spessore mm 80	R_d	m^{2}K/W	2,00	2,22	2,22	2,35	2,42	2,42	EN 12667
Spessore mm 90	R_d	m^{2}K/W	2,25	2,50	2,50	2,65	2,73	2,73	EN 12667
Spessore mm 100	R_d	m^{2}K/W	2,50	2,78	2,78	2,94	3,03	3,03	EN 12667
Spessore mm 110	R_d	m^{2}K/W	2,75	3,06	3,06	3,24	3,33	3,33	EN 12667
Spessore mm 120	R_d	m^{2}K/W	3,00	3,33	3,33	3,53	3,64	3,64	EN 12667
Lunghezza	L2	mm	±2	±2	±2	±2	±2	±2	EN 822
Larghezza	W2	mm	±2	±2	±2	±2	±2	±2	EN 822
Spessore	T2	mm	±1	±1	±1	±1	±1	±1	EN 823
Ortogonalità	S2	mm/m	±2/1000	±2/1000	±2/1000	±2/1000	±2/1000	±2/1000	EN 824
Planarità	P3	mm	±10	±10	±10	±10	±10	±10	EN 825
Stabilità dimensionale	DS (N)	%	±0,2	±0,2	±0,2	±0,2	±0,2	±0,2	EN 1603
Reazione al Fuoco	Euroclas		E	E	E	E	E	E	EN 13501-1
Resistenza a Compressione al 10% di deformazione	CS(10)	KPa Kg/cm^2	30 0,30	80 0,80	100 1,00	120 1,20	150 1,50	200 2,00	EN 826
Resistenza a Flessione	BS	KPa	50	125	150	170	200	250	EN 12089
Resistenza diffusione di vapore	μ_{med}	Adim	20-40	20-40	30-70	30-70	30-70	40-100	EN 12086
Permeabilità al vaopre acqueo	δ_{med}	mg/mhPa	0,018-0,036	0,018-0,036	0,010-0,024	0,010-0,024	0,010-0,024	0,007-0,018	EN 12086

Fig. 3.4-6 - Characteristics of EPS products by Ferramati. Source: Ferramati International s.r.l.

Paying attention to the environmental and economic sustainability, the establishment is also equipped with a plant devoted to the waste milling and a bagging machine for packing the resulting material. It is reintegrated into the production chain or sold as lightweight component of mortars and concretes. The waste milling permits to shatter the EPS blocks and brings them back to the beads state with a diameter varying from 2 mm and 25 mm. The amount of dust that the grinding machine produces is very low, hence, Ferramati's recycled pearls appear entire and defined. Contrary to the virgin, for the recycled EPS, the choice of the material density is difficult because in the grinder the waste is not classified by quality and density. Therefore, it may vary from about 8 kg/m^3 to 18 kg/m^3. Figure 3.4-7 compares virgin (a) and recycled EPS (b) beads by Ferramati.
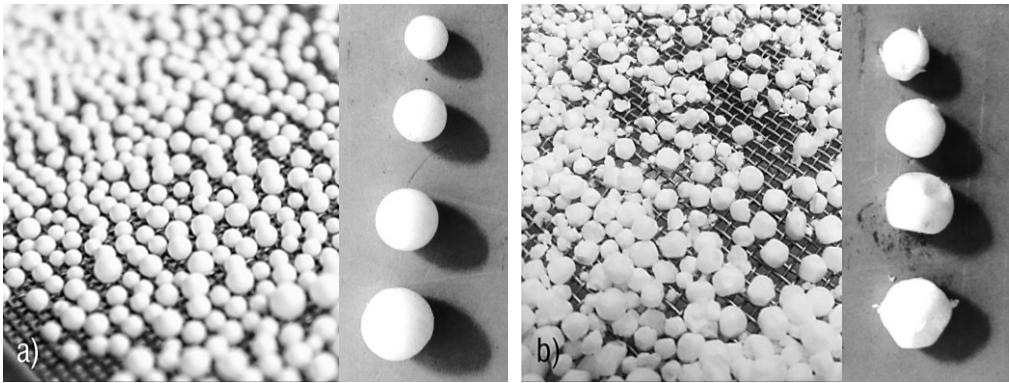
Fig. 3.4-7 - Ferramati's EPS beads: a) virgin EPS; b) recycled EPS. Source: Author

3.5 The existing building typologies and facades

The analysis of the existing buildings constructed throughout 20th century aims to individuate the widely diffused building typology with poor energy performance and technical characteristics in order to begin the project of the retrofitting system.

The first part of this section is an overall view of the European scenario in which the characteristics of the existing building stock belonging to the 27 European Member States (EU27) are compared. Then, going into the detail of the case of Italy and Spain, a more accurate classification of building façade typologies and performance is provided.

3.5.1 The European overview

The importance of building performance in the effort to mitigate climate change, defined by the EPBDs and the EED, underlines the necessity to monitor the advancements of the EU28. In particular, it is aimed at the existing building stocks which require improvements in energy performance.

Starting from the classification of the countries by climate zones carried out by EPISCOPE project (Figure 3.5-1), it is possible to better frame the results of the following studies about building typologies of the EU27 thanks to comparable climates (EPISCOPE, 2016).

Fig. 3.5-1 - *Classification of European countries by climate zones. Source: EPISCOPE, 2016*

The overall knowledge about European building stock characteristics, edge and energy performance is helpful to understand the effectiveness of national building policies under the European directives and compare the results of the EU27 with the intended values.

The recent EU's web platform called Building Stock Observatory makes this monitoring, providing consistent and comparable data according to specific topics e.g. building stock characteristics, shell performance, technical building systems, building renovation and others (The European Commission, 2020a). Concerning the study of the building typologies, the Figure 3.5-2 shows a heterogeneous classification of the floor area. The share varies considerably, though, the majority is composed by residential buildings. Italy, with 89%, has the highest value.
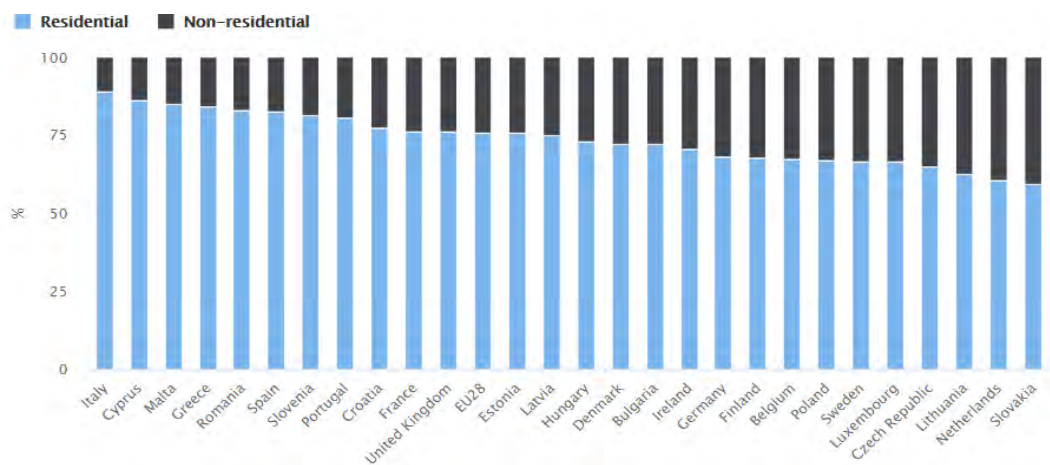
Fig. 3.5-2 - Breakdown of building floor area. Source: https://ec.europa.eu/energy/eu-buildings-factsheets_en

The data of average age of existing buildings and the new buildings share from the total stock are useful indicators to evaluate the overall building stock efficiency.

The Figure 3.5-3 shows the breakdown of residential building by construction year of the EU27, revealing that in most countries, half of the residential stock was built before 1970, thus, before the first thermal regulations. Indeed, from the EU Building Database the thermal transmittance values (U-value) of the external walls of the EU27's residential buildings, updated to 2017 and referred to constructions built before 1945 and between 1945 and 1969 are very high and equal to 2.18 W/m^2K and 1.86 W/m^2K, respectively (The European Commission, 2020b).
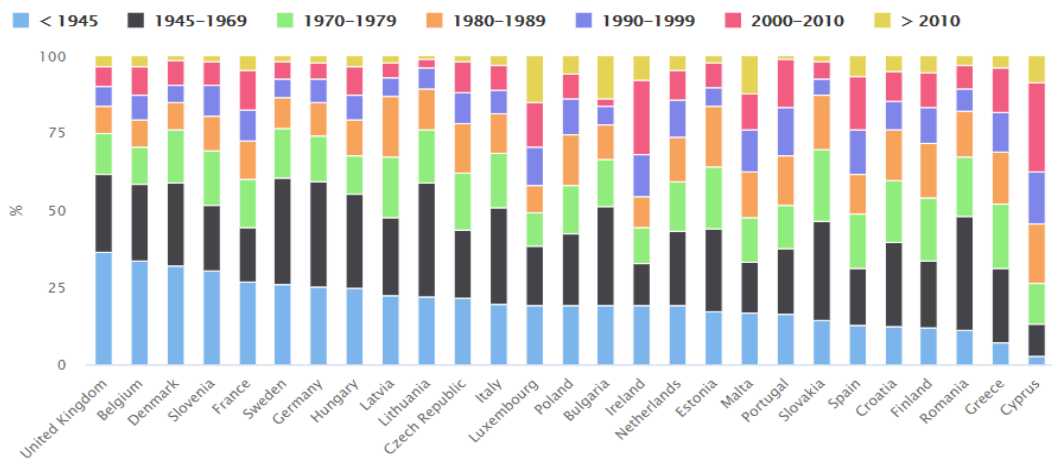
Fig. 3.5-3 - Breakdown of residential building by construction year. Source: https://ec.europa.eu/energy/eu-buildings-factsheets_en

The knowledge of the building typologies is central to draw an accurate portrait of the EU building stock. Since different insulation characteristics imply specific heating consumption for the contact surface with the outdoors, the dwelling types have a great impact on heating energy performance. Figure 3.5-4 permits comprehending the distribution of the two main typologies of residential buildings in EU27. It differs significantly across the EU: in Ireland and United Kingdom the dominant type is single-family dwelling with a percent value of almost 80%, while in Italy and Spain, the percentage is inverted i.e. multi-family dwellings represent more than 70% of all buildings. The EU average value is almost 49% for multi-family dwellings.
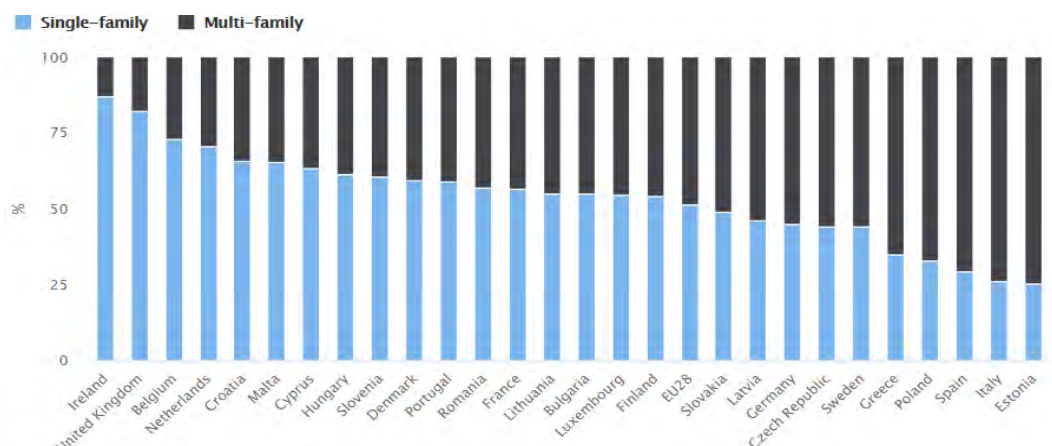
Fig. 3.5-4 - Distribution of multi and single-family residential buildings in EU27. Source: https://ec.europa.eu/energy/eu-buildings-factsheets_en

3.5.2 The case of Italy

Starting from the study of the Italian territory from the climate point of view, six climate zones (from A to F), are identified in function of the degree-days (DD), according to the Republic President Decree n. 412/1993 and 74/2013. The degree-days are parameters that quantify the average thermal requirement necessary to maintain an indoor comfortable climate during the year in a specific location. Zone A needs less heating energy than zone F. They are calculated as the sum of the daily positive differences between the indoor conventional temperature and the average outdoor daily temperature of the annual heating period (Italian Decree, 1993).

For each climate zone, Annex B of the Italian Ministerial Decree of 06/26/2015 and its further updates establishes the maximum limit U-values the walls should have in case of building renovations (Ministerial Decree, 2015). Table 3.5-1 shows the classification of the Italian territory by climate zones, associating to each the limit U-values.

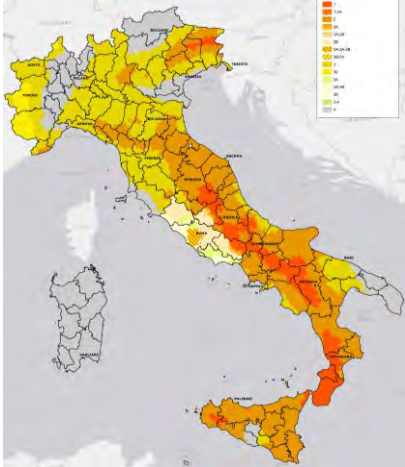**Table 3.5-1.** Classification of Italian territory by climate zones according to the DD

GEOGRAPHICAL DISTRIBUTION	CLIMATE ZONE	DD	LIMIT U-VALUES
	A	$DD \leq 600$	0.40 W/(m²K)
	B	$600 < DD \leq 900$	0.40 W/(m²K)
	C	$900 < DD \leq 1400$	0.36 W/(m²K)
	D	$1400 < DD \leq 2100$	0.32 W/(m²K)
	E	$2100 < DD \leq 3000$	0.28 W/(m²K)
	F	$DD > 3000$	0.26 W/(m²K)

Source: http://venetiangeostatistics.altervista.org/ (Accessed November 07, 2020)

As concern the seismic hazard, according to the Ordinance of the President of the Ministers Council n. 3519/2006, Italy is divided in four seismic zones, from the most dangerous (zone 1) in which the probability that a strong earthquake occurs is high, to the less dangerous (zone 4) in which the probability is very low. The reference ranges

associated to each zone are the values of the peak acceleration on hard ground (Consiglio dei Ministri, 2006) (Table 3.5-2).

Table 3.5-2. Classification of Italian territory by hazard seismic zones

GEOGRAPHICAL DISTRIBUTION	SEISMIC ZONES	ACCELERATION (AG) $[m/s^2]$
	1	$AG > 0.25$
	2	$0.15 < AG \leq 0.25$
	3	$0.05 < AG \leq 0.15$
	4	$AG \leq 0.05$

Source: http://www.protezionecivile.gov.it/attivita-rischi/rischio-sismico/attivita/classificazione-sismica (Accessed November 07, 2020)

The study of the Italian existing building stock is carried out in accordance with the TABULA Italian database inserted into the general EPISCOPE Project that aims to analyse the energy performance of the existing buildings to quantify the starting point for their energy renovation.

The evaluation of building energy efficiency is performed considering three different parameters that permit to identify the existing building typologies and define their performance: climate zone, construction age and dimension (Ballarini *et al.*, 2011).

As regard the parameters of construction age and dimension, TABULA distinguishes eight epoch classes that cover a time period between 1900 and 2005, and four-dimensional types, i.e. single-family houses (SFH), terraced houses (TH), multi-family houses (MFH), and apartment blocks (AB). It elaborates a "building-typology 8x4 matrix" in which the columns are the four building types by dimension and the rows are the eight construction epoch classes (Table 3.5-3) (Corrado, Ballarini and Corgnati, 2014).
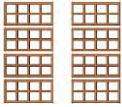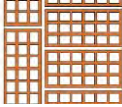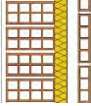
Table 3.5-3. Italian "building-typology matrix"
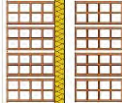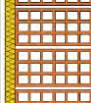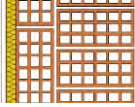
BUILDING AGE CLASS		BUILDING SIZE CLASS			
		SINGLE-FAMILY HOUSES	TERRACED HOUSES	MULTI-FAMILY HOUSES	APARTMENT BLOCKS
Up to 1900	I				
1901-1920	II				
1921-1945	III				
1946-1960	IV				
1961-1975	V				
1976-1990	VI				
1991-2005	VII				
After 2005	VIII				

Source: Corrado V, Ballarini I, Corgnati SP. Building Typology Brochure

The classification of the widely diffused facades and their U-values is performed in compliance with TABULA project and the technical regulations in force in the eight construction periods defined above. Since the proposed technological system intends to retrofit the existing RC buildings, among all, the facades in hollow bricks are considered (Table 3.5-4) (Martiradonna, Fatiguso and Lombillo, 2020).

Table 3.5-4. Façade typologies in hollow bricks mainly diffused in Italy and their U-value

FACADE TYPOLOGY	SECTION	THICKNESS	MAIN DIFFUSION PERIOD	U-VALUE
	[Indoor/Outdoor]	[cm]	[years]	[W/(m²K)]
Double hollow brick wall with air chamber		30	1930-1975	1.09

Double hollow brick wall with air chamber		40	1930-1975	0.96
Hollow brick wall		30	1950-1975	1.25
Double hollow brick wall		40	1950-1975	1.05
Double hollow brick wall with air chamber and low level of insulation		30	1976-1990	0.66
Double hollow brick wall with air chamber and low level of insulation		40	1976-1990	0.64
Hollow brick wall with low indoor level of insulation		25	1976-1990	0.69
Double hollow brick wall with low indoor level of insulation		40	1976-1990	0.60

Source: Martiradonna, Fatiguso, and Lombillo (2020). Thermal improvements of existing reinforced concrete buildings by an Innovative Precast Concrete Panel system

The façade typologies in hollow brick which present less performing thermal characteristics belong to the period between 1930 and 1975, when, in Italy, any legislation considered the quality of materials and building thermal behaviour. In particular, in the years between 1950 and 1975, better identified as post-World War II (WW2), the energy performance of buildings worsens due to the haste of the government to rebuild the cities, destroyed during the War.

3.5.3   The case of Spain

Italy and Spain are comparable countries under several aspects i.e. climate, building typologies, architecture, energy policies and others. Assuming that the technical proposal may be used for renovating the buildings located into the same climate area, the design

criteria should take in account also the studies of Spanish territory and its existing building stock. The methodological study phases used for Italy are also valid for Spain. Therefore, it starts from surveying the Spanish territory from the climate point of view. Spain has a very disparate climate due to its geographical location, the presence of the Mediterranean Sea and the Atlantic Ocean. It is divided into twelve climatic zones as the combination of the letters from A to E and numbers from 1 to 4. The letters represent the winter weather severity (SCI), instead, the numbers the summer weather severity (SCV). The climatic severity combines the degree-days and the solar radiation e.g. if two locations have the same SCI, the heating energy demand of the same building in both places is equal (IVE, 2011). Table 3.5-5 shows the geographical distribution of the 12 climatic zones in shadows of colours according to the combinations of the 5 SCI and 4 SCV. Moreover, the limit U-values for walls in contact with the outdoor temperatures in winter climatic zones, are specified (Ministerio de Fomento, 2019).

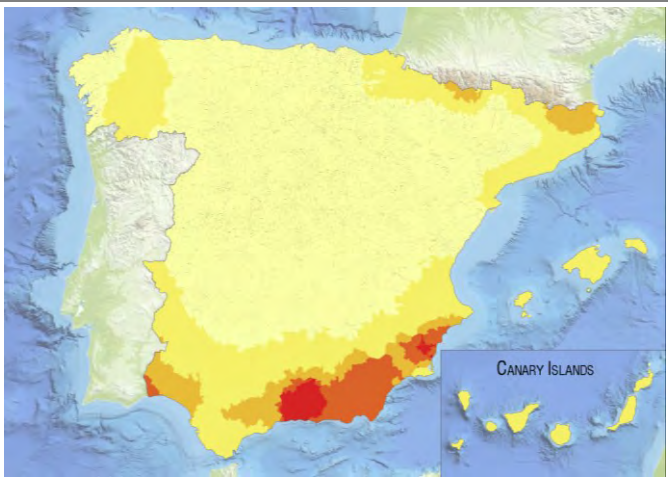**Table 3.5-5.** Classification of Spanish territory by climate zones

GEOGRAPHICAL DISTRIBUTION		CLIMATE ZONES				
			C1	D1	E1	**1** $SCV \leq 0.6$
			C2	D2		**2** $0.6 < SCV \leq 0.9$
		A3	B3	C3	D3	**3** $0.9 < SCV \leq 1.25$
		A4	B4	C4		**4** $SCV > 1.25$
		A	B	C	D	E
		$SCI \leq 0.3$	$0.3 < SCI \leq 0.6$	$0.6 < SCI \leq 0.95$	$0.95 < SCI \leq 1.3$	$SCI > 1.3$

CANARY ISLANDS

LIMIT U-VALUES	A	B	C	D	E
	0.70 W/(m²K)	0.56 W/(m²K)	0.49 W/(m²K)	0.41 W/(m²K)	0.37 W/(m²K)

Source: https://www.construmatica.com/construpedia/España:_Zonas_Climáticas_por_Provincia (Accessed November 07, 2020)

Concerning the seismic hazard in Spain, the regulation for seismic-resistant construction divides the territory into five seismic zones in function of the basic values of the ground

horizontal acceleration (AB*) and gravity acceleration (g) (Ministerio de Fomento, 2009). From the geographical division by seismic zones, showed in table 3.5-6, it is observed that most of the Spanish territory is classified as a zone with very low seismic risk, however some southern zones may reach very high seismic acceleration values.

Table 3.5-6. Classification of Spanish territory by hazard seismic zones

GEOGRAPHICAL DISTRIBUTION	SEISMIC ZONES	ACCELERATION (AB)
	1	$AG \geq 0.16g$
	2	$0.12g \leq AG < 0.16g$
	3	$0.08g \leq AG < 0.12g$
	4	$0.04g \leq AG < 0.08g$
	5	$AG < 0.04g$

Source: https://www.geamap.com/it/sismologia-espana (Accessed November 07, 2020)

The study of the Spanish existing building stock is carried out in accordance with the TABULA Spanish database inserted into the general EPISCOPE Project. To simplify the classification of the existing building typologies in function of climate, the subdivision into three macro zones by the SPAHOUSEC project is took in account. They are distinguished in function of the average minimum, half and maximum temperatures, region geographic location and seas: Atlantic, Continental, and Mediterranean climate (IDAE, 2016). To make a comparison between Spain and Italy, the building typologies of the Mediterranean climate zone by Spanish TABULA database is considered. Hence, the "building-typology 6x4 matrix" follows (table 3.5-7). The rows are the six building age classes, going from before 1900 to after 2007, and the columns are the four building size classes: SFH, TH, MFH, AB (García-Prieto Ruiz, Serrano Lanzarote and Ortega Madrigal, 2016).

Table 3.5-7. Spanish "building-typology matrix" of the Mediterranean climate zone

BUILDING AGE CLASS		BUILDING SIZE CLASS			
		SINGLE-FAMILY HOUSES	TERRACED HOUSES	MULTI-FAMILY HOUSES	APARTMENT BLOCKS
Up to 1900	I				
1901-1936	II				
1937-1959	III				
1960-1979	IV				
1980-2006	V				
After 2007	VI				

Source: García-Prieto Ruiz, Serrano Lanzarote, and Ortega Madrigal. Catálogo de tipología edificatoria residencial Ámbito: España

In Spain, the most diffused construction methodology is the load-bearing brick masonry, used until 1940, despite the widespread use of RC buildings in Europe. Between 1940 and 1960, the post-Civil War buildings are in RC and filling walls in solid bricks or hollow bricks. The spacing between the pillars is limited and the overall dimensions are reduced. The wall average thermal transmittance for these buildings is 3.03 W/m^{2}K. From 1960, the building dimensions grow, and the infill walls are composed by two brick layers interposed by an air cavity (U-value=1.43 W/m^{2}K). With the first energy technical code in 1979 (NBE CT-79), the insulating layer appears into the air cavity, although, a more economic hollow brick is used (U-value=1.33 W/m^{2}K) (García-Prieto Ruiz, Serrano Lanzarote and Ortega Madrigal, 2016).

4 STRATEGICAL DESIGN PROCESS

According to the general methodology provided in section 2.1, this chapter is devoted to deepen the *Design Stage* aiming at describing the strategical process to develop the innovative technology for the existing RC buildings retrofitting.

Thanks to the critical analysis of the state-of-the-art regarding the prefabricated elements, lightweight compounds, and industrial processes by Ferramati Int., in the first section of this chapter (4.1), the specific goals of the project with the related design criteria are established. In the section 4.2, the boundary conditions, the building typology and the façade for which performing the system design, are specified, deriving from the review of the building characteristics carried out in the previous section.

In the section 4.3, the technological proposal is described with the illustration of the final design concept derived from the approval by the technical team of Ferramati International. Hence, the study of the system portions is carried out. It is articulated according to the deepening of three scales of detail: *Material, Component,* and *System*.

At *Material scale* the experimental phases about mortar with light aggregates in rEPS are outlined (section 4.4) aiming at characterizing the most performant mixture to use as insulating layer of the PC panel. Hence, starting from these results, at *Component scale* the design of the panel layers is carried out (section 4.5). Assuming that the sum of more panels generates the external layer of the system, at the *System scale,* the connection, reinforcement and completing technology are designed (section 4.6) in relation with the building typology chosen in the section 4.2. Finally, the approaches to preliminarily assess the thermal and structural system behaviour are presented.

4.1 Design goals

The proposal of the innovative PC panel system dedicated to the retrofit of existing RC buildings arises from the need to find a solution that improves, at the same time, the building thermal protection, the structural safety, and monitoring the building performance over time. The project goals related to the specific criteria derived from the literature review are specified in the Figure 4.1-1.
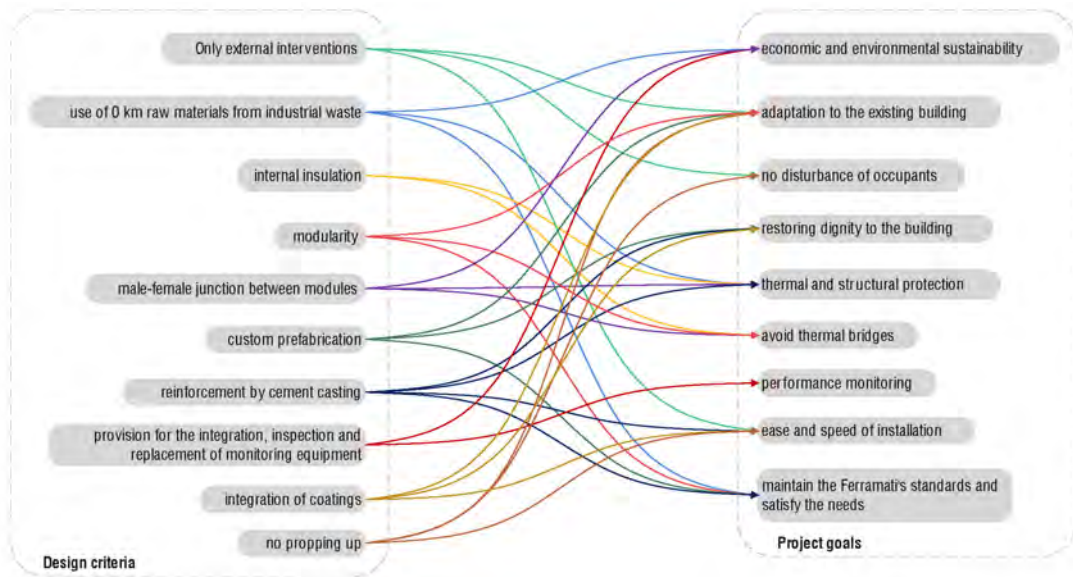

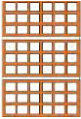**Fig. 4.1-1 -** Design criteria and Project goals. Source: Author

The figure above may be translated into the following provisions. The application of novel technology has to be performed only at the external side of the building façade through the implementation of PC panels, containing recycled materials. The junctions among the panels have to be according to the male-female configuration to avoid the generation of thermal bridges and optimize the thermal protection of the building. They can integrate the external cladding, to restore aesthetic dignity to the building and speed up the installation phases. The connection between the panels and the façade has to be ensured by elements that avoid the use of props in order to minimize the occupant disturbance. The completion technology that assures the connection and the building stiffening has to be in concrete according to the Ferramati's practice. Finally, to achieve the goal of building

monitoring, the system has to contain elements to place and inspect any time, devices to control the trends of performance.

4.2 Boundary conditions

In the light of the studies on climatic and seismic hazard, this section outlines the boundary conditions for the development of the technological system project devoted to the existing RC building retrofitting. They are summarised in the Table 4.2-1.

Table 4.2-1. The boundary conditions for the project of the novel technological system

Italian Region | District	Climate zone	Seismic zone	Building typology	Facade typology	Section	U-Value
Apulia | Bari	C - DD=1185 - limit U-value= 0.36 W/(m²K)	3 0.05<AG≤0.15	MFH	- Hollow brick wall - Thickness 30 cm - Post-WW2		1.25 W/(m²K)

Source: the Author

The average conditions of temperature (T) and relative humidity (RH) to consider for carrying out the thermo-hygrometric studies are defined as follows:

- indoor conditions, corresponding to the ideal comfortable values, are T 293.15 K and RH 52%.
- outdoor conditions are T 281.55 K and RH 68%. The data are selected from Bari Karol Wojtyla weather station, Italy (WMO: 162700) by ASHRAE Climatic Design Conditions 2003/2013/2017. The mean values from the table of "Monthly Climatic Design Conditions in 2017" are considered, in particular, in February, the coldest month of the year. Despite in the referred month lower peak values of T and RH occur, the design criteria of the analyses are the mean values.

The choice of MFH typology of the post-WW2, in particular the economic-popular buildings (EPBs), is purposed by different factors. In the literature review, great deficiencies in terms of thermal and structural performance of this building category appear. Being the widespread typology in Italy and in many other countries, as illustrated in the Figure 3.5-4, they are responsible of a great energy consumption and endanger the health of citizens. Moreover, they have a very simple shape, and their constructive and technical

characteristics are approximately the same in the European countries with similar climate conditions such as Italy and Spain. Normally, they are in peripheral areas outside the city centre, along wide roads that allow the ease transit of heavy vehicles. In fact, an important requirement for the installation of prefabricated modules is the sufficient space for handling the panels and assembling the necessary equipment to perform the work in safety. The external RC frame usually stay along the perimeter of the building to anchor and link the existing structure to the modules.

In the southern Italy, EPBs may present balconies or lodges that embody physical impediments to the system uniform application and also may be supported on pilotis (supports that lift a building above the ground). Therefore, the project of the PC panel system considers the hypothesis of integrating typical retrofit techniques in specific building portions to obviate the problem of the balconies and lodges, and double-PC panel walls in the space between the external pillars to close the building ground floor.

Finally, it is assumed that, improving the less performing building façade with the proposed system, thus, complying with the national codes, similar existing buildings in the same boundary condition, with better thermal characteristics, may be improved too. However, for those buildings, a specific project is necessary.

4.3   Design concept

The proposal of the novel technology, in accordance with the specific goals and criteria established from the literature review, has been presented to the technical team by Ferramati Int. that approved and apported improvements to the solution until the final configuration. Therefore, the novel technology has been named "Intelligent PC panel system". It redefines the concept of the double layered RC slab for walls used by Ferramati for new constructions. It is configured as a double slab system in which the external layer is an innovative PC panel, instead the internal one is the existing building façade. The connections between the two layers are ensured by steel anchors and reinforcements directly installed on the existing RC frame which remain embedded in the site cast concrete. It makes the system and the existing building a unique reinforced entity. To
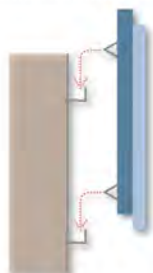
achieve the objective of building performance monitoring, the elements used to anchor the PC panels to the façade, are shaped to leave several empty spaces along the section in which inserting, inspecting, and substituting the monitoring equipment at any time. The Figure 4.3-1 illustrates the concept of the technological system design.

Materials from industrial wastes

Modular composition; male-female junctions

Rapid and easy anchoring system

Technological predisposition for placing monitoring devices

1. Existing RC building   2. Steel mullions   3. Steel reinforcement   4. PC panels   5. Cast in site concrete
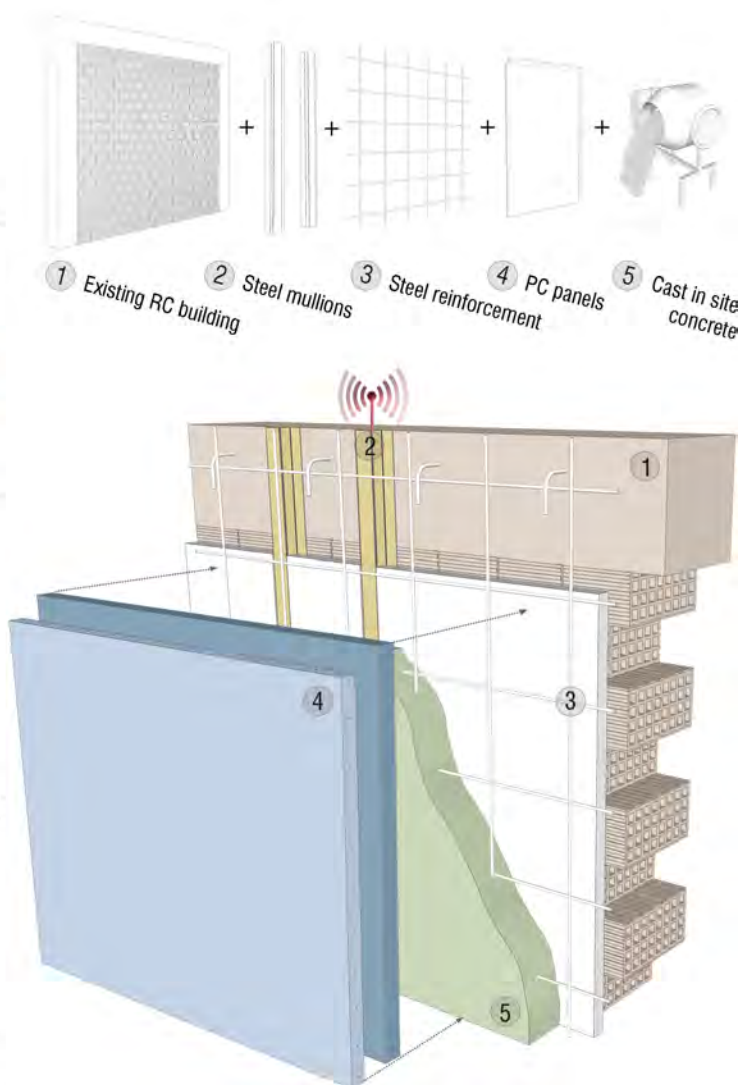
Fig. 4.3-1 - The concept of the technological system design. Source: Author

4.4 Novel lightweight mortar (LWM) with recycled EPS (rEPS)

According to the methodological subdivision of the *Design* Stage into three scales of details, this section develops the analyses at the *Material scale.*

As results of the auditing of Ferramati's needs and future perspectives, the problem of the PC modules insulation have emerged. Despite the use of high-density EPS blocks, the external insulation is damaged by the panel self-weight during its fabrication and transportation. Instead internally, the steel rebars embody geometric discontinuity which impede to insulate uniformly the module.

Therefore, the idea of the novel lightweight mortar (LWM) in rEPS is born, acting as internal non-structural thermo-insulating layer of the PC panel. Since the mortar binder is the cement, the LWM has the advantage of limiting the process of the lattice oxidation by the passivating effect of cement in contact with steel. Moreover, according to the criterion of environmental sustainability and circular economy, the LWM contains recycled EPS beads, coming from the wastes of other Ferramati's works.

To individuate the mortar with the better characteristics in terms of thermo-hygrometric insulation and workability, many samples have been produced and tested. The characteristics of mechanic resistance have been evaluated in the hypothesis of non-structural mortar. Assuming that there is a relationship between the thermal conductivity, compressive strength, and bulk density of the EPS dry mortar (EN 16025-1, 2013), the samples have been designed to have low density in order to reach low thermal conductivity values ($\lambda_{int} \leq 0.06$ W/mK) (American Concrete Institute, 2013).

4.4.1 Materials and methods

The materials employed to compose the rEPS mortars are cement CEM I 42.5 R (EN 197-1:2011), drinking water (EN 1008:2003) and rEPS from Ferramati International. High-density (18 kg/m^3) recycled polystyrene (rEPSa) and low-density (12 kg/m^3) recycled polystyrene (rEPSb) are considered to understand what type of aggregate is most suitable for achieving the intended thermal conductivity. A low-density mortar (12 kg/m^3) based on virgin beads (vEPSb) is also considered to make a direct comparison with the

correspondent recycled. No sand is employed, since the goal is investigating mortars with very low densities. The EPS beads are the only aggregates of the mixtures.

In order to prevent the segregation of the mixture and obtain a uniform distribution of the light aggregate in the section, a natural resin-based hydrophobic additive for EPS pearls are used. It is covered by industrial secrecy, thus the characteristic and doses can not be reported. The investigation is carried out in accordance with the methods provided by EN 16025-1:2013.

The first step consists in characterize the rEPS aggregate by a particle size analysis, performed by visual inspection and mechanical sieving to understand the size distribution of the aggregate samples and choose the size to be used in the mortar mix design (Figure 4.4-1 a). The sieves used belong to the R20 series of the Italian standard ISO 2331 with square openings in accordance with UNI EN 933-2. For every test screen, the percentage by mass of retained material f is obtain by the following formula (EN 933-1:2012):

$$f = \frac{100P}{M_1} \qquad (1)$$

where P is the mass of retained material and M_1 is the total mass of the sample.

After choosing the particle size of rEPS with more coherent distribution of pearls to use in the mix design, it is treated with the hydrophobic additive at least 30 minutes before preparing the mortars (Figure 4.4-1 b). It is the time needed for beads to absorb the additive. For the composition of the mortars, a premixture of the beads with cement (Figure 4.4-1 c) is necessary to avoid the loss of aggregate during the mixing phase, executed in compliance with EN 196-1:2016.
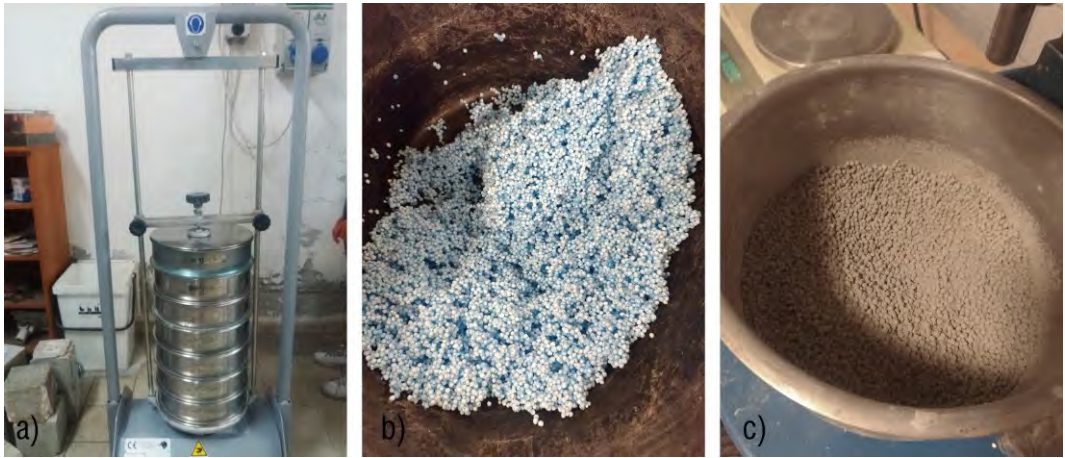
Fig. 4.4-1 - LWM characterization - preliminary phases: a) particle size analysis; b) rEPS treatment with hydrophobic additive; c) rEPS premixture with cement. Source: Author

The flow test is performed by the flow table method of the EN 7044:1972, in order to analyse the mortar consistency and workability. The consistency percentage $C\%$ is calculated according to the following formula:

$$C\% = 100 \times \frac{d_m - d}{d} \qquad (2)$$

where d_m is the average value of the measured diameters on the flow table and d is the lower diameter of the tunnel ring.

For the evaluation of the thermal conductivity and mechanical strength tests, cylindrical specimens (100 mm diameter and 50 mm high) and prismatic specimens (40mm x 40mm x 160mm) are prepared, respectively. For the hygrometric tests, dish-shaped samples (150 mm diameter and 10 mm high) are composed. Figure 4.4-2 shows the set of mortar specimens, cylinder-shaped, prism-shaped, and dish-shaped.

Fig. 4.4-2 - LWM characterization - preliminary phases: a) particle size analysis; b) rEPS treatment with hydrophobic additive; c) rEPS premixture with cement. Source: Author

The cylindrical and dish-shaped samples are dried in the oven at 60° C until the constant mass of $\pm$0.5%, then brought to room temperature in special laboratory dryers to prevent them from encountering the environment humidity. For each mortar, the dry density, ρ (kg/m3), is calculated by weighting and measuring the samples by means balance accurate and electronic gauge.

Thermal conductivity, λ (W/mK), thermal volumetric capacity, $c\rho$ (106 J/m³K), as well as dry thermal diffusivity, α_{dry} (10-6 m²/s), of the cylindrical specimens are measured through the Applied Precision ISOMET 2104 instrument with precision probe for thermal conductivity between 0.3 and 0.03 (W/mK) (Figure 4.4-3).


Fig. 4.4-3 - Thermal analysis through the Applied Precision ISOMET 2104 instrument. Source: Author

For each sample, the specific heat value is determined as follows:

$$c_p = \frac{10^6 c \rho}{\rho} \qquad \text{[J/kgK]} \qquad (3)$$

The evaluation of water vapour diffusion resistance is carried out on the dish-shaped samples in accordance with EN 12086:2013 under test conditions C. The d-type test assembly is chosen from the annex B of the standard (Figure 4.4-4 a, b).
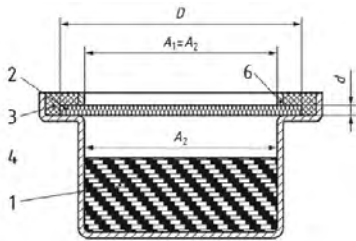
1   desiccant/aqueous saturated salt solution
2   test specimen
3   sealant
4   tape
5   template
6   limiting ring

A_1 is the upper exposed area;
A_2 is the lower exposed area; the mean exposed area:
        $A = (A_1 + A_2)/2$
D is the area of the test specimen
d is the thickness of the test specimen
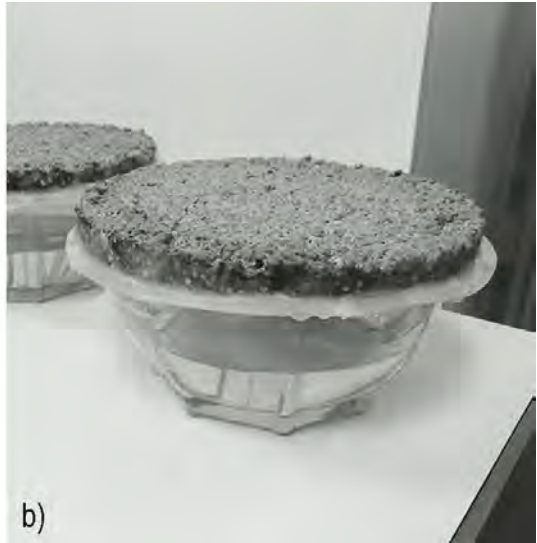
Fig. 4.4-4 - Determination of water vapour transmission properties: test assembly a) from EN 12086-ANNEX B; b) from investigation. Source: EN 12086-ANNEX B; Author

Before storing the specimens into the wet chamber (Figure 4.4-5), the assemblies are weighted and the date as well as the time of weighing are marked. These data correspond to the specimen mean values.

Fig. 4.4-5 - Determination of water vapour transmission properties: wet chamber. Source: Author

The procedure is repeated at regular intervals of 24 hours until five successive determinations of change in mass per unit time, G, are constant within $\pm 5\%$ of the mean value. They are calculated for the selected time intervals using the following formula:

$$G_{1,2} = \frac{m_2 - m_1}{t_2 - t_1} \qquad \text{[mg/h]} \qquad (4)$$

where m_1 is the mass of the test assembly at time t_1; m_2 is the mass of the test assembly at time t_2; t_1 and t_2 are the successive times of weightings.

The water vapour transmission rate, g, is calculated as follows, considering the mean of the upper and lower exposed areas of the test specimen, A:

$$g = \frac{G}{A} \qquad \text{[mg/m²h]} \qquad (5)$$

In accordance with the test condition C, the water vapour pressure difference Δp is equal to 1210 Pa. Thus, the water vapour permanence is determined with formula (6):

$$W = \frac{G}{A \times \Delta p} \qquad \text{[mg/m²hPa]} \qquad (6)$$

Therefore, water vapour resistance, Z, is calculated as the mutual value of W by formula (7), while, considering the specimen thickness, d, the water vapour permeability of the specimens, δ, is determined with formula (8):

$$Z = \frac{1}{W} \qquad \text{[m²hPa/mg]} \qquad (7)$$

$$\delta = W \times d \qquad \text{[mg/mhPa]} \qquad (8)$$

Before calculating the water vapour diffusion resistance factor, μ, it is necessary to know the water vapour permeability of the air, δ_{air} which depend on the barometric pressure of the measuring site of which the meteorological features should be taken in account. The conventional value of δ_{air} for the barometric pressure of Bari, where the measures are performed, is equal to 0,695 mg/mhPa. Thus, formulae (9-10) are used to calculate the dimensionless factor μ and the water vapour diffusion air layer thickness s_d:

$$\mu = \frac{\delta_{air}}{\delta} \qquad (9)$$

$$s_d = \mu \times d \qquad \text{[m]} \qquad (10)$$

The mortar mechanical resistance under flexural and compressive loads is evaluated following the procedure of European standard EN 196-1:2006. The tests are carried out on the prismatic samples after 28 days of maturation (Figure 4.4-6 a, b).

Fig. 4.4-6 - Mechanical resistance tests under a) flexural and b) compressive loads. Source: Author

After testing the samples and marking the flexural (F_f) and compressive (F_c) breaking load values, flexural resistance, R_t, and compressive strength, R_c, are calculated using the following formulae:

$$R_f = \frac{1.5 \times F_f \times l}{b^3} \qquad \text{[MPa]} \qquad (11)$$

$$R_c = \frac{F_c}{1600} \qquad \text{[MPa]} \qquad (12)$$

where b is the side of the square section of the prism, l is the distance between the supports of the flexural test machine, and 1600 is the area of the plates (40 x 40 mm^2) of the compressive test machine.

Regarding to the evaluation of the dry mortars water absorption, the empirical procedure by Petrella, Di Mundo and Notarnicola is carried out by using a Premier series dyno-lite (Taiwan) portable microscope in order to study the time evolution of the drop, with a rate ranging of 30 frames per second (Petrella, Di Mundo and Notarnicola, 2020).

A scanning electron microscope FESEM-EDX Carl Zeiss Sigma 300 VP (Carl Zeiss Microscopy GmbH (Jena, Germany)) is used to characterize the mortar morphology, chemical composition and verify the adhesion between the rEPS and the cement matrix for the samples with and without additive applied onto aluminium stubs (Figure 4.4-7).

Fig. 4.4-7 - Analysis of mortar morphology and chemical composition by SEM. Source: Author

4.4.2 Particle size analysis

From the visual inspection of the two materials, the rEPSa appeared as lumps of beads with a diameter up to 15 mm due to the solid links between the pearls (Figure 4.4-8 a). The rEPSb beads looked entire and defined (Figure 4.4-8 b) similar to the vEPS (Figure 4.4-8 c) with the maximum diameter of 8 mm. The rEPSa and rEPSb samples have been classified respectively in PS10 and PS8 levels, in conformity with EN 933-1.

Fig. 4.4-8 - Visual inspection: a) rEPSa; b) rEPSb; c) vEPS. Source: Author

Both rEPS types have been mechanically sifted in order to understand the percentage by mass of retained material in each sieve, according to formula (1). Table 4.4 1 shows the average results for size-type sieve for rEPSa and rEPSb.

Table 4.4-1. Mechanical sieving: average percentage of retained material in each sieve

CONVENTIONAL SIZE NAME	TEST SIEVE OPENING R20 series - ISO 2331	PERCENTAGE BY MASS OF RETAINED MATERIAL	
		rEPSa	rEPSb
Ø8	8 mm	19.2 %	9.7 %
Ø6.5	6.3 mm	13.8 %	6.7 %
Ø4.5	4.5 mm	9.0 %	8.8 %
Ø3.5	3.15 mm	9.9 %	18.8 %
Ø2.5	2 mm	45.7 %	52.5 %
Ø1.5	1 mm	2.3 %	3.4 %
Ø0.8	0.5 mm	0.1 %	0.1 %
Ø0.3	0.25 mm	0.0 %	0.0 %
Ø0.15	0.125 mm	0.0 %	0.0 %
Ø0	0.063 mm	0.0 %	0.0 %

The amount of dust, resulting from the milling, was less than 1% of the sample volumes, hence, the products were classified in the class of dust percentage D0, according to the law EN 933-1.

The average particle size fractions chosen for designing the lighter cement mortars were Ø3,5 and Ø2,5, retained respectively in the 3,15 mm and 2 mm sieves, because of they had a more consistent distribution of pearls without the presence of agglomerated portions. The mixed fraction from size Ø1.5 to Ø6.5 was considered too.

4.4.3 Mix design and consistency analysis

Fifteen mortars were designed with water-cement ratio varying from 0.45 and 0.70 and with the amount of rEPS calculated in function of the volume of the cement paste. Two sets of mortars by densities and a reference set with vEPSb and rEPSb not additivated were defined.

The first set of mortars was composed with the use of rEPSa in the percentages varying from 55% to 80% with the particle sizes Ø2.5 and Ø3.5. The water-cement ratio was kept unchanged at 0.5 for mortars with rEPSa up to 75%. For mortar with 80% of rEPSa was necessary to increase the cement portion, otherwise insufficient to contain the large amount of aggregate.

The second set of mortars was composed maintaining the percentage of rEPSb (Ø2.5, Ø3.5 and Ø1.5-6.5) at 75% for all mortars except M8 which was designed with 70% of rEPSb Ø3.5.

The reference set contained the mortar M_v14 (75% of vEPSb Ø1.5-6.5) and $M_{na}15$ (75% of rEPSb Ø1.5-6.5 not additivated).

Table 4.4-2 shows the mortars mix design and their water-cement ratio (w/c). Figure 4.4-9 illustrates the fresh conditions of mortars from M1 to M12 at the beginning and at the end of the flow test.

Table 4.4-2. Mix design of the three sets of mortars and their consistency percentage

MORTAR	SET	PARTICLE SIZE	rEPS		CONCRETE	WATER	W/C
			Type	%	gr	gr	
M1	1	Ø2.5	rEPSa	55	450	225	0.50
M2		Ø2.5		65	450	225	0.50
M3		Ø2.5		70	450	225	0.50
M4		Ø2.5		75	450	225	0.50
M5		Ø2.5		80	500	225	0.45
M6		Ø3.5		75	450	225	0.50
M7		Ø3.5		75	450	225	0.50
M8	2	Ø3.5	rEPSb	70	450	225	0.50
M9		Ø2.5		75	500	225	0.45
M10		Ø3.5		75	450	292.5	0.65
M11		Ø3.5		75	450	315	0.70
M12		Ø1.5-6.5		75	450	315	0.70
M13		Ø1.5-6.5		75	450	292.5	0.65
M_v14	Ref. set	Ø1.5-6.5	vEPSb	75	450	315	0.70
$M_{na}15$	Ref. set	Ø1.5-6.5	rEPSb	75	450	292.5	0.65
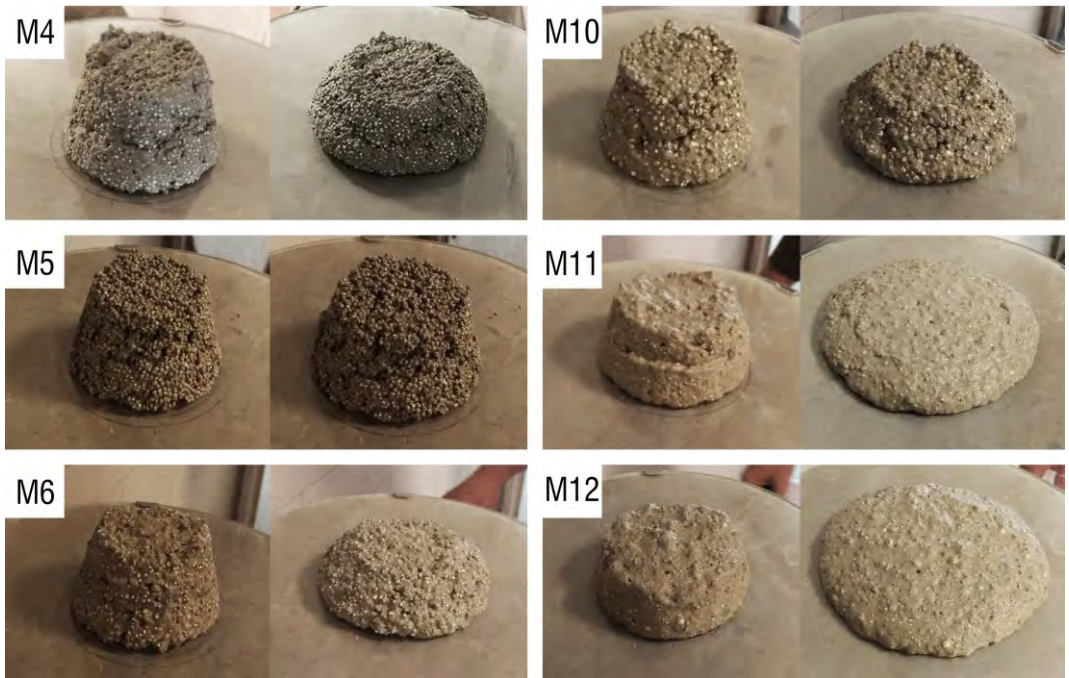
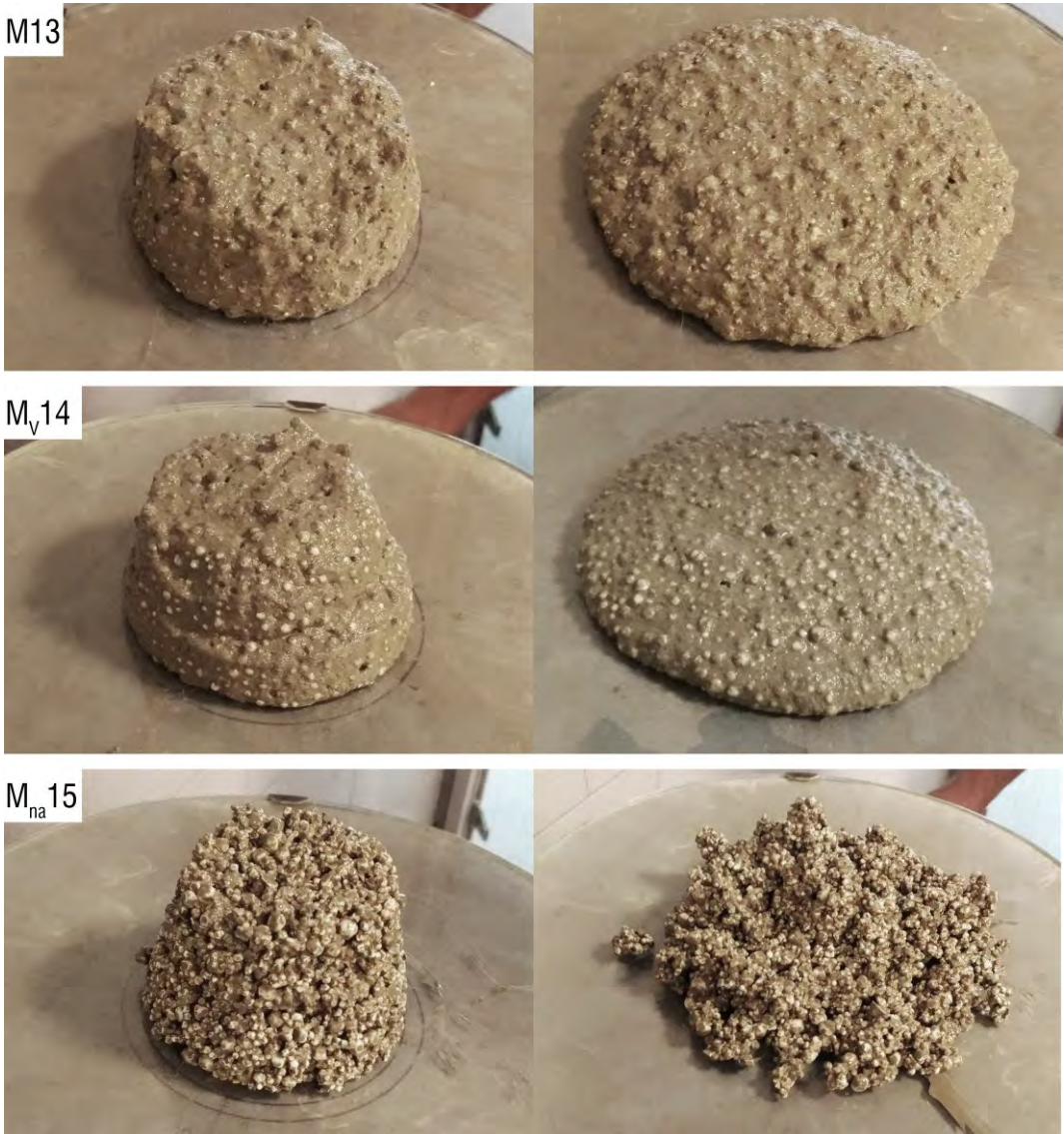**Fig. 4.4-9** - Consistency analysis - Flow test: fresh mortars M1-M12 at the beginning and at the end of the flow test. Source: Author

From the flow test visual survey, it was deduced that as the percentage of rEPS in the mortar increased, the consistency of the mortar increased too at the expense of workability. The dryness of the mortars M5, M7, M8 and M9 was detected and underlined the lack of water in the dough to maintain unchanged the shape-cone after the flow test. The M10 (w/c=0.65) had a good distribution on the table but not sufficiently workable to industrial use. On the other hand, M11 and M12 (w/c=0.7) showed an optimal workability, almost recalling the standard mortars. However, M12 appeared too fluid and rich in air bubbles that would have made too brittle the mortar in its dry conditions. Therefore, M13 was designed as M12 with a reduced w/c ratio of 0.65 and since it presented a good consistency and workability without too much air voids, it was compared with the reference mortars M_v14 and $M_{na}15$ designed with the same EPS quantity (Figure 4.4-10).

Fig. 4.4-10 - Consistency analysis – Flow test: fresh mortars M13, M_v14 and M_{na}15 at the beginning and at the end of the flow test. Source: Author

Despite the use of two different types of additivated EPS (rEPSb and vEPSb) with the same bulk density, the consistency of M13 and M_v14 was comparable. On the contrary, M_{na}15, designed like rEPSb not additivated, appeared too dried and without consistency. It was deduced that, in fresh conditions, the hydrophobic additive influenced the mortars

workability and consistency (Babu and Babu, 2003). Therefore, M13 was identified as the best mortar for further and deeper investigations.

The observation from visual inspection were validated by the percent results calculated according to formula (2) (Figure 4.4-11).
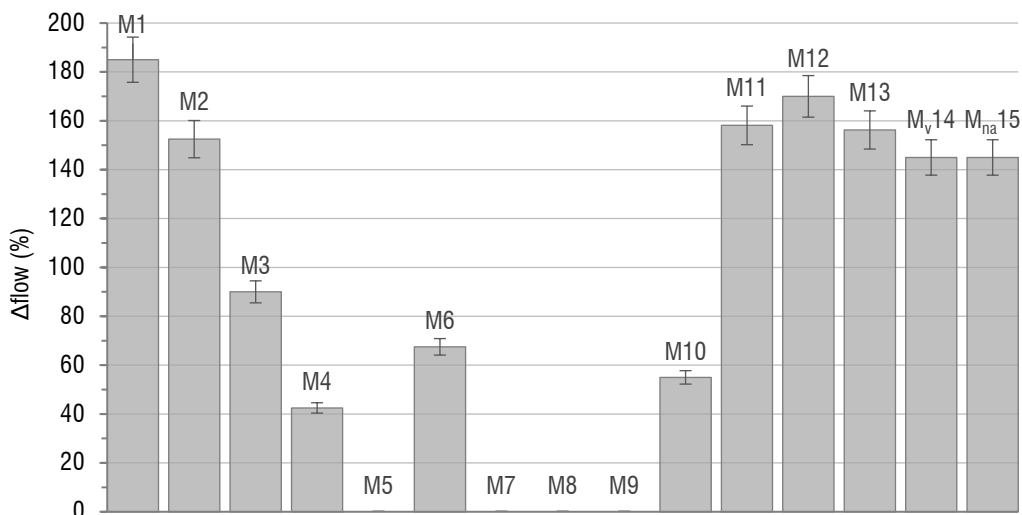
Fig. 4.4-11 - Flow test results. Source: Author

From the comparison of these results, it was deduced that the second mortar set needed to be mixed with greater quantity of water, otherwise non-workable. Comparing M6 and M7 which had the same composition but different rEPS densities, rEPSa and rEPSb respectively, the total non-workability of the mortar M7 was remarked. It could be explained by the material characteristics declared by Ferramati pursuant to EN 13163:2017. Indeed, associating rEPSa to EPS100 and rEPSb to EPS30 by density, the mean values of water absorption (δ_{med}) of the materials varied between 0.010 and 0.024 mg/mhPa for EPS100 and between 0.018 and 0.036 mg/mhPa for EPS30. Moreover, since rEPS showed a more porous surface, as investigated by Kekanović et al., its water absorption was assumed to be higher than vEPS. In addition, as this feature depends on the material density, it was concluded that mortars belonging to the second set needed more water than the first. Therefore, it is assumed that reducing the density of rEPS, the water requirement in the mixture increases.

4.4.4 Thermo-hygrometric analysis

For every mortar, two cylindric-shaped samples were composed to perform the thermal conductivity analysis and individuate the best lightweight mortar in terms of thermal insulation. Three further samples of the best mortars resulting from the consistency analysis, M11, M12 and M13, were produced to obtain a more accurate mean value of thermal conductivity. Thermal measurements of M12 could not be carried out as the test specimen surfaces were not sufficiently smooth and without voids to allow the planar support of the probe. Table 4.4-3 compares the measured average values of density (ρ), thermal conductivity (λ_{dry}), thermal diffusivity (α_{dry}), volumetric heat capacity ($c\rho$) as well as sample mean temperature (T_m) of the fourteen mortar. It includes the specific heat values (c_p) calculated with formula (3).

Table 4.4-3. Thermal analysis

MORTAR	ρ	λ_{dry}	α_{dry}	$c\rho$	c_p	T_m
	Kg/m^3	W/mK	10^{-6} m^2/s	10^6 J/m^{3}K	J/kgK	K
M1	342.43	0.0873	0.177	0.520	1519.52	303.47
M2	278.76	0.0743	0.166	0.450	1612.49	303.67
M3	261.14	0.0708	0.181	0.392	1499.19	302.81
M4	223.43	0.0637	0.173	0.369	1649.28	303.79
M5	212.94	0.0593	0.174	0.344	1613.13	300.82
M6	216.92	0.0627	0.166	0.379	1744.87	301.27
M7	213.20	0.0625	0.185	0.340	1592.39	300.73
M8	245.85	0.0703	0.171	0.413	1679.90	301.51
M9	341.39	0.0829	0.168	0.495	1449.96	301.83
M10	186.80	0.0608	0.190	0.325	1739.87	300.77
M11	186.48	0.0580	0.184	0.315	1690.09	299.38
M12	179.09	---	---	---	---	---
M13	187.70	0.0587	0.190	0.315	1679.08	299.82
M_v14	131.50	0.0504	0.186	0.271	2056.99	299.86
M_{na}15	238.79	0.0711	0.194	0.375	1570.44	299.80

The results obtained showed the gradual reduction of the thermal conductivity value as the density of the mortar decreased, thus as the percentage of rEPS in the mixture increased. The mortars M4, M5, M6 were the most performing of the first set, with thermal

conductivity values varying between 0.059 W/mK and 0.064 W/mK. In particular, the M4 and M6 which had the same composition but with aggregates belonging to two different particle size, respectively Ø2.5 and Ø3.5. It was observed that, by increasing the size of the rEPS beads, the density of the mortar was reduced, hence the thermal conductivity due to the presence of greater quantity of air voids inside the beads. At the same density, they reached the volume of the vessel containing the Ø2,5 pearls with less material. Similarly, the M6 mortar specimens, having the same volume as the M4 mortar, were lighter, thus with lower density as they contained less aggregate.

M10, M11, M13 were the most performing mortars of the second set, with thermal conductivity values ranging from 0.058 W/mK to 0.0608 W/mK. However, only M11 and M13 were considered for further studies for their ease workability.

Comparing the reference set containing the M_v14 and $M_{na}15$ with M13, the effect of the additive also on dry samples was evident. At the same volume and EPS percentage, the three samples had very different densities and λ values. The absence of the additive provoked on $M_{na}15$ the segregation of the mortar components and the increasing in weight and consequently in thermal conductivity, probably due to the minimal quantity of air voids as shows Figure 4.4-12.

Fig. 4.4-12 - Comparison of dry condition mortars: M_v14 (left); M13 (middle); $M_{na}15$ (right). Source: Author

The relationship between the thermal conductivity and the dry density of the two mortar sets is better explained in the curves showed in Figure 4.4-13.
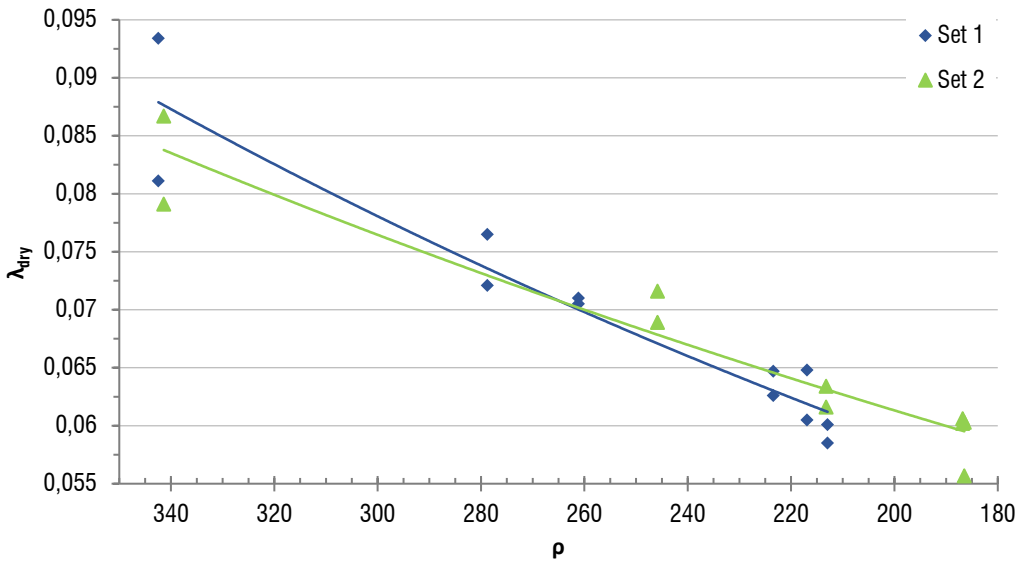
Fig. 4.4-13 - Correlation curves between thermal conductivity and dry density of the two mortar sets. Source: Author

The evaluation of water vapour diffusion resistance was carried out for mortars M11 and M13 on five dish-shaped samples each. Nine measurements were carried out until five successive determinations of change in mass per unit time, G, were constant within $\pm5\%$ of the mean value. The hygrometric parameters were calculated according to formula from (4) to (10). The values obtained were negative due to the evaporation of water contained into the cup with intervals of 24 hours. Table 4.4-4 reports the outstanding mean values of the hygrometric parameters of the last five measurements on the five test assemblies which decreed the test concluded.

Table 4.4-4. Mean values of the hygrometric parameters for the determination of the water vapour diffusion resistance value

MORTAR	G_m	g	W	Z	δ	μ	s_d
	mg/h	mg/m²h	mg/m²hPa	m²hPa/mg	mg/mhPa	-	m
M11	235.72	12254.21	10.13	0.0988	0.101	6.87	0.069
M13	249.79	12985.38	10.732	0.0935	0.107	6.50	0.065

The water vapour diffusion resistance values (μ) of the two mortars were almost the same.

Comparing them with the declared values of a conventional EPS blocks which μ-value vary from 20 to 60, it was deduced that the designed mortars were very performing materials for their transpiration capacity which impedes the creation of interstitial humidity into the section of a building component.

4.4.5   Mechanical resistance evaluation

For mortars aiming at thermal insulation according to EN 16025-1:2013, the mechanical characterization is not required. Although, to have a complete overview of the mortar characteristics, mechanical tests under flexural and compressive loads were carried out on the prism-shaped samples of all mortars excepted M12 which dry conditions were unsuitable due to its fragility (the samplings broke during the mould-release phase). Table 4.4-5 compares the values of flexural and compressive strength of the mortars calculated using formulae (11-12).

Table 4.4-5. Flexural and compressive strength of the designed mortars

RESISTANCES	M1	M2	M3	M4	M5	M6	M7	M8	M9	M10	M11	M13
R_f [MPa]	0.67	0.55	0.73	0.63	0.41	0.38	0.39	0.39	0.78	0.34	0.09	0.19
R_c [MPa]	1.05	0.83	0.69	0.56	0.33	0.28	0.30	0.46	0.60	0.16	0.13	0.28

For M11 and M13, the best mortars in terms of workability and thermo-hygrometric characteristics, the stress-strain curves were drawn during the tests to understand their behaviour during the load increasing. In particular, the performance of M13 was deepen investigated. The expected behaviour was a fragile breakage which occurred under bending loads (Figure 4.4-14 a) but not under compressive loads (Figure 4.4-14 b).
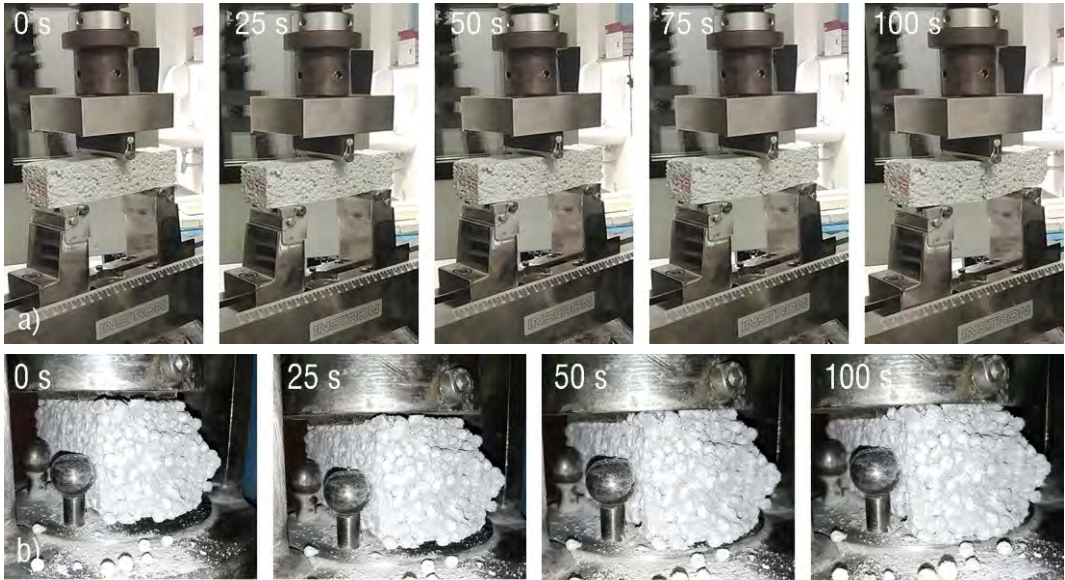
Fig. 4.4-14 – Mechanical resistance tests under a) flexural and b) compressive loads. Source: Author

The end of the test was decreed since the samples could no longer withstand the load. They presented a flexural crack opened in the opposite side to the load at the end of the flexural test (Figure 4.4-15 a), instead the typical cracks from crushing showed at compressive test concluded, not reaching the final rupture (Figure 4.4-15 b).
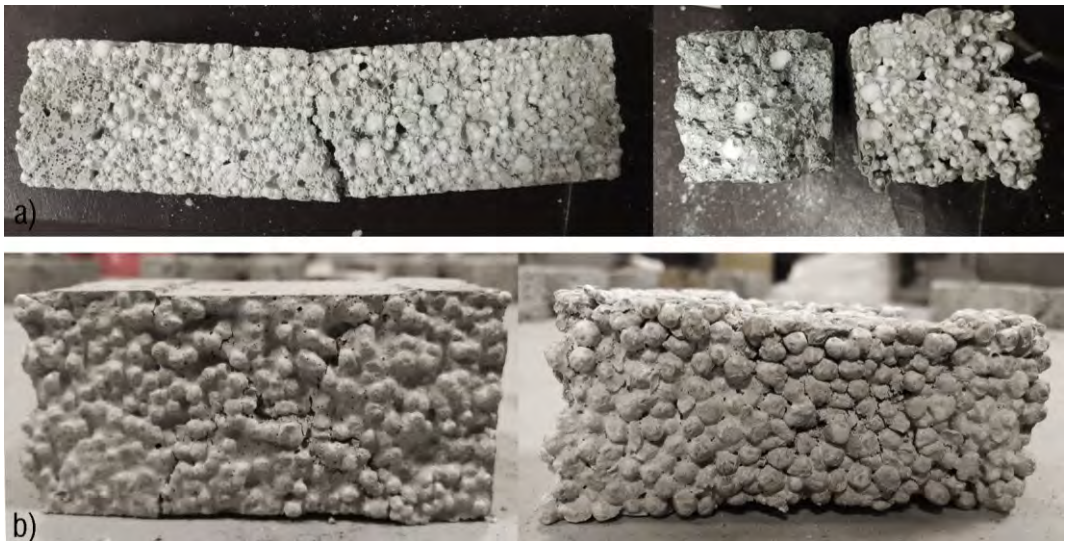

Fig. 4.4-15 - M13 mechanical characterization under a) flexural and b) compressive loads. Source: Author

This behaviour was confirmed by the stress-strain (σ-ε) curve (Figure 4.4-16) which showed a ductile behaviour due to the large amount of rEPS beads in the section. It was renamed "bearing behaviour" since during the test, the samples underwent a large deformation and lost some surface beads, then regaining, part of their original shape.

$y = 0,0409\ln(x) + 0,0003$
$R^2 = 0,916$

Stress-Strain by compressive test

Time-Strain

Log. (Stress-Strain by compressive test)

$\sigma = 0.25$ MPa

$\varepsilon = 7.3$ %

$E_{tan} = 49.73$ MPa
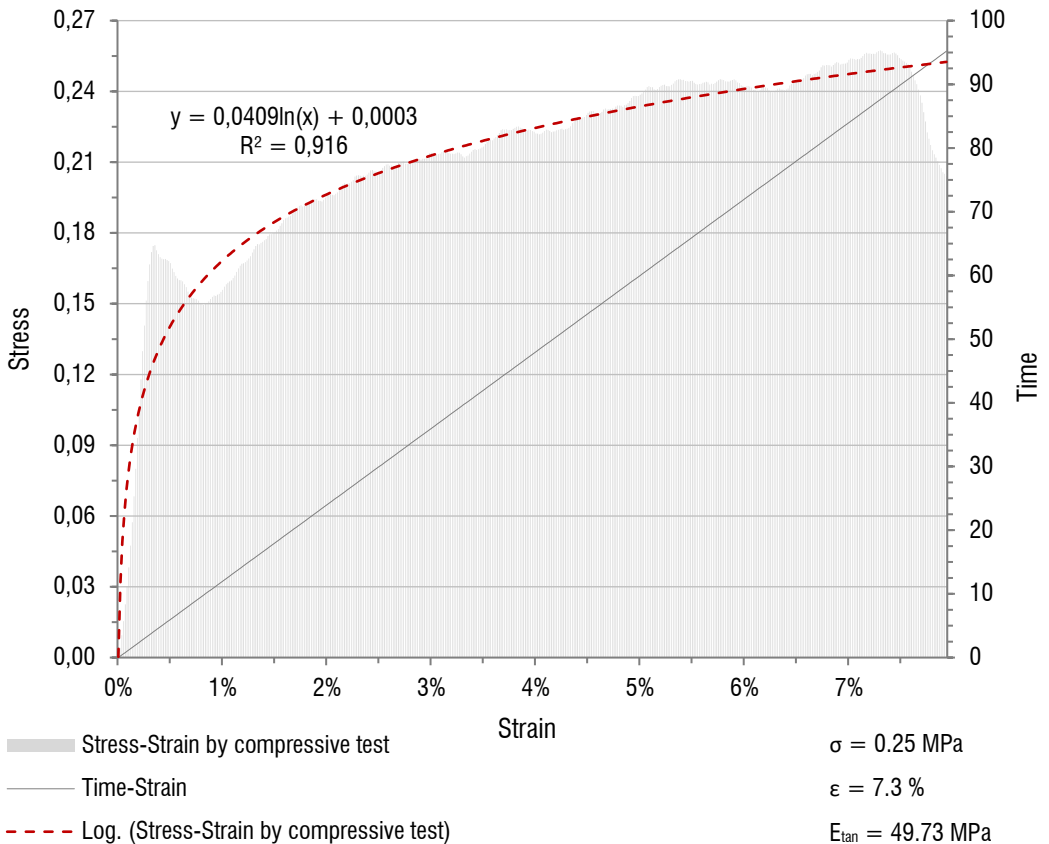
Fig. 4.4-16 – Compressive strength of mortar M13: example of stress-strain curve. Source: Author

4.4.6   Water absorption evaluation

The wetting characterization of the sample surface of mortar M13 was carried out. The drops of water were released on three different parts of the sample to understand if the water absorption was uniform everywhere. On a rEPS bead the drop remained unaltered. At the interface between a rEPS pearl and the cement matrix, a gradual absorption

occurred, instead in correspondence of the only cement matrix, water penetrated quickly (Figure 4.4-17). It was due to the heterogeneous distribution of the rEPS into the mortar which created air voids and made the mortar porous. As assessed during thermal-hygrometric analysis, this feature involved good insulating performance, although in presence of wet environmental, it might absorb water and invalidate its function. However, since the mortar has been designed to be included into building components, away from water sources, its thermo-insulating performance should not be affected.
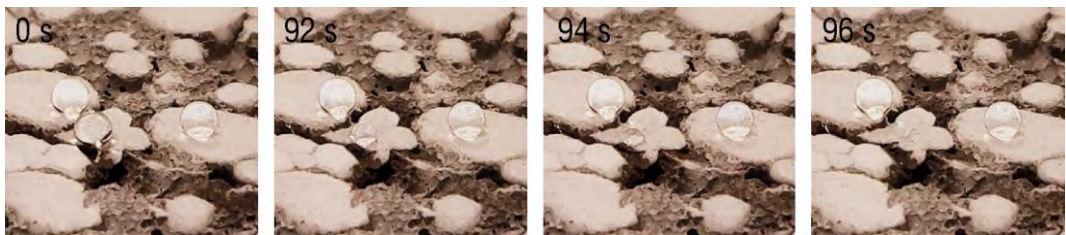
Fig. 4.4-17 - Optical microscope observations on mortar M13. Source: Author

4.4.7 Scanning electron microscope analysis

The purpose of this study is examining the morphology, the chemical composition as well as the adhesion between the cement matrix and the lightweight aggregate of the mortar M13. It was also compared with the reference mortars M_v14 and $M_{na}15$ to better understand the effect of rEPS and the additive on the dry mortars.

Deepening the study of mortar M13, it was observed that the additivated lighter rEPSb aggregate was closely linked to the cement matrix without any cracks at the interface between the parts (Figure 4.4-18). Many times, the images reading has been arduous due to the difficulty in recognizing the cement from the aggregate due to the presence of air bubbles in the cement. In such cases the spectrum study was necessary to individuate the component by chemical elements (Figure 4.4-19).

Moreover, it was confirmed that the rough surface of the beads allowed a better adhesion with the cement paste due to the capacity of pearls surface to absorb the additive during the pre-mixing phase and favouring the cement grip. As proof of this, it was possible to acquire detailed images of the cement inside the open cells of rEPS (Figure 4.4-20).
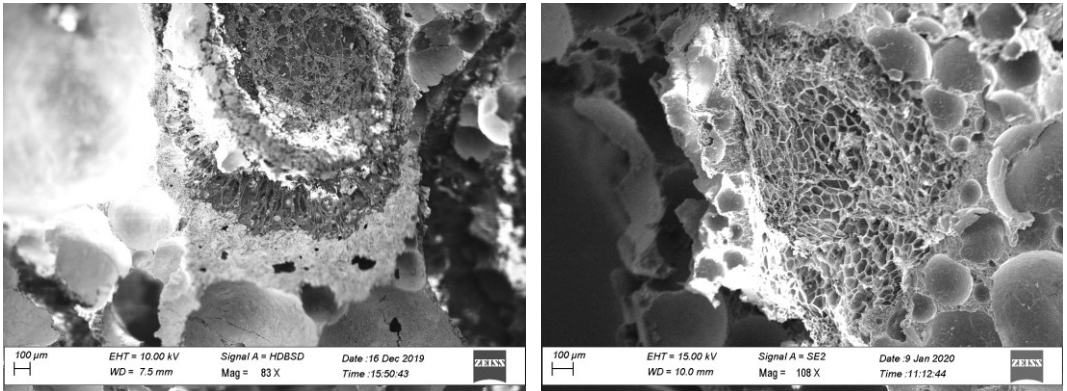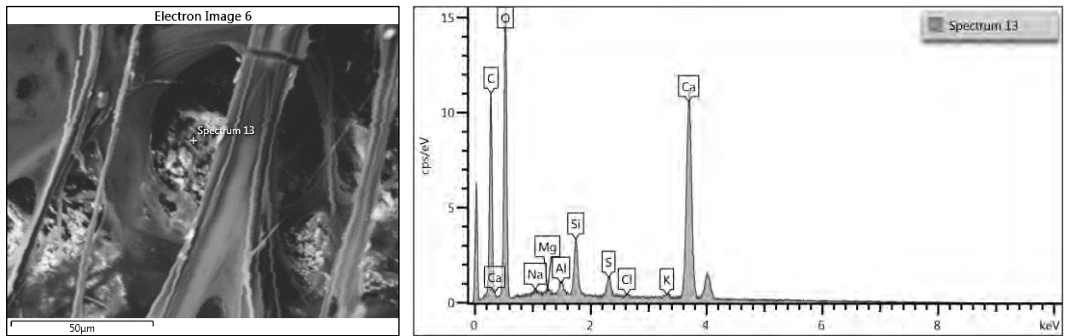
Fig. 4.4-18 - SEM analysis on M13: strong adhesion between rEPS and cement matrix. Source: Author

Element	C	O	Na	Mg	Al	Si	S	Cl	K	Ca	Total
Wt%	10.84	42.73	0.18	0.21	0.77	3.85	1.86	0.11	0.51	38.95	100
Wt% Sigma	0.17	0.29	0.06	0.05	0.06	0.09	0.08	0.03	0.07	0.27	

Fig. 4.4-19 - SEM analysis on M13: Chemical spectrum study. Source: Author
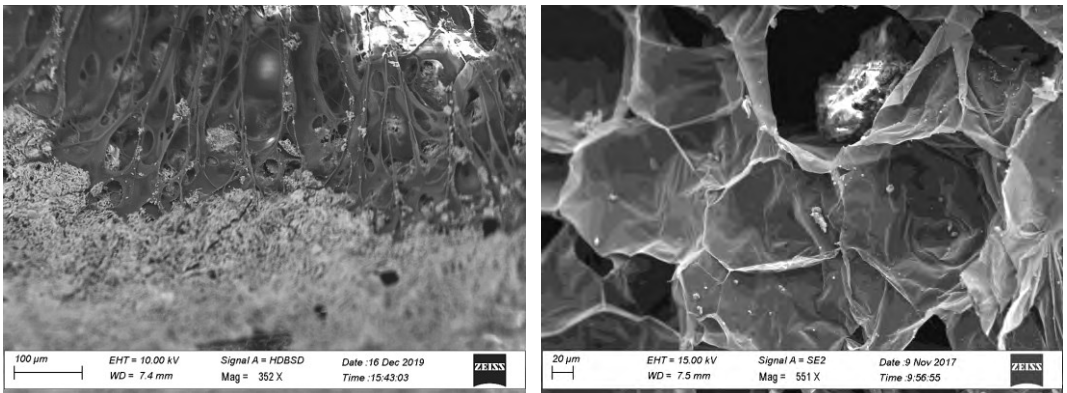
Fig. 4.4-20 - SEM analysis on M13: presence of cement into the rEPS open cells. Source: Author

In some cases, it was possible to observe the dry state of the additive that appeared under the microscope as filaments that kept the aggregate connected to the cement matrix (Figure 4.4-21 a). It was detectable also on the surface of the vEPS aggregate, configured as venous ramifications on which was found the presence of cement dough (Figure 4.4-21 b). Comparing the mortar M13 with the corresponding M_v14, apparently there were no differences. In both, the aggregate was connected to the cement matrix, even though, many times, it did not occur with M_v14. Indeed, the homogeneous and closed-cell surface of the virgin EPS, did not allow the beads to absorb the additive which appeared not homogeneously distributed on the particle surface. In that cases a crack section at the interface between the cement and the aggregate occurred (Figure 4.4-22 a). The same situation appeared in the mixture without additive, $M_{na}15$ (Figure 4.4-22 b).
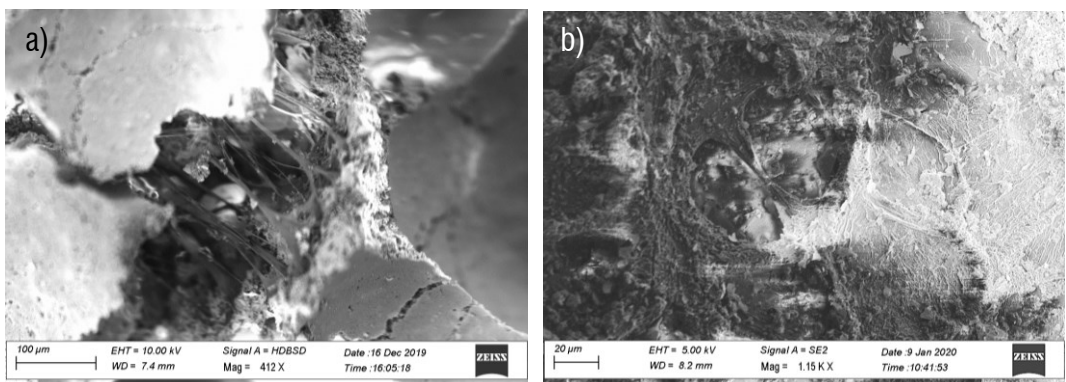
Fig. 4.4-21 - SEM analysis: dry state of the additive as filaments - a) M13; b) vEPS. Source: Author
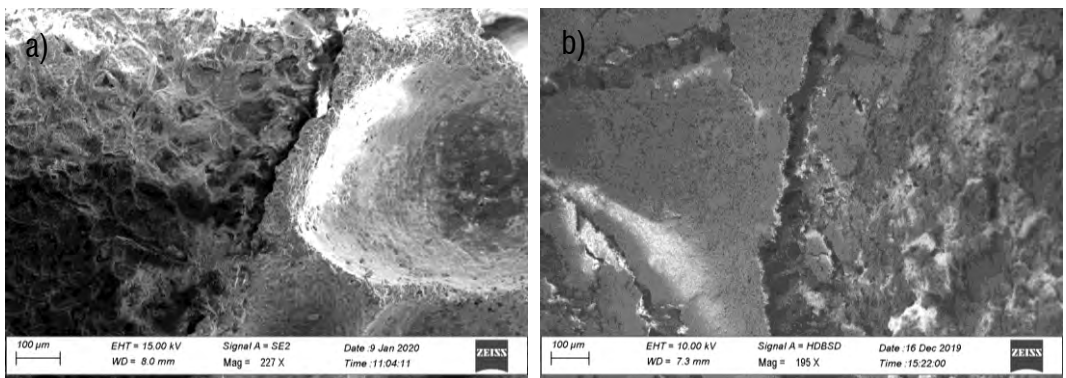
Fig. 4.4-22 - SEM analysis: crack section at the interface between the aggregate and the cement matrix – a) M_v14; b) $M_{na}15$. Source: Author

4.4.8 Patent Declared characteristics for patent application

The investigation on non-structural mortars for thermo-insulation functions has led to individuate the optimum mix design which could satisfy the requirement of good workability for industrial production and high thermo-hygrometric properties by using economic materials coming from industrial wastes. The use of a natural resin-based additive on the rEPS apports many advantages on the mixture i.e. it increases the mortar workability, conferring it a good consistency, and prevents the phenomena of segregation due to the creation of a hydrophobic film around the rEPS beads which can robustly bind at the cement matrix in each point of the mixture. It has greater advantages on the recycled EPS for the beads physical properties deriving from the industrial recycling process. The break of the bonds between the particles, gives the surface a porous aspect.

Among the thirteen mortars analysed, M13 is the most performing in terms of mix design, consistency, thermo-hygrometric insulation, ease, and speed of industrial reproduction. The low coefficient of thermal conductivity and resistance to the water vapour diffusion provide to the mortar a high thermal insulation capacity without the risk of interstitial condensation. Therefore, it can be used as a non-structural and insulating filling material for building components i.e. as an under-roof insulation cover as well as a completion casting for prefabricated double-slab wall or traditional constructions. Unlike normal thermal insulation materials, M13 can be used in the presence of steel because its cementitious matrix creates a protection cover from the phenomenon of oxidation.

It has been subjected to a patenting process since from the search for precedence, no mortars have presented such good characteristics. The declared properties are summarised in Table 4.4-6.

Table 4.4-6. Declared properties for mortar patent

MORTAR	MIX-DESIGN	ADDITIVES	W/C	ρ Kg/m^3	λ W/mK	μ -	R_c MPa
M13	- CEM I 42.5R - Water - rEPSb (12 kg/m^3)	- Water retainer - Superplasticizer	0.65	187.70	0.0587	6.50	0.25÷0.31

4.5   Precast concrete modules

Proceeding at the *Component scale* of detail, this section aims at designing the innovative precast concrete panels which are the base elements of the innovative PC panel system. Despite they follow the characters of Ferramati's chain of product, they present new components that assign them the characteristics of thermal insulation, contributing to the structural purpose and anchoring the modules to the existing RC building. In general, the PC module consist of two layers: the external reinforced concrete slab and the internal insulation sheet in LWM and rEPS blocks. This internal insulating coat is disposed on the inner slab surface in a staggered way to create the male-female configuration of junctions with the aim to prevent the generation of possible thermal bridges. The panel reinforcement is designed to anchor the module to the existing façade and consists in steel lattices disposed along the panel width and steel rebar arranged in both directions and embedded into the slab thickness. Figure 4.5-1 shows the axonometric representation of the panel in its front (a) and back side (b).
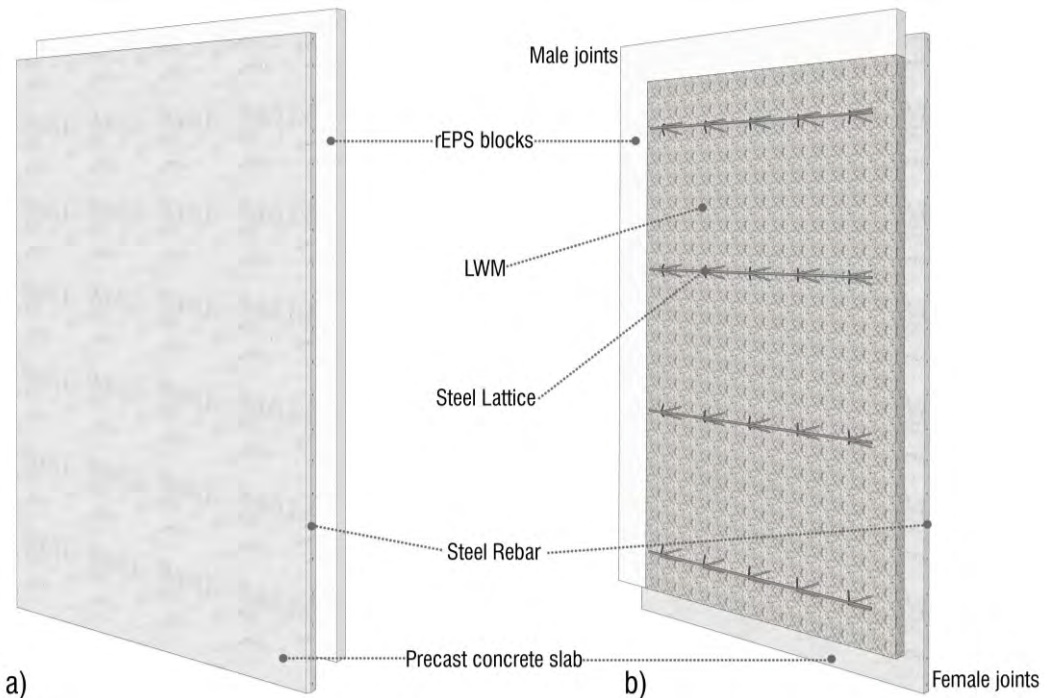
Fig. 4.5-1 - The axonometric representation of the panel (a) front and (b) back sides. Source: Author

4.5.1 Materials and design methodology

All the materials used for the panel design derive from the need to follow the traditional product chain by Ferramati Int. to industrially produce the novel module with the machines and workers at its disposal and do not interrupt the production of the conventional artifacts. Therefore, the external slab is composed by reinforced concrete which characteristics are certified by Ferramati in accordance with the Italian NTC18, EC2, EN 206:2013 and EN 197/1:2011. The declared concrete characteristics, derived from Ferramati's technical sheet, are the following:

- Class of compressive resistance: C28/35
- Exposition class: XC2
- Maximum dimension of aggregates: D_{max} 20mm (sand, breach, gravel)
- Maximum water/cement ratio: 0.55
- Consistency class: S4
- Cement type and class: CEM I 52.5 R

The panel reinforcement in improved adhesion steel is type B450C for structural use in accordance with EN 13369:2018. The inner insulating layer is designed to be in LWM (M13) which characteristics are explained in section 4.4. It is casted with 7 cm offset from the edges along all directions inside a partial frame of rEPS blocks to avoid the damaging of the LWM in correspondence of the panels' joints and the generation of thermal bridges. The referred rEPS blocks protrude 7 cm from the panel on the top and right side to create the male joint to be associated with the female of the next panel (Figure 4.5-1). Hence, every panel has two male and female joints. The material properties of the panel layers for thermal investigation are summarized in the Table 4.5-1.

Table 4.5-1. Properties of panel materials

MATERIAL	ρ	λ	μ	c_p
	Kg/m³	W/mK	-	J/kgK
Concrete	2400	1.80	34	880
Steel	7800	52	2000000	1990
LWM	187.7	0.0587	6.50	1679.08
rEPS	10	0.037	30	916.67

The calculation of the slab minimal rebar is carried out in accordance with the Italian Decree DM 12/3/1987 which provides the guidelines for the design, execution and testing of prefabricated buildings. In particular, the rules to design in seismic zones are considered. It establishes that the section reinforcement should be at least 200 mm²/m in each direction.

After individuating the diameter of the rebar necessary to comply with the requirements, the correct concrete cover is calculated in accordance with NTC18, EC2, EN 13369:2018 ANNEX A, to ensure the panel protection from the environmental agents and reduce the risk of corrosion. The durability constraints and the environmental conditions are considered to delineate the requirements for which the cover calculation should be performed. Therefore, the value of the building nominal life, the concrete compressive strength class, the element shape, and the steel typology are defined in function of the project characteristics. The exposition conditions are chosen in function of the physical and climatic characteristic of the application site from the nominal scale in Figure 4.5-2 a provided by EN 13369:2018, ANNEX A, in which the recommended values of minimum concrete cover (c_{min}) for prefabricated products are also reported. The calculation of the reinforcement cover is carried out considering the range of minimal values of the table illustrated in Figure 4.5-2 b.

a)

Environmental conditions	Aggressivity	Exposure classes of EN 206
A	Null	X0
B	Low	XC1
C	Moderate	XC2-XC3
D	Normal	XC4
E	High	XD1-XS1
F	Very high	XD2-XS2
G	Extreme	XD3-XS3

b)

Environmental conditions	C_{min}	C_0	Ambient conditions	Slab reinforcing bars		Reinforcing bars for products other than slabs		Slab pretensioned tendons		Pretensioned tendons for products other than slabs	
				$\geq C_0$	$< C_0$	$\geq C_0$	$< C_0$	$\geq C_0$	$< C_0$	$\geq C_0$	$< C_0$
A	C20/25	C30/37	A	10	10	10	10	10		10	
B	C20/25	C30/37	B	10	10	10	10	15		15	
C	C25/30	C35/45	C	10	15	15	20	20	25	25	30
D	C30/37	C40/50	D	15	20	20	25	25	30	30	35
E	C30/37	C40/50	E	20	25	25	30	30	35	35	40
F	C30/37	C40/50	F	25	30	30	35	35	40	40	45
G	C35/45	C45/55	G	30	35	35	40	40	45	45	50

Fig. 4.5-2 - Minimum concrete cover: a) Environmental conditions; b) Recommended values of minimum concrete cover (c_{min}). Source: EN 13369:2018 - ANNEX A

To calculate the nominal value of the concrete cover (c_{nom}) the formula (13) by NTC18 is used:

$$c_{nom} = c_{min} + \Delta c_{dev} \qquad [mm] \qquad (13)$$

where Δc_{dev} is the execution tolerance that is equal to 5 mm.

The lattice girder dimensions are chosen from the table of standard typologies provided by the producer from which Ferramati supplies. Since the bottom rebar of the lattices collaborate with the concrete reinforcement mesh, the choice depends on the rebar diameter and the height necessary to ensure the panel anchoring to the façade.

Despite the disposition of the lattices of the conventional PC panels by Ferramati follows the longitudinal direction of the module, in the novel PC panel they are arranged along the transversal direction where the crossing between the bracket and the upper rebar creates the accommodation of the anchors for the coupling with the façade. Furthermore, they facilitate the insertion of the hooks for the panel handling, avoiding the introduction of further elements. Therefore, only with the lattices it is possible to perform the fundamental functions of the panel reinforcement, handling, and anchoring. The lattices spacing should not exceed 50 cm to avoid the panel instability.

The dimensions of the panel are chosen, respecting the widthwise of the trays of the carousel system and to optimize the production. It can contain two next panels of 1.2 m in width. The length can vary as request by the need to adapt to the existing building, though the maximum dimension is set at 2 m for the requirements of ease handling and installation of the panel on the façade. The minimal PC slab thickness is chosen in function of the calculated steel cover, while for the insulating layer in LWM, it can vary from 5 cm to 7 cm in function of the thermal protection requirements. It should not exceed 7 cm as a greater thickness would lead to the LWM maturation times longer than 48 h.

4.5.2 The designed module

The novel PC panel has been designed in accordance with the boundary conditions defined in the section 4.2, which permitted to delineate the durability constrains and the exposition conditions for the panel concrete cover calculation. They were so specified:

- Nominal life of the intervention: 50 years;
- Environmental condition: C (Figure 4.5-2 a);
- Exposition class: XC2 (Figure 4.5-2 a).

Assuming the standard dimension of the panel 1.2 m in width and 2 m in length, the minimal surface of the reinforcement was calculated and the amount and diameter of rebars were determined. The Table 4.5-2 records the resulting values.

Table 4.5-2. Panel rebar calculation and steel cover definition

REQUIREMENT BY DM 12/3/1987				As $_{min}$/dir	200	mm²/m
PANEL DIMENSIONS	WIDTH	2 m		As$_{w,min}$	400	mm²
	LENGTH	1.2 m		As$_{l,min}$	240	mm²
PANEL REINFORCEMENT	TYPE	Φ	QNT	RODS		As
		mm²	unit	unit		mm²
LATTICE	Φ5|7|5	19.63	4	8		157.08
REBAR	Φ5	19.63	26	26		510.51
TRANSVERSAL ARMOUR	13Φ5	-	-	13		255.25
LONGITUDINAL ARMOUR	21Φ5	-	-	21		412.33

Thus, the steel cover of the PC panel was calculated in compliance with Figure 4.5-2 and formula (13). In particular, the raw of the environmental condition C and the column of slab reinforcing bars were considered. Since, the compressive strength class of the PC panel concrete was C28/35, hence minor than C35/45, the minimal cover value (c_0) was 15 mm. Therefore, the c_{nom} was determined:

$$c_{nom} = 15 + 5 = 20mm$$

Consequently, the thickness of the panel was established and was equal to 4.5 cm.
As concern the dimension in height of the lattice girders, three typologies i.e. 95 mm, 125 mm, and 165 mm, were selected from the standard sheet, considering the type 5/7/5 resulting from the calculation in Table 4.5-2. Assuming the thickness of 5 cm of the LWM layer, the lattice girder selected was the type 125 mm 5/7/5. In the standard panel (1.2m x 2m) were arranged four lattices spaced 50 cm from each and 25 cm from the edges. The overall weight of the panel is almost 286 kg. Table 4.5-3 details the calculation for each component. The panel reinforcement was arranged as in Figure 4.5-3. The technical drawings of the overall panel are illustrated in the Figures 4.5-4.

Table 4.5-3. Panel weight

COMPONENT	QNT	DENSITY	DIMENSIONS	VOLUME	WEIGHT
	unit	Kg/m^3	m	m^3	kg
LATTICE	4		0.8		3.616
REBAR	13		2		4.00
	13		1.2		2.40
PCS		2400	2 x 1.2 x 0.045	0.11	259
LWM		187.7	1.8 x 1 x 0.05	0.09	16.89
rEPS		10	1.2 x 0.1 x 0.05	0.006	0.06
			2 x 0.1 x 0.05	0.010	0.10
Total					**286.28**
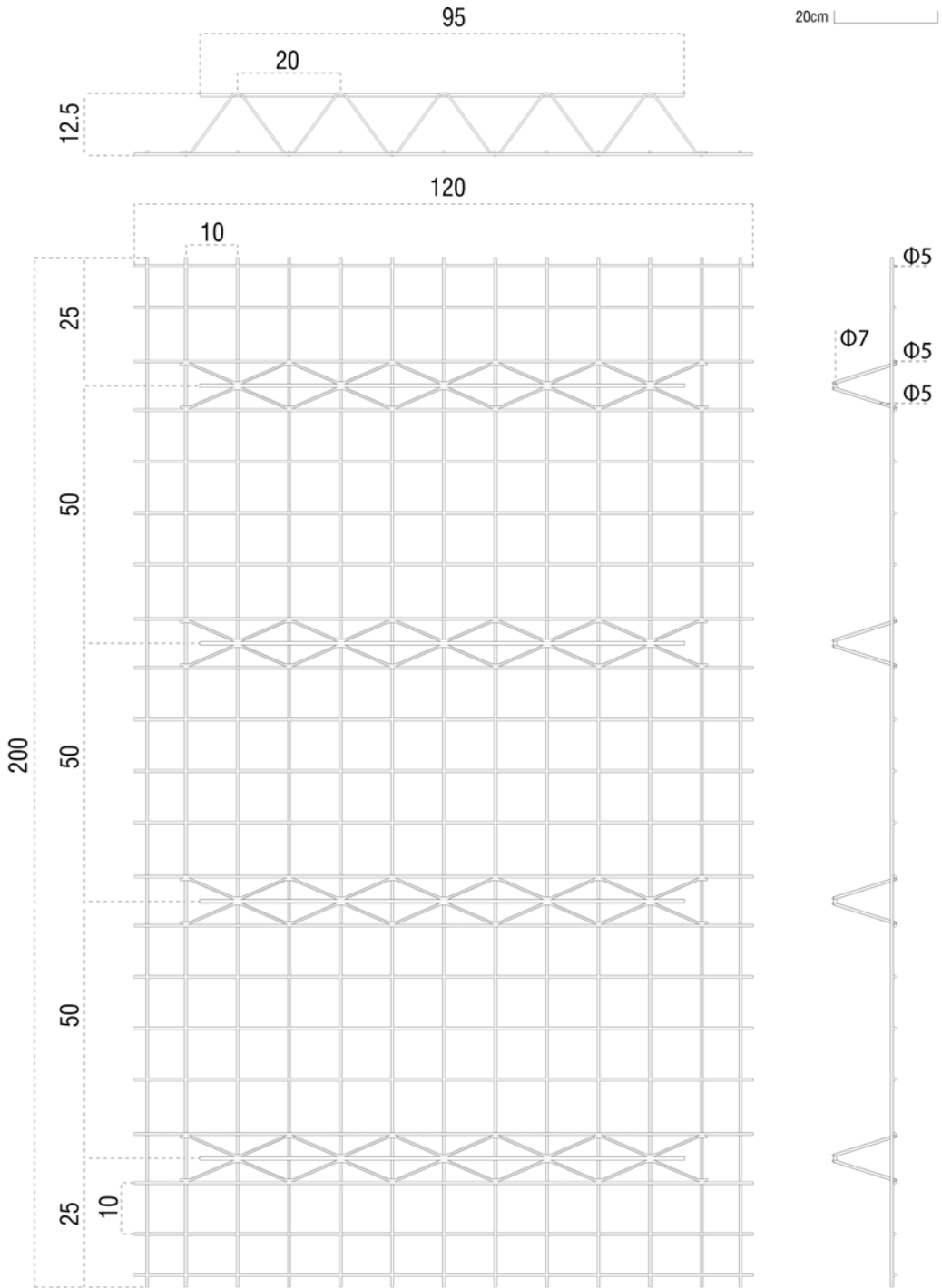
Fig. 4.5-3 - Arrangement of the module reinforcement. Source: Author

94

SECTION A-A

SECTION D-D

SECTION C-C

20cm

SECTION B-B
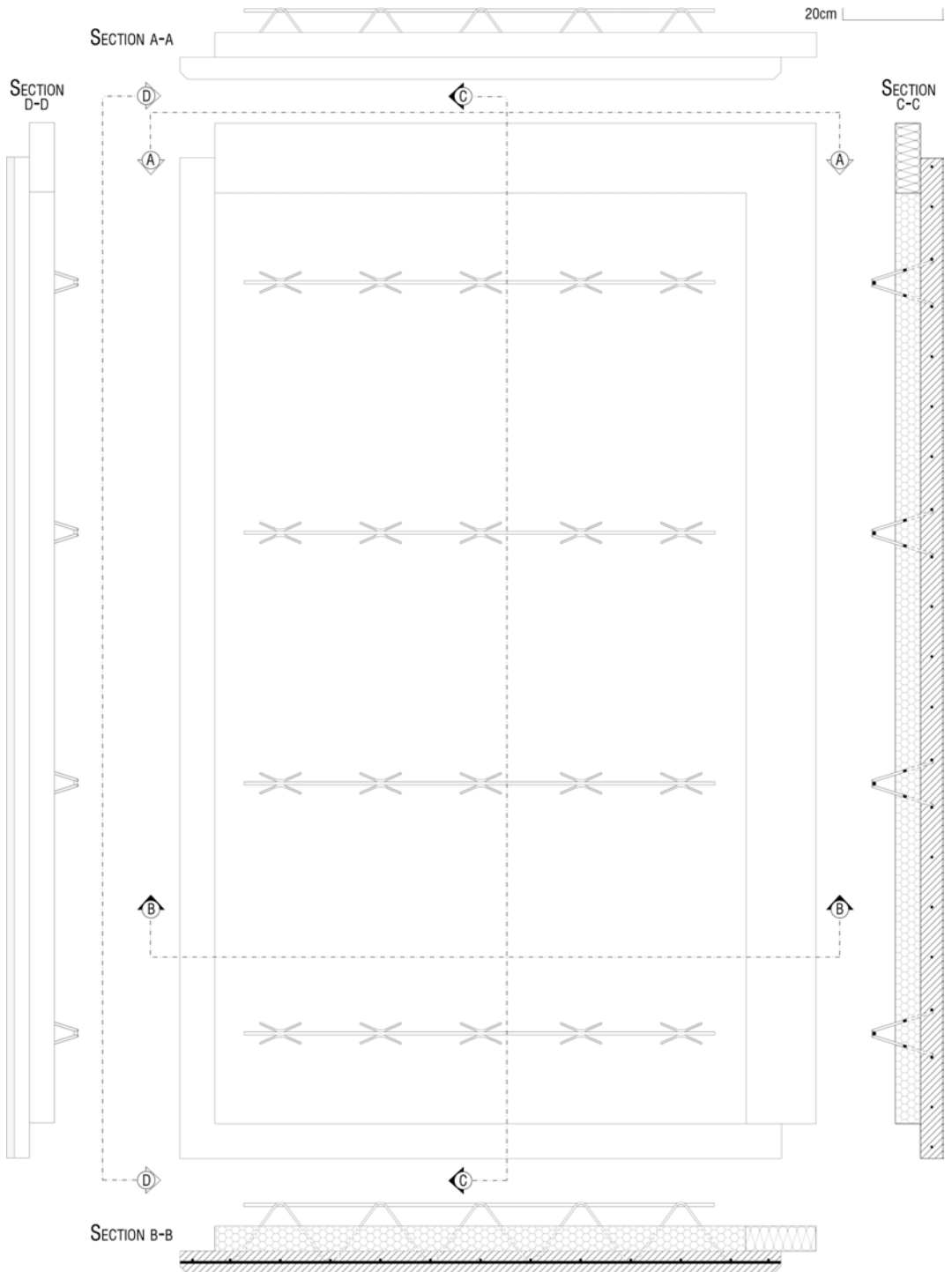
Fig. 4.5-4 - The technical drawings of the novel PC panel. Source: Author

4.5.3   Composition and junctions

The novel PC panels are designed to be composed as "puzzle pieces" due to their internal layer staggered from the external slab to create the male-female junctions. The two layers have the same size (1.2m x 2m), although, as the inner layer slides upwards and to the right side, protruding 7 cm from the top and right edges of the panel, they create the male waiting joints for the juxtaposition of the next and upper panel.

Since they have the same configuration, their female joints assemble with the male of the waiting panel (Figure 4.5-5).
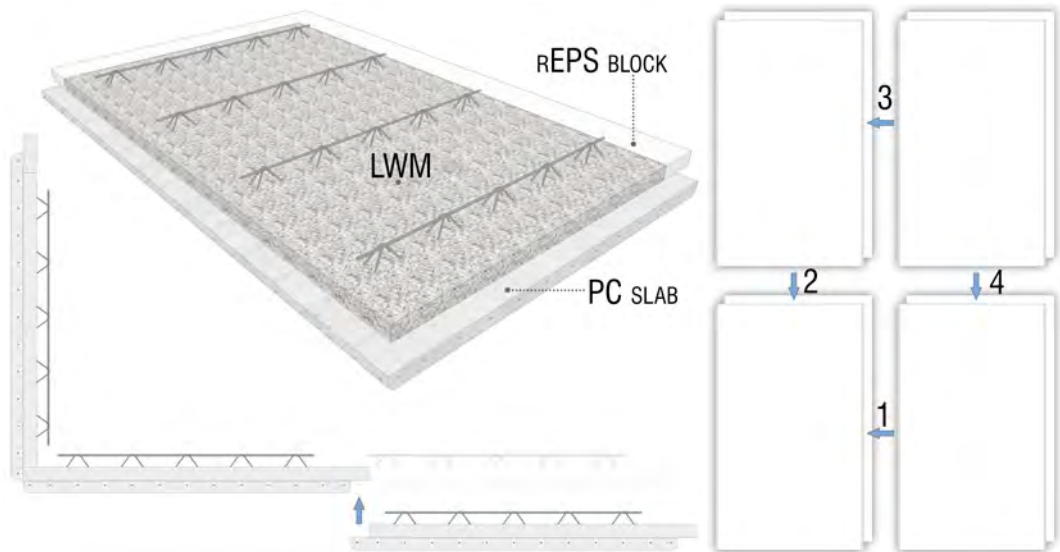
Fig. 4.5-5 - The panel composition: male-female junctions. Source: Author

In this way, the risk of generating thermal bridges at the connections between the panels is eliminated. To validate such assumption and verify that the presence of steel reinforcements does not influence excessively the heat flow in the section, a graphical assessment was carried out. In this way, a finite element method by means the software COMSOL Multiphysics for heat transfer studies in steady-state conditions was employed, to verify the heat flux and temperature distribution in the panel sections. The boundary conditions set for the study are been explained in the section 4.2. The overall 3D evaluation of the junctions in correspondence of the juxtaposition of four panels was carried out through the observation of the isocurves evolution (Figure 4.5-6). In addition, more

detailed 2D analyses were carried out, taking into account several significant sections in which thermal bridges occurring (Figure 4.5-7a) section xy; b) section xz).
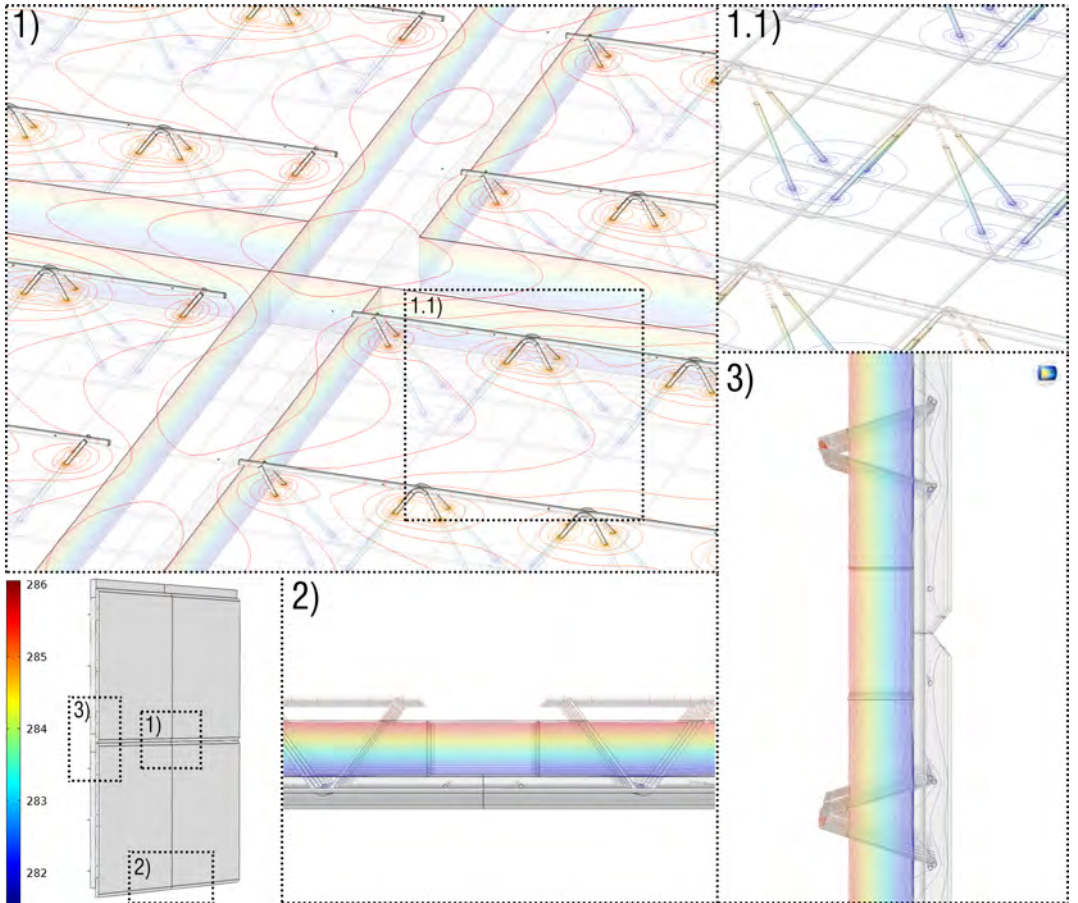
Fig. 4.5-6 - 3D evaluation of the heat flux through the junctions of the four panels. Source: Author
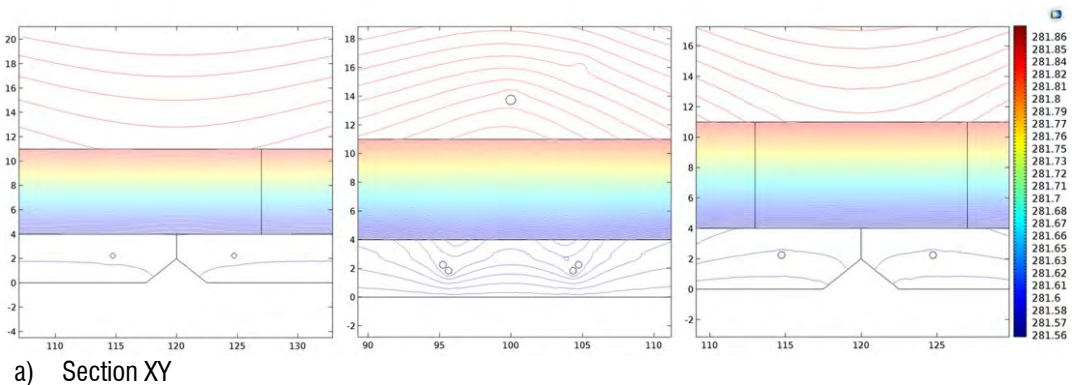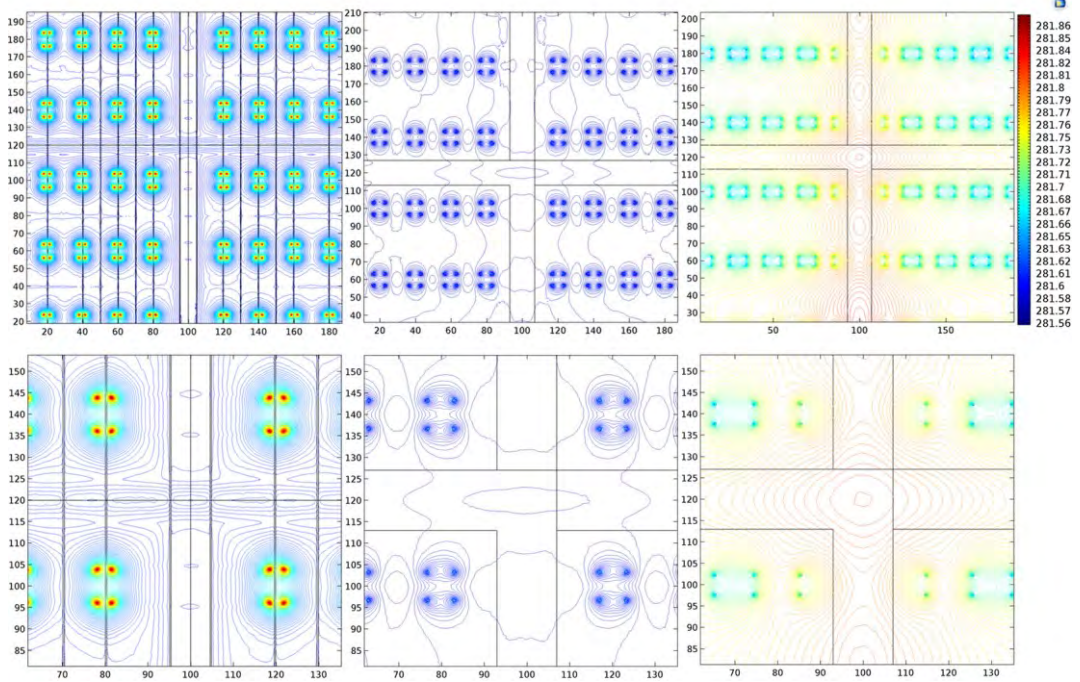
a)   Section XY

b) Section XZ

Fig. 4.5-7 - 2D evaluation of the heat flux in significant sections. Source: Author

The distribution of the isocurves into the sections was uniform and confirm the absence of thermal bridges. If they occurred, a flux deviation would be created in correspondence of the junction between the panels. It became irregular in presence of the steel rebar and lattices, in which a sudden temperature change occurred due to the property of the iron to conduct the heat. Therefore, as the lattices crossed the panel layers having different temperatures, they conducted the heat toward the outside of the panel, deflecting the flow. Nevertheless, the thermal performance was not affected, validating the panel composition.

4.5.4   Cladding typologies

One of the advantages in using the PC panels is the possibility to integrate the external cladding already during the prefabrication process, avoiding the typical waste of time due to the building finishes after retrofitting. Many types of cladding may be embedded into the concrete casting i.e. bricks (Figure 4.5-8 a), ceramic tiles (Figure 4.5-8 b), stones

(Figure 4.5-8 c), and others. However, the PC panel can be used also without any cladding, leaving the concrete exposed (Figure 4.5-8 d) or covered in situ with the plaster technique (Figure 4.5-8 e). At any case, they can restore aesthetic dignity to the building and increase the thermal properties of the external wall.

a)　　　　　　　b)　　　　　　　c)　　　　　　　d)　　　　　　　e)
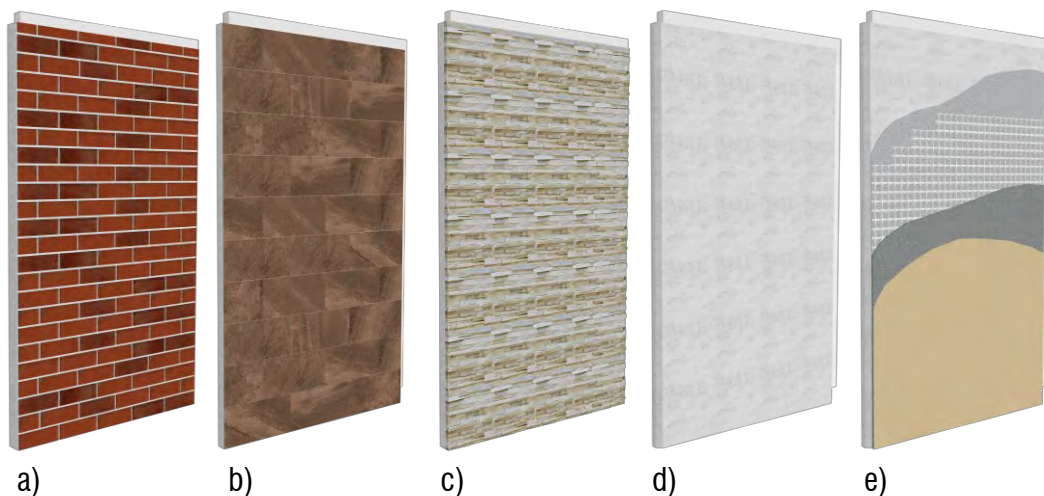
Fig. 4.5-8 - Panel cladding: a) brick cover; b) ceramic cover; c) stone cover. Source: Author

However, the junctions between the panels remains visible. They should be filled in situ, at panel installation completed. To overcome this problem, a partial prefabricated cladding methodology can be used. It consists in embedding some light aluminium shaped mullions into concrete, which clip technology allows mounting the strips in site and hide the junctions. Therefore, it permits using materials that need maintenance e.g. wood products thanks to the possibility to remove easily the elements from the façade (Figure 4.5-9).

PLAN VIEW

1. PC panel
2. Aluminium mullion
3. Wood strip
4. Clip device

SIDE VIEW
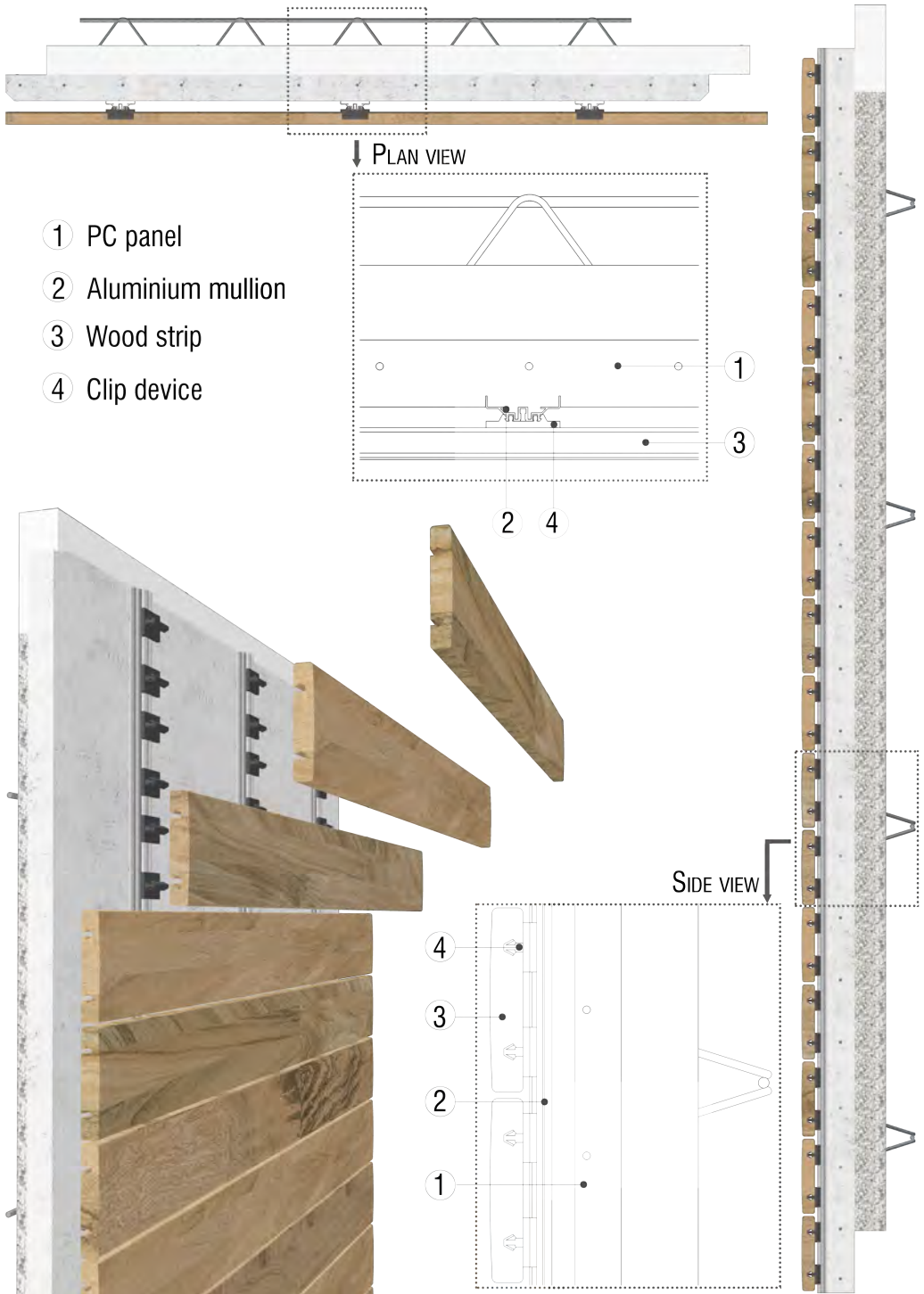
Fig. 4.5-9 - Panel cladding: wood cover with the mullion-clip system. Source: Author

The choice of the cladding type depends on several factors related to the context in which should be inserted, e.g. climate, neighbourhood, and technical aspects e.g. time and needs of production, installation, technical properties, and economic sustainability.

The use of heavy materials provokes the increasing in panel thickness and weight involving specific machineries and more caution in the handling, transportation and installing phases. Many particular measures for the correct work execution in the factory and in the construction site should be taken in account, according to the rules of workers prevention and protection on the work. In particular, the caution during the movement phases should be considered as well as the need of scaffolds, props and anchorages. It also requires a retail labour for arranging the pieces on the formwork, increasing the times and costs for fabrication. Moreover, the type of vehicle required and the number of trips to deliver the panels from the factory to the construction site depend on the size, the weight, the arrangement, and the maximum number of panels. Since several wooden beams to separate the panels in height and protect their cladding should be considered, the permissible load of vehicle would reduce of about 2%. Therefore, loading the vehicle with a limited number of panels, more trips are required.

In general, the most used vehicles for conventional precast modules up to 3 m in height are the articulated lorry and the combined truck with tractor and trailer. The Italian road regulation lays down the limits in size and the permissible weight of vehicle bodies. Indeed, articulated lorry shall not exceed 16.50 m in length and 2.50 m in width with bodies 12.50 m or 13.60 m long. The elements should be arranged in height up to 2.50 m with a limit in load of 300 quintals.

The combined truck can be 8 m long maximum, 2.50 m wide with a 6 m long trailer. The permissible load and height are 150 quintals and 2.50 m, respectively. If they enclose the crane to move and install the elements on the building façade, the deliverable load decreases of about the crane weight (DM n. 495, 1992).

In order to have a reference frame of the criteria to consider in the cladding choice regarding the realization complexity (Figure 4.5-10 a), the type of vehicles to involve and the numbers of trips required (Figure 4.5-10b), a rough estimate has been performed, considering a load of 200 panels and six different cladding types: exposed concrete (the base panel without any coating), wood strips (Figure 4.5-9), bricks (Figure 4.5-8 a), ceramic tyles (Figure 4.5-8 b), stones (Figure 4.5-8 c) and traditional plaster.

REALIZATION COMPLEXITY

a)

CLADDING TYPE	ADDITIONAL WORK IN FACTORY	INSTALLATION ON SITE	ADVANTAGES
EXPOSED CONCRETE	EPS formworks production for the substrate elements protection	Props are needed along the corners and in the presence of openings	Speed of production and installation
WOOD STRIPS	Formworks disposition on the manufacturing tray and aluminium mullions inserting; Caution during the movimentation phases	Final wooden strips installation on the panels; Scaffold installation is required; Longer installation times; All the requirements for the base panel are valid	Uniform cladding of the facade; Joints between panels not visible; good aestetic aspect
BRICKS	Detailed bricks' disposition along the rows and staggering the vertical joints; Longer production times	Stiffening of anchors due to the weight increasing; Scaffold installation required; Filling of joints between the panel after installation; All the requirements for the base panel are valid	Good aestetic aspect
CERAMIC TYLES	Detailed tiles' disposition along the rows	Scaffold installation is required; Filling of joints between the panel after installation; All the requirements for the base panel are valid	Good aestetic aspect
STONES	Disposition of the stones according to the architectural design	Stiffening of anchors due to the weight increasing; All the requirements for the base panel are valid	Good aestetic aspect
PLASTER		Supply and installation of exterior plaster and painting according to the project; Scaffold installation is required; All the requirements for the base panel are valid; Longer working times	

REQUIRED VEHICLES AND TRIPS

b)

	PANEL DETAILS			ARTICULATED LORRY								REQUIREMENTS					TOTAL TRIPS	
CLADDINGS	WEIGHT	THICKNESS (production)	THICKNESS + WOOD BEAMS	MAXIMUM NUMBER OF PANELS height	length	[kg]	outwight excess		PANELS PER TRIP	TRIPS (full capacity)		TOTAL PANELS DELIVERED	REMAINING PANELS	[kg]	REQUIRED VEHICLE	TRIPS	A	D
	[kg/panel]	[m]	[m]		[m]	[kg]			[n]	[n]		[n]	[n]	[kg]	[n]	[n] [condition]		
EXPOSED CONCRETE	286,28	0,15	0,40	6	12	19753	-	-	72	2,78	2	144	57	16318	A	0,56 1 HALF LOAD	2	-
WOOD STRIPS	331,28	0,18	0,43	5	12	21125	-	-	60	3,33	3	180	21	6957	D	0,24 1 HALF LOAD	3	-
BRICKS	388,28	0,18	0,43	5	12	24760	-	-	60	3,33	3	180	21	8154	D	0,28 1 HALF LOAD	3	-
CERAMIC TYLES	341,48	0,16	0,41	6	12	22937	-	-	72	2,78	2	144	57	19464	A	0,66 1 ALMOST FULL	2	-
STONE	482,12	0,18	0,43	5	12	30744	1344	3	57	3,50	3	172	29	14155	D	0,48 1 HALF LOAD	3	-
PLASTER	286,28	0,15	0,40	6	12	19753	-	-	72	2,78	2	144	57	16318	A	0,56 1 HALF LOAD	2	-

ARTICULATED LORRY (A) 29400 kg (maximum capacity)
DRIVING MACHINERY (D) 14700 kg (maximum capacity)

Fig. 4.5-10 - Rouge estimation of the parameters " Realization complexity" and " Required vehicles and trips" to consider to choose the panel cladding

4.6   The intelligent PC panel system

The "Intelligent PC panel system" (IPCS) is a novel technological proposal for the existing RC building retrofitting aiming at the energy and structural performance improvement. It is also predisposed to be easily equipped with monitoring devices to control the performance trend of the building façade over time. The system provides the possibility to inspect, maintain and replace them anytime in case of malfunctioning.

The technology is designed to be applied only on the external side of the existing façade, without the need to evacuate occupants from the building. Moreover, its components allow executing quickly and easily the installing phases, requiring the installation of the props only in correspondence of the openings. Since the system intents to improve the economic-popular buildings (EPBs) built in the post-WW2 which are often degraded and neglected from the aesthetic point of view, it can restore their dignity, conferring a new architectural aspect thanks to the integration of the cladding in the PC modules, personalized as required. It can adapt easily to the context and the façade on which is applied. If the building has balconies or loggias, it is assumed the integration of traditional methods of energy recovery, e.g. the External Thermal Insulation Cladding System (ETICS). If it had ornamental elements without artistic importance, they would be covered by the system and reproduced in EPS, if required.

The Figure 4.6-1 shows the model of the innovative retrofitting PC panel system.

After designing the PC panel that characterizes the system, according to the *System scale* of detail of the general design strategy, the project of the connections, reinforcement and completing of the system, applied at the existing building, is carried out.

In particular, the following subsections aim to define the procedure to estimate the detailed physical and dimensional properties of the system components as well as to individuate the approach for the preliminary assessments of the thermo-hygrometric and structural behaviour of the system by performing only numerical attempts and qualitative analyses. In addition, a preliminary method to choose the system cladding is presented based on analytical hierarchy process (AHP) approach since many qualitative criteria should be considered. Finally, a pilot monitoring approach is described and illustrated.
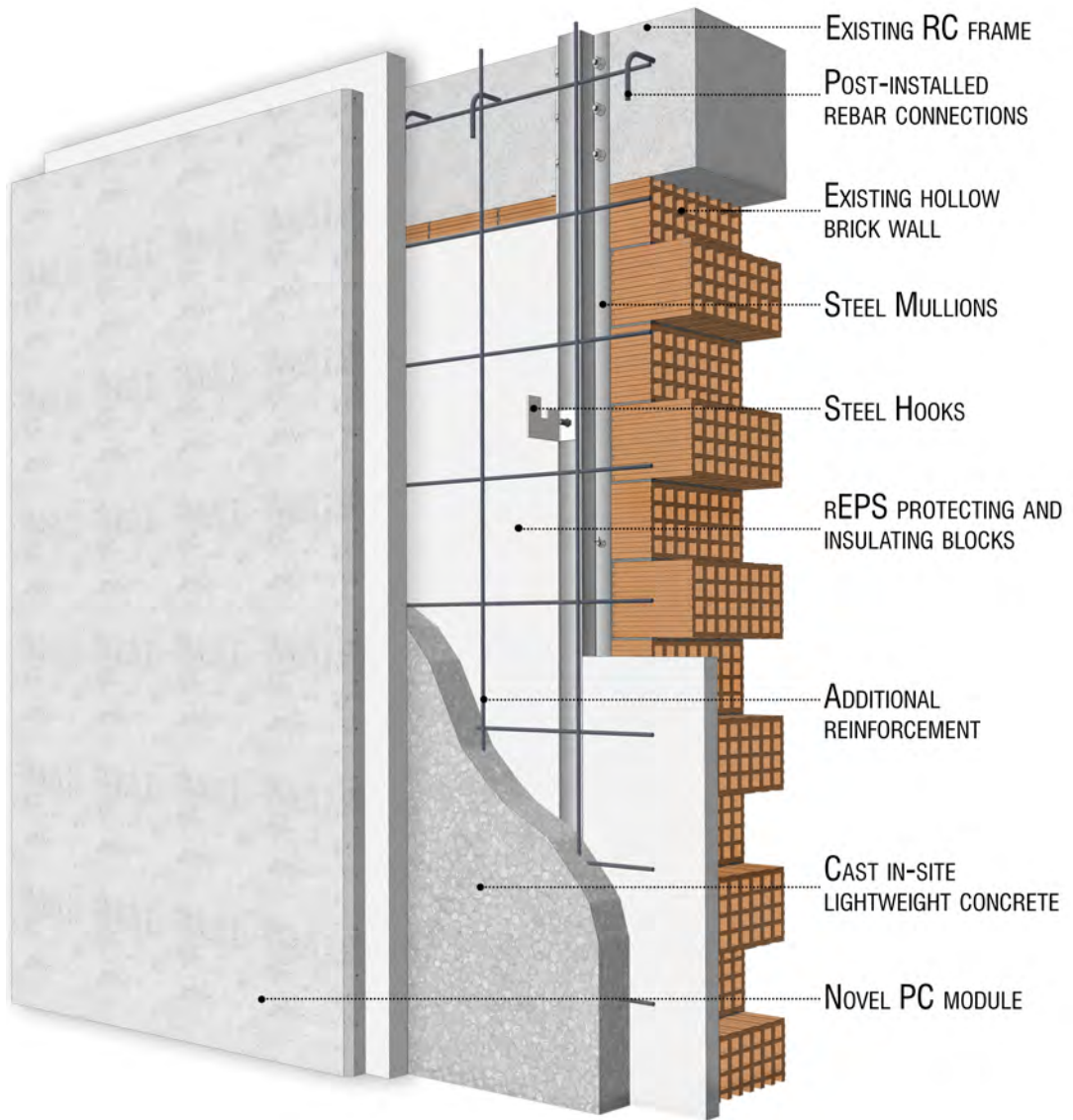
Fig. 4.6-1 - The innovative retrofitting PC panel system. Source: Author

Labels in figure:
- Existing RC frame
- Post-installed rebar connections
- Existing hollow brick wall
- Steel Mullions
- Steel Hooks
- rEPS protecting and insulating blocks
- Additional reinforcement
- Cast in-site lightweight concrete
- Novel PC module

4.6.1 System components and design technology

The design ideology of the technological system takes in account the compatibility of the novel building components with the existing materials and constructed methods. Since every existing building has its characteristics and technical properties, this doctoral thesis proposes the design and the preliminary assessment of the system technology for the retrofit of the building typology specified in the section 4.2. However, from a technological point of view, the system is easily adaptable to different building typologies; the technical details, the element dimensioning, calculation, and the performance assessment should be carried out case by case in function of the properties, dimensions, and loads. To assess the energy and structural performance for the definition of the thermal coat and structural layer thickness of the system, a preliminary building survey should be carried out.

In general, the technological system is a sort of double layered RC slab wall in which the external layer is the innovative PC module, described in the previous section, and the internal one is the existing façade, joined by a lightweight structural concrete (LWSC) casting onsite. More in detail, the technology consists in integrating the existing facade with a series of empty steel mullions equipped with some hooks positioned to receive the PC modules, connect them to the facade and ensure their vertical position. The mullion-hooks technology replaces the props as it performs the function of retaining the panel from the inside. The mullions have a hollow section allowing the insertion of the performance monitoring devises. The system is placed close to the facade and connected to the RC frame by means of suitable post-installed rebars. It does not burden the existing structure because it has its own continuous foundation along the portions to which it is applied, also connected to the existing one by post-installed rebars. In this way, the renovated building would result stiffened and strengthened.

The building wall is protected with a rEPS coat to avoid the expulsion of the bricks towards the inside for the hydrostatic pressure due to the LWSC casting onsite. It also improves the energy performance of the whole system. The insulating blocks are disposed up to 5 cm from the frame, leaving free the joints between beams, pillars and wall

to strengthen them by means the cast-in-place concrete. Since the mullions are in steel, they may create punctual thermal bridges in the wall section. Hence, at the contact with the wall, the mullions are insulated by thermal joints running along its height.

The system components can be classified into four macro categories: PC elements, thermo-insulating materials, metallic components, and conglomerates. The precast concrete elements are the novel PC panels described in the section 4.5. Their dimensions and trusses arrangement may vary for aesthetic needs and adaptation to the existing building, within the specified limits. However, in this doctoral thesis, the standard module is considered (1.2 m in width and 2 m in length).

The thermo-insulating material, used for the brick protecting coat is in 0 km recycled EPS, from Ferramati's industrial waste, in accordance with the project goal of the environmental sustainability. It is in blocks with mean density of 10 kg/m^3 and λ-value of 0.04 W/mK. As it can be associated to the virgin type EPS30 from the Ferramati's technical sheet, the other characteristics are specified in the section 3.4.2.

The characteristics and the design methodology of the metallic components and the conglomerates are explained below.

4.6.1.1 Metallic components

The distinguishing elements of the system are the steel mullions and hooks used to connect the PC modules to the existing building façade. Thanks to accurately designed anchoring elements, used to fix them to the existing RC frame, they are fundamental for the system tightness during the mounting phase of PC modules, the cast-in-place LWSC and for the monitoring stage. The mullions are in hot galvanised steel for structural use, type S235JR, thickness (t) 30/10 mm, classified according to NTC18, EN 10025:2-2019 and EC3. In particular, they have a hot rolled omega profile, suitably shaped for the monitoring sensors lodging in the core and for the anchoring positioning into the slots, dimensioned and spaced according to the anchoring determination.

The hooks are specially designed to meet the lattices girders and sustain the PC panels. They are in hot galvanised steel for structural use, type S235JR like the mullions to avoid electrochemical incompatibility, t 50/10 mm to withstand the traction forces induced by

the panels from the moment of the installation to the cast-in-place concrete. Their length determines the concrete layer thickness which have to be defined in accordance with the results of the preliminary structural analyses aiming at understanding the building behaviour with the applied system. The methodological approach employed to perform such analyses is outlined in the next sections. Preliminary, the hooks length is supposed to be 9.5 cm. The table 4.6-1 summarized the technical characteristics of the steel type S235JR used for mullion and hooks by NTC18, EN 10025-2:2019, and EC3.

Table 4.6-1. Steel S235JR: technical characteristics

f_{yk}	f_{tk}	f_{yd}	ν	E_s	G	ε_y	ρ	λ
MPa	MPa	MPa	-	MPa	MPa	%	kg/m³	W/mK
235	360	204.35	0.3	210000	80769	15.70	7850	79

where:
- f_{yk} is the characteristic yield strength;
- f_{tk} is the characteristic tension strength;
- f_{yd} is the design strength;
- ν is the Poisson's ratio;
- E_s is the modulus of elasticity;
- G is the transverse modulus of elasticity;
- ε_y is the characteristic deformation;
- ρ is the steel density;
- λ is the thermal conductivity coefficient

The hooks are hold to the mullions through bolted connections, suitably designed at shear and traction forces in accordance with NTC18 and EC3. In particular, after estimating the values of the design shear and tensile forces ($F_{v,Ed}$, $F_{t,Ed}$) and assuming the bolt resistance class of 8.8 and diameter d_0, 12 mm (M12), the design shear, and tensile resistances ($F_{v,Rd}$, $F_{t,Rd}$) are calculated with the following formulas:

- Resistance to shear loads
$$F_{v,Rd} = \frac{0.6 f_{ub} A_s}{\gamma_{Ms}} \qquad \text{[N]} \qquad (14)$$

- Resistance to tension loads
$$F_{t,Rd} = \frac{0.9 f_{ub} A_s}{\gamma_{Ms}} \qquad \text{[N]} \qquad (15)$$

where:
- f_{ub} is the nominal value of the ultimate tensile strength for bolts by EC3:

Bolt class	4.6	4.8	5.6	5.8	6.8	8.8	10.9
f_{yb} (N/mm²)	240	320	300	400	480	640	900
f_{ub} (N/mm²)	400	400	500	500	600	800	1000

- A_s is the tensile resistance area of the bolt equal to 84 mm² for bolts M12;

- γ_{Ms} is the steel partial safety factor equal to 1.25.

The first verification of the bolt eligibility is performed with the following formulas:

$$F_{v,Ed} \leq F_{v,Rd} \qquad (16)$$

$$F_{t,Ed} \leq F_{t,Rd} \qquad (17)$$

The combined shear and tension action are also verified by the next proof:

$$\frac{F_{v,Ed}}{F_{v,Rd}} + \frac{F_{t,Ed}}{1.4F_{t,Rd}} \leq 1.0 \qquad (18)$$

If such checks are satisfied, the bolt in question is suitable for the use for which it is designed. The minimum value of the bolt distance from the plate edge e_1 is $1.2d_0$ (CEN, 2004). In Figure 4.6-2 a) the characteristics of the bolts and b) the combined shear and tension actions to which the bolted mullion-hook is subjected are illustrated in accordance with EC3 and DIN EN ISO 4032. The Figure 4.6-3 illustrates the bolted mullion-hook technology.
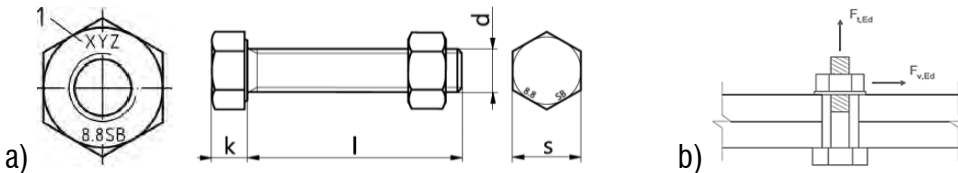
Fig. 4.6-2 – Bolted unions: a) dimensions; b) combined actions. Source: DIN EN ISO 4032

STEEL MULLION

STEEL HOOK

Fig. 4.6-3 – Steel mullion, anchor and the bolted technology. Source: Author

To assure a strength connection of the mullions to the existing RC beams the chemical anchoring method is used. The anchorages are hot galvanized steel threaded bars, nuts and washers of resistance class 8.8 and the injection mortar is a two-component epoxy resin with characteristics in compliance with the European Technical Approval ETA-07/0260. The mechanical properties of the steel threaded bars are supplied by the EN ISO 898-1:2013 which classifies the values according to the resistance classes and the bar diameters. In the Table 4.6-2 the mechanical characteristics of the steel threaded bars with resistance class 8.8 are reported.

Table 4.6-2. Threaded bar physical properties, class 8.8, according to EN ISO 898-1:2013

MECHANICAL PROPERTY		TREATED BAR DIAMETER										
		M8	M10	M12	M16	M20	M24	M27	M30	M33	M36	M39
Characteristic nominal ultimate strength [MPa]	f_{uk}	700	700	700	700	700	700	700	700	700	700	700
Characteristic yield strength [MPa]	f_{yk}	450	450	450	450	450	450	450	450	450	450	450
Nominal stress area [mm²]	A_s	36.6	58	84.3	157	245	353	459	561	694	817	976

The design of the dimensional characteristics i.e. the bar diameter and the anchor length is fundamental to ensure the good connection between the elements and prevent the release or breakage of the anchors. The methodological approach follows the procedure of the ETAG 001 and its Annex C and EOTA TR 029, assuming as standard assessment that the value of the design actions S_d does not exceed the value of the design resistance R_d (EOTA TR 029, 2007; ETAG 001-ANNEX C, 2010; ETAG 001, 2013). Therefore, after evaluating the loads acting on the anchors in function of the connection conditions (Figure 4.6-4), the design method consists in computing the steel resistances of the anchors at the ultimate limit state of steel and concrete failures under tension and shear loads.
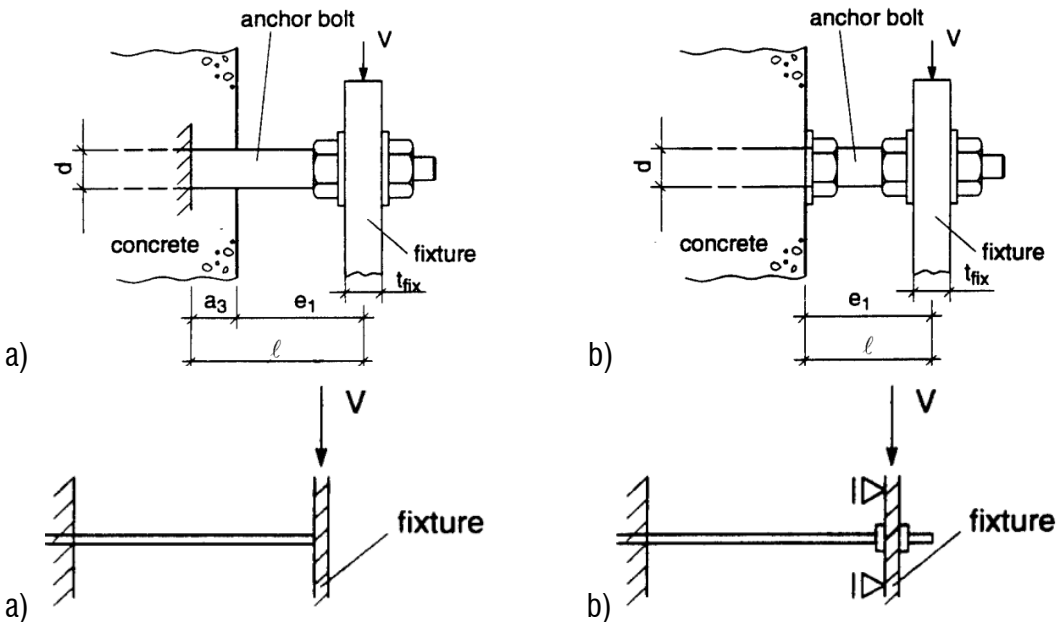
Fig. 4.6-4 – Anchor bolt conditions. Source: ETAG 001-ANNEX C

Thanks to the ETA-07/0260, the reference values of the installation parameters of the anchors are expressed, guiding to the preliminary choice of the anchor characteristics, illustrated in Figure 4.6-5a (ETA-07/0260, 2017). In Figure 4.6-5b the spacing parameters of the anchor group to estimate are illustrated.

a)   b)
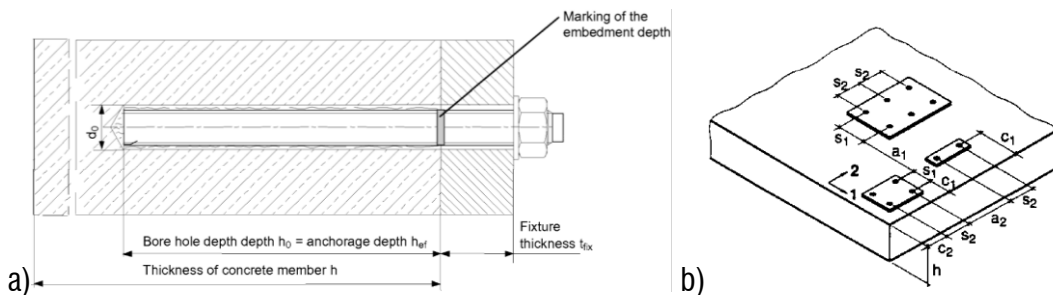
Fig. 4.6-5 – Chemical injection: a) anchor geometric characteristics by ETA-07/0260; b) spacing parameters of anchor groups by ETAG 001

Hence, considering these data, the values of steel failure $N_{Rd,s}$, combined pull-out and concrete cone failure $N_{Rd,p}$, the only concrete cone failure $N_{Rd,c}$ and splitting failure $N_{Rd,sp}$ are calculated and assessed with the related design values as in Figure 4.6-6.

	single anchor	anchor group	
steel failure	$N_{Sd} \leq N_{Rk,s} / \gamma_{Ms}$	$N_{Sd}^h \leq N_{Rk,s} / \gamma_{Ms}$	
pull-out failure	$N_{Sd} \leq N_{Rk,p} / \gamma_{Mp}$	$N_{Sd}^h \leq N_{Rk,p} / \gamma_{Mp}$	
concrete cone failure	$N_{Sd} \leq N_{Rk,c} / \gamma_{Mc}$		$N_{Sd}^g \leq N_{Rk,c} / \gamma_{Mc}$
splitting failure	$N_{Sd} \leq N_{Rk,sp} / \gamma_{Msp}$		$N_{Sd}^g \leq N_{Rk,sp} / \gamma_{Msp}$

Fig. 4.6-6 – Proofs to evaluate of the anchor resistance to tension load. Source: ETAG 001-ANNEX C

$N_{Rd,p}$ and $N_{Rd,c}$ are tabulated in ETA-07/0260 by steel classes and bar diameters. The other resistances are obtained by the following formulas:

Steel Failure
$$N_{Rd,s} = \frac{N_{Rk,s}}{\gamma_{Ms}} = \frac{A_s \cdot f_{uk}}{\gamma_{Ms}} \qquad \text{[kN]}$$
(19)

Splitting failure $$N_{Rd,sp} = \frac{N_{Rk,c} \cdot f_B \cdot f_{1,sp} \cdot f_{2,sp} \cdot f_{3,sp} \cdot f_{h,N} \cdot f_{re,N}}{\gamma_{Msp}} \quad [kN] \quad (20)$$

where:

- γ_{Ms} is the partial safety factor for steel failure under tension loads, equal to 1.4;
- γ_{Msp} is the partial safety factor for splitting failure, equal to 1.5;
- A_s, f_{uk} are tabulated in table 4.6 2;
- $f_B, f_{1,sp}, f_{2,sp}, f_{3,sp}, f_{h,N}, f_{re,N}$ are the influencing factors which depends on the concrete class and are tabulated in ETA-07/0260 (Figure 4.6-7) according with the setting details in Figure 4.6-8:

Concrete strength designation (ENV 206)	C 20/25	C 25/30		C 30/37	C 35/45		C 40/50	C 45/55		C 50/60
$f_B = (f_{ck,cube}/25 N/mm^2)^{1/2}$ [a]	1	1,1		1,22	1,34		1,41	1,48		1,55
$c/c_{cr,N}$ / $c/c_{cr,sp}$	0,1	0,2	0,3	0,4	0,5	0,6	0,7	0,8	0,9	1
$f_{1,N} = 0,7 + 0,3 \cdot c/c_{cr,N}$ / $f_{1,sp} = 0,7 + 0,3 \cdot c/c_{cr,sp}$	0,73	0,76	0,79	0,82	0,85	0,88	0,91	0,94	0,97	1
$f_{2,N} = 0,5 \cdot (1 + c/c_{cr,N})$ / $f_{2,sp} = 0,5 \cdot (1 + c/c_{cr,sp})$	0,55	0,60	0,65	0,70	0,75	0,80	0,85	0,90	0,95	1
$s/s_{cr,N}$ / $s/s_{cr,sp}$	0,1	0,2	0,3	0,4	0,5	0,6	0,7	0,8	0,9	1
$f_{3,N} = 0,5 \cdot (1 + s/s_{cr,N})$ / $f_{3,sp} = 0,5 \cdot (1 + s/s_{cr,sp})$	0,55	0,60	0,65	0,70	0,75	0,80	0,85	0,90	0,95	1
h_{ef} [mm]	40	50		60	70		80	90		≥ 100
$f_{re,N} = 0,5 + h_{ef}/200mm \le 1$	0,7 [a]	0,75 [a]		0,8 [a]	0,85 [a]		0,9 [a]	0,95 [a]		1

Fig. 4.6-7 – Tabulated concrete influencing factors. Source: ETA-07/0260

Anchor size			M8	M10	M12	M16	M20	M24	M27	M30
Nominal diameter of drill bit	d_0	[mm]	10	12	14	18	24	28	30	35
Effective anchorage and drill hole depth range [a)]	$h_{ef,min}$	[mm]	40	40	48	64	80	96	108	120
	$h_{ef,max}$	[mm]	160	200	240	320	400	480	540	600
Minimum base material thickness	h_{min}	[mm]	h_{ef} + 30 mm ≥ 100 mm			h_{ef} + 2 d_0				
Diameter of clearance hole in the fixture	d_f	[mm]	9	12	14	18	22	26	30	33
Minimum spacing	s_{min}	[mm]	40	50	60	80	100	120	135	150
Minimum edge distance	c_{min}	[mm]	40	50	60	80	100	120	135	150
Critical spacing for splitting failure	$s_{cr,sp}$		2 $c_{cr,sp}$							
Critical edge distance for splitting failure [b)]	$c_{cr,sp}$	[mm]	**1,0·h_{ef}** for h / h_{ef} ≥ 2,0; **4,6 h_{ef} – 1,8 h** for 2,0 > h / h_{ef} > 1,3:; **2,26 h_{ef}** for h / h_{ef} ≤ 1,3:							
Critical spacing for concrete cone failure	$s_{cr,N}$		2 $c_{cr,N}$							
Critical edge distance for concrete cone failure [c)]	$c_{cr,N}$		1,5 h_{ef}							
Torque moment [d)]	T_{max}	[Nm]	10	20	40	80	150	200	270	300

Fig. 4.6-8 – Setting details. Source: ETA-07/0260

The tensile resistance of the anchor is the lower value of the four calculated resistances. If the proofs are not verified, another anchor size should be considered.

Similarly, the steel failure under shear loads $V_{Rd,s}$, concrete pry-out failure $V_{Rd,cp}$, and concrete edge failure $V_{Rd,c}$ are calculated and compared with the related characteristic values as in Figure 4.6-9.

	single anchor	anchor group	
steel failure, shear load without lever arm	$V_{Sd} \leq V_{Rk,s} / \gamma_{Ms}$	$V_{Sd}^h \leq V_{Rk,s} / \gamma_{Ms}$	
steel failure, shear load with lever arm	$V_{Sd} \leq V_{Rk,s} / \gamma_{Ms}$	$V_{Sd}^h \leq V_{Rk,s} / \gamma_{Ms}$	
concrete pry-out failure	$V_{Sd} \leq V_{Rk,cp} / \gamma_{Mc}$		$V_{Sd}^g \leq V_{Rk,cp} / \gamma_{Mc}$
concrete edge failure	$V_{Sd} \leq V_{Rk,c} / \gamma_{Mc}$		$V_{Sd}^g \leq V_{Rk,c} / \gamma_{Mc}$

Fig. 4.6-9 – Proofs to evaluate of the anchor resistance to shear load. Source: ETAG 001-ANNEX C

$V_{Rd,s}$ is tabulated in ETA-07/0260 by anchor diameters, instead $V_{Rd,cp}$ and $V_{Rd,c}$ are calculated as follows:

Pry-out Failure

$$V_{Rd,cp} = lower(kN_{Rd,p}; kN_{Rd,c}) \qquad [kN] \qquad (21)$$

Concrete edge failure

$$V_{Rd,c} = \frac{V^0_{Rk,c} \cdot f_B \cdot f_\beta \cdot f_h \cdot f_4 \cdot f_{hef} \cdot f_c}{\gamma_{Mc}} \qquad [kN] \qquad (22)$$

where:
- $k = 1$ for $h_{ef} < 60 \ mm$; $k = 2$ for $h_{ef} \geq 60 \ mm$;
- γ_{Mc} is the partial safety factor for concrete and is equal to 1.5;
- $V^0_{Rd,c}$ is tabulated in ETA-07/0260 (Figure 4.6-10):

Anchor size		M8	M10	M12	M16	M20	M24	M27	M30
Non-cracked concrete									
$V^0_{Rd,c}$	[kN]	5,9	8,6	11,6	18,7	27,0	36,6	44,5	53,0
Cracked concrete									
$V^0_{Rd,c}$	[kN]	4,2	6,1	8,2	13,2	19,2	25,9	31,5	37,5

Fig. 4.6-10 – Tabulated values of design concrete edge resistance for one anchor. Source: ETA-07/0260

- $f_B, f_\beta, f_h, f_{hef} f_c$ are the influencing factors which depends on the concrete class and are tabulated in ETA-07/0260 and reported in Figure 4.6-11.

Angle ß		0°	10°	20°	30°	40°	50°	60°	70°	80°	≥ 90°
f_β		1	1,01	1,05	1,13	1,24	1,40	1,64	1,97	2,32	2,50
h/c		0,15	0,3	0,45	0,6	0,75	0,9	1,05	1,2	1,35	≥ 1,5
f_h =	$\{h/(1,5 \cdot c)\}^{1/2} \leq 1$	0,32	0,45	0,55	0,63	0,71	0,77	0,84	0,89	0,95	1,00
h_{ef}/d		4	4,5	5	6	7	8	9	10	11	
f_{hef} =	$0,05 \cdot (h_{ef} / d)^{1,68}$	0,51	0,63	0,75	1,01	1,31	1,64	2,00	2,39	2,81	
h_{ef}/d		12	13	14	15	16	17	18	19	20	
f_{hef} =	$0,05 \cdot (h_{ef} / d)^{1,68}$	3,25	3,72	4,21	4,73	5,27	5,84	6,42	7,04	7,67	
c/d		4	6	8	10	15	20	30	40		
f_c =	$(d / c)^{0,19}$	0,77	0,71	0,67	0,65	0,60	0,57	0,52	0,50		

Fig. 4.6-11 – Tabulated concrete influencing factors. Source: ETA-07/0260

- $f_4 = \left(\frac{c}{h_{ef}}\right)^{1.5} \cdot \left(1 + \frac{s}{3c}\right) \cdot 0.5$ for $\frac{c}{h_{ef}}$ values tabulated in Figure 4.6-12.

c/h_ef	Single anchor	Group of two anchors s/h_ef														
		0,75	1,50	2,25	3,00	3,75	4,50	5,25	6,00	6,75	7,50	8,25	9,00	9,75	10,50	11,25
0,50	0,35	0,27	0,35	0,35	0,35	0,35	0,35	0,35	0,35	0,35	0,35	0,35	0,35	0,35	0,35	0,35
0,75	0,65	0,43	0,54	0,65	0,65	0,65	0,65	0,65	0,65	0,65	0,65	0,65	0,65	0,65	0,65	0,65
1,00	1,00	0,63	0,75	0,88	1,00	1,00	1,00	1,00	1,00	1,00	1,00	1,00	1,00	1,00	1,00	1,00
1,25	1,40	0,84	0,98	1,12	1,26	1,40	1,40	1,40	1,40	1,40	1,40	1,40	1,40	1,40	1,40	1,40
1,50	1,84	1,07	1,22	1,38	1,53	1,68	1,84	1,84	1,84	1,84	1,84	1,84	1,84	1,84	1,84	1,84
1,75	2,32	1,32	1,49	1,65	1,82	1,98	2,15	2,32	2,32	2,32	2,32	2,32	2,32	2,32	2,32	2,32
2,00	2,83	1,59	1,77	1,94	2,12	2,30	2,47	2,65	2,83	2,83	2,83	2,83	2,83	2,83	2,83	2,83
2,25	3,38	1,88	2,06	2,25	2,44	2,63	2,81	3,00	3,19	3,38	3,38	3,38	3,38	3,38	3,38	3,38
2,50	3,95	2,17	2,37	2,57	2,77	2,96	3,16	3,36	3,56	3,76	3,95	3,95	3,95	3,95	3,95	3,95
2,75	4,56	2,49	2,69	2,90	3,11	3,32	3,52	3,73	3,94	4,15	4,35	4,56	4,56	4,56	4,56	4,56
3,00	5,20	2,81	3,03	3,25	3,46	3,68	3,90	4,11	4,33	4,55	4,76	4,98	5,20	5,20	5,20	5,20
3,25	5,86	3,15	3,38	3,61	3,83	4,06	4,28	4,51	4,73	4,96	5,18	5,41	5,63	5,86	5,86	5,86
3,50	6,55	3,51	3,74	3,98	4,21	4,44	4,68	4,91	5,14	5,38	5,61	5,85	6,08	6,31	6,55	6,55
3,75	7,26	3,87	4,12	4,36	4,60	4,84	5,08	5,33	5,57	5,81	6,05	6,29	6,54	6,78	7,02	7,26
4,00	8,00	4,25	4,50	4,75	5,00	5,25	5,50	5,75	6,00	6,25	6,50	6,75	7,00	7,25	7,50	7,75
4,25	8,76	4,64	4,90	5,15	5,41	5,67	5,93	6,18	6,44	6,70	6,96	7,22	7,47	7,73	7,99	8,25
4,50	9,55	5,04	5,30	5,57	5,83	6,10	6,36	6,63	6,89	7,16	7,42	7,69	7,95	8,22	8,49	8,75
4,75	10,35	5,45	5,72	5,99	6,27	6,54	6,81	7,08	7,36	7,63	7,90	8,17	8,45	8,72	8,99	9,26
5,00	11,18	5,87	6,15	6,43	6,71	6,99	7,27	7,55	7,83	8,11	8,39	8,66	8,94	9,22	9,50	9,78
5,25	12,03	6,30	6,59	6,87	7,16	7,45	7,73	8,02	8,31	8,59	8,88	9,17	9,45	9,74	10,02	10,31
5,50	12,90	6,74	7,04	7,33	7,62	7,92	8,21	8,50	8,79	9,09	9,38	9,67	9,97	10,26	10,55	10,85

Fig. 4.6-12 – Influence factor of anchor spacing and edge distance for concrete edge. Source: ETA-07/0260

The design shear resistance of the anchor is the lower value among $V_{Rd,s}$, $V_{Rd,cp}$, and $V_{Rd,c}$. The calculation is carried out for an anchor, so if the proofs are verified, they are also valid for the group of the six anchors provided in the project.

Since the hooks are positioned along the overall mullion length and not only near to the connection with the beams, they may provoke the deflection of the mullion when they receive the traction load of the panel. To prevent this phenomenon, several anchors in the hollow brick wall are required. Their alternate configuration along the wings of the mullion instead of two side-by-side, works to prevent the generation of tensions within a single brick, breakage or pulling out. Therefore, they keep the mullions close to the wall and in some cases help correcting factory imperfections.

The anchoring methodology is the chemical injection of hot galvanized steel threaded bars, nuts and washers of resistance class 8.8. The injection mortar is a two-component epoxy resin for anchorages in masonry which characteristics are in compliance with the ETA-13/1036 (ETA-13/1036, 2017). As the masonry is in hollow bricks, the use of the screen capsule that avoids the dispersion of the mortar inside the brick, is necessary. The design of the steel anchors follows the method by ETAG 029-ANNEX C on the basis

of ETA-13/1036 (ETAG 029-ANNEX C, 2013). In particular, it depends on the wall typology in which the anchoring is performed. Hence, it is necessary to identify the type of brick, its geometrical (Figure 4.6-13) and physical characteristics that ETA-13/1036 partially provides. Since the wall typology is defined in the section 4.2 of this thesis, the brick type is already determined. Its characteristics, derived from the manufacturer's data sheets, are reported in the table 4.6-3.
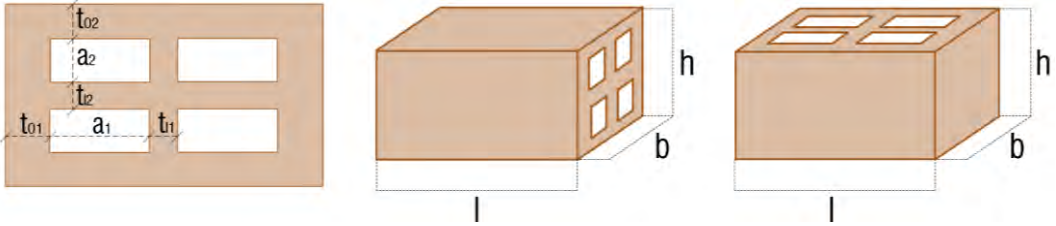
Fig. 4.6-13 – Identification of brick typology by its geometrical parameters. Source: ETA-13/1036

Table 4.6-3. Brick type characteristics

BRICK TYPE	l	b	h	t_{01}	t_{02}	t_{l1}	t_{l2}	a_1	a_2	ρ	f_b
	mm	mm	mm	mm	mm	mm	mm	mm	mm	Kg/dm^3	MPa
	250	250	120	12	12	10	12	22	24	1.1	27

As for the design of the anchorages in concrete, the geometric characteristics of the anchors are chosen from the reference tables of the technical approval reports. Figure 4.6-14 illustrates the two possible anchoring configuration and the related geometric parameters to estimate by the design approach.
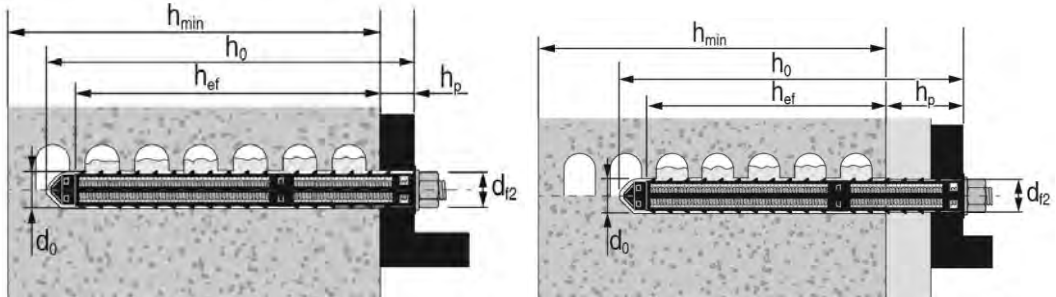
Fig. 4.6-14 – Anchoring configuration and geometric parameters. Source: ETA-13/1036

Hence, the anchor resistance to tension load is identified as the lower value among the resistances for failure of the metal part $N_{Rd,s}$, pull-out failure of the anchor $N_{Rd,p}$, brick breakout failure $N_{Rd,b}$, pull out of one brick $N_{Rd,pb}$, and if influenced by joints $\alpha_j N_{Rd,p}, \alpha_j N_{Rd,b}$. As for the previous procedure, $N_{Rd,s}$ is calculated with formula (19). $N_{Rd,p}$ normally equal to $N_{Rd,b}$ are tabulated in ETA-13/1036 by anchor and brick type. The other values are estimated using the following formulas:

Pull out of one brick
$$N_{Rd,pb} = 2 \cdot l \cdot b \cdot \frac{0.5 \cdot f_{vko} + 0.4 \cdot \sigma_d}{2.5 \cdot 1000} \qquad \text{[kN]} \qquad (23)$$

Influence of joints
$$N_{Rd,p} = N_{Rd,b} = \frac{\alpha_j N_{Rk,p}}{\gamma_{Mm}} \qquad \text{[kN]} \qquad (24)$$

where:
- f_{vko} is the initial shear strength by ETAG 029-ANNEX C:

Brick type	Mortar strength	f_{vko} [N/mm^2]
Clay brick	M2,5 to M9	0,2
	M10 to M20	0,3
All other types	M2,5 to M9	0,15
	M10 to M20	0,2

- σ_d is the design compressive stress perpendicular to the shear;
- α_j is a reductive factor used if the joints of the masonry are not visible;
- γ_{Mm} is the partial safety factor for masonry, equal to 2.5.

At the same way, to define the anchor shear resistance, the values of the failure of the metal part for shear loads $V_{Rd,s}$, local brick failure $V_{Rd,b}$, brick edge failure $V_{Rd,c}$, pushing out of one brick $V_{Rd,pb}$, and influence of joints $\alpha_j V_{Rd,p}, \alpha_j V_{Rd,b}$ are calculated by the next formulas:

Metal part
$$V_{Rd,s} = \frac{0.5 \cdot A_s \cdot f_{uk}}{\gamma_{Ms}} \qquad \text{[kN]} \qquad (25)$$

Hollow brick edge failure
$$V_{Rd,c,\|} = \frac{2.5}{\gamma_{Mm}} ; V_{Rd,c,\perp} = \frac{1.25}{\gamma_{Mm}} \qquad \text{[kN]} \qquad (26)$$

Pushing out of one brick

$$V_{Rd,pb} = 2 \cdot l \cdot b \cdot \frac{0.5 \cdot f_{vko} + 0.4 \cdot \sigma_d}{2.5 \cdot 1000} \qquad \text{[kN]} \qquad (27)$$

where:

- γ_{Ms} is the partial safety factor for steel failure under shear loads, equal to 1.25;

The proofs to perform are illustrated in Figure 4.6-15 by ETAG 029-ANNEX C. If they are verified, the anchor tensile and shear resistances are the lower values among the estimated ones.

Failure of the metal part	$N_{Sd}^h \leq N_{Rk,s} / \gamma_{Ms}$
Pull-out failure of the anchor	$N_{Sd}^h \leq N_{Rk,p} / \gamma_{Mm}$
Brick breakout failure	$N_{Sd} \leq N_{Rk,b} / \gamma_{Mm}$ $N_{Sd}^g \leq N_{Rk}^g / \gamma_{Mm}$
Pull out of one brick	$N_{Sd} \leq N_{Rk,pb} / \gamma_{Mm}$
Influence of joints	$N_{Sd} \leq \alpha_j N_{Rk,p} / \gamma_{Mm}$ $N_{Sd} \leq \alpha_j N_{Rk,b} / \gamma_{Mm}$

a)

Failure of the metal part, shear load without lever arm	$V_{Sd}^h \leq V_{Rk,s} / \gamma_{Ms}$
Failure of the metal part, shear load with lever arm	$V_{Sd}^h \leq V_{Rk,s} / \gamma_{Ms}$
Local brick failure	$V_{Sd} \leq V_{Rk,b} / \gamma_{Mm}$ $V_{Sd}^g \leq V_{Rk}^g / \gamma_{Mm}$
Brick edge failure	$V_{Sd} \leq V_{Rk,c} / \gamma_{Mm}$ $V_{Sd}^g \leq V_{Rk}^g / \gamma_{Mm}$
Pushing out of one brick	$V_{Sd} \leq V_{Rk,pb} / \gamma_{Mm}$
Influence of joints	$V_{Sd} \leq \alpha_j V_{Rk,b} / \gamma_{Mm}$ $V_{Sd} \leq \alpha_j V_{Rk,c} / \gamma_{Mm}$

b)

Fig. 4.6-15 – Required proofs to evaluate the anchor resistance to a) tension load and b) shear load. Source: ETAG 001-ANNEX C

As regard the connection between the existing RC frame rebars with the novel wall reinforcement, the post-installed rebar technology is employed in accordance with the

procedure by NTC18, EC2, and EOTA TR 023. In particular, the chemical anchoring method is used and the parameters of the ETA-07/0260 are considered. The bars are in improved adhesion steel, type B450C for structural use, shaped as hooks complying with EC2 directive (Figure 4.6 16).
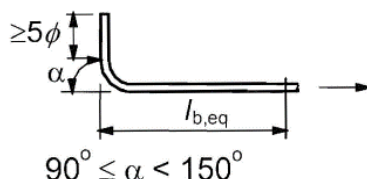
Fig. 4.6-16 – Geometric characteristics of the post-installed rebar. Source: EC2

It is assumed that they are installed into the existing RC frame to ensure the adequate iron cover, safely transmitting the forces to the concrete avoiding longitudinal cracking or spalling (The European Union, 2005).The calculation aims to determine the type, the diameter Φ, the anchor length l_{bd}, the wheelbase and amount of anchors to install. It is supposed that the anchoring length is calculated considering the iron cover value (c_1) at the anchor end, using the following formula:

$$l_v \geq l_0 + c_1 \qquad \text{[mm]} \qquad (28)$$

where l_0 is the required overlapping length.
The minimum c_1 is calculated by the formula (28.1) or (28.2) in function of the drilling machine employed to execute the holes into concrete.

with hammer drill $\qquad c_{min} = 30 + 0.06 \, l_v \geq 2\Phi \qquad$ [mm] $\qquad (28.1)$

with air drill $\qquad c_{min} = 50 + 0.08 \, l_v \geq 2\Phi \qquad$ [mm] $\qquad (28.2)$

Depending on the concrete strength class in which the rebars are inserted, the concrete strength is involved to estimate the anchoring length, starting from the design values of the ultimate bond resistance for good bond conditions f_{bd}. Its values are tabulated in EOTA TR 023 for the most common concrete strength classes (Figure 4.6-17).

Concrete strength class (1)	Design values of the ultimate bond resistance according to EC2 for good bond conditions f_{bd} (N/mm²) (2)	Required bond resistance for post-installed rebars f_{bm}^{req} (N/mm²)
C12/15	1,6	7,1
C16/20	2,0	8,6
C20/25	**2,3**	**10,0**
C25/30	2,7	11,6
C30/37	3,0	13,1
C35/45	3,4	14,5
C40/50	3,7	15,9
C45/55	4,0	17,2
C50/60	**4,3**	**18,4**

Fig. 4.6-17 – Ultimate bond resistance design values. Source: EOTA TR 023.

Considering the design stress of the rebar calculated with formula (29), the basic required anchorage length $l_{b,rqd}$, is determined by formula (30) according with EC2.

$$f_{yd} = \frac{f_{yk}}{\gamma_s} \qquad \text{[MPa]} \qquad (29)$$

$$l_{b,rqd} = \frac{\Phi \cdot f_{yd}}{4 \cdot f_{bd}} \qquad \text{[mm]} \qquad (30)$$

The anchorage length l_{bd} varies depending on whether the bars are subject to traction or compression, according to the following formulas:

$$l_{bd} = \alpha_1 \cdot \alpha_2 \cdot \alpha_3 \cdot \alpha_4 \cdot \alpha_5 l_{b,rqd} \geq l_{b,min} \qquad \text{[mm]} \qquad (31)$$

$$l_{b,min} \geq max\{0.3 l_{b,rqd}; 10\Phi; 100 \ mm\} \qquad \text{[mm]} \qquad (31.1)$$

$$l_{bd} = \alpha_4 l_{b,rqd} \geq l_{b,min} \qquad \text{[mm]} \qquad (32)$$

$$l_{b,min} \geq max\{0.6 l_{b,rqd}; 10\Phi; 100 \ mm\} \qquad \text{[mm]} \qquad (32.1)$$

where:
- α_1 is for the effect of the form of the bars and is equal to 0.7 for hook shapes;
- α_2 is for the effect of concrete minimum cover;
- α_3 is for the effect of confinement by transverse reinforcement;
- α_4 is for the influence of welded transverse bars (0.7 for tensioned bars; 1.0 for compressed bars);
- α_5 is for the effect of the pressure transverse along the design anchorage length

- $\alpha_2 \, \alpha_3 \, \alpha_5 \geq 0.7$

To evaluate how many rebars it is necessary to anchor to the existing RC frame to ensure the correct transfer of efforts and make the two structures cooperate as a single wall, the procedure of section 7.3.2 of EC2 is considered. In particular, the minimum area of reinforcing steel within the tensile zone is calculated as follows:

$$A_{s,min} \geq \frac{k_c k f_{ctm} A_{ct}}{f_{yk}} \qquad \text{[mm}^2\text{/m]} \qquad (33)$$

where:
- A_{ct} is the area of concrete within tensile zone;
- f_{yk} is the yield strength of the reinforcement;
- k is the coefficient which lead to a reduction of restraint forces;
- k_c is a coefficient which considers the stress distribution within the section and is equal to 1.0

The number of post-installed rebars (n) and the spacing (s_p) between the rebars are calculated considering the heavy-duty section of the relevant diameter bar (A_s) provided by ETA-07/0260 and the length of the existing beam (l), through formulas (34) and (35):

$$n = \frac{A_{s,min}}{A_s} \qquad (34)$$

$$s_p = {}^l/_n \qquad \text{[mm]} \qquad (35)$$

The novel wall in lightweight structural concrete (LWSC) is identified as a weakly armed concrete wall which design of steel reinforcement is regulated by the Italian legislation LL.GG. 117/2011. It establishes some standard requirements regarding to rebars diameter, spacing, amount of rebar in function of geometric percentage. In particular, the diameter of the horizontal and vertical bars shall not exceed a maximum of one-tenth of the wall thickness and be spaced apart up to 300 mm. Both vertical and horizontal geometric percentage of rebar should be at least 0.20%, considering a minimum diameter of 8 mm. The geometric percentage of vertical reinforcement (ρ_v), is obtained by dividing the area of the vertical bars (A_{va}), for the area of the horizontal section (A_{hc}) of the cast-in-place concrete. Instead, the geometric percentage of horizontal reinforcement (ρ_h), is

the area of the horizontal reinforcement bars (A_{ha}) divided for the area of the vertical section (A_{vc}) of the concrete cast in place.

The reinforcement mesh is in improved adhesion steel, type B450C for structural use.

4.6.1.2 Conglomerates

The cast-in-place concrete used to strengthen and stiffen the whole structure is a light-weight structural concrete (LWSC). In particular, its light aggregates are in recycled EPS coming from industrial wastes which confer to the mixture good thermal insulating characteristics. Thanks to its physical properties it is classified as lightweight structural concrete type LC_3, i.e. having average density between 1200 and 2000 Kg/m^3 and characteristic compressive strength more than 25 N/mm^2. Its consistency class is S5.

The reference patent number is BA2015A000027 (Amati *et al.*, 2015). The declared properties of such concrete are summarized in the Table 4.6-4.

Table 4.6-4. Declared properties of LWSC

MECHANICAL PROPERTIES			THERMO-HYGROMETRIC CHARACTERISTICS			
R_{ck}	f_{ck}	E_m	ρ	λ	c_p	μ
MPa	MPa	MPa	Kg/m^3	W/mK	J/kgK	-
29.06	24.12	31221.6	1974.89	1.35	825.36	42.46

The LWSC casting between the novel PC modules and the existing building façade is the completing phase of the system installation. It is the most difficult and dangerous step because the concrete hydrostatic pressure may generate several problems to the structure, damaging irreversibly the building. It may provoke the ejection of the brick wall toward the internal environmental, the pulling out of the anchors, the hooks breakage, as well as the instability of the modules and the overturning out of the plane due to the tension exerted on the surfaces. Therefore, the determination of its action is fundamental for the overall design system because it is considered for the pre-dimensioning and verification of the system.

The procedure used to predict the behaviour of the fresh concrete follows the directives of the standard DIN 18218:2010-01 on the basis of the related scientific literature (Graubner, Motzko and Proske, 2009; Kwon *et al.*, 2010; Proske *et al.*, 2014; Perrot *et*

al., 2015). Many factors are considered to evaluate the maximum lateral pressure of the concrete $\sigma_{hk,max}$ i.e. the concrete consistency (F_n), the casting height (H), the casting rate (v), the specific concrete weight (γ_c), the setting time (t_E), the stiffening and setting concrete factors (K1) and the factor for specific weight (K2). They depend on each as in the Figure 4.6-18 by DIN 18218:2010-01.

Consistency class	Flow (a) DIN EN 12350-5 (cm)	Slump-flow (sf) DIN EN 12350-8 (cm)	
F1	≤ 34		Stiff
F2	35–41		Plastic
F3	42–48		Soft
F4	49–55		Very soft
F5	56–62	~ 55	Flowable
F6	63–69[a]	~ 60[b]	Very flowable
SCC	≥ 70	≥ 65[c]	Self-compacting

Consistency class	Maximum lateral form pressure, $\sigma_{hk,max}$ (kN/m^2)
F1	$((5 \cdot v + 21) \cdot K1 \geq 25) \cdot K2$
F2	$((10 \cdot v + 19) \cdot K1 \geq 25) \cdot K2$
F3	$((14 \cdot v + 18) \cdot K1 \geq 25) \cdot K2$
F4	$((17 \cdot v + 17) \cdot K1 \geq 25) \cdot K2$
F5	$(25 + 30 \cdot v \cdot K1 \geq 30) \cdot K2$
F6[a]	$(25 + 38 \cdot v \cdot K1 \geq 30) \cdot K2$
SCC	$(25 + 33 \cdot v \cdot K1 \geq 30) \cdot K2$

Consistency class	Coefficient K1			
	General equation for setting time (t_E)[b]	Setting time $t_E = 5$ h	Setting time $t_E = 10$ h	Setting time $t_E = 20$ h
F1[a]	$1 + 0.03 \times (t_E - 5)$	1.0	1.15[c]	1.45
F2[a]	$1 + 0.053 \times (t_E - 5)$		1.25	1.80
F3[a]	$1 + 0.077 \times (t_E - 5)$		1.40	2.15
F4[a]	$1 + 0.14 \times (t_E - 5)$		1.70	3.10
F5, F6, SCC	$t_E/5.0$		2.00	4.00

Fig. 4.6-18 - Maximum concrete lateral pressure: design parameters. Source: Proske et al., (2014)

Therefore, it is possible to evaluate the maximum values of theoretical pressure (σ_{hd}), characteristic pressure ($\sigma_{hk,max}$), hence, the design fresh concrete pressure ($\sigma_{hd,max}$) through the following formulas:

$$\sigma_{hd} = \sigma_{hk} \cdot \gamma_F \tag{36}$$

$$\sigma_{hk,max} = (25 + 30 \cdot v \cdot K1) \cdot K2 \tag{37}$$

$$\sigma_{hd,max} = \gamma_F \cdot \sigma_{hk,max} \tag{38}$$

where:
- γ_F is the partial safety factor equal to 1.5;
- $K2 = \gamma_c/25$ kN/m³.

It is possible to draw the bilinear pressure distribution from which the behaviour of the fresh concrete can be observed. It assumes hydrostatic behaviour until the maximum characteristic pressure $\sigma_{hk,max}$ at the height h_s and becomes constant in the remain section due to the height h_E which value is the casting rate for the initial setting time ($h_E = v \cdot t_E$). The theoretical distribution is illustrated in the Figure 4.6-19 by Proske et al., in accordance to DIN 18218:2010-01.
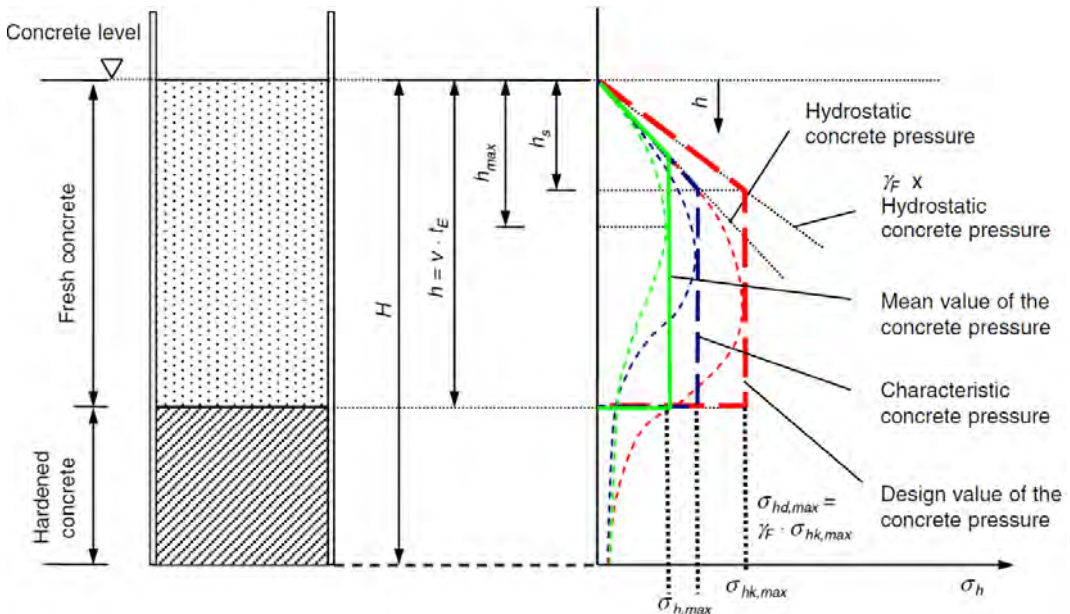
Fig. 4.6-19 - Distribution of the fresh concrete lateral pressure. Source: Proske et al., (2014)

Following such method, the evaluation of the fresh LWSC behaviour between the PC modules and the existing façade starts establishing the initial parameters of setting time, casting rate, and taking in account the concrete characteristics. Since the concrete cavity is narrow, it is assumed that the casting speed is very low to avoid the vibrating phase and aggravate the load. The theoretical, characteristic and design fresh concrete pressure are calculated with the formulas (36), (37) and (38). Finally, the h_s is identified. Figure 4.6-20 illustrates the results of calculation.

SETTING DATA

$\gamma_c = 19.74$ kN/m³

$F_n = F5$

$H = 2$m

$t_E = 5$h

$v = 0.7$ m/h

$K1 = 1$

$K2 = 0.8$

PRESSURES

$\sigma_{hd} = 39$ kN/m³

$\sigma_{hk,max} = 30.8$ kN/m³

$\sigma_{hd,max} = 46.20$ kN/m³
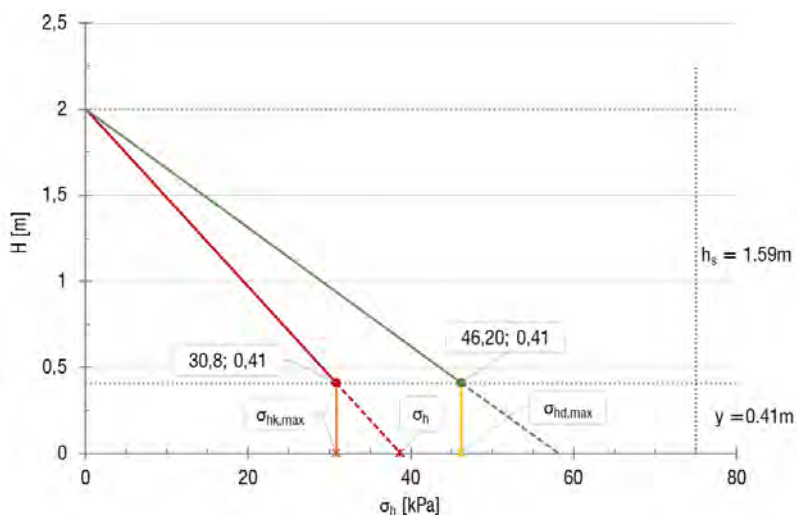
Fig. 4.6-20 – LWSC pressure distribution along the panel height. Source: Author

From the concrete behaviour prediction in figure, it is possible to observe that it assumes a hydrostatic behaviour up to 41 cm where reached the maximum value of the LWSC pressure of 46.20 kN/m³. Then it remains constant, until the upper the panel foot. Since, it depends on the casting rate, at higher values, the maximum pressure increases and vice-versa.

These results are important for the design stage and the in-site phases. In fact, the value of pressure is involved in the loads analysis to perform the design and the verification of the steel components, while the setting data define the criteria of the work execution i.e. the method and speed of the concrete casting.

4.6.2 Technical drawings and technological choices

The purpose of this section is to show the geometric characteristics and composition of the technological system through the graphical representation. The focus is understanding the components of the system as well as the different connection levels: mullion-panel; mullion-RC frame; mullion-masonry brick; RC frame-new concrete wall. Many sections are provided in various heights of the wall. Moreover, the case of the pilotis building is analysed aiming at showing the benefits in terms of versatility and adaptability the PC module provides. The Figures from 4.6-21 to 4.6-29 follow.

① EXISTING BRICK WALL
② EXISTING RC CONCRETE ELEMENT
③ STELL MULLION AND HOOK
④ ADDITIONAL REINFORCEMENT
⑤ PC MODULE
⑥ EPS INSULATING LAYER
⑦ METAL ANCHOR IN BRICK (CI)
⑧ METAL ANCHOR IN CONCRETE (CI)
⑨ POST-INSTALLED REBAR (CI)
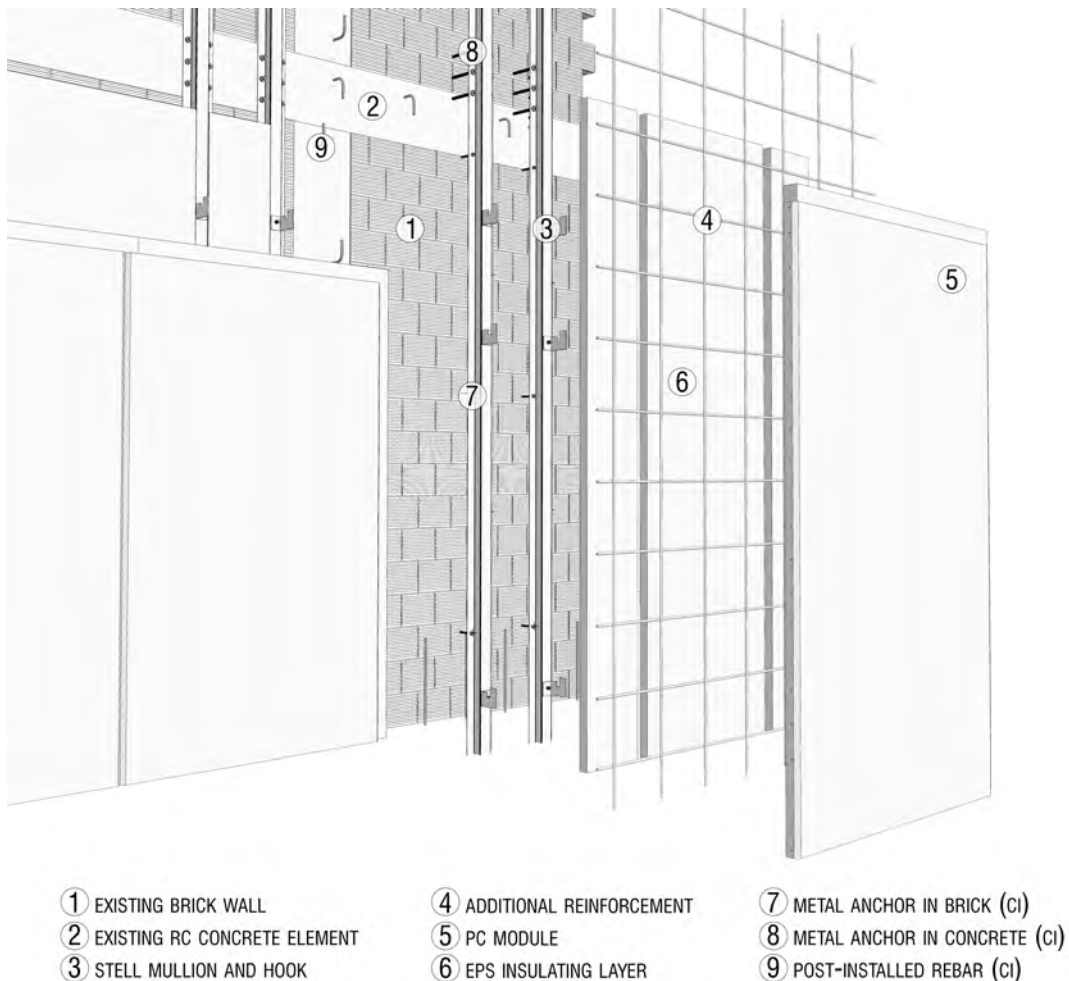
Fig. 4.6-21 – Axonometric view of the technological proposal. Source: Author

(1) EXISTING BRICK WALL	(4) ADDITIONAL REINFORCEMENT	(7) METAL ANCHOR IN BRICK (CI)
(2) EXISTING RC CONCRETE ELEMENT	(5) PC MODULE	(8) METAL ANCHOR IN CONCRETE (CI)
(3) STELL MULLION AND HOOK	(6) EPS INSULATING LAYER	(9) POST-INSTALLED REBAR (CI)
		(10) CASTED-ON-SITE LIGHTWEIGHT STRUCTURAL CONCRETE
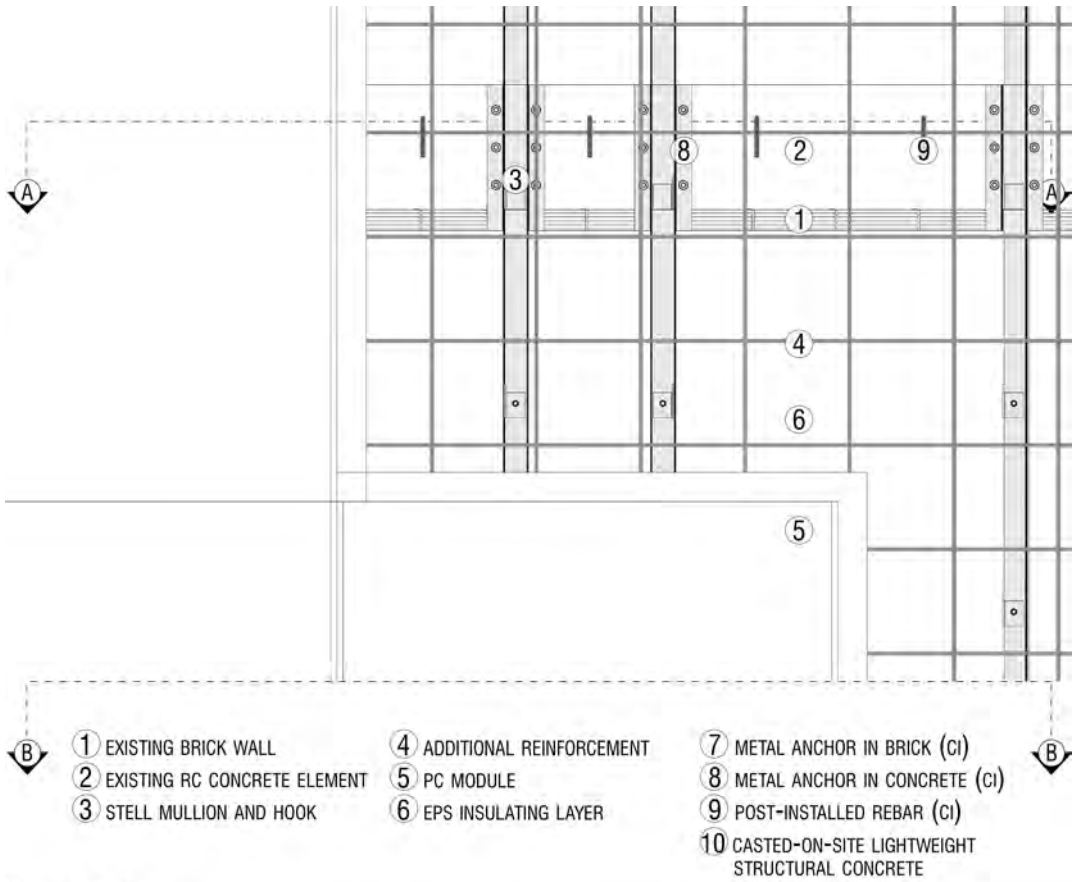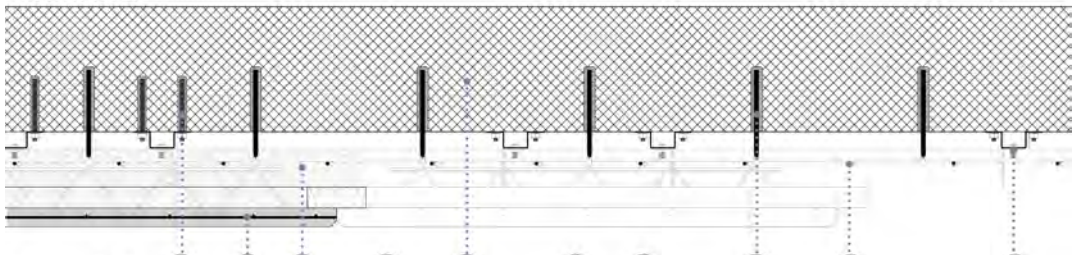
SECTION A-A
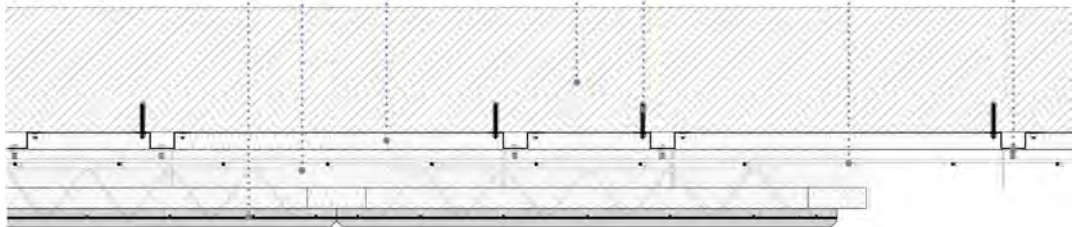
SECTION B-B

Fig. 4.6-22 – Portion of the façade with cut sections: A-A in concrete; B-B in brick wall. Source: Author
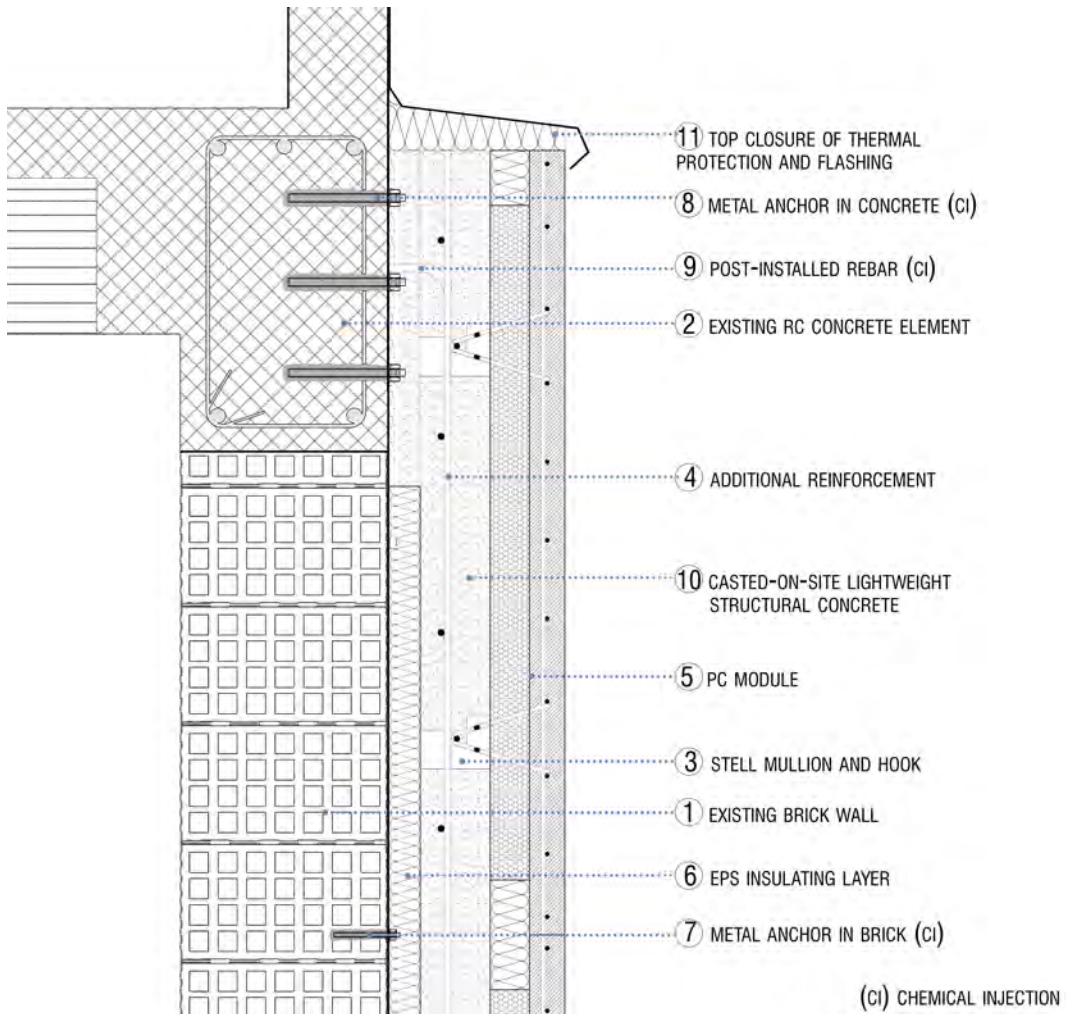
Fig. 4.6-23 – Vertical section: top ending. Source: Author

11 TOP CLOSURE OF THERMAL PROTECTION AND FLASHING

8 METAL ANCHOR IN CONCRETE (CI)

9 POST-INSTALLED REBAR (CI)

2 EXISTING RC CONCRETE ELEMENT

4 ADDITIONAL REINFORCEMENT

10 CASTED-ON-SITE LIGHTWEIGHT STRUCTURAL CONCRETE

5 PC MODULE

3 STELL MULLION AND HOOK

1 EXISTING BRICK WALL

6 EPS INSULATING LAYER

7 METAL ANCHOR IN BRICK (CI)

(CI) CHEMICAL INJECTION
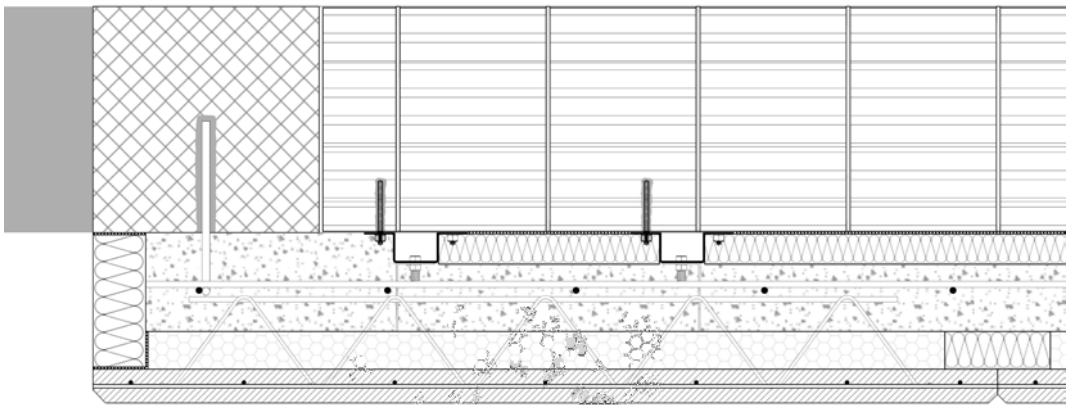
Fig. 4.6-24 – Plan section: lateral ending in presence of another building. Source: Author

128
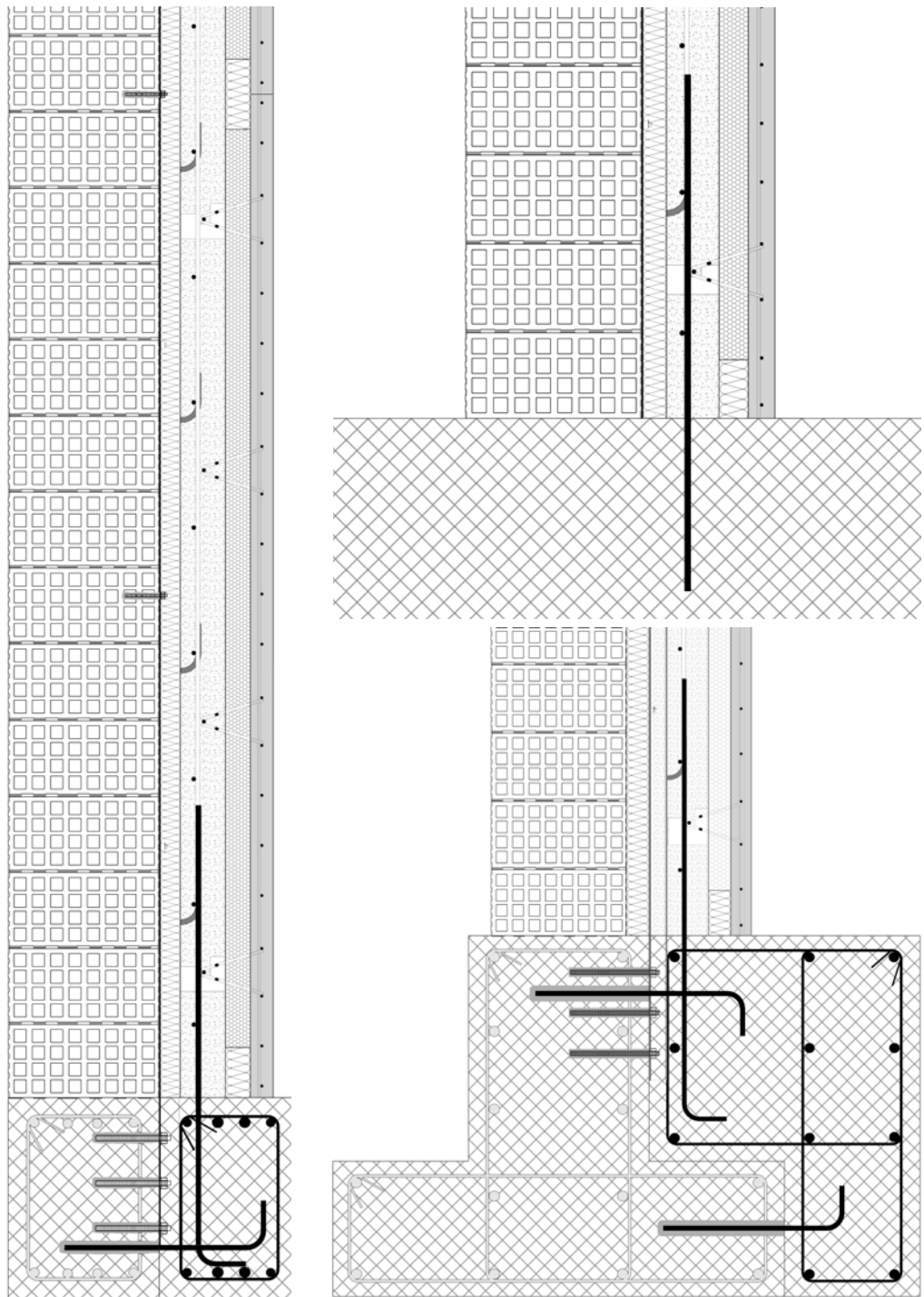
Fig. 4.6-25 – Base connection: three existing type of foundation. Source: Author

In function of the existing building foundation, the order of the layers may vary to better fit to the geometric requirements of the structure. For instance, in order to achieve the connection of the mullions at the foundation plinth, the insulating layer in EPS may be placed behind the mullions as the Figure 4.6-26 shows.

It also illustrates the intersection of the panels near the corner of the building and the interlocking between the different layers to avoid the generation of thermal bridges. The post installed connections on the pillar are alternated in the two main directions of development of the façade to ensure a better connection at different heights.
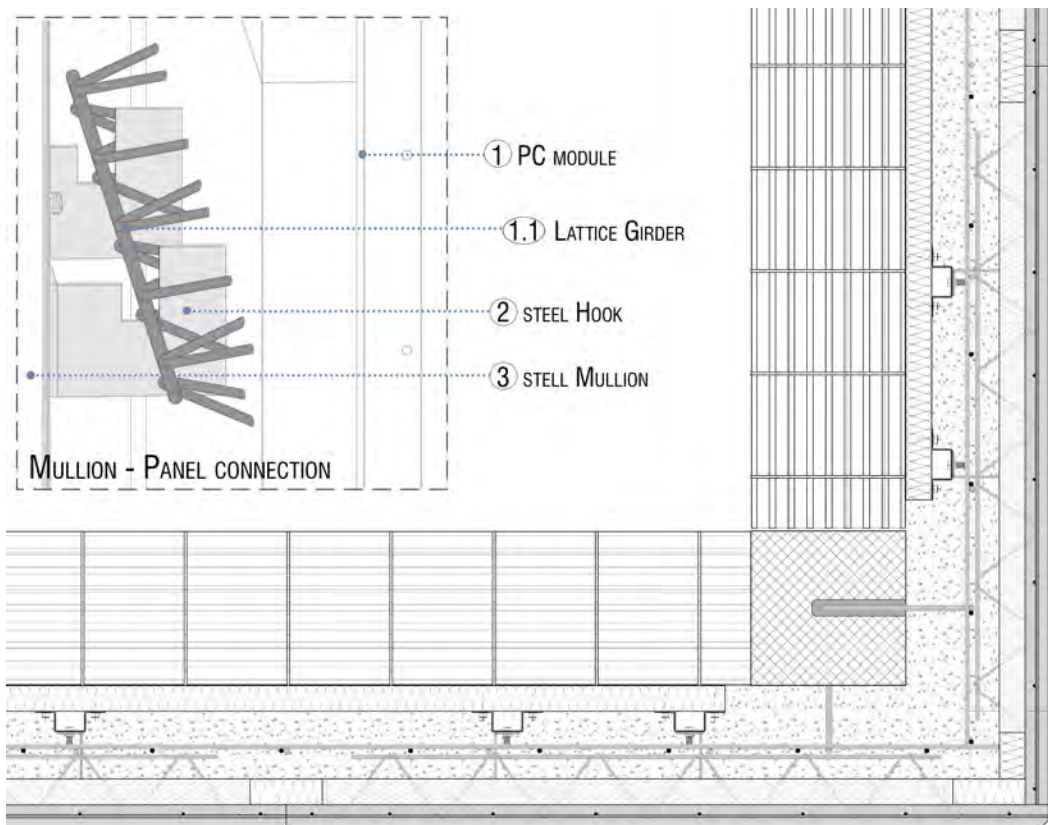
Fig. 4.6-26 – Corner section and focus on the mullion-panel connection. Source: Author

In the South of Italy, one of the most common typology of RC building constructed in the post-WW2 was the pilotis building which consists in raising the first floor leaving the ground floor uncovered and usable. However, this solution endangers the safety of the building, especially under seismic action. Therefore, the application of the solution to this type of building implies an increase in the safety of the building due to an increase in rigidity at the base.

Thanks to the use of prefabricated elements and the custom prefabrication implemented by the company Ferramati Int., the solution can easily adapt to the structure through the combination of multiple elements. In particular, the PC module can easily be converted into a double-slab wall by coupling with a single slab in reinforced concrete. Approaching the pillar, the wall generates a new armed continuous wall, also completed with the cast-on-site concrete, which generates the support base for standard modules to be applied from the first floor of the building. Moreover, by closing the ground floor, the solution has an additional advantage of generating new accessory volumes usable by users.

From a constructive point of view, the upper edge of the second slab is at a higher height than the facade slab, as it avoids creating a section of less resistance at the intersection of the panels at the time of the concrete casting. The joint between modules of different heights will be guaranteed by the male-female joints of the panels. How shown in the Figure 4.6-28, special elements can also be produced to better adapt to the dimensional requirements of the building.

In the double-plate version of the standard module PC, it is necessary to use higher lattice girders in such a way as to generate a suitable cast-on-site concrete cavity and maintain the section of constant with that realized above. In the case in the figure, 20.5 cm high lattice girders are used with reinforcement $\Phi 5|8|5$.

In the presence of openings (4.6-29), the distribution of the panels is interrupted in order to meet the geometric requirements of the building. An EPS panel is placed inside the opening pad to thermally protect the wall.

GROUND FLOOR
PILOTIS

LATTICE GIRDER 12.5CM
(5|7|5)

COMBINED PC MODULE
(SPECIAL PIECE)

COMBINED PC MODULE

LATTICE GIRDER 20.5CM
(5|8|5)
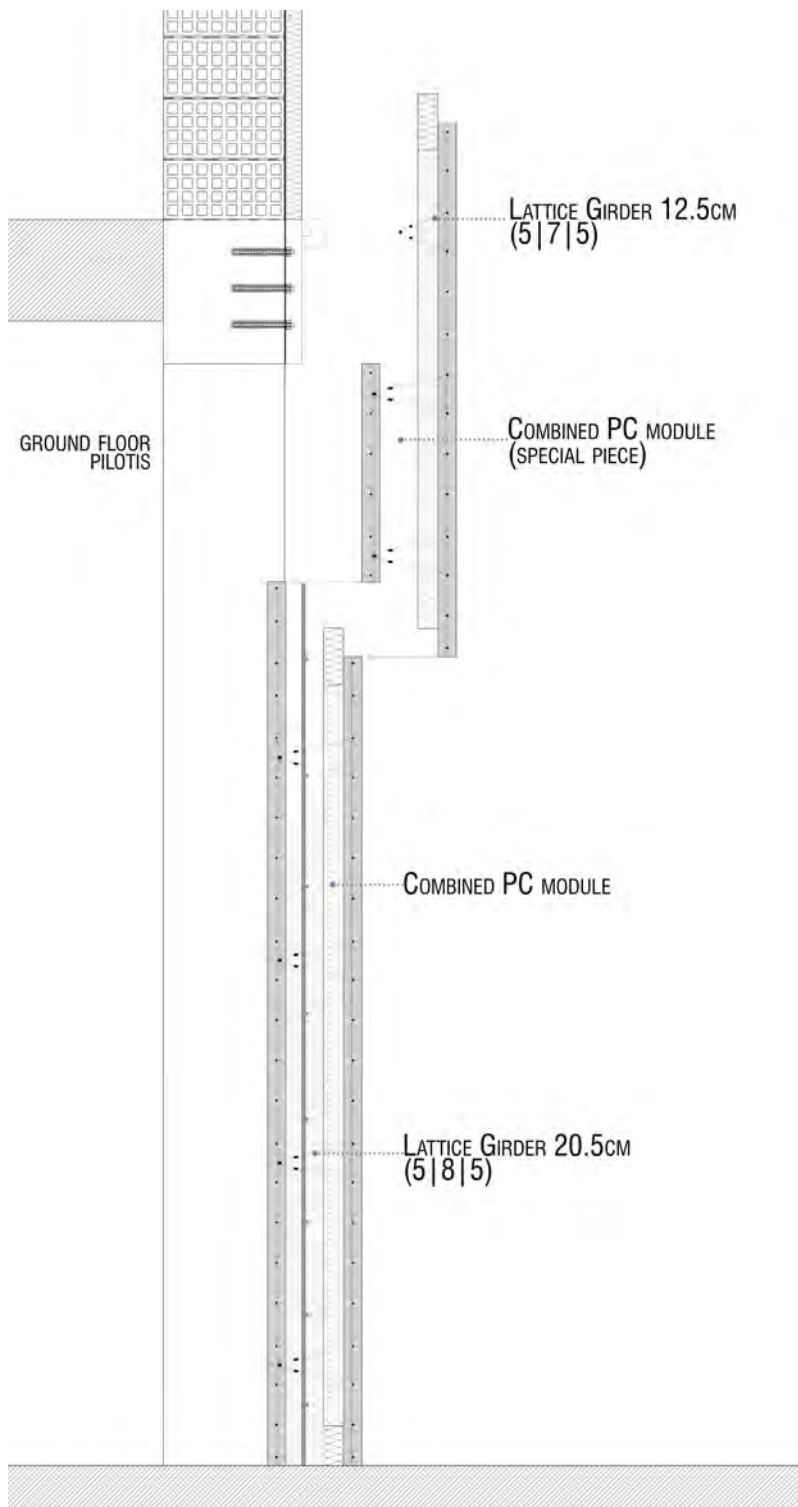
Fig. 4.6-27 – Particular case: Pilotis building. Source: Author

132
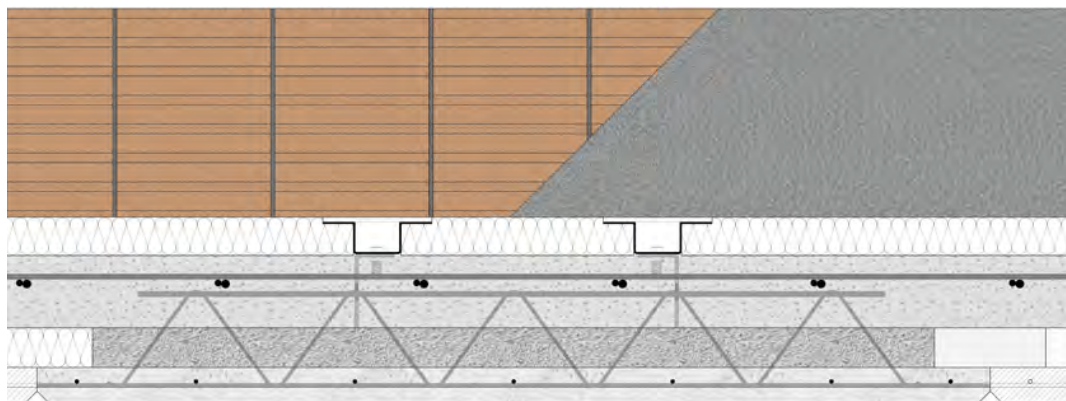
Fig. 4.6-28 – Plan view. Source: Author
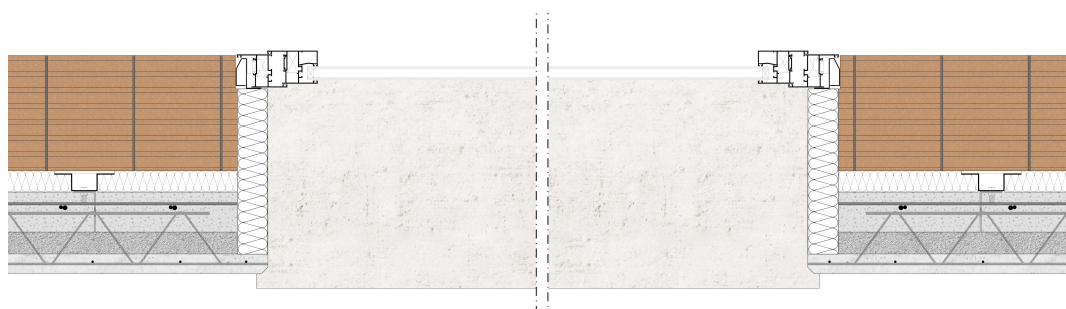
Fig. 4.6-29 – Plan section: windows. Source: Author

4.6.3 Methods of preliminary performance evaluation and monitoring

The purpose of the proposed technology is the renovation of the existing RC building from thermo-insulating and structural point of view. The definition of the geometric and physical characteristics as well as the constrains between the novel system and the existing structure, allow carrying out some preliminary assessments to understand the system behaviour under certain climatic conditions and seismic loads, according to section 4.2. However, no experimental tests have been performed. The evaluation has been carried out by numerical models on the basis of several assumptions, specified for the two application fields. The methodology employed, from the model setting to the results reading, is based on the actual standards and the methods proposed in the scientific literature. The numerical attempts and qualitative evaluation are carried out thanks to the creation of finite element (FE) models both for the thermal and structural evaluations. In particular, to better understand the methodologies employed a reduced framed wall

model (3x3 m) is considered (Figure 4.6-30). The purpose is comprehending the wall behaviour with the system in order to predict the overall performance that an entire building may behave.
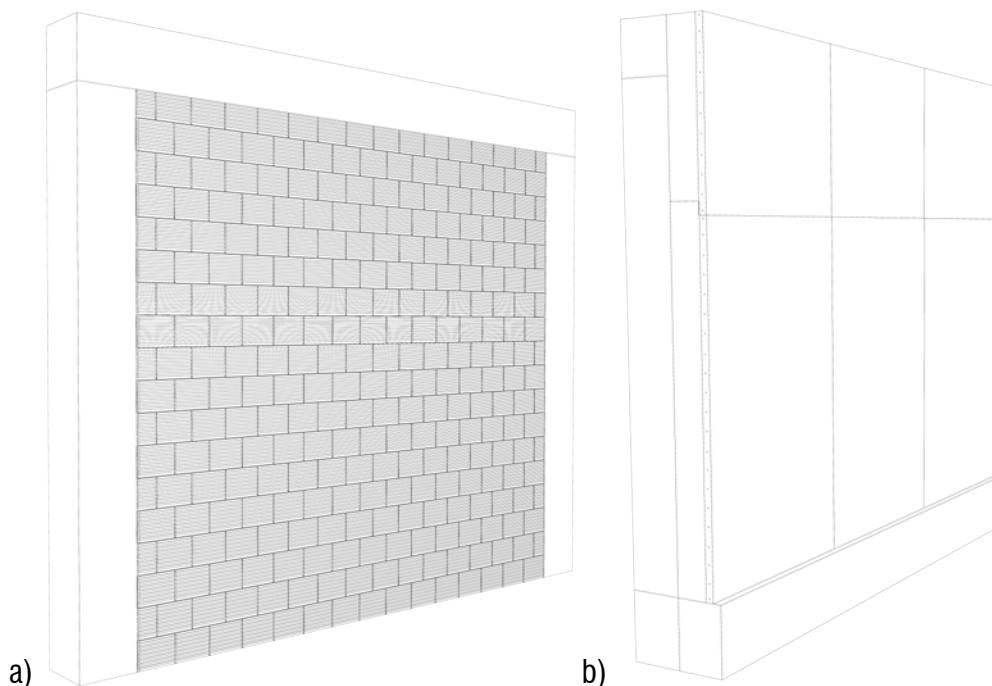
Fig. 4.6-30 – Reduced model for preliminary evaluation: a) existing wall model; b) retrofitted wall model. Source: Author

4.6.3.1 Thermo-Hygrometric behaviour

The evaluation of the thermal behaviour of the façade typology chosen in accordance with section 4.2, is carried out under the stationary and dynamic climatic conditions in to appraise the thermal resistance and thermal inertia. In addition, the estimation of the resistance to vapour diffusion is performed in order to study the hygrometric behaviour wall, considering the steady-state procedure by EN ISO 13788:2013. Starting from the definition of these parameters, the evaluation methodology is specified.

According to EN ISO 6946:2018, the thermal resistance (R-value) in stationary conditions, is the capacity of the wall to resist to the heat flow (EN ISO 6946, 2018). It is the mutual value of the coefficient of heat transmission between surfaces namely thermal

134

transmittance (U-value), which represents the heat flow that through a unit thickness (d) surface subjected to a temperature difference of a Kelvin degree (EN ISO 6946, 2018). It depends on the thermal conductivity coefficient (λ) which represents the capacity of a material to heat transferring. The Italian standard, MD 6/26/2015, fixes the limit R-value of the existing building walls subjected to energy improvements to 2.77 m^2K/W which correspond to the U-value of 0.36 W/m^2K (U_{max}). At lower U-values correspond a better thermal performance of the building component (Ministerial Decree, 2015).

The resistance to vapour diffusion is the capacity of the wall to impede the water vapour diffusion through its layers. It depends on the dimensionless coefficient of vapour diffusion resistivity (μ) which characterizes each material (EN ISO 13788, 2013).

To evaluate the wall thermal capacity in dynamic conditions i.e. at temperature variation, the thermal inertia has to be considered. According to EN ISO 13786:2018, it is the capacity of a building component to mitigate the indoor temperature fluctuations due to the variation of thermal loads throughout the day, and to accumulate and release heat after several hours (EN ISO 13786, 2018). To appreciate the wall thermal inertia in a simplified way, the principle dynamic parameters are considered: the periodic thermal transmittance (Y_{ie}) and the periodic internal thermal capacity (k_1). The first estimates the heat shift for 24 hours and it is defined as the ratio of the flow induced internally by a periodic sinusoidal variation of the external temperature to the variation itself. The second is the effective thermal accumulation capacity of the wall and it is the product between the specific wall heat and the surface thermal mass (m_s).

High performance of the wall, thus a reduced energy requirement for summer cooling, is determined by a periodic thermal transmittance value lower than 0.10 W/m^2K (with a time shift coefficient (φ), greater than 12 hours and attenuation factor, f_d, lower than 0.15), and a high value of periodic internal thermal capacity (Perna *et al.*, 2009). These parameters are calculated thanks to the excel calculation sheet proposed by Ursini Casalena (2018). The Italian standard, MD 6/26/2015, also establishes the limit values of the dynamic parameter below:

- $Y_{ie,lim} < 0.10$ W/m^2K;
- $k_{1,lim} \geq 50$ kJ/m^2K;

- $m_{s,lim} > 230$ kg/m³

- $f_{d,lim} < 0.6$

For the preliminary assessment of the steady-state thermo-hygrometric behaviour of the reduced wall considered for this study, four main portions are taken in account due to the variation of the stratigraphy:

a. 30 cm hollow brick + 5 cm rEPS block + 10 cm LWSC + 5 cm LWM + 4,5 cm Concrete slab (table 4.6-5);

b. 30 cm hollow brick + 4 cm air + 0.3 cm steel mullion + 10 cm LWSC + 5 cm LWM + 4,5 cm Concrete slab (table 4.6-6);

c. 30 cm RC (beam) + 15 cm LWSC + 5 cm LWM + 4,5 cm Concrete slab (table 4.6-7);

d. 30 cm RC (beam) + 4 cm air + 0.3 cm steel mullion+ 10 cm LWSC + 5 cm LWM + 4,5 cm Concrete slab (table 4.6-8);

Table 4.6-5. Wall stratigraphy type a

WALL LAYER		d	ρ	λ	μ	STRATIGRAPHY
		mm	kg/m³	W/mK	-	
INDOOR HEAT TRANSFER COEFFICIENT				7.70		
1	HOLLOW BRICK	300	1200	0.50	9.30	
2	rEPS BLOCK	50	10	0.04	20	
3	LWSC	100	1978	1.35	42.46	
4	LWM	50	187.7	0.0587	6.50	
5	CONCRETE SLAB	45	2400	2.00	47.85	
OUTDOOR HEAT TRANSFER COEFFICIENT				25.0		

Table 4.6-6. Wall stratigraphy type b

WALL LAYER		d	ρ	λ	μ	STRATIGRAPHY
		mm	kg/m³	W/mK	-	
INDOOR HEAT TRANSFER COEFFICIENT				7.70		
1	HOLLOW BRICK	300	1200	0.50	9.30	
6	AIR	40	1.225	0.026	1	
7	STEEL MULLION	3	7850	79	2×10^6	
3	LWSC	100	1978	1.35	42.46	
4	LWM	50	187.7	0.0587	6.50	
5	CONCRETE SLAB	45	2400	2.00	47.85	
OUTDOOR HEAT TRANSFER COEFFICIENT				25.0		

Table 4.6-7. Wall stratigraphy type c
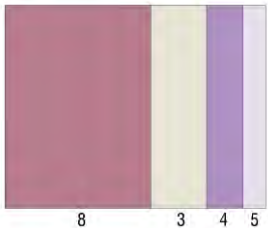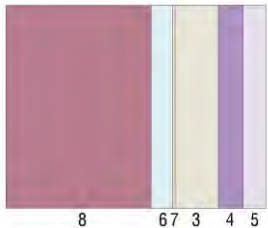
WALL LAYER		d	ρ	λ	μ	STRATIGRAPHY
		mm	kg/m³	W/mK	-	
INDOOR HEAT TRANSFER COEFFICIENT				7.70		
8	RC (BEAM)	300	1200	0.50	9.30	
3	LWSC	150	1978	1.35	42.46	
4	LWM	50	187.7	0.0587	6.50	
5	CONCRETE SLAB	45	2400	2.00	47.85	
OUTDOOR HEAT TRANSFER COEFFICIENT				25.0		

Table 4.6-8. Wall stratigraphy type d

WALL LAYER		d	ρ	λ	μ	STRATIGRAPHY
		mm	kg/m³	W/mK	-	
INDOOR HEAT TRANSFER COEFFICIENT				7.70		
8	RC (BEAM)	300	1200	0.50	9.30	
6	AIR	40	1.225	0.026	1	
7	STEEL MULLION	3	7850	79	2×10^6	
3	LWSC	100	1978	1.35	42.46	
4	LWM	50	187.7	0.0587	6.50	
5	CONCRETE SLAB	45	2400	2.00	47.85	
OUTDOOR HEAT TRANSFER COEFFICIENT				25.0		

Hence, the thermal transmittance values of the four wall portions are calculated in accordance with the procedure of EN ISO 6946:2018, Martiradonna (2020) and Garay (2017), and compared with the limit value, U_{max}, established by MD 6/26/2015:

a. $U_a = 0.31$ W/m²K; ($<U_{max}$)
b. $U_b = 0.28$ W/m²K; ($<U_{max}$)
c. $U_c = 0.77$ W/m²K; ($>U_{max}$)
d. $U_d = 0.36$ W/m²K; ($=U_{max}$)

The overall U-value of the wall (U_w) is the mean value of the four types and is equal to 0.44 W/m²K. It is clear that it does not comply with the standard due to the high values reached in type c and d. Although, thanks to the panel configuration (i.e. the horizontal direction of the girders), it is possible to vary the distribution of the insulating materials in order to match the section of the beam the panel portion with the rEPS block,

positioned within the spacing of the lattices. Type e and type f would be the new stratigraphy that replace type c and type d, respectively:

e. 30 cm RC (beam) + 15 cm LWSC + 8 cm rEPS block + 4,5 cm Concrete slab (table 4.6-9);

f. 30 cm RC (beam) + 4 cm air + 0.3 cm steel mullion+ 7 cm LWSC + 8 cm LWM + 4,5 cm Concrete slab (table 4.6-10).

Table 4.6-9. Wall stratigraphy type e

WALL LAYER		d	ρ	λ	μ	STRATIGRAPHY
		mm	kg/m³	W/mK	-	
INDOOR HEAT TRANSFER COEFFICIENT				7.70		
8	RC (BEAM)	300	1200	0.50	9.30	
3	LWSC	120	1978	1.35	42.46	
2	rEPS BLOCK	80	10	0.04	20	
5	CONCRETE SLAB	45	2400	2.00	47.85	
OUTDOOR HEAT TRANSFER COEFFICIENT				25.0		

Table 4.6-10. Wall stratigraphy type f

WALL LAYER		d	ρ	λ	μ	STRATIGRAPHY
		mm	kg/m³	W/mK	-	
INDOOR HEAT TRANSFER COEFFICIENT				7.70		
8	RC (BEAM)	300	1200	0.50	9.30	
6	AIR	40	1.225	0.026	1	
7	STEEL MULLION	3	7850	79	2×10^6	
3	LWSC	70	1978	1.35	42.46	
2	rEPS BLOCK	80	10	0.04	20	
5	CONCRETE SLAB	45	2400	2.00	47.85	
OUTDOOR HEAT TRANSFER COEFFICIENT				25.0		

The U_e-value and U_f-value are 0.35 W/m²K and 0.25 W/m²K respectively. Therefore, the U_w-value is equal to 0.2975 W/m²K which complies with the standard.

Considering the climatic conditions fixed in the section 4.2 (indoor: T=293.15 K; RH=52%; outdoor: T=281.55 K; RH=68%), the evaluation of the hygrometric behaviour of the wall starts from the calculation of the superficial temperature of each layer. The software COMSOL Multiphysics is used to create the FE 3D model of the wall, calculate the temperature distribution in the specific sections and observe the heat flux

development through the temperature iso-curves. The visual survey of the 3D models and in particular the temperature variation scale, provides information about the thermal bridges' generation (Martiradonna, Fatiguso and Lombillo, 2020).

Applying the procedure by EN ISO 13788:2013, the Glaser's diagrams are drawn in order to understand the interstitial condensation hazard, in particular in the sections with the steel mullions. The interstitial condensation occurs if the saturation pressure curve intersects the vapour pressure one. The following figures investigate the temperature distribution (a), the related Glaser's diagrams (b), the thermal bridges (c) for the sections: type a (Figure 4.6-31), type b (Figure 4.6-32), type e (Figure 4.6-33) and type f (Figure 4.6-34). The section with the post-installed connection is analysed too in Figure 4.6-35.
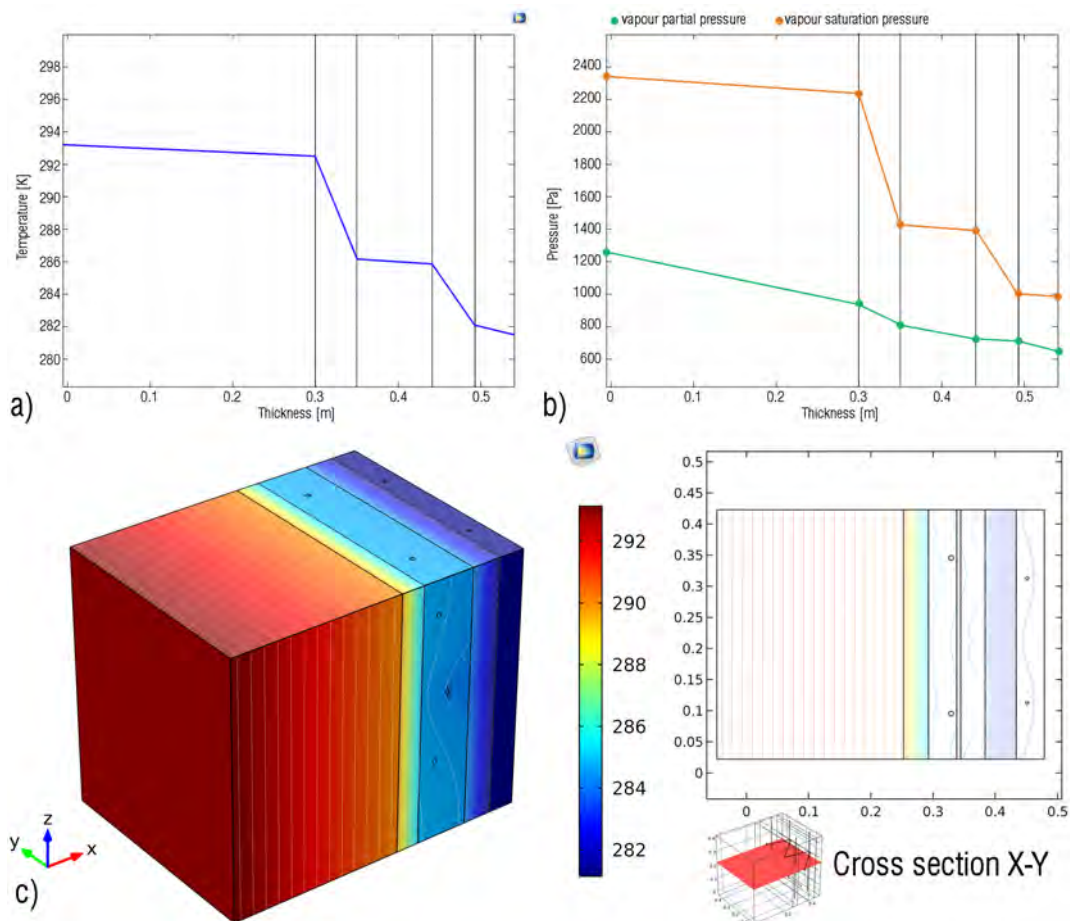
Fig. 4.6-31 –Hygrometric behaviour and thermal bridges formation: wall portion type a. Source: Author
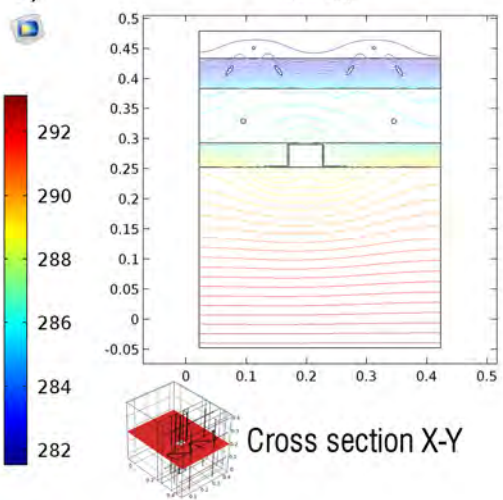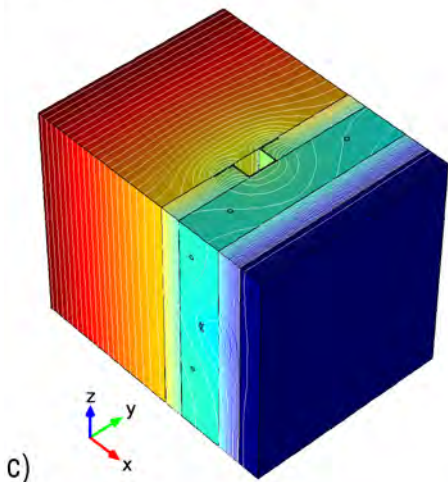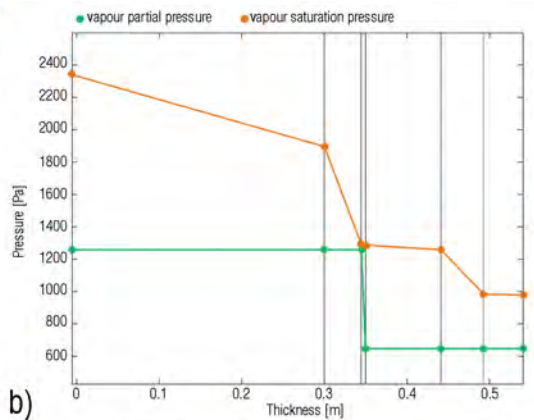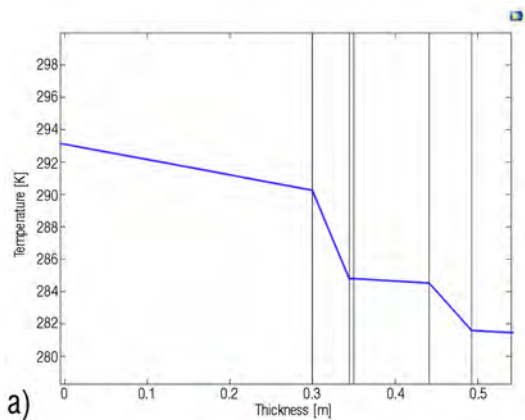
Fig. 4.6-32 – Hygrometric behaviour and thermal bridges formation: wall portion type b. Source: Author
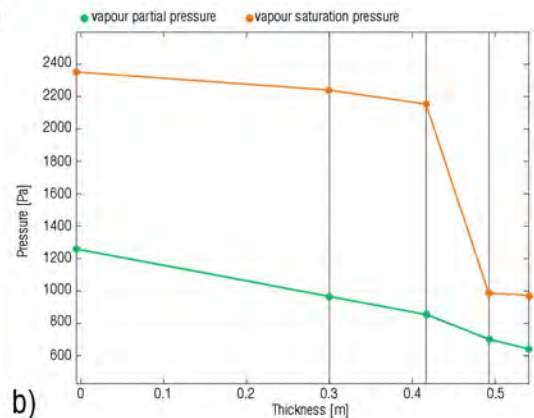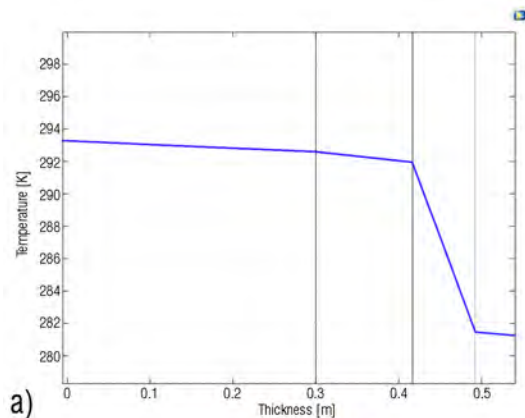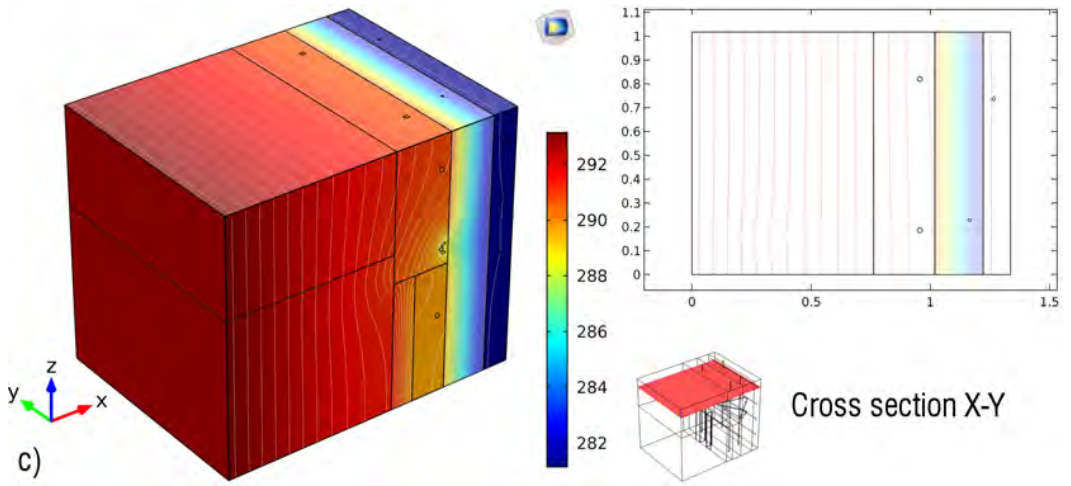
Fig. 4.6-33 – Hygrometric behaviour and thermal bridges formation: wall portion type e. Source: Author
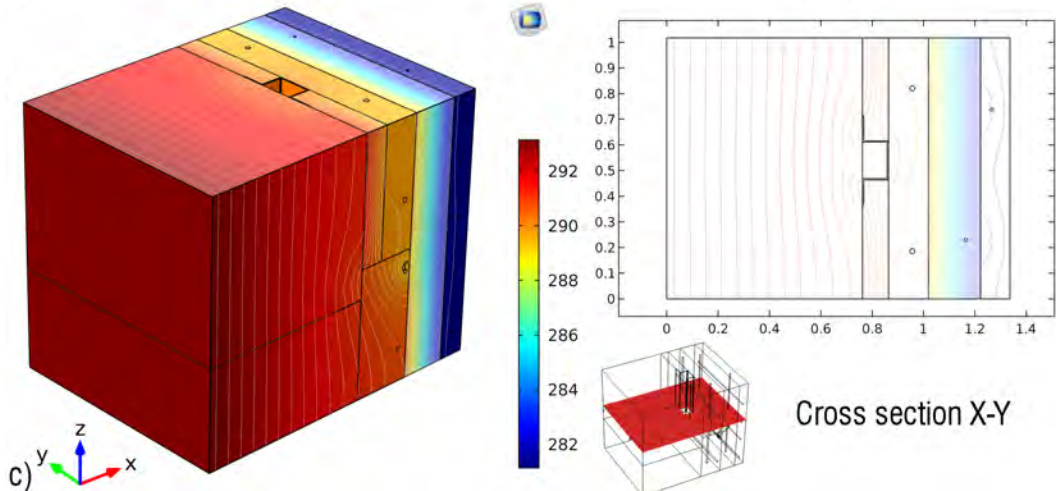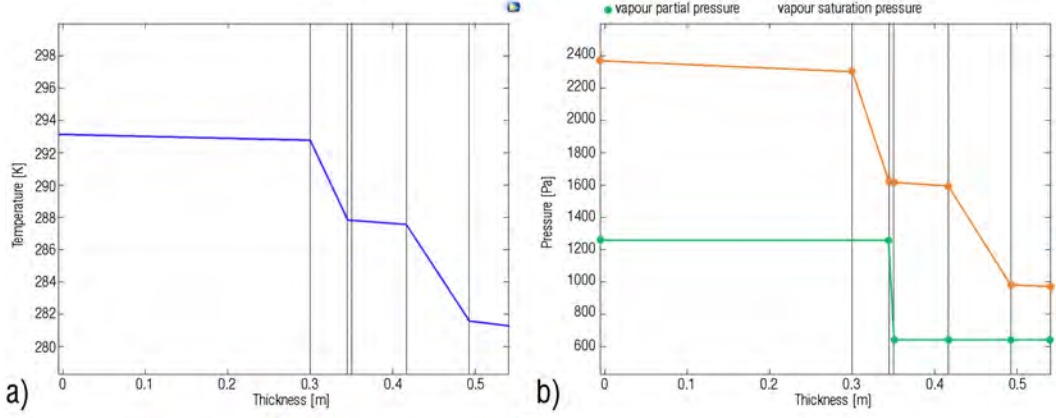
Fig. 4.6-34 – Hygrometric behaviour and thermal bridges formation: wall portion type f. Source: Author
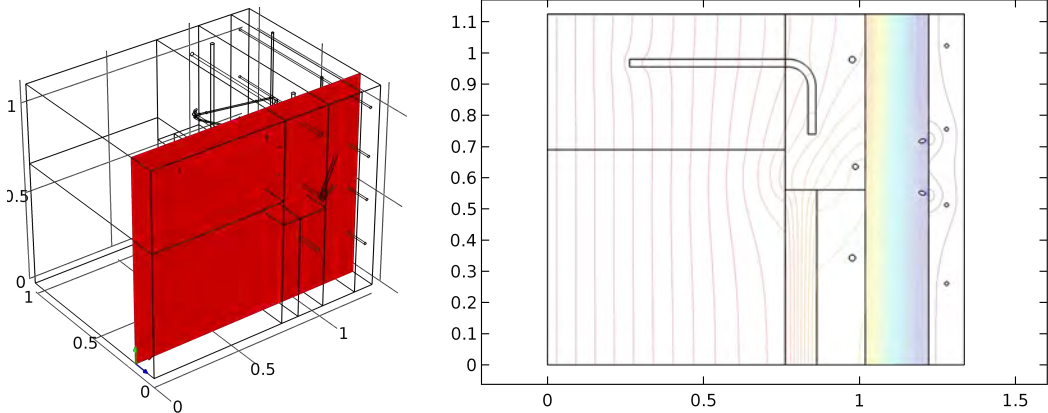
Fig. 4.6-35 – Heat flux distribution in the section X-Z: post-installed connection. Source: Author

Thanks to the distribution, thickness, and properties of the layers, no condensation occurs in any section for the values of temperature and relative humidity considered. In the wall section type b, especially in correspondence of the steel mullion, the curves of vapour partial and saturation pressures peak due to the waterproof properties of the mullion that does not spread water vapour. However, for the mean conditions considered for the analysis, the curves do not intersect, thus, no condensation occurs. It is not excluded that it generates in more severe climatic situations. However, considering the results of the other sections and that iron is a good heat conductor, the temperature along the mullions would be the weighted average of all the temperatures of the individual sections. Therefore, the surface temperature value of the mullion on the resulting curve would have a higher value than that of section type b. This would result in a deviation of the pressure curves, thus removing the risk of condensation. Certainly, further insights will be developed in the future, through the use of global behaviour assessment software as performed by Silva (2013) and experimental tests.

The 3D analysis of the temperature iso-curves shows that, despite the presence of steel elements in all sections, no thermal bridges occur. Thermal flux disturbances are observed near to the reinforcements; however, they do not affect the overall performance of the system.

As regard the evaluation of the thermal performance in dynamic-state, thus, the wall thermal inertia, the computation of the periodic thermal transmittance and the periodic

142

internal thermal capacity is carried out thanks to the calculation sheet proposed by Ursini (2018), taking in account the resulting values of the time shift coefficient and attenuation factor. The results of the calculation are reported below:

- Y_{ie} = 0.003 W/m²K; ($<Y_{ie,lim}$)

- k_1 = 53.5 kJ/m²K; ($>k_{1,lim}$)

- m_s = 714 kg/m³; ($>m_{s,lim}$)

- f_d = 0.01 ($<f_{d,lim}$)

- φ = 21.3 h

The values comply with the standard limit values. In particular, the time shift value φ is very high, meaning that the wall is able to retain and release the heat only after 21 hours of exposure to hot summer temperatures, keeping the indoor environment at temperatures lower than outside, thus, decreasing the energy requirement for cooling. Therefore, agreeing with the considerations by Perna (2009), the system presents excellent performance in dynamic regime.

4.6.3.2 Explorative numerical modelling of the Seismic behaviour

It should be noted that the objective of the proposal is to provide a strategy for energy, architectural and structural upgrading able to minimize the interruption of use and the invasiveness of the interventions. The nature of the designed system involves a substantial change in the response of the structure to which it is applied, as a result of the increase in mass and stiffness provided, especially in the presence of seismic actions. From this point of view, it is necessary to evaluate how the structural capacity is modified, both in terms of resistance and ductility. To this end, an exploratory analysis has been carried out, adopting a panel modelling approach, described below, which is sufficiently lean and manageable, especially considering that currently no experiments have been carried out for the mechanical characterization of materials and structural tests on prototypes, and therefore no specific reference data are available.

This approach will therefore be applied to a case study to globally test the effects on structural response. Of course, it must be stressed that the evaluations made on the effectiveness and limitations of the results obtained will have to be supported by a more

extensive campaign of experiments, both real and numerical. In particular, it must be remembered that the type of intervention proposed always requires, in all cases of application, that a complete procedure of vulnerability assessment is carried out on the focused building, which includes the path of knowledge, in-situ investigations on materials and structural elements, verification of existing structural elements (possibly assume the configuration of secondary structural elements) for all combinations of actions provided by the standard. It cannot be a priori excluded, therefore, that interventions on the existing structural elements are still necessary.

The preliminary numerical simulations performed are based on a simple but effective model that incorporates structural, non-structural and new components, even if, as already mentioned, only general literature data about materials are used, since structural experimental tests have not been performed yet. In addition, some further boundary assumptions had to be made about the features of the retrofit system. In particular, three assumptions have been considered in the finite element (FE) model: (a) the connections that bind the existing structural elements to the PC panels are rigid and resistant; (b) the corresponding nodal degrees of freedom (DOFs) of infill RC frame, PC panel and filling RC concrete are constrained; (c) only in-plane (IP) behaviour is simulated, whereas out-of-plane (OOP) behaviour is neglected. While the condition (b) retains a physical sense, due to the technology of the retrofit system, condition (a) should be carefully assessed, because the failure of steel connectors could affect the final performance (they have not been specifically designed and verified). Still, condition (c) needs some additional remarks.

First of all, the retrofit system, as conceived, interacts with the masonry infill panels as an additional structural system, creating a single vertical ribbed plate, anchored to a RC frame structure. Provided that the condition (a) is satisfied, the overturning of masonry panel under seismic action is prevented. It is expected a relevant increase of the stiffness after the introduction of the additional retrofit system and a mainly elastic response characterized by a higher strength.

The FE model is conceived by referring to the proposal in Mondal and Jain (2008) and after revisited in Ozturkoglu, Ucar and Yesilce (2017), which studied the effects of the

openings in the infill RC frames under seismic actions with a mesoscale approach. Using SAP2000 software (CSI, 2016), beams and columns are simulated as frame elements having in-plan three DOFs (two translational and one rotational), while infill panels are modelled as shell elements having in-plan two DOFs (two translational). The interface between frame and shell are simulated through rigid springs. Similarly to the FEM approach used for modelling masonry infill panels in RC frames, filling cast-in-place reinforced concrete (LWSC) and PC panel are simulated through shell elements having, the two nodal DOFs indicated in Figure 4.6.36. The three layers are linked among them through rigid springs to constrain the DOFs of all internal and external shell nodes. Figure 4.6-36 shows a schematic representation of the numerical model.
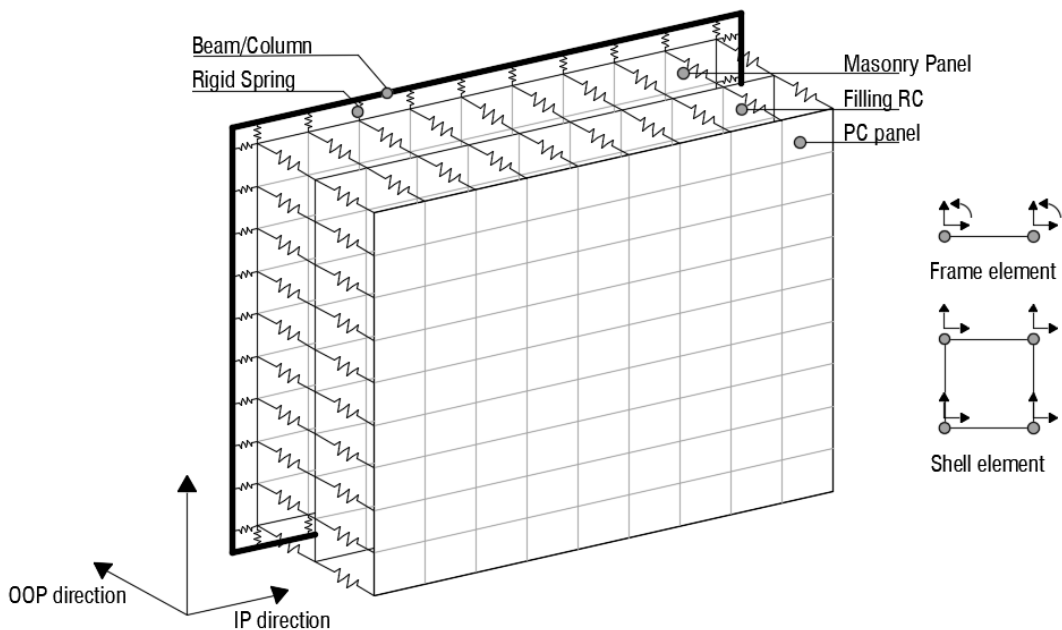
Fig. 4.6-36 – Schematization of the proposed FE model and available DOFs for frame and shell elements. Source: Martiradonna, S., Ruggieri, S., Fatiguso, F., Uva, G. (under drafting)

The external restraints are simulated through fixed supports applied at the base of columns and simple supports at the base of meshed shell nodes, assuming the foundation (including the existing and the new one added for the retrofit technique) as rigid. Concerning to the nonlinear behaviour, a fiber approach has been implemented. Frame

elements are modelled through the "section design" tool, by assigning the constitutive laws of concrete (confined and unconfined Mander, Priestley and Park, (1988) assumptions) and steel rebar to each fiber of beams and columns and the resultant fiber hinges are located at the end sections of frames. Shell elements are characterized through "layered nonlinear shell" tool, by defining the geometry of the three package components and by assigning to each fiber the related constitutive law. Regarding to masonry infill panel, each fiber is modelled according to the constitutive law proposed by Kaushik, Rai and Jain (2007) while, for PC panels and filling cast-in-place RC the unconfined Mander constitutive law is implemented.

Since no experimental data are available for a validation of the effectiveness of this proposal under seismic actions, especially for the masonry infill frame configuration, the results obtained by the numerical model are now compared with the ones obtained by adopting the consolidate macroscale approach (Uva *et al.*, 2012), which consist in the simulation of the masonry panel behaviour with a single strut that links opposite joints. The nonlinear behaviour of the strut for employing the macroscale approach has been simulated by using an axial plastic hinge, accounting for the Panagiotakos and Fardis (1996) constitutive law and by considering the elastic properties through a strut section defined according to (Shing and Mehrabi, 2002). Then, to investigate the seismic behaviour of the developed prototype, four numerical models have been developed, subjected to a nonlinear static analysis approach:

1. Bare frame model;
2. Infill frame model, by using a macroscale approach;
3. Infill frame model, by using a mesoscale approach;
4. Retrofit model, with multi-layer shells.

The results of the numerical analyses are shown in Figure 4.6-37, where 2 graphs are reported. The first one shows the comparison of bare and infill frame models in terms of base shear (V_b) and roof displacement (δ_R). In the second graph, the comparison is made for the bare, infill with mesoscale and retrofit models.
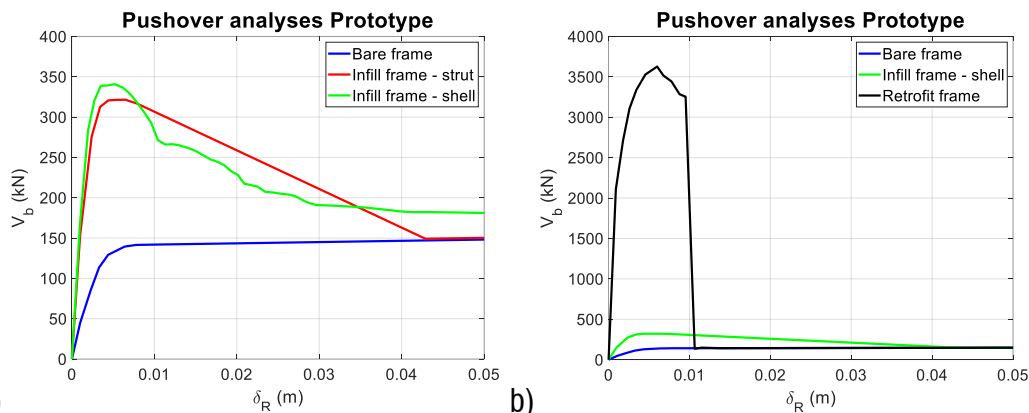
Fig. 4.6-37 – Pushover analyses on prototype FE model: a) comparison among bare and infill frames with strut and shell models; b) comparison among bare, infill and retrofit frames elements. Source: Martiradonna, S., Ruggieri, S., Fatiguso, F., Uva, G. (under drafting)

Pushover results show that the assumption made for infill frames are in accordance (Figure 4.6-37), with comparable values in terms of initial stiffness, peak V_b and δ_R and softening branch. Regarding to the retrofit method, as expected (Figure 4.6-37 b), the results show the proposed methodology provides a high increment of initial stiffness and peak strength (about 10 times of the infill frame one) and a strongly reduced displacement capacity. As a matter of fact, in terms of seismic behaviour, this system shows a low ductility capacity, especially in the post-yield branches. On the other hand, the high stiffness and strength contribution allows to assimilate the entire system to an elastic RC wall, with the related benefit in energetic retrofit terms. From the numerical point of view, when the failure of the masonry and retrofit layers is attained, the pushover curve re-joins that of the bare frame model, even if at this point the entire system should be considered as collapsed.

4.6.3.3   Choice of system cladding

This section provides the methodology employed to choose the cladding of the IPCS, hence, the coating material of the PC modules, in function of several qualitative and quantitative factors. In the field of the existing buildings refurbishment, only aspects relating to technical performance issues cannot be considered. The impact that an

intervention may have on society is a fundamental parameter to bear in mind as it can be decisive in the phases of choice of materials and technical solutions to be adopted. For instance, the choice of the building cladding may have repercussions on the building aesthetics, performance characteristics, installation methods as well as on costs and times of realization. Therefore, many parameters, both quantitative and qualitative, should be taken in account, making the choice a difficult problem to solve. Nevertheless, several mathematical tools, based on multicriteria decision making approach, may speed up this process and support the evaluation in order to select the best alternative. The widely used tool in different construction areas is the Analytic Hierarchy Process (AHP). It allows to decompose complex problems in basic components with the aim to individually analyse every aspect according to different criteria. Each component is weighted and judged by professional subjects to be later reassembled to recompose the whole problem pieces and give the resulting priority scale to the decision maker. An in-depth analysis of the methodology underlying the AHP is provided by Barzilai (1992), Saaty (2002) and Sangiorgio (2018). Figure 4.6-38 illustrates the problem structuring (a) and the base methodology of the AHP development by a flowchart (b).

a)
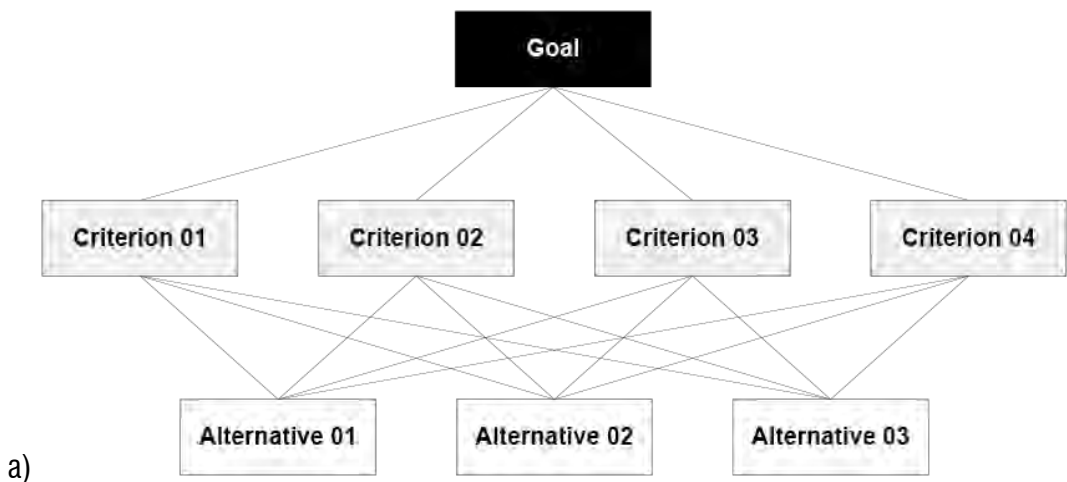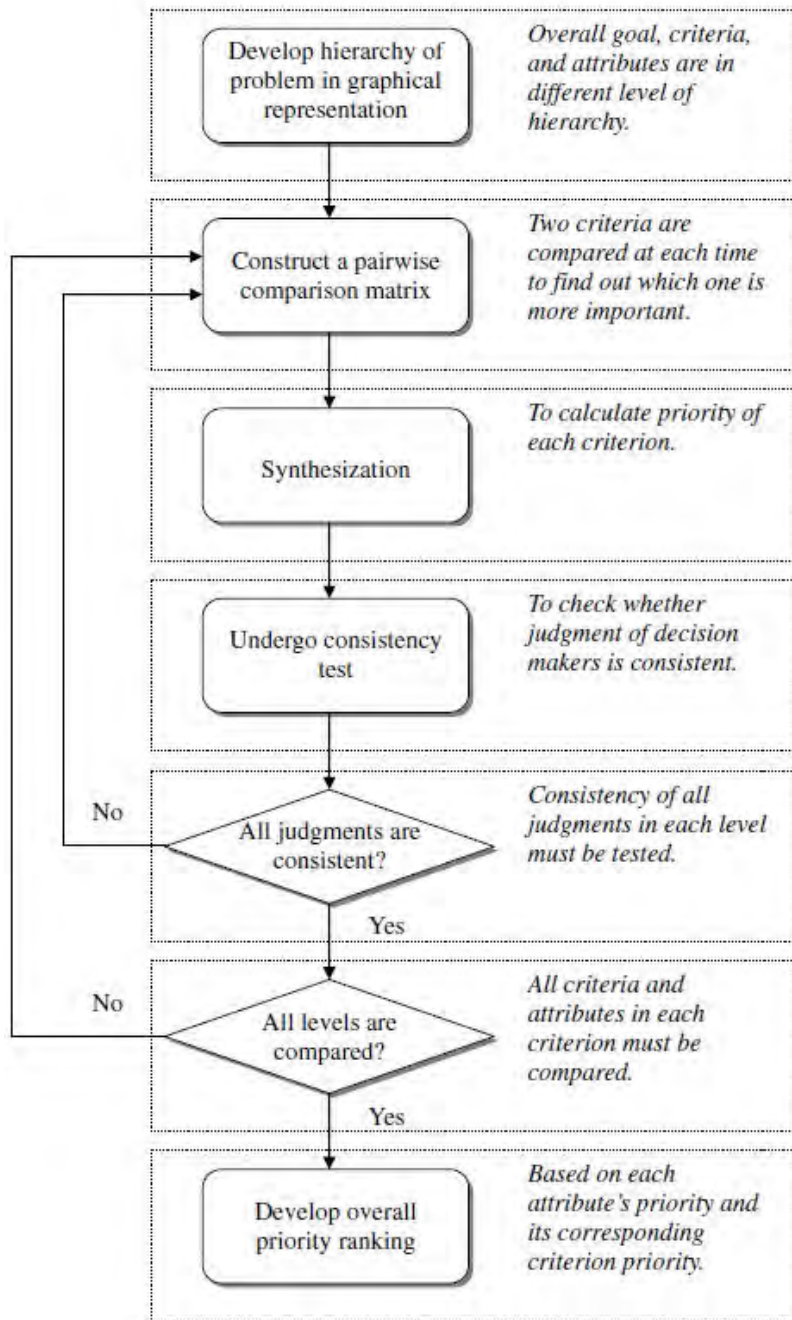
b)

Fig. 4.6-38 – Multicriteria analysis by AHP: a) problem structuring; b) AHP flowchart. Source: Viana Vargas, (2010); Ho, (2008)

In the literature related to the AHP application to the construction field, several authors have characterized the design work (Nassar, Thabet and Beliveau, 2003) according the contribution to sustainability (Guzmán-Sánchez *et al.*, 2018), by evaluating efficiency, user comfort, safety, reliability, functionality, and maintainability factors, in order to weight benefits in comparison with costs (Shapira and Goldenberg, 2005; Kwon *et al.*, 2014) and environmental impact (Bobylev, 2011). Furthermore, it is used to evaluate green building rating (Ali and Al Nsairat, 2009), energetic renovation (Gigliarelli, Cessari and Cerqua, 2011; Wang and Shen, 2013), building safety performance level (Sangiorgio *et al.*, 2017, 2019) and for many other building aspects.

In the context of the building refurbishment through the Innovative PC panel system, the complex decision problem that needs to be analysed by the AHP approach is the choice of the cladding of the PC modules to apply to the system because of the great amount of qualitative and quantitative parameters to consider. As already reported in the subsection 4.5.4 of this chapter, the use of a material rather than another can affect the characteristics of the panel in terms of aesthetic impact, time and requirements of production, installation, technical features, and economic sustainability.

Therefore, to determine an effective choice regarding the best selection of the cladding for the PC modules, the problem structuring is the first step. Four macro-criteria are considered: aesthetics, production and executive needs, thermal behaviour and costs. In turn, six criteria i (with $i=1,\ldots,6$) are defined: aesthetic impact, required construction vehicles, realization complexity, thermal transmittance, thermal inertia, expected cost. The set of the six different module coverings illustrated in the subsection 4.5.4 are proposed as alternatives j (with $j=1,\ldots,6$): exposed concrete, wood coated, brick coated, ceramic coated, stone coated, plastered. Criteria and alternatives are structured in a hierarchical flowchart showed in the Figure 4.6-39:
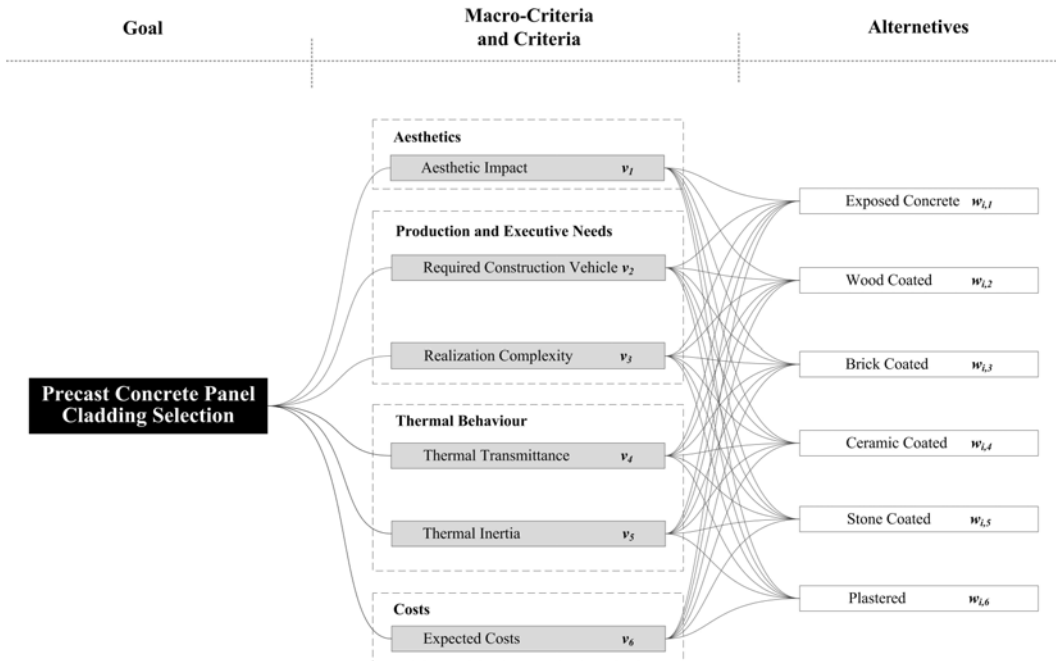
Fig. 4.6-39 – Structure of the Problem: criteria and alternatives to choose the best cladding for the Intelli-gent PC panel system. Source: Sangiorgio *et al.*, (2021)

The rationality of the specified criteria and alternatives is related to the context in which the IPCS is developed. In particular, the conditions expressed in the section 4.2 and the partner company requirements are considered.

The first qualitative macro-criterion and criterion regard the aesthetic aspects.

a. *Aesthetic Impact* ($i = 1$) is the factor that may have a strong effect on the society. Indeed, since the system is born for EPBs, a low aesthetic impact may have some negative effects such as marginalization and social discrimination. Instead, a high aesthetic impact may return dignity to the building, integrate the residents with the rest of the city and makes the building gain value (Pittau *et al.*, 2017).

The second qualitative macro-criterion is about production and executive needs of the company. the criteria regard the vehicles required to transport the panels from the factory to the construction site and the complexity in realizing and installing the modules.

b. *Required construction vehicles* ($i = 2$) is related to the typology of lorry employed to deliver the panels to the construction site. It is better specified in the subsection 4.5.4.

c. *Realization complexity* ($i = 3$) considers the different requirements and measures for the PC module production and the system installation in the construction place (according to the rules of workers prevention and protection on the work). In particular, caution during the movement phases, scaffolds, props and stiffening of anchors are considered according to the already illustrated Figure 4.5-10.

The third macro-criterion regards the thermal behaviour of the building renovated by the application of the system. According to the subsection 4.6.3.1 of this chapter, the two quantitative criteria to assess the preliminary thermal behaviour of the buildings are the following:

d. *Thermal transmittance* ($i = 4$);

e. *Thermal inertia* ($i = 5$).

The final macro-criterion considers a preliminary evaluation of costs. The related quantitative criterion is defined as follows:

f. *Expected cost* ($i = 6$) is the economic parameter that considers the percentage increasing of the panel costs in function of the cladding material chosen and its assemblage technology. It also includes the preliminary evaluation of the costs of the labour in the factory and in the construction site, the increasing in production, installation, refinement times and the mere costs of the materials.

Assuming that the retrofitting technological system remains unvaried, the six alternatives of the PC panel cladding are defined in the table 4.6-11 below:

Table 4.6-11. Six cladding alternatives of the PC modules

ILLUSTRATION	DESCRIPTION
	Exposed Concrete ($j = 1$) is the standard module applied to the Innovative PC panel system. Its external finish is smooth and shows the typical grey color of Portland cement concrete. Its characteristics are deepened in section 4.5.
	Wood Coated ($j = 2$) is the PC module integrating the wooden strips used for external surfaces covering. The technology is better specified in the subsection 4.5 and in particular, by the figure 4.5-9. This type of cladding permits hiding the junctions among the panels.
	Brick Coated ($j = 3$) is the standard PC panel integrated with ceramic solid bricks during the prefabrication process. The considered bricks are 25 cm long, 12 cm wide and 2.5 cm thick, arranged in rows along the width and with offset vertical joints. Hence, the panels leave the factory already with the brick coat.
	Ceramic Coated ($j = 4$) is the base module cladded with ceramic tiles before the concrete casting. They can be arranged according to the architectural design and with various shape tiles. Those considered are 20x40 cm in brown shadows. Also in this case, the modules leave the factory integrated with the ceramic cladding.
	Stone Coated ($j = 5$) is the PC panel cladded using the "Trani's stone" tiles. They are widely used in Apulian region, for its characteristics and white aspect. The tiles are arranged in the casting formwork of the carousel plant as first layer. The stone coated PC modules arrive to the construction site ready to be mounted on the building.

Plastered ($j = 6$) is the most common cladding of the southern Italy and consists in integrating the PC modules with four layers: first cement mortar, plaster net, second cement mortar, and the coloured tint. It is performed directly in the construction site, after concluding the system installation. It is necessary to fill the junctions between the panel, before executing the plaster application.

Source of figures: Author

The next step of the AHP approach consists in involving a group of users operating in the construction field to perform the pairwise comparisons between the alternatives, and then between the criteria, and provide a weight to each, in accordance with the literature (v_i for the criteria; $w_{i,j}$ for the alternatives). Hence, following the procedure offered by Saaty (2002), the global weights referred to the alternatives are calculated (w_i') in order to generate a hierarchical scale of the different claddings and choose the best one for the application for which the AHP has been developed. This approach has been applied to a case study, which results are afforded in the forward section 5.4.

4.6.3.4 Monitoring technology

The programming of maintenance activities may preserve the building from failures and damages and keep the performance unaltered during its life cycle, especially after having been subjected to renovation interventions. However, these activities are difficult to manage and programming, in particular if the building apparently does not present damages or deficiencies. Therefore, the monitoring activity is essential in order to obtain information about the health status of the building and to avoid situations of irreversibility. In addition, the automation in this field is crucial in the data acquisition and processing phases. It avoids the constant presence of a professional on the building site and, above all, it speeds up the monitoring procedure, allowing a constant, faster and correct reading of the results. It is achieved by the synergic work of performance devices integrated into the buildings and a computing platform which thanks to the implementation of the modern technology of the Internet of Things, may constantly communicate in real time in order to offer a more detailed overview of building performance. They may provide information about climate (Lesecq *et al.*, 2017), building structural health (Scuro *et al.*, 2018) in order to have a more efficient building toward a sustainable development (Wang *et al.*, 2017). Recently it has been implemented also in prefabricated elements to achieve real-time visibility and traceability of the building (Zhong *et al.*, 2017) or to detect energy deficiencies and structural anomalies by integrating psychrometer and accelerator meter devices (Zaglio *et al.*, 2018) etc.

Since one of the goals of the thesis was to provide a technological solution that could integrate devices for the building performance monitoring, this section is intended to illustrate the technological design choices for the inclusion of monitoring equipment within the system. Furthermore, a primarily idea of monitoring and processing data platform is provided.

The IPCS is so called because it provides the possibility to insert into its section wireless sensors for the temperature and relative humidity control which can be inspected from the top of the building. Equipped with an airtight cap and protected by a thermo-isolated flashing, the environment into the mullion does not suffer the influence of the outdoor climatic conditions, making the measurements of the devices truthful and reliable. The

advantage of this solution is the possibility to place, maintain and remove the sensors at any time, also during the installation phases, after anchoring the mullions at the frame structure.

As the example illustrated in the Figure 4.6-40, the sensors should be placed into the omega-profile mullions having an empty core which develops along all the height of the building. The sensors can detect the data in any portion of the building at the required height because the mullions have been designed to be integrated with a telescopic rail that can be elongated and retracted as needed. However, this aspect of the project remains as idea proposal as technical constructive issues have been majorly explored.

Fig. 4.6-40 – The "Intelligent" PC panel system: technological solution for the positioning of monitoring devices. Source: http://www.bamip.it/it/montanti,-profilati-e-staffe-ad-elica/item/116-profilati-multiforo-telescopici

From the commissioning of sensors equipped with the IoT technology, the monitoring process starts. In order to read the data collected by the devices into the building, it is necessary to design a computing platform calibrated according to several parameters.

Hence, this section provides a preliminary design of a generic Performance Detecting Platform (PDP) which founded on the database of an Information System (IS), analyses and processes the data collected by the sensors, comparing them with predefined limit values. A box transmission is required into the building to collect the data of the sensors and transmit them to the PDP. The methodological design of the platform is developed in accordance with the approach by Martiradonna (2019).

The information flow from the sensors to the PDP of the IS consists in three main phases: data-setting phase, data acquisition phase, and data processing phase. It is illustrated in Figure 4.6-41.
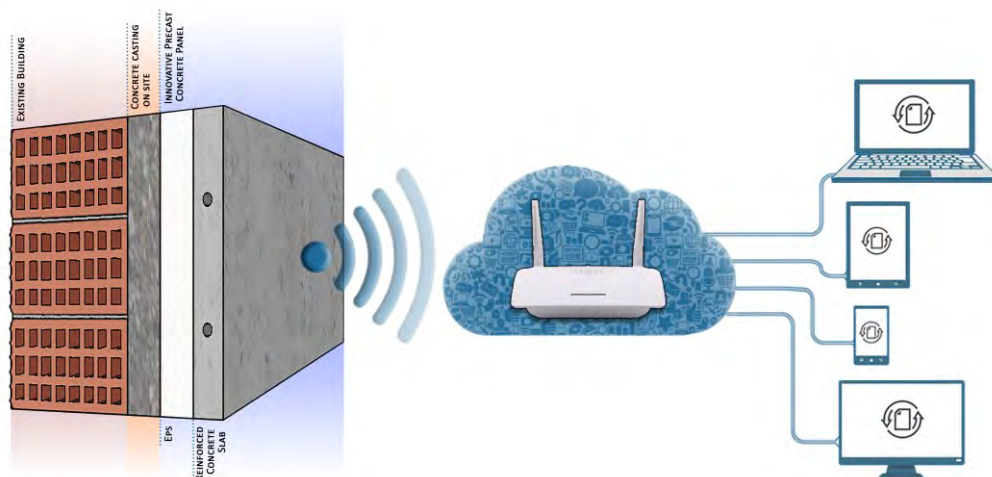
Fig. 4.6-41 – Information flow from the sensors to the PDP of the IS. Source: (S. Martiradonna, Lombillo and Fatiguso, 2019)

In the first phase the PDP is set with the risk parameters deriving from the study of the local climate conditions and by European and national directives. Some geographic, typological and geometry information are also added. Hence, an *Identification Tab* of the building is generated as shown in Figure 4.6-42 a. In this phase, a 3D model of the refurbished building is generated and connected to the PDP. The model includes the matrix of points indicating the position of the sensors. Thus, the PDP generates the first *Matrix of survey* for climate data (Figure 4.6-42 b) and positioning data (Figure 4.6-42 c). It is the graphical schematization of the panels with their related devices installed on the building and the values detected by them. It is divided into two principal portions: the interactive box and the values spectrum acquired by the sensors. The interactive box contains the 3D model divided according to the disposition of the PC panels on the facade. The columns of the grid are assigned an identification letter (a, b, c, etc.), while the rows contain the floor indication in descending order (P2, P1, P0). Moreover, a series

of points is visible into the grid, representing the sensors recognized by an identification number.
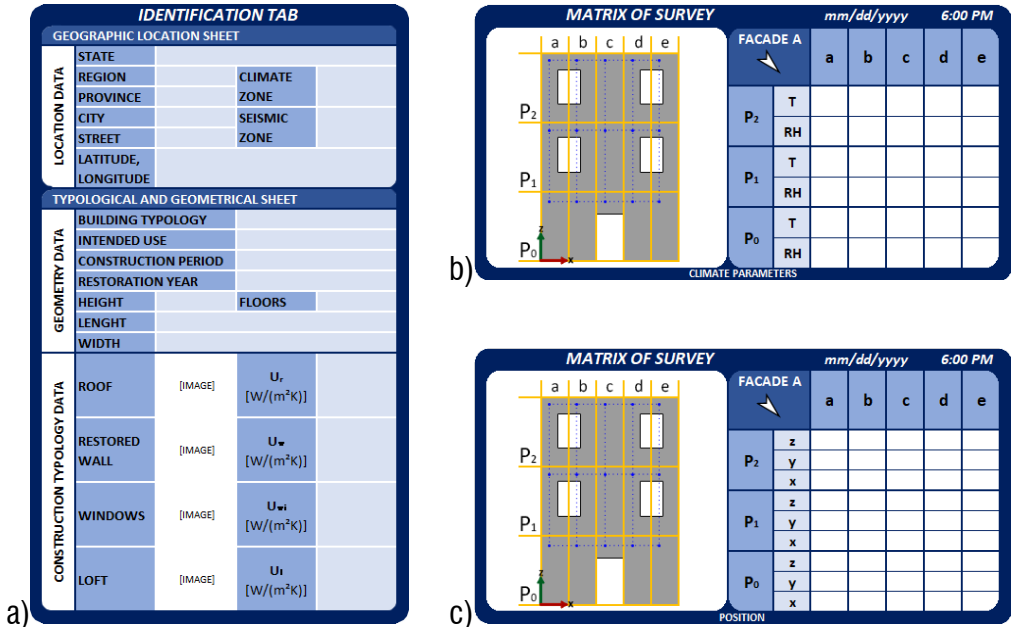
Fig. 4.6-42 – Data setting: example models of a) building *Identification Tab;* b) climate *Matrix of survey*; c) position *Matrix of survey*. Source: Martiradonna, Lombillo and Fatiguso, (2019).

In the second phase, data acquisition is performed both by the devices and the PDP. The first ones detect their absolute and relative three-dimensional position and the thermo-hygrometric parameters into the wall section. The box transmission collects these data and sends the information to the PDP.

In the data processing phase, the PDP automatically elaborates and compares the acquired data with the risk limit values and generates graphs of performance trends. If the risk limit values are exceeded, it notifies the event. In parallel, the information of the building 3D model is updated with the new matrix of point surveyed. The PDP overlaps the new matrix with the original one, indicating the new absolute or relative movements of the structure. if there are movements in the order of few millimetres, the platform notifies the risk in the matrix and in the 3D model, colouring in red the cells and the panels that are undergoing the movements. Thus, the matrix is tagged as *Matrix of risk* in which the

3D model generates a new grid of points on the original one to understand if the problem concerns a local part or the global structure (Figure 4.6-43 a, b).
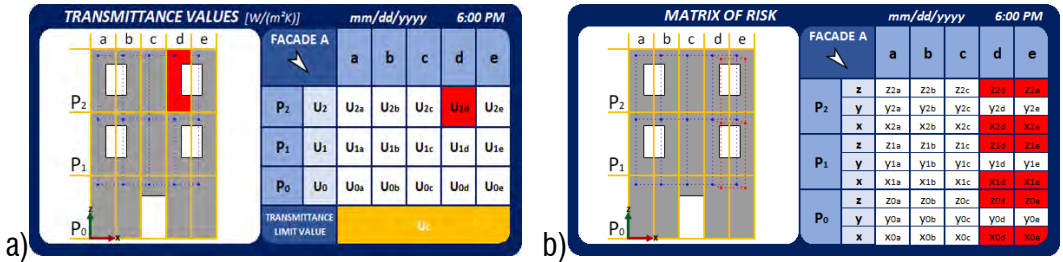
Fig. 4.6-43 – Data processing phase: example models of a) thermal *Matrix of risks*; b) position *Matrix of risks*. Source: S. Martiradonna, Lombillo and Fatiguso, (2019).

In the future developments, a more deepen project of the PDP will be performed.

5 PILOT CASE STUDY

The methodology approaches employed to design the "Intelligent PC panel system" (IPCS), i.e. the technological proposal for the energy and structural retrofit of the existing RC buildings in the South of Italy, has been applied to a pilot case study to assess preliminarily the global structural response of the system on the specific type of building chosen.

In this chapter, both the thermal and seismic behaviour of the building have been studied, with further investigations on specific portions. As reported in the methodology at sub-sections 4.6.3, the analyses have been carried out basing on the approach defined by FE modelling, since no experimental tests have been performed.

Finally, the AHP approach proposed to choose the PC module cladding has been applied to select the best envelope for a typical economic-popular building (EPB) of the Apulian region.

First of all, it worth mentioning that on the selected pilot case study, all the analyses and the numerical elaborations are aimed to assess the efficiency of the proposed approach, by completely neglecting the necessary phases for a reliable seismic assessment of an existing building. In other words, before designing any kind of retrofit solution on a building, it is necessary to carry out a systematic preliminary phase to achieve a complete knowledge of the building: in-situ characterization of structural materials and structural elements, assessment of the constructive details. Only after these steps it will be possible to perform the evaluation of the capacity for all structural elements under gravity and seismic actions , accounting for ductile and brittle mechanisms. On this basis, the safety level of the structure can be assessed and the retrofit solution chosen. With regard to the pilot case study, the building analysed is part of the residential housing complex in the

west-side of Trani, a city few kilometres far from Bari. It is located in a peripheral zone along a wide street. It was constructed between 1958 and 1963 and contains most of the peculiar traits of the post-War World II buildings in the South of Italy, remained almost unaltered over the years. It has been designed according to the older Italian code, only accounting for gravity loads and not considering any anti-seismic roles. Figure 5-1 illustrates the case study building through a real photo (a) and the 3D base-model (b).

a)

b)
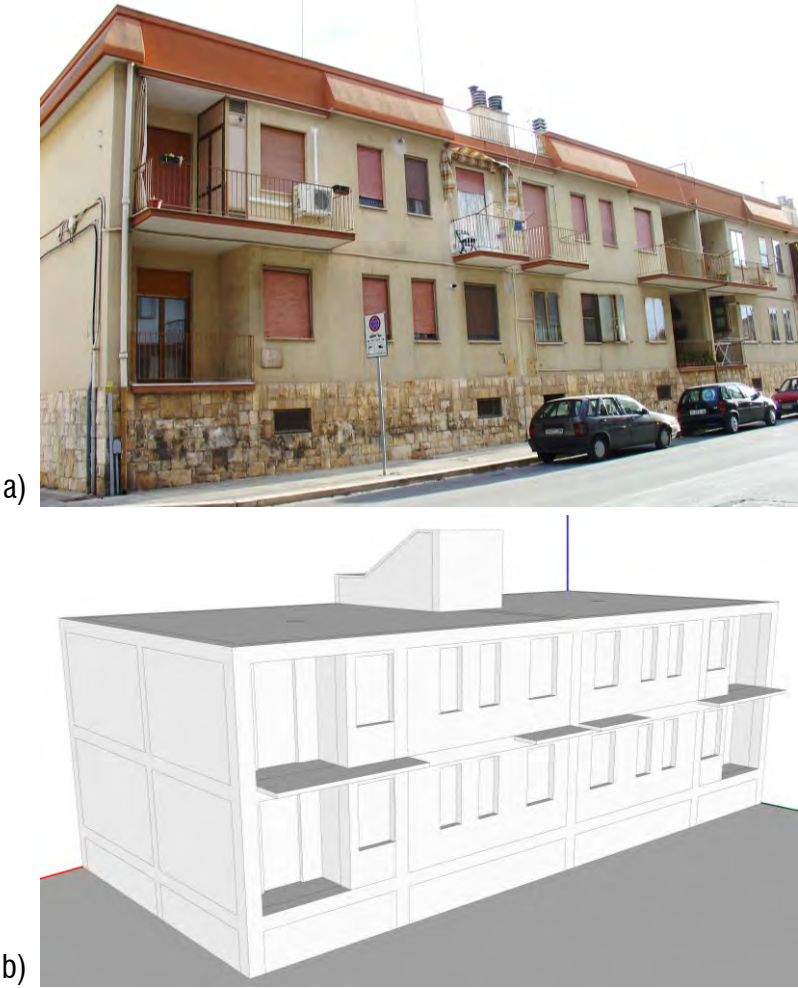
Fig. 5-1 – Pilot case study: a) real photo; b) 3D base-model. Source: Author

In detail, it is a multi-family building, regular in-plan and in-height, presenting a rectangular shape of 21.8 m x 10.9 m, two plants of 3 m height (H), and moment-resisting frames in one direction, with a central staircase. Beam and column sections do not present variations between first and second levels and footings connected by beams constitute the foundations. Both storeys present RC ribbed slab, as in the greater part of the Mediterranean buildings, having constant joists of fixed dimensions (height 20 cm, width 10 cm, and spaced 50 cm) interspersed with hollow clay masonry blocks, all covered by a RC concrete layer of 4 cm thick. The infill walls are in hollow brick of 25 cm x 25 cm x 12 cm as the type considered in the table 4.6-3 of the section 4.6, casted in place with Portland cement 325 and quarry sand mortar. No insulating layers are included, thus, the U-value of the wall is 1.25 W/m^{2}K.

From a visual inspection of the building, the windows have open-joint aluminium frames, with single glass and no insulating chamber. Figure 5-2 illustrates some examples of window surveyed.

Fig. 5-2 – Case study: Survey of the windows. Source: Author

As regard the structural frame, Table 5-1 provides information about gravity loads (dead and live ones, respectively indicated with G and Q), information for the estimation of the seismic loads (coordinates (Lat, Lon), nominal life (N_L), usage class (U_c) and indexes of soil category and topography (Cat and Top)).

Table 5-2 show the hypothesized mechanical parameters of the elements i.e. mean compressive strength of in situ concrete (f′$_{cm}$), mean tensile strength of steel rebars (f′$_{ym}$), elastic modulus of concrete (E$_c$) and elastic modulus of reinforcement steel (E$_s$). The

values of typical mechanical parameters of masonry are provided too, i.e. the elastic moduli E_w, $E_{w\theta}$ and G_w, respectively, vertical, diagonal and shear ones, the compression strength σ_m and the tensile strength f_{tp}.

Table 5.1-1. Report about case study building: loads and geometrical information

BUILDING FEATURE	GRAVITY LOADS			HEIGHT	SEISMIC LOADS				SOIL	
	G_1	G_2	Q	$H_1 = H_2$	LAT	LON	N_L	U_c	CAT	TOP
	kN/m^2	kN/m^2	kN/m^2	m	°	°				
VALUE	3.50	2.50	2.00	3.00	16.416	41.274	50	1	C	T_2

Table 5.1-2. Report about case study building: mechanical parameters

BUILDING FEATURE	IN SITU CONCRETE		STEEL REBAR		MASONRY ELEMENTS				
	f'_{cm}	E_c	f'_{ym}	E_s	E_w	$E_{w\theta}$	G_w	σ_m	f_{tp}
	MPa	MPa	MPa	MPa	MPa	MPa	MPa	MPa	MPa
VALUE	20.00	29962	440.00	205000	3080	1495	1233	2.5	0.36

The characteristics of the elements are summarized in Figure 5-3, wherein there are beams and column sections and the related steel reinforcement.
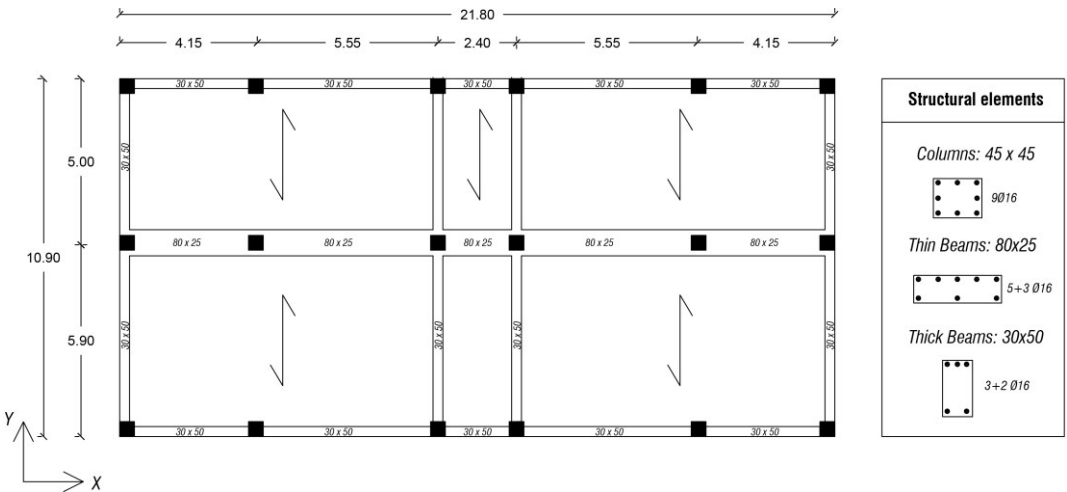
Fig. 5-3 – Carpentry of the case study and detail of end sections of structural elements. Source: Martiradonna, S., Ruggieri, S., Fatiguso, F., Uva, G. (under drafting)

5.1   Design of the intervention

The IPCS has been designed to adapt to the geometry of the pilot case study, assuming that in correspondence of the loggias and balconies the traditional intervention of external insulation coating has to be performed in order to thermally protect the building portions in which the system cannot be installed. The structural layer of the system were connected to the RC beams, pillars and curbs of balconies by post-installed rebars strengthened with chemical injections as explained in the subsection 4.6.1.1. Figure 5.1-1 shows the section about the connection of the system to the particular beam-curb node. Thanks to the panel configuration i.e. the shifted layers, the innovative system and the traditional retrofitting interventions were adapted to each other, creating a unique thermal-insulating layer outside the building. The dimensions of the modules remained unaltered for most of the building. Only in some cases they have been varied in accordance with the panel design requirements, to better adapt to the structure.

For the simulation of the system application to the pilot case study, the design of the intervention has regarded only the dimensional adaptability, thus the composition of the panel around the building. The specific anchoring project have not been performed. The minimum anchor dimensions, spacing and length have been considered in accordance with the related regulations, specified in the subsection 4.6.1.
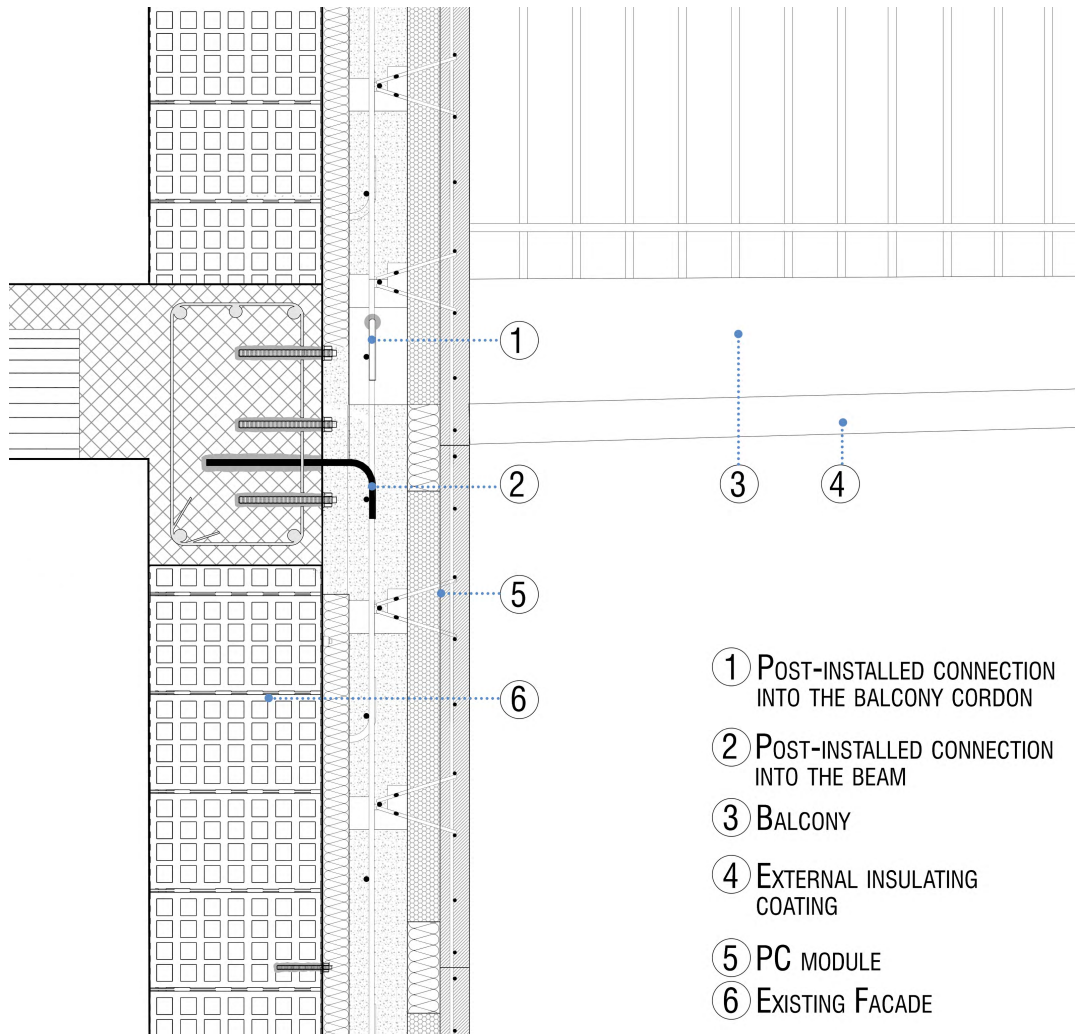
Fig. 5.1-1 – Particular sections: a) connection to the beam-curb node; b) innovating system integrated with the traditional external thermal-insulation. Source: Author

5.2   Thermal Behaviour assessment

The case study considered presented the wall typology of the most common RC building constructed in the post-WW2 in the South of Italy. It corresponded to the building façade chosen for the development of the IPCS design methodology. Therefore, the U-value of the wall has been considered equal to 1.25 W/m²K since no insulation layer was included

into the section. The analysis of the actual state of the building was performed according to the methodology reported in the subsection 4.6.3.1 with the mean Trani's climate conditions below, selected from Bari Karol Wojtyla weather station, Italy (WMO: 162700) by ASHRAE Climatic Design Conditions 2003/2013/2017:

- $T_i = 293.15$ K; $RH_i = 52\%$;
- $T_e = 281.55$ K; $RH_e = 68\%$.

The thermal behaviour was observed through a qualitative approach using the software COMSOL Multiphysics in steady-state conditions. In particular, the heat flux in a specific building portion was deepened. Hence, a reduced model of the building which contained an half part of the balcony/loggia between two apartments, was imported in the software, Figure 5.2-1 shows the considered building portion from the outside (a) and inside (b) in the FEM environment. The two views were called OUT and IN, respectively. Figure 5.2-2 illustrates the results of the analysis of the building actual state, in the plan view (xy), while Figure 5.2-3 in OUT view (a) and IN view (b).
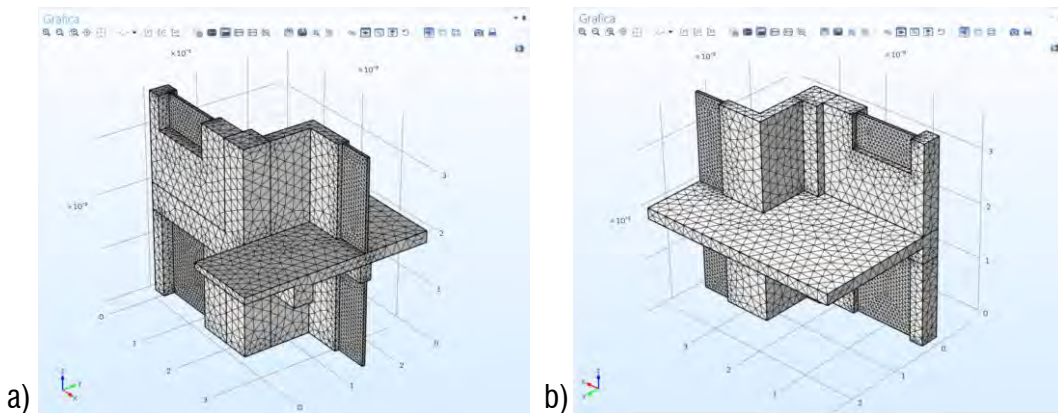
Fig. 5.2-1 – Thermal behaviour assessment: building portion in FEM environment a) from outside; b) from inside. Source: Author
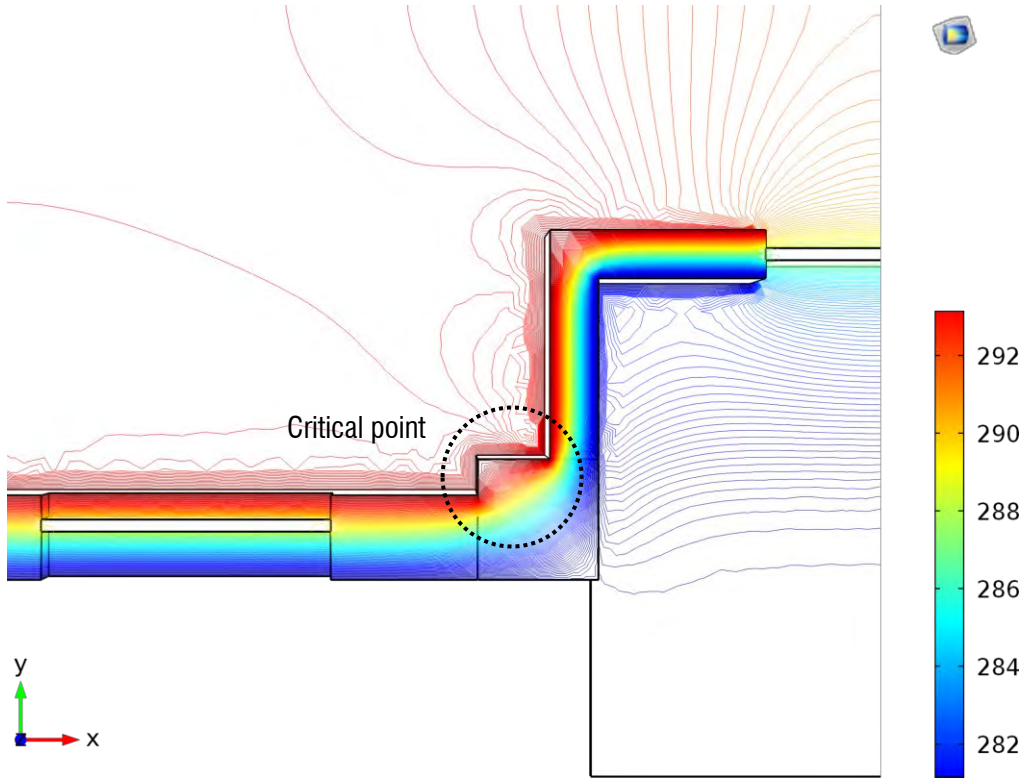
Fig. 5.2-2 – Thermal behaviour assessment - actual state: plan view. Source: Author

a)   b)
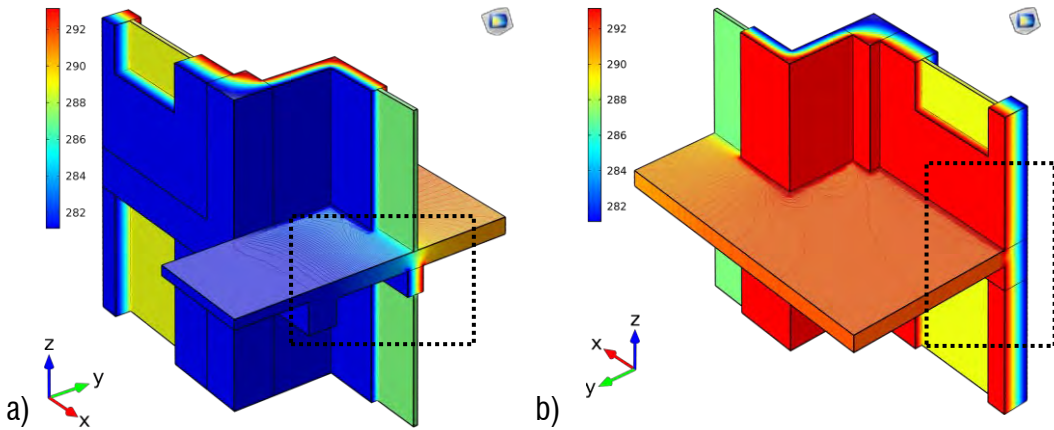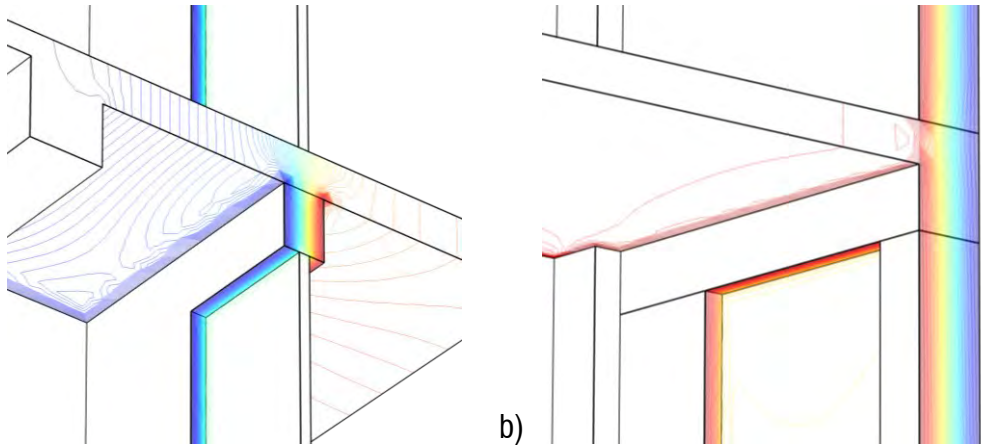
Fig. 5.2-3 – Thermal behaviour assessment - actual state a) OUT view; b) IN view. Source: Author

At the actual state, the temperature difference between the inner and outer faces of the building was about 11.4 K. It generated a great outgoing thermal flux with heat losses of about 70% in the section. It was accentuated at the intersections between the wall and the balconies, especially in correspondence of the windows. Thermal bridges were not surveyed due to the thickness of the external walls. Although, a critical point was identified at the junction between the pillar and the thinner wall of the lodge in the indoor corners.

Therefore, the simulation of the refurbishment through the novel system was performed. Since the pilot building had the same characteristics of the model employed to explain the methodology and the climate conditions were similar to those for the characterization of the IPCS, the preliminary analysis about thermo-hygrometric behaviour is explained in the subsection 4.6.3.1. Instead, the heat flux and the thermal bridges assessment was conducted in order to understand the effectiveness of the system in preventing thermal dispersions.

Since the simulations have regarded only the retrofit of the external walls, the windows and the other aspects have been leaved unaltered. Therefore, among the results, an excellent thermal insulation capacity is expected from the new system but a strong thermal dispersion on the surfaces of the windows that are not equipped with any protection. Fig. 5.2-4 illustrates the results: a) global behaviour; b) global section X-Y view; c) section X-Y (window); d) section Y-Z (wall-windows); e) section Y-Z (wall).
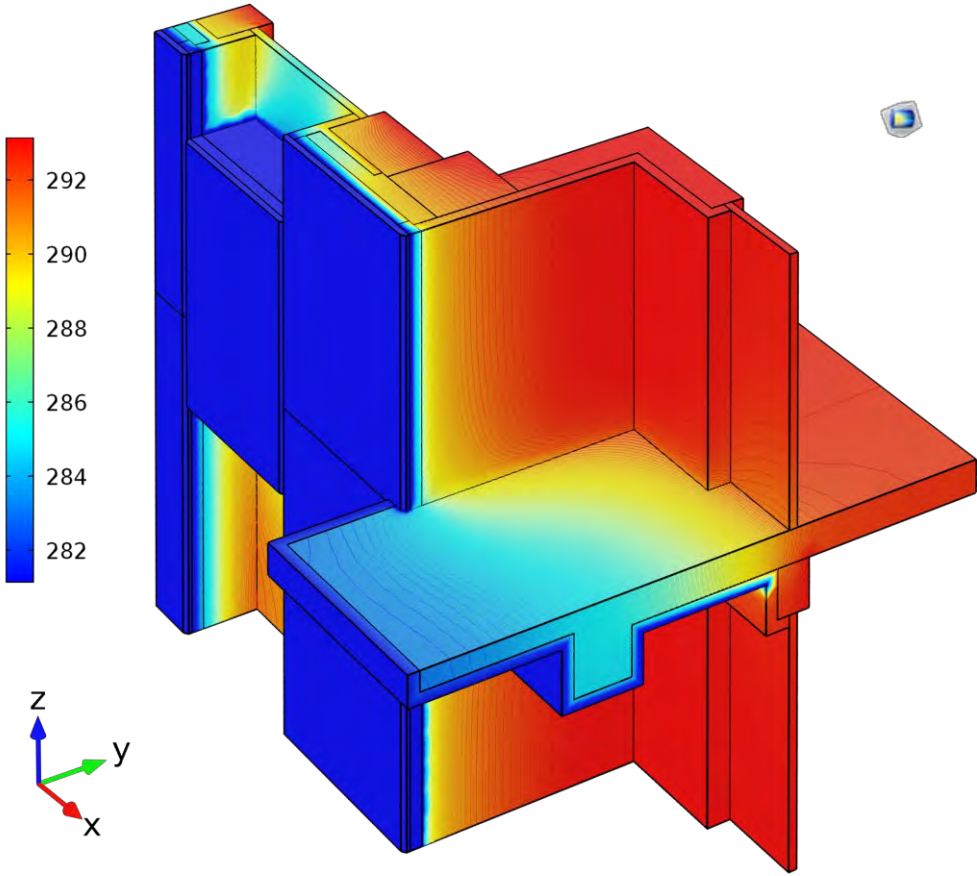
a)
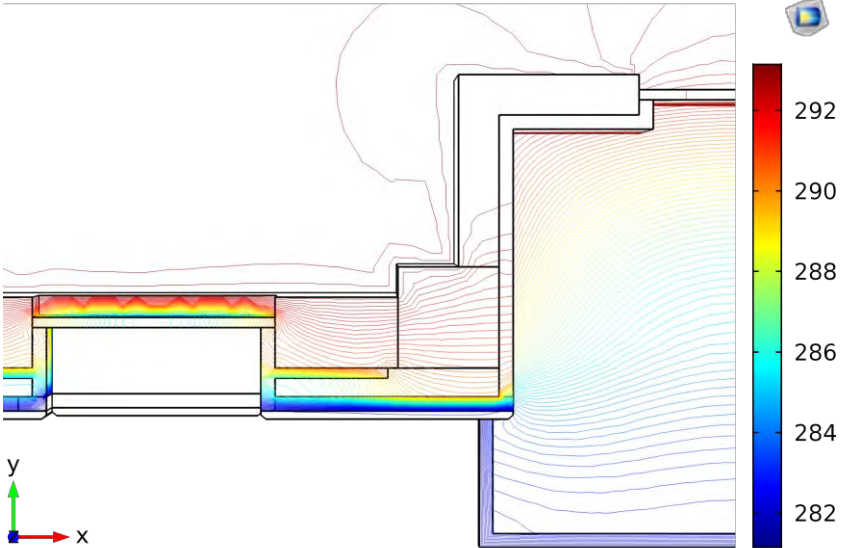
b)
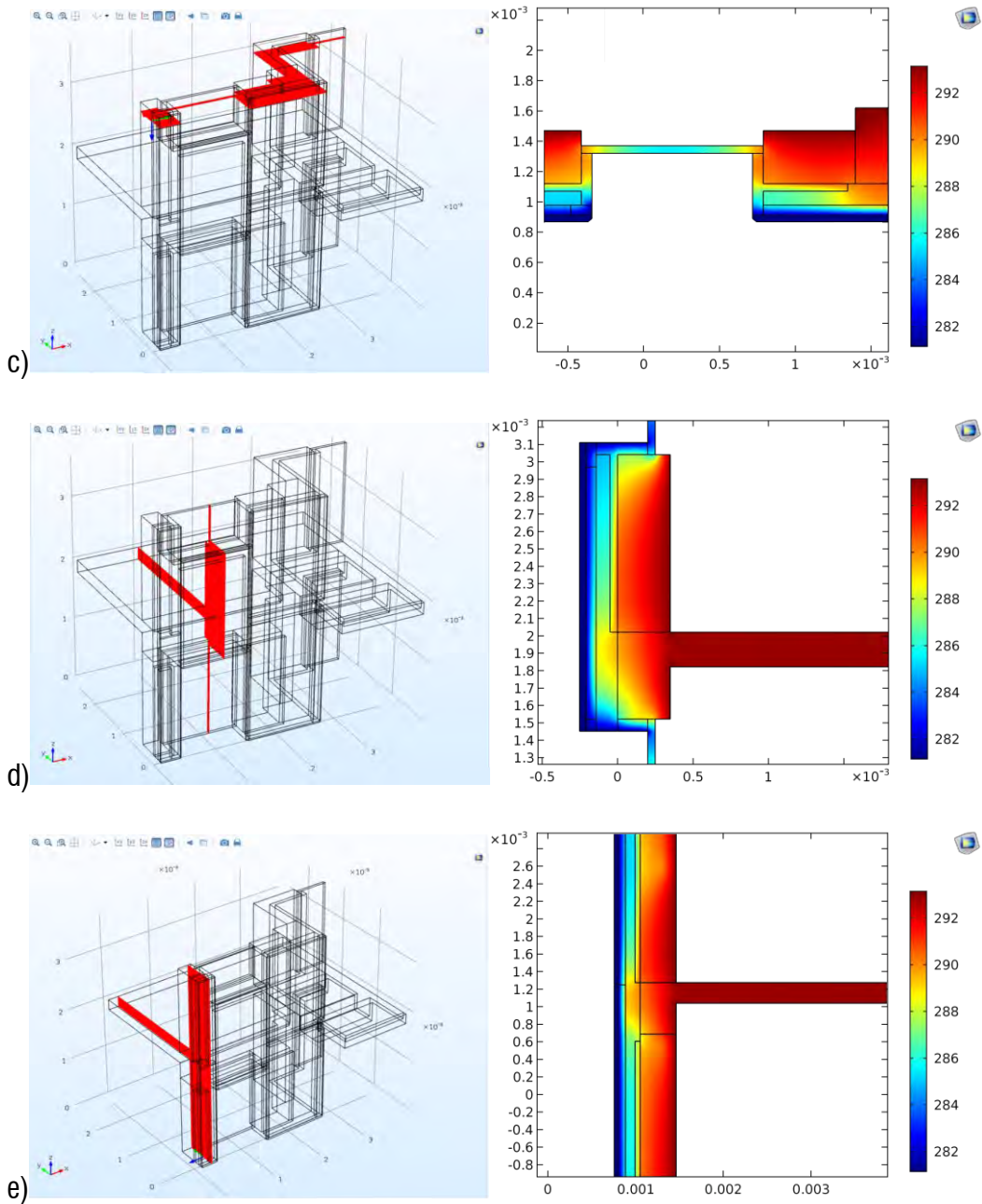
Fig. 5.2-4 – Results of the visual analyses of the system thermal advances: a) global behaviour; b) global section X-Y view; c) section X-Y (window); d) section Y-Z (wall-windows); e) section Y-Z (wall). Source: Author

The overall behaviour of the building portion with the applicatin of the Intelligent PC panel system is very good. The walls stay warm almost along the whole section with temperature difference between the inner and outer side of about 3 K and a reduction of the heat losses of about 74%. However, as expected, in correspondence of the windows, the heat flux became irregular with a huge temperature variation at the intersection with the system, between the insulating wall and the external coating. It is visible in the plan section in figure 5.2-4 c and vertical section in d. The windows caused a high dispersion of heat, also affecting the performance of the system and the outer coat. In addition, the presence of different materials in the section of the building, eg. the concrete of the beams and the ceramic of the brick wall, generated an uneven distribution of temperature in the upper and lower part of the wall. It was due to the presence of a thinner outer lining insulation layer. A thicker insulation panel would solve this problem.

5.3   Seismic valuation: analyses and results

The case study building has been modelled by using SAP2000 software. According to the methodology employed for the prototype FE model (subsection 4.6.3.2), a fiber approach has been implemented. In particular, nonlinear behaviour of frame elements has been defined by assigning fiber hinges at the beams and columns end sections through "Fiber P-M2-M3" library, while shell and link elements are defined as for the prototype model. For the structural performance estimates, eight FE models have been developed (four configurations in the 2 main directions, X and Y, as defined in Figure 5), by considering bare frame (BF), infill with masonry panel simulated with shell elements (IF) and two retrofit configurations (RF1; RF2).

The differences between RF1 and RF2 are related to technologic aspects in the application of PC panels on an existing RC building. In particular, RF1 consists in the application of the proposed retrofit technique only on the "full" parts of the building envelope and by neglecting the parts in correspondence with the openings; RF2 consists in the application of the retrofit on the entire building envelope, in the hypothesis that PC panels can be resized in order to accommodate all openings (both windows and doors).

In the practice, both solutions included in RF1 and RF2 could be employed. For sure, RF1 results the easier way to apply the PC panel, considering the vertical connections and

the possible presence of overhangs, which can interrupt the desired interaction. On the other hand, for achieving a full energetic retrofit, it is necessary to forecast a thermal coat on the uncovered parts of the building envelope. RF2 is going to be the best way to obtain an elevate performance from the energetic and seismic point of view, but it could hold some difficulties in the PC panel application, due the assignment of an irregular shape to PC panel and the related connections with the structural elements. Assuming a prefect reliability of the retrofit about technologic and structural local aspects, all numerical models present base columns fixed at the base, while shells are restrained at the base with simple supports. An internal constraint has been predisposed for simulating a rigid diaphragm, which can represent a correct assumption in the case of perfect box behaviour. Loads G and Q are applied as distributed on the frame elements, according to the seismic combination provided by Eurocode 8. Regarding to shell elements, both in infill and retrofit configurations, the presence of openings for doors and windows have been accounted.

Regarding to the ductile and shear capacities of elements, the automatic definition of the nonlinear properties of frames and shells allows to fix the trend of failure mechanisms on the stress-strain behaviour of the several materials employed. In particular, concrete fibres are characterized with an unconfined Mander constitutive law, while steel fibres are modelled with an elasto-plastic constitutive law with hardening behaviour. At the same, the acceptance criteria for defining the achievement of the limit-states for frame elements have been automatically defined. Looking at the concrete stress-strain, the immediate occupancy (IO) limit-state is defined a strain value of fibres equal to 0.08%; the life-safety (LS) limit-state is defined for a strain value of fibres equal to 0.22%; the near collapse (NC) limit-state is defined for a strain value of fibres equal to 0.35%. Figure 6 shows the eight numerical models, subdivided for the two main directions, besides to report some modelling details regarding to the link among frame and shell elements. It is worth noting that the shell elements have been meshed, according to the schematization proposed in Figure 5.3-1, by assuring that the results obtained with a fitter mesh presents a maximum scatter of 3% and by linking each joint with perpendicular rigid link.

3D view - BF Model (Same for X and Y directions)
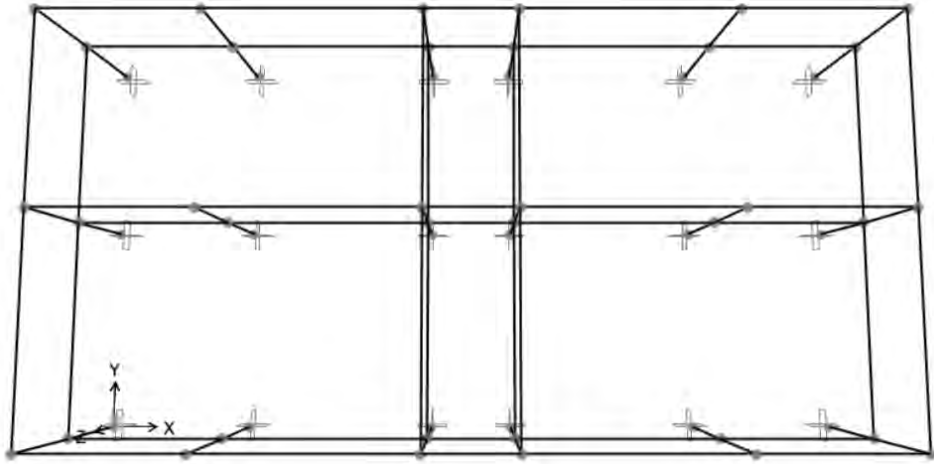
Plane X-Z - IF Model (X direction)
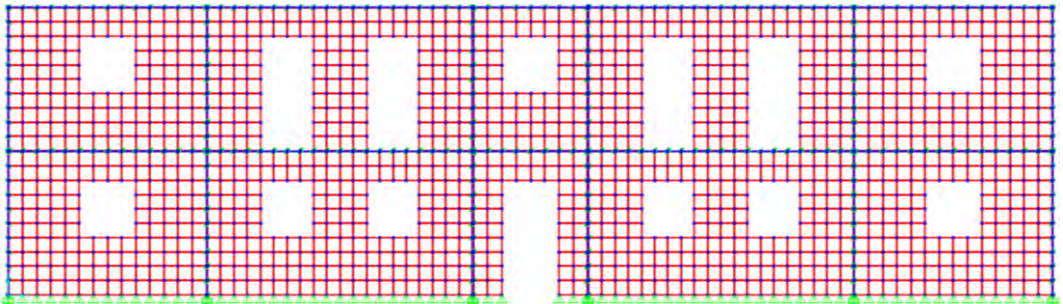
Plane X-Z – RF2 Model (X direction)
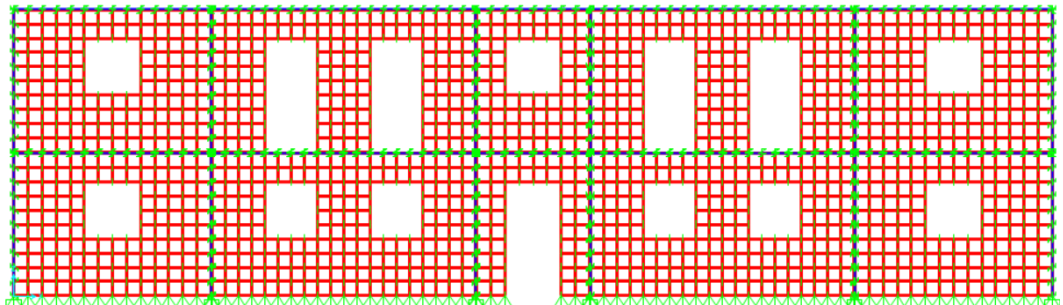
Plane Y-Z - IF Model (Y direction)　　　　Plane Y-Z – RF2 Model (Y direction)
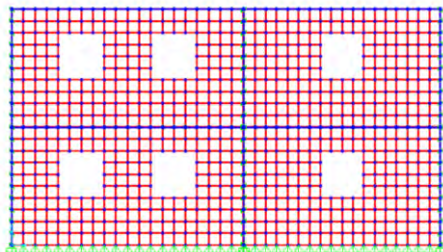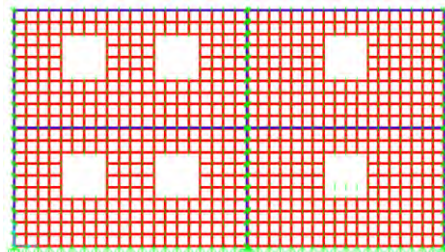
3D view - FE models details: particular of RF1 model and link among shell and frame elements
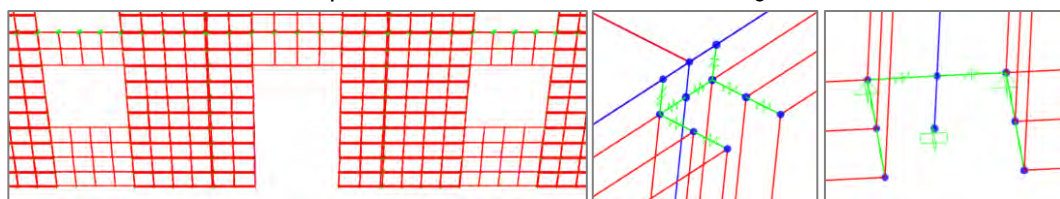
Fig. 5.3-1 – Seismic valuation: Numerical models and FE model details. Source: Martiradonna, S., Ruggieri, S., Fatiguso, F., Uva, G. (under drafting)

Firstly, eigenvalue analyses have been carried out on the eight numerical models. Table 5.3-1 reports main periods (T) and the related participation mass (M[%]) per direction. As expected, going from the BF model to IF, RF1 and RF2 configurations, the T values reduce and the same evidence can be noted for M[%]. The complexity of retrofit numerical models leads to shift the main mode per direction to the higher ones. Nevertheless, these expected effects does not bring the M[%] values under the thresholds of 75%, which means that according to the provisions of Eurocode 8 (CEN, 2004), the nonlinear behaviour of all models can be investigated with unimodal pushover analysis.

Table 5.3-1. Main periods and participating mass for the numerical models of the case study building

NUMERICAL MODEL	T	M[%]
	s	%
BF – X	0.2418	85.92
BF – Y	0.3074	88.28
IF – X	0.1147	84.45
IF – Y	0.1497	85.18
RF1 – X	0.0299	77.53
RF1 – Y	0.0372	81.65
RF2 – X	0.0272	76.54
RF2 – Y	0.0349	80.95

Accordingly, unimodal pushover analyses were performed on the eight numerical models and the results can be displayed in Figures 5.3-2 and 5.3-3, by assuming as control node the centre of the mass of the last storey, by neglecting any sources of eccentricity and by representing the resultant curves in terms of V_b-δ_R.
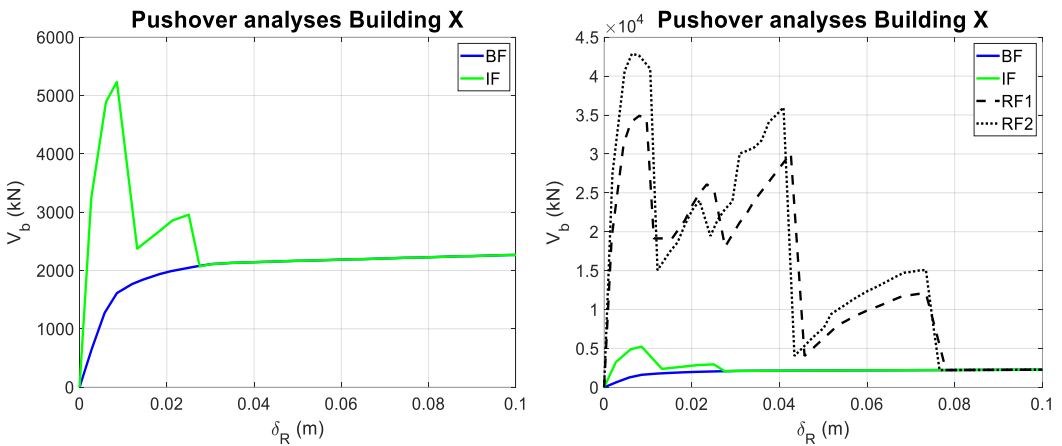
Fig. 5.3-2 – Pushover analyses in X direction for bare, infill and retrofit configurations. Source: Martiradonna, S., Ruggieri, S., Fatiguso, F., Uva, G. (under drafting)
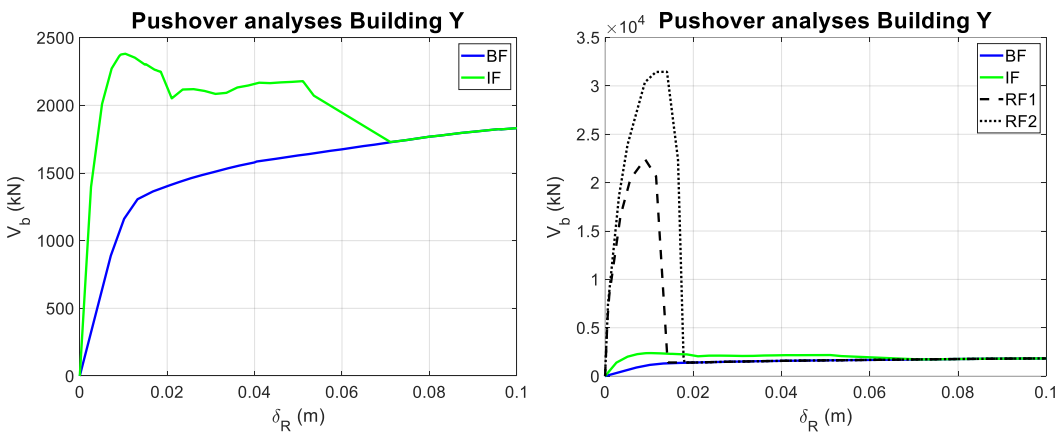
Fig. 5.3-3 – Pushover analyses in Y direction for bare, infill and retrofit configurations Source: Martiradonna, S., Ruggieri, S., Fatiguso, F., Uva, G. (under drafting)

As expected, the pushover curves show that IF models in both main directions (left graphs in Figures 5.3-2 and 5.3-3) present an initial peak which after returns on the BF model trend. For infill models, the numerical complexity given by shell elements employ-ment provokes a "Saw-Tooth" trend, given by numerical convergence problems. Similar

effects can be shown by the comparison among the previous curves and RF1 and RF2 (right graphs in Figures 5.3-2 and 5.3-3). Especially in X direction, pushover curve shows some resurrections, also due to the presence of a large set of openings. In the Y direction this effect did not occur, probably because the openings surface is reduced. The total collapse of shell elements (more rigid than the frame) occurs before than moment-resisting frame and bring back the curve on the BF trend, as well as displayed for IF model. Comparing the results obtained for RF1 and RF2, it is evident the slight difference in term of strength, especially around the peak values in both directions. In terms of δ_R, RF1 shows a similar capacity in X and a lower one in Y. These results suggest that, from the global structural performance point of view, both RF1 and RF2 provide similar behaviour in terms of strength, stiffness and ductility and the possible advantages of the one or of the other method are only related to technological aspects. Also in this application, as highlighted for the prototype model, this retrofit technique increases the stiffness and the strength of the structural system, with a peak V_b of about 10 times (in the case of RF2) the IF value. On the other hand, the deformation capacity and the related ductility is strongly reduced, which means that the building behaves like an elastic (or low-ductile) structural system.

From the physical point of view, the obtained results need of some interpretations. As a matter of fact, the resurrections occurred in X direction are the result of a numerical elaboration, but we believe that at the first significant strength loss, the retrofit system could be declared as collapsed. At the same time, considering that the real interaction between the frame and the added PC panels is rigid, a strength decay effect could lead some structural elements to achieve their strength capacity limits. Then, in a conservative view, the achievement of the LS limit-state (NC also, the two limit-states can be confused in this case) for RF1 and RF2 is signalled at the first significant strength decay shown by pushover curves. For the same reasons, in this case it does not physical sense to establish a criterion for defining the violation of the IO limit-state.

For the other structural configurations (BF and IF), the limit-states definition can be assumed in a practice-oriented view, such as summarized in Ruggieri et al. (2020b). More in detail, LS limit-state is achieved when shear failure appears in any element or when e

certain percentage of elements achieve the 75% percent of the ultimate rotation (in this case, the ultimate rotation is automatically defined from the moment-rotation law of each section); IO limit-state is achieved at the 0.5% of the inter-storey drift ratio for the bare frame configuration and at the displacement on pushover curve correspondent to the first significant strength loss for the IF configuration. The limit-states thresholds, as above defined and as reported in Table 5.3-2, show that going from BF to IF and after to RF1 and RF2, the IO and LS values of δ_R decrease, caused by the stiffness and strength variations among the models. The definition of these limit-states thresholds are necessary for the comparison of the building capacity (in all simulated configurations) and the seismic demand, which represents the standard procedure of global seismic assessment, according to the N2 method in Eurocode 8 (for more details, see Ruggieri and Uva, 2020). For the case at hand, the assumption of δ_R like engineering demand parameter to determine the transition to a higher damage state is due to the nature of our evaluations, which is aimed to identify a global performance and, to the nature of the analysis method performed. Assuming as seismic demand the code spectra for the IO and LS limit-states and comparing them with the capacity curves, opportunely scaled to the single DOF system, it is possible to compute the capacity/demand (C/D) ratios. The results are plotted in Figure 5.3-4, wherein the C/D ratios are always greater than 1, which means that for the seismic demand considered the building is always verified. Still, from the C/D ratios evaluation, it is worth noting that the obtained values for RF1 and RF2 are strongly greater than the related values obtained from the BF and IF models, for both main directions. For example, in X direction RF2 presents a C/D ratio value about 15 times greater than of the IF value. Despite this benefit is not obtained in terms of displacement capacity (or in terms of ductility), it is clear that the stiffness of RF1 and RF2 causes low values of T, which somehow reduces the seismic demand (the mass increases, but in a lower measure than stiffness). This means that the proposed retrofit method allows to obtain strongly higher safety levels for the entire structural system than the IF configuration.

Table 5.3-2. Values of IO and LS limit-state thresholds, for all FE models, in terms of δ_R

NUMERICAL MODEL	IO - δ_R	LS - δ_R
	m	m
BF – X	0.0183	0.0373
BF – Y	0.0205	0.0389
IF – X	0.0089	0.0171
IF – Y	0.0133	0.0210
RF1 – X	/	0.0131
RF1 – Y	/	0.0152
RF2 – X	/	0.0112
RF2 – Y	/	0.0149
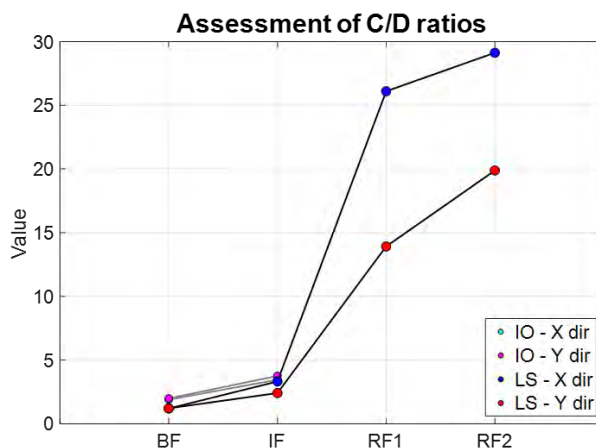
Fig. 5.3-4 – C/D ratios for all models, for IO and LS limit-states and for both main directions (X and Y dir). Source: Martiradonna, S., Ruggieri, S., Fatiguso, F., Uva, G. (under drafting)

In the end, as mentioned in the first part of this Section, the global seismic assessment presented does not take into account of some key aspects that should be always considered in this kind of analysis. In particular, in the case study, even if existing structural elements have been considered to obtain the global response, the specific capacity assessment (in terms of resistance, ductility and stiffness) of structural and non-structural elements is not performed, as well as the design and verification of the connections that ensure the working of the entire system. Overall, the retrofitted building will work as a dual frame-wall system, in which seismic actions are mainly entrusted to by the new wall system. Anyway, it is not possible to state that the building is completely safe toward seismic actions only basing on the presented analyses. Albeit several assumptions have been made in the definition of the system and in its numerical model, the general approach shows a good potentiality as a reliable retrofit system.

5.4   The choice of cladding

The proposed methodology based on the AHP aiming at choosing the best system cladding, has been applied for the case study analysed in this chapter. The criteria and alternatives explained in the section 4.6.3.3 have been considered in relation with the context in which the real building was inserted. Since the methodology already provides the structure of the problem and defines the criteria and alternative to compare, in this section, the results of the pairwise evaluations are afforded.

Therefore, in order to achieve accurate and consistent judgments, a group of experts in the construction field weighted the alternatives and criteria of the problem, taking in account the previous analyses regarding the specific technological aspects related to each panel cladding (section 4.5.4). The results are outlined in the Table 5.4-1.

Table 5.4-1. Tabulated weights obtained by the pairwise comparison of the alternatives and criteria.

CRITERION		WEIGHT (v_i)	ALTERNATIVE		WEIGHT (w_{ij})
Aesthetic Impact	v_1	0.18	Exposed Concrete	$w_{1,1}$	0.10
			Wood Coated	$w_{1,2}$	0.03
			Brick Coated	$w_{1,3}$	0.07
			Ceramic Coated	$w_{1,4}$	0.31
			Stone Coated	$w_{1,5}$	0.28
			Plastered	$w_{1,6}$	0.21
Required Construction Vehicle	v_2	0.03	Exposed Concrete	$w_{2,1}$	0.18
			Wood Coated	$w_{2,2}$	0.15
			Brick Coated	$w_{2,3}$	0.15
			Ceramic Coated	$w_{2,4}$	0.18
			Stone Coated	$w_{2,5}$	0.14
			Plastered	$w_{2,6}$	0.18
Realization Complexity	v_3	0.09	Exposed Concrete	$w_{3,1}$	0.30
			Wood Coated	$w_{3,2}$	0.13
			Brick Coated	$w_{3,3}$	0.03
			Ceramic Coated	$w_{3,4}$	0.27
			Stone Coated	$w_{3,5}$	0.07
			Plastered	$w_{3,6}$	0.20
Thermal Transmittance	v_4	0.24	Exposed Concrete	$w_{4,1}$	0.16
			Wood Coated	$w_{4,2}$	0.17
			Brick Coated	$w_{4,3}$	0.17
			Ceramic Coated	$w_{4,4}$	0.17
			Stone Coated	$w_{4,5}$	0.17
			Plastered	$w_{4,6}$	0.17
Thermal Inertia	v_5	0.26	Exposed Concrete	$w_{5,1}$	0.19
			Wood Coated	$w_{5,2}$	0.02
			Brick Coated	$w_{5,3}$	0.20

			Ceramic Coated	$w_{5,4}$	0.19
			Stone Coated	$w_{5,5}$	0.20
			Plastered	$w_{5,6}$	0.20
			Exposed Concrete	$w_{6,1}$	0.19
			Wood Coated	$w_{6,2}$	0.14
Expected Costs	v_6	0.21	Brick Coated	$w_{6,3}$	0.16
			Ceramic Coated	$w_{6,4}$	0.18
			Stone Coated	$w_{6,5}$	0.17
			Plastered	$w_{6,6}$	0.17

Following the methodology provided by Saaty (2008), it was possible to obtain the synthesis of the priority by calculating the global weights (w_i'), illustrated in the Table 5.4-2 below:

Table 5.4-2. Synthesis of the priority: global weights

ALTERNETIVE	w_i'
Exposed Concrete	0.18
Wood Coated	0.11
Brick Coated	0.15
Ceramic Coated	0.21
Stone Coated	0.17
Plastered	0.18
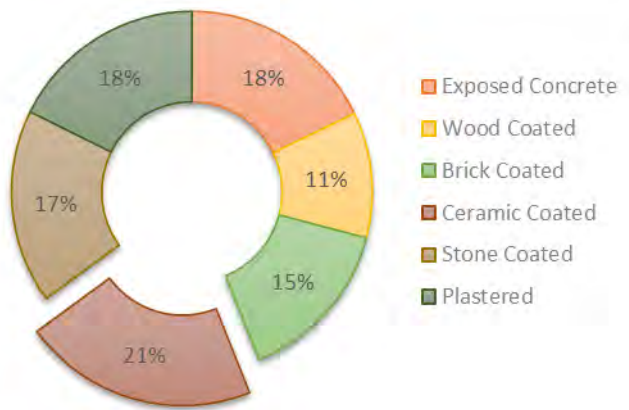
The results show that the group of users preferred the Ceramic Coated as cladding of the IPCS applied to the case study for its good performance in all the criteria. The global weight expressed in percentage was equal to 21%. They have judged Stone Coated, Exposed concrete and Plastered PC panels in a similar way as the ranging was between 17% and 19%. Finally, Brick Coated and Wood Coated PC panel were individuated as worst claddings for the considered case study with a weight of 15% and 10%, respectively. To understand these results and observed the aesthetic impact that the cladding would be on the building, the models of the refurbished case study with the application of the six cladding types have been provided in Figure 5.3-5.

Ceramic coated

Plastered

Exposed concrete

Stone coated

Brick coated

Wood coated
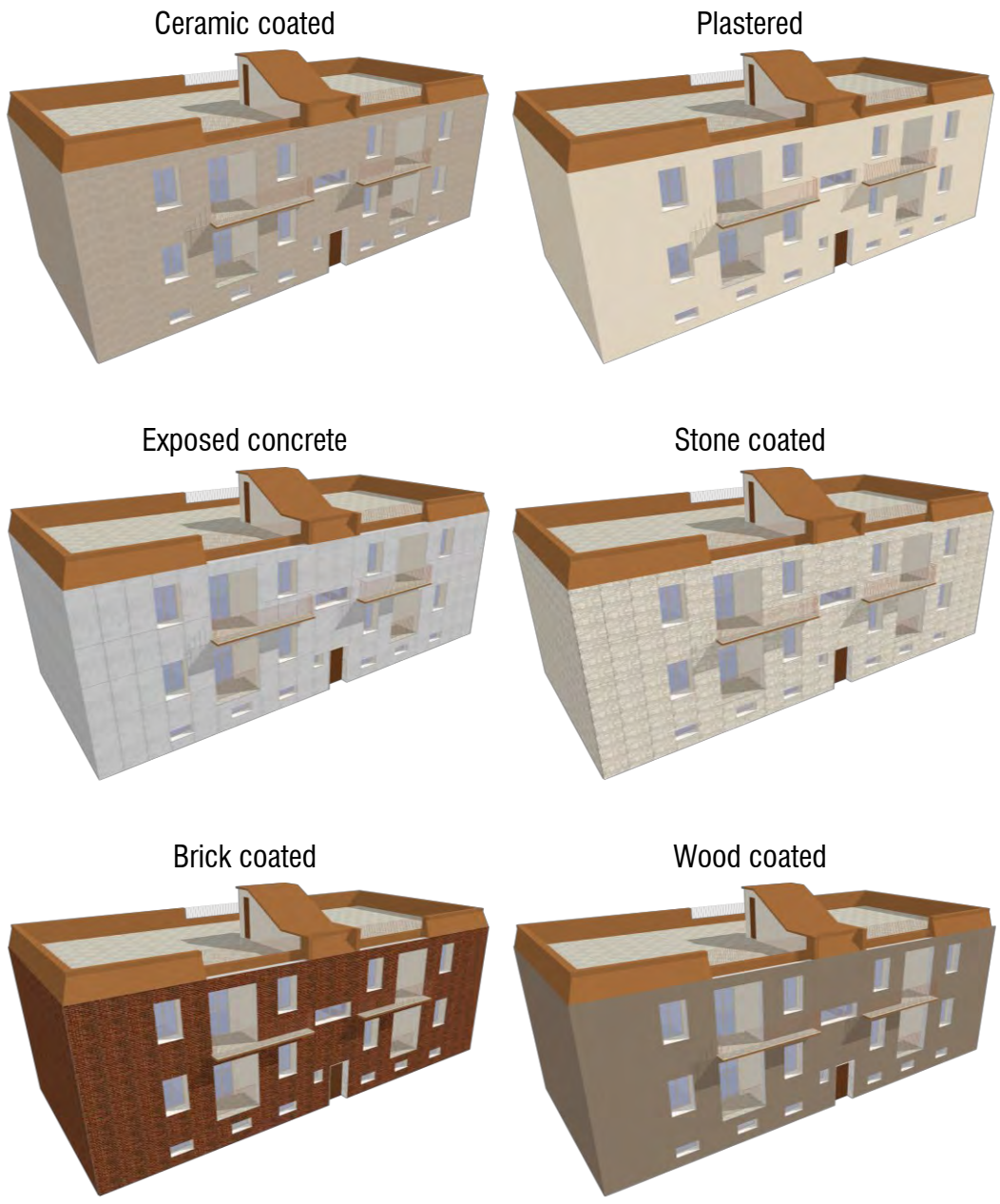
Fig. 5.4-1 – Case study models with the application of the six cladding types. Source: Author

The same analyses have been performed and implemented with the novel method called Augmented Reality based Decision Making (AR-DM) by Sangiorgio et al., (2021) to get a powerful multicriteria analysis approach. It makes use of virtual environment to visually provide a large amount of information during the decision process. In this way, even nonexpert users of the specific problem can successfully carry out the procedure thanks to the useful information displayed in the virtual 3D models, speed up and optimise the decision-making process. The figure 5.4-2 shows how the 3D model can be rotated and displayed at the real scale in AR environment, in order to comprehend many aspects of the PC module, including the composing element, the installation methods, the materials, the stratigraphy and the final result. In particular, the Wood Coted PC module, applied to the existing façade, is shown allowing. A more in depth explanation of the method is presented in Sangiorgio, Martiradonna and Fatiguso, (2020) and Sangiorgio et al., (2021).

Fig. 5.4-2 – Virtual application on site during the building retrofit displayed in AR. Source: Sangiorgio *et al.*, (2021)

184

6 PROTOTYPE STAGE

The last phase of the investigation regards the aspects related to the industrial realization of the "Intelligent PC panel system" with the purpose of validating the technological choices, defining the production phases, individuating possible constructive gaps and proposing further optimizations to improve the solution. In view of the technological system patenting, thus, the future standardized production of its components, this phase has been carried out directly in the Ferramati International plants, implementing the materials, tools and the automatic systems of prefabrication. Therefore, the production requirements have been individuated, also thanks to the collaboration of the company's technical team who reorganized the normal working activities to insert the production of the system components into the scheduled production sheet as if it had been commissioned by a client. From it, the production times have been defined and verified.

Starting from the reproducibility of the novel lightweight mortar (LWM) with the recycled EPS beads coming from the industrial waste, six PC module prototypes have been produced by two different dimensional categories to assess the versatility of the panels intended to adapt to the geometric requirements of the existing buildings. Hence, a real scale sample of an existing façade has been constructed with the technical requirements of the older Italian construction code. It consisted in a 3.60 x 3.00m wall, 30 cm thick, in which pillars and beam had a regular square section 30 x 30 cm. The bricks employed were the types considered for the system design i.e. 25 x 25 x 12 cm blocks in ceramic according to table 4.6-3 of the subsection 4.6.1.1 of this thesis. The foundation was constituted by a continuous beam with rectangular section 30x40 cm, 3.60m long. It was employed to simulate the installation of the system, starting from the chemical injections of the post-installed rebars in the foundation, pillars, and beams.

The entire prototyping process was supported by a 3D model with which the dimension of the components as well as the spacing between the façade and the panels, mullions, post-installed rebar, anchorages etc. have been previously verified. It was fundamental to the sizing of the hooks and to observe the anchorage section with the panels in order to predict possible troubles and simulate the mounting operations.

In this phase, the methods proposed to design the mullions, hooks, anchors, post-installed rebars, additional reinforcements and the other system components have been put into practice. The resulting computation sheets showed the effectiveness of the design calculations. they have been fundamental to produce the related production schedules to be delivered to the operators of the prefabrication plants.

Unfortunately, the issues related to the supply and installation of sensors within the prototype as well as the phases of verification of the real thermal and structural performance were not deepened due to the health emergency linked to the infection with COVID-19.

This chapter purposes to describe and illustrate the prototyping phases (the calculation sheets and the production schedules are included), to propose optimization solutions to speed up the work and improve the results. It is organized according to the strategical design methodology proposed for the investigation, hence, by the three scales of details individuated: *Material scale, Component scale* and *System scale.* Therefore, section 6.1 regards the large-scale production of the novel LWM; section 6.2 the fabrication of the six PC module prototypes, and section 6.3 the phase of the system installation. In the attachment C the photographic documentation of the entire process is provided.

6.1 Large scale production of the novel LWM

The mortar under patenting, chosen for the large-scale industrial production, was the mixture M13 of the three tested sets of mortars proposed in the section 4.4 of this thesis. Having been tested in the laboratory with a variable particle size ranging from 1.5 mm to 6.5 mm for the composition of reduced samples, in the Ferramati's plant, the mechanical sieving phase have not been required for the great quantity of mortar to produce. in fact, the particle size distribution and grain characteristics of the rEPS permitted to use the whole quantity of material supplied in order to speed up and facilitate the mortar composition in the plant. The recycled EPS used for the industrial production has been the same employed for testing procedure in the laboratory, hence it had density of almost 10-12 Kg/m^3. In order to confer better consistency in the casting phase, a superplasticizer additive has been used during the mixing process in quantity equal to 30% of the cement weight. Therefore, to produce a cubic meter of LWM the following volume percentages have been used (Table 6.1-1):

Table 6.1-1. Volume percentages to produce 1 m^3 of LWM

MATERIALS	W/C	DENSITY Kg/m^3	%VOL
CEM I 42.5 R	0.65	2400	7.56%
WATER		1000	11.79%
rEPSb		10	80.65%
SUPERPLASTICIZER ADDITIVE		880	0.02%

The mortar composition phases, showed in the Figure 6.1-1, has been: 1) rEPS additivation; 2) pre-mixing phase; 3) mixing phase; 4) casting phase, according to the procedure used in the laboratory. Unlike normal cement mortars produced on site which can be mixed with the drill, the LWM must be composed exclusively in the cement mixer because the uniformity in mixing conferred to the mortar the aspect of a cream, as obtained in the laboratory. It was determining of the workability on large surfaces.

During the third phase the mixer has been always in operation in order to obtain a uniform mixing of the materials. The temporal scanning of the phases has been fundamental to achieve a good consistency, workability, and dry state aspect. Two minutes after pouring the water into the cement mixer, a part of superplasticizer additive was added to the mortar. The remaining part was inserted after other two minutes to make sure the additive

was well mixed to the mortar. From that moment, the mortar remained working for ten minutes at least i.e., the time necessary to make the additive be activated. Exceeding or reducing these production times, experimentally proved, it was observed that a too dry of too porous dough were produced, unfit for the use.Since the mortar do not contains sand, the setting times are shorter than the normal, thus, it was necessary to spread the mortar on the surface within 8-10 min, after it lost workability because it began to settle on the surface. As tested in the laboratory, no segregation phenomena were generated by the addition of pearls in the first phase. No vibration was needed. The mortar was ripe already after 24 hours, however, to get a completely dry state, it was necessary to wait until 48 hours. In the Table 6.1-2 the mortar production times are reported according to the five phases.

1. rEPS additivation   2. pre-mixing phase   3. mixing phase   4. casting phase

Fig. 6.1-1 – Mortar composition phases

Table 6.1-2. Times and procedure to produce the LWM

PRODUCTION PHASES	TIMES	PROCEDURE
1 rEPS additivation	At least 45 min before starting the next phase	- put the rEPS beads in the mixing machine; - add the additive (quantities are covered by trade secret); - operate the machine for 10 minutes; - switch off the machine and allow the additive to absorb for at least 30 minutes.
2 Pre-mixing phase	10 minutes	- add the cement to the additivated rEPS - leave operating the machine for 10 minutes before starting the phase 3.
3 Mixing phase	15 minutes	- add all the water while the machine is already working and leave mixing for 2 minutes; - add the half part of the plasticizer and wait 2 minutes for inserting the second part; - leave the mortar mixing for no more than 10-15 minutes.
4 Casting phase	8-10 minutes	- spread and smooth the mortar on the surface.
5 Setting phase	48 hours	- leave the mortar setting

A more in-depth photographic documentation is provided in the Annex.

6.2 Standardized production of the innovative PC modules

The technological configuration of the innovative PC module was validated and approved by the Ferramati's technician team with which the prefabrication procedures were discussed and optimized. Since its characteristics and materials follow the company standards, the modules have been easily manufactured with the carousel system of the prefabrication plant. In particular, two different sizes of panels have been proposed to comprehend the aspects related to the adaptability to the existing building, the versatility, handling and safety in assembling. Hence, the standard module (A), of 1.2 x 2 m, and the reduced module (B), of 1.2 x 1 m, have been projected in accordance with the procedure explained in the section 4.5.2. In total, three A prototypes and three B prototypes were produced. The production process started with the spreading of the disarming liquid on the metal formwork and the disposition of the banks stop jet magnet according to the panel dimensions. Thus, some specific plastic spacers were placed to ensure the steel cover as calculated (2 cm), then the reinforcement was arranged following the dispositions of the production sheets (Figure 6.2-1 and 6.2-2). Unlike the traditional slabs for which the lattices and the rebars are composed directly on the formwork, for the novel module, the steel components have been already assembled in the iron plant because the spacing between the lattices had to comply as closely as possible with the design. Therefore, the assessment of the spacing between the lattices and the formwork borders has been carried out. The next phases were the concrete casting up to reach 4.5 cm thickness and vibration to eliminate air voids and distribute the material on the formwork surface. As specified in the section 3.4.1, the setting phase of the modules was carried out in the maturation tower for 24 hours. Since the internal layer in LWM had to set back 7 cm from the slab boundaries and the rEPS frame had to protrude 7 cm from the panel along two sides to create the male-female junction system (see section 4.5.3), the problem of the banks firm jet occurred. In addition, as the mortar had not yet been tested on a large, porous concrete surface, to produce these first prototypes, a manual approach was adopted which consisted in gluing the rEPS frame and other wooden firm jets (in accordance with the production sheet in the Figure 6.2-3), only after the slab has matured. Later, the LWM was casted up 5 cm of thickness on the resulting space and smooth to create a uniform layer. After 48 hours, the panels were ready to be installed on the wall sample. Figure 6.2-4 illustrates briefly the production phases.

189

Pezzi	Descrizione	m/m2		
4	Traliccio 12,5 5/7/5	1.20	d: 4.0 cm	
13	Tondini Φ5	2.00	Calces: Area: 2.40 m2	
13	Tondini Φ5	1.20	Vol.: 0.096 m3 CCls: C28/35	
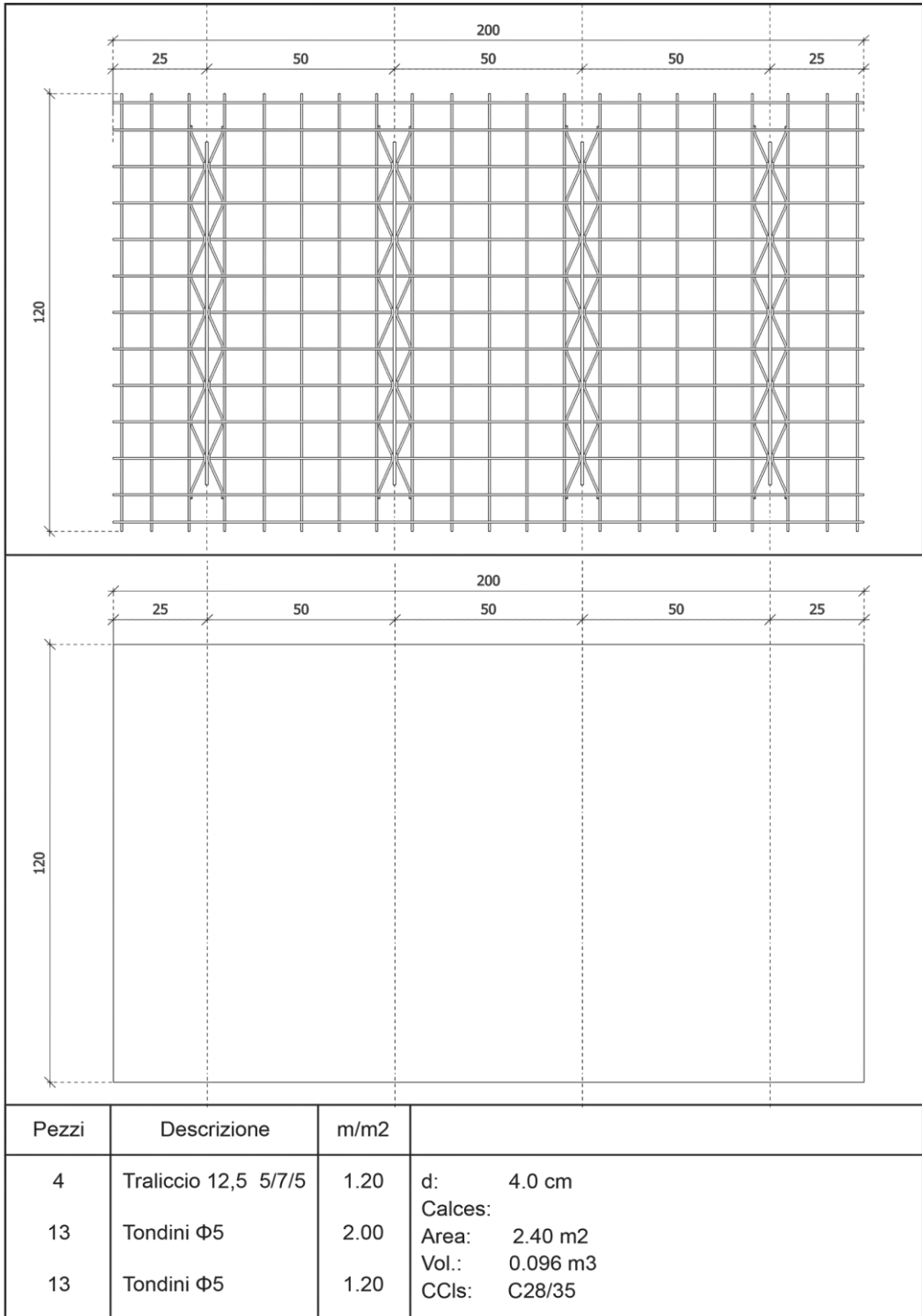
Fig. 6.2-1 – Production sheet for the A assembly. Source: Author

190

Pezzi	Descrizione	m/m2		
2	Traliccio 12,5 5/7/5	1.20	d:	4.0 cm
			Calces:	
13	Tondini Φ5	1.00	Area:	1.20 m2
			Vol.:	0.048 m3
7	Tondini Φ5	1.20	CCls:	C28/35
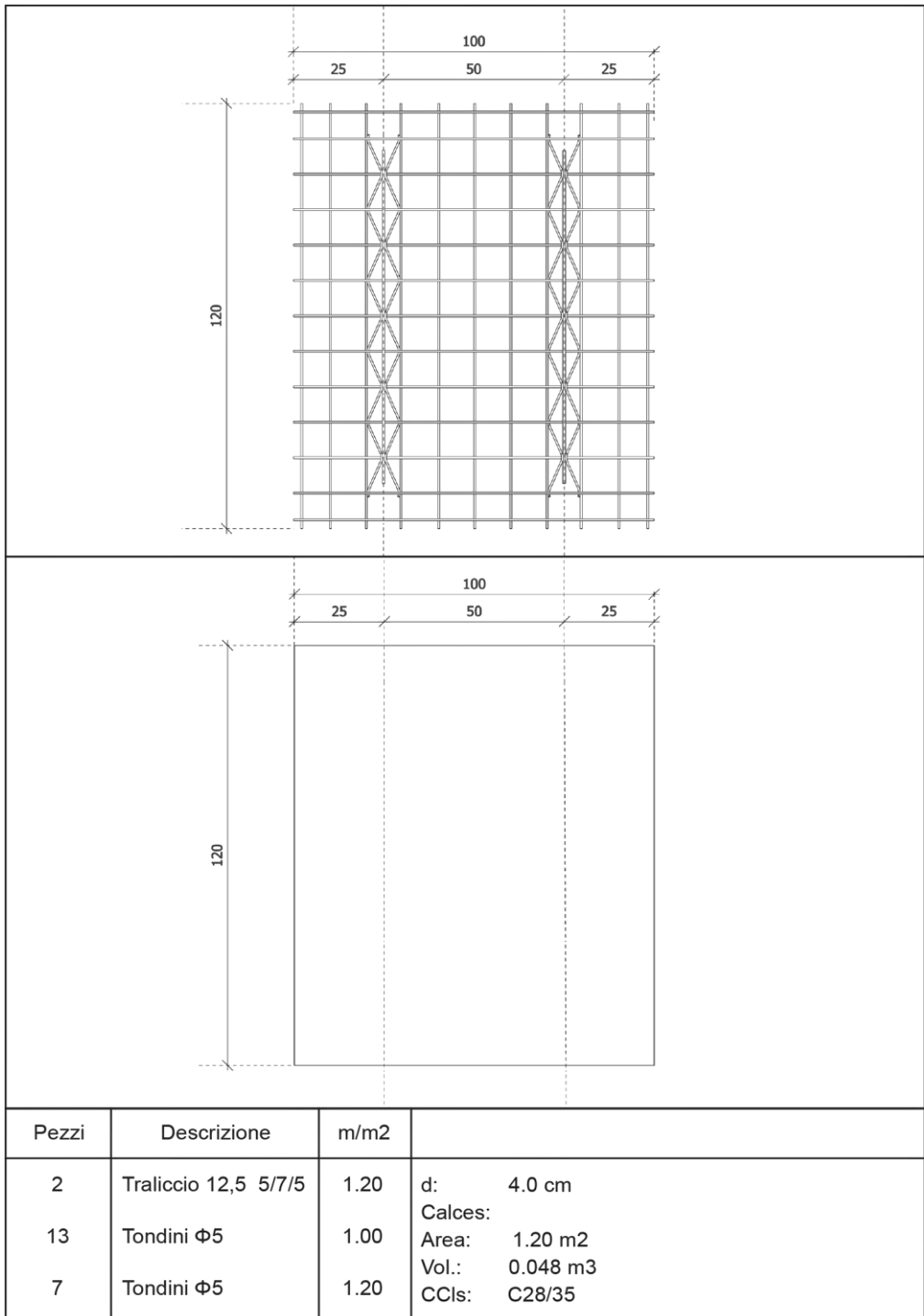
Fig. 6.2-2 – Production sheet for the B assembly. Source: Author
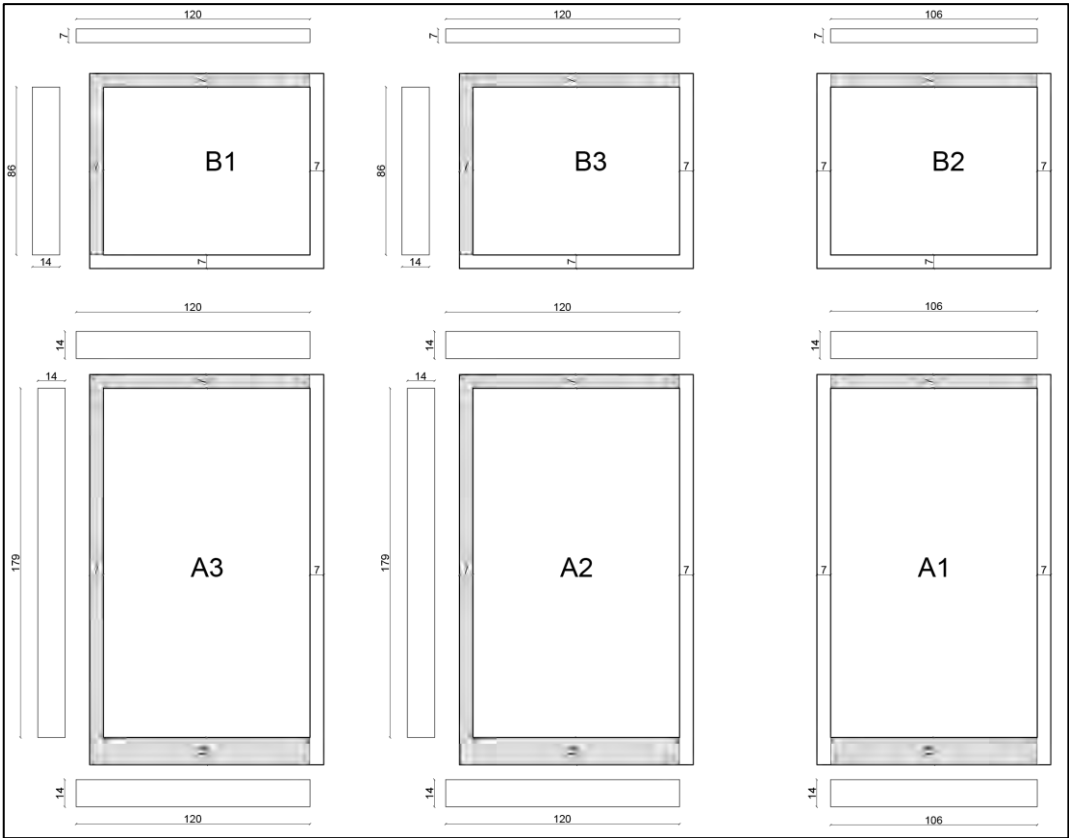
Fig. 6.2-3 – Disposition of the rEPS blocks on the A and B modules. Source: Author

Fig. 6.2-4 – PC module production phases. Source: Author

The manual approach employed was too complex due to the involvement of many workforce and three-day working time. The optimization of this procedure consists in placing, on the fresh concrete layer, two EPS blocks as jetty banks, 7 cm wide and 5 cm thick, along the female joints of the panel and on the other sides, two rEPS puzzle-shaped blocks. The second half of the puzzle blocks are glued to interlocking with the firsts, in a second time, to create the male junction. At the end of the bonding phase, the LWM can be casted into the remaining space on the fresh concrete surface. Hence, the panel is stored into the maturation tower for a day. As the two layers dry together, the panel is configured as a solid block with improved characteristics. This optimized procedure allows using the panel already the day after its fabrication, saving time and labour. Unfortunately, the optimized panels have not been produced. In the Figure 6.2-5 the optimization proposal of the panel realization procedure is illustrated. Table 6.2-5 summarizes the times needed to produce a panel A with the improvements proposed.
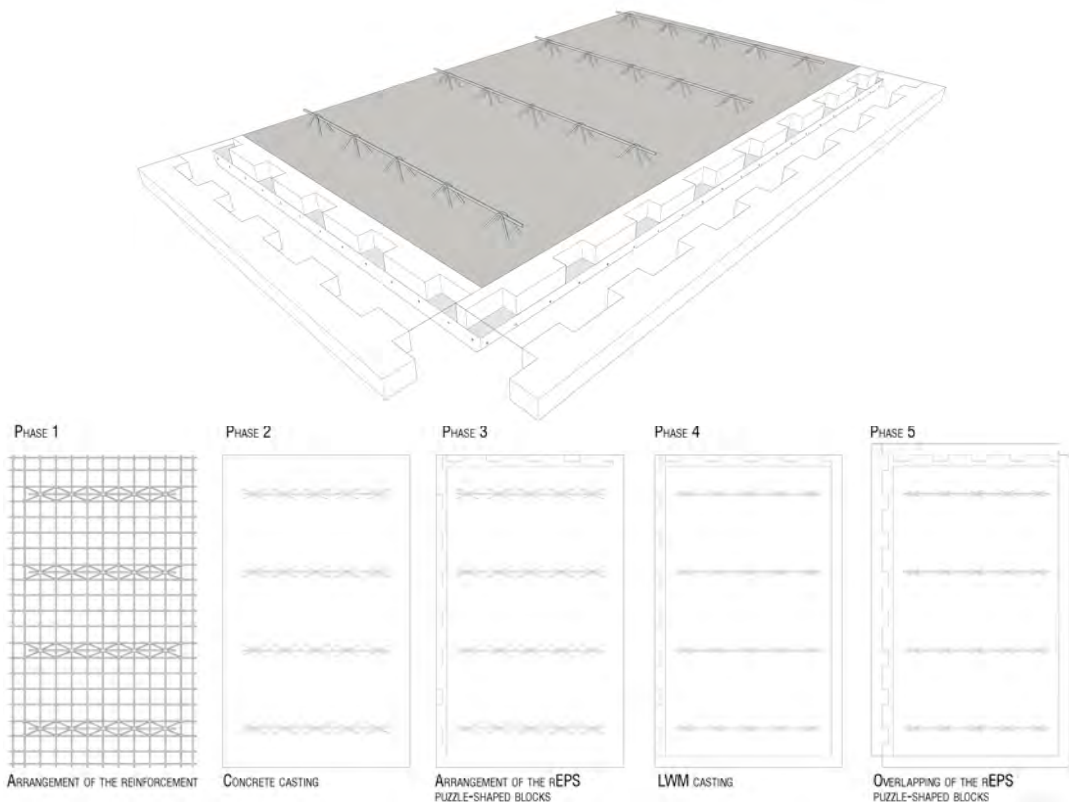
Fig. 6.2-5 – Optimization proposal of industrial realization procedure of the PC module. Source: Author

Table 6.2-1. Times and procedure to produce a PC module in the carousel system

	PRODUCTION PHASES	TIMES	PROCEDURE
1	Reinforcement disposition	8-10 minutes	- place the spacers 2 cm high on the formwork; - arrange the reinforcement on the spacers (lattices and rebars are already assembled); - check the distance of the lattice girders from the formwork edges.
2	Concrete casting	5-7 minutes	- move the formwork to the casting station; - cast the concrete in the formwork up to 4.5 cm of thickness - vibrate the formwork
3	EPS jet firm disposition	5 minutes	- arrange the puzzled rEPS blocks along the upper and left side of the fresh concrete panel by adhering the shaped side to the formwork - arrange other stop jet along the bottom and right edge of the formwork
4	LWM casting	8-10 minutes	- spread and smooth the mortar on the surface.
5	Maturation phase	36 hours	- leave the module dry out

On average, the carousel system produces 550 square metres of single slabs per day according to the Ferramati's chain (subsection 3.4.1). In agreement with the technician who manages the production plant, the carousel system would produce an average of 480 square meters of modules A per day, thus about 200 units.

After concluding the production of the modules of the set A and B, the compositional order was established by verifying the vertical alignment between the lattice girders with the aim to begin the system installation phase, analysed in the next section. The aspects of the modules A and B at their production phase concluded is illustrated in the Figure 6.2-6 below. A more in-depth photographic documentation is reported in the Annex.

a)   b)
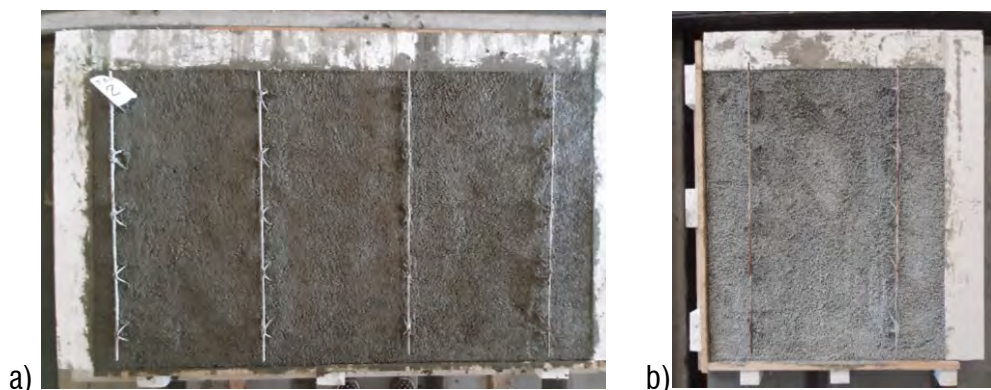
Fig. 6.2-6 – The PC modules: a) The standard module A; b) the reduced module B. Source: Author

6.3 Technological system design and installation

In the *Prototype phase* at the *System_scale*, the methods proposed in the section 4.6 to calculate the specific dimensions of the system components have been effectively applied. The procedure started by analysing the loads of the panel and the possible kinematics that could occur during the assembly and completion phases of the system (e.g. panel overturning). Therefore, the considered actions were the panel weight, the hydrostatic pressure, and the overturning moment as illustrated in the sketches made during this phase (Figure 6.3-1).
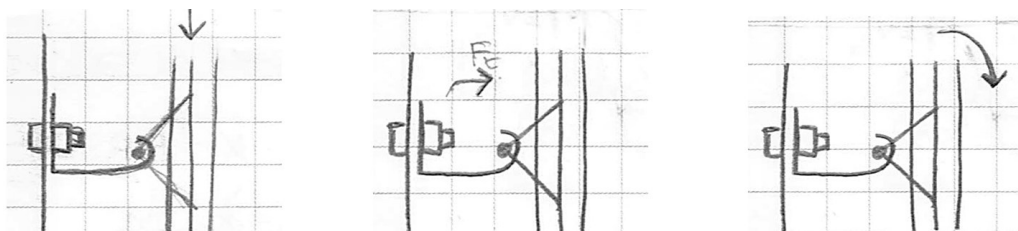
Fig. 6.3-1 – Sketches of the forces at play. Source: Author

After calculating the centre of mass and choosing the anchor bolt condition b illustrated in Figure 4.6-4 the calculation of the anchors to fix the mullion in concrete was performed. Since the design of the system provides for the anchoring of the PC module through two mullions and four hooks, in turn anchored to the base and upper beam by means of six anchors each, three side by side, as reported in the Figure 4.6-3 of the subsection 4.6.1.1, the anchor M12 was chosen in accordance with Table 4.6-2.

In function of the action loads, its resistance to tension and shear loads were calculated in compliance with the formulas from (19) to (22) of the methodology proposed in the subsection 4.6.1.1. The Figure 6.3-2 (a) reports the assessment of the anchor resistance to the tension load compared with the design values and (b) the related calculation sheets. At the same way, Figure 6.3-3 (a) reports the assessment and (b) the calculations for shear loads. It was assumed that the concrete was in cracked state.

VERIFICATION			
$N_{Rd,s}=$	$N_{Rk,s}/\gamma_{Ms}=$	44,70 kN	TRUE
$N_{Rd,p}=$	$N_{Rk,p}/\gamma_{Mp}=$	17,3 kN	TRUE
$N_{Rd,c}=$	$N_{Rk,c}/\gamma_{Mc}=$	23,1 kN	TRUE
$N_{Rd,sp}=$	$N_{Rk,sp}/\gamma_{Msp}=$	14,98 kN	TRUE

a)

Design steel resistance

$N_{Rk,s} = A_s * f_{uk}$

$N_{Rd,s}=$	44,7	kN
$N_{Rk,s}=$	59,01	kN
$\gamma_{Ms}=$	1,4	
A_s	84,3	mm^2
f_{yk}	450	MPa
f_{uk}	700	MPa

Design combined pull-out and concrete cone resistance

Cracked concrete

Temperature range I

$N^0_{Rd,p}=$	17,3	kN
$N_{Rk,p}=$	25,95	kN
$\gamma_{Mp}=$	1,5	

Typical embedment depth

$h_{ef,typ}=$	110 mm

Effective anchorage depth

$h_{ef}=$	144 mm

Minimum base material thickness

$h_{min} = h_{ef} + 30\ mm \geq 100\ mm$

$h_{min}=$	174 mm
$h_{reale}=$	300 mm

b)
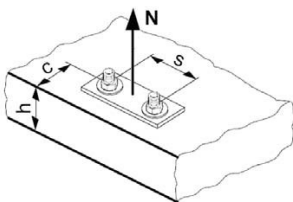
Design concrete cone resistance

$N^0_{Rd,c}=$	23,1	kN
$N_{Rk,c}=$	34,65	kN
$\gamma_c=$	1,5	

Design splitting resistance

$N^0_{Rd,sp} = N^0_{Rd,c} * f_B * f_{1,sp} * f_{2,sp} * f_{3,sp} * f_{h,N} * f_{re,N}$

$N^0_{Rd,sp}=$	14,98	kN
$N_{Rk,sp}=$	22,47	kN
$\gamma_{Msp}=$	1,5	

Influence of concrete strength on concrete cone resistance (C25/30)

$f_B=$	1,1		

Influence of edge distance

$f_{1,sp}=$	$0,7 + 0,3*c/c_{cr,sp}$		0,83
$h/h_{ef}=$	2,1	>2	
$c_{cr,sp}=$	144	mm	$1*h_{ef}$
$c_{min}=$	60	mm	
$c/c_{cr,sp}=$	0,42	mm	
$f_{2,sp}=$	$0,5*(1+c/c_{cr,sp})$		0,71
$f_{3,sp}=$	$0,5*(1+s/s_{cr,sp})$		0,67
$s_{min}=$	60	mm	100
$s_{cr,sp}=$	$2c_{cr,sp}$		288
$s/s_{cr,sp}=$	0,35		

Influence of embedment depth on concrete cone resistance

$f_{h,N}=$	$(h_{ef}/h_{ef,typ})^{1,5}$	1,50

Influence of reinforcement

$f_{re,N}=$	$0,5 + h_{ef}/200mm \leq 1$	1

Fig. 6.3-2 – Resistance of the anchor M12 to tension loads in concrete: a) verification; b) calculation sheets. Source: Author

196

VERIFICATION			
$V_{Rd,s}=$	$V_{Rk,s}/\gamma_{Ms}=$	27,20 kN	TRUE
$V_{Rd,cp}=$	$V_{Rk,cp}/\gamma_{Mc}=$	34,6 kN	TRUE
$V_{Rd,c}=$	$V_{Rk,c}/\gamma_{Mc}=$	5,86 kN	TRUE

a)

Steel failure

$V_{Rk,s}=\alpha_M*M_{Rk,s}/l$	47,21	kN
$M^0_{Rk,s}=1,2*W_{el}*f_{uk}$	105 Nm	

Design steel resistance

$V_{Rd,s}=$	27,2	kN
$V_{Rk,s}=$	34	kN
$\gamma_{Ms}=$	1,25	

Design pry-out failure

$V_{Rd,cp}=$ lower$(k*N_{Rd,p}; k*N_{Rd,c})$		
$V_{Rd,cp}=$	34,6	kN
$V_{Rk,cp}=$	51,9	kN
$\gamma_{Mc}=$	1,5	
$k=$	1	$h_{ef}<60$ mm
$k=$	2	$h_{ef}\geq 60$ mm
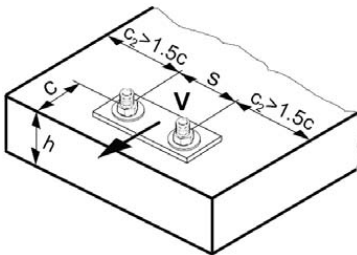
Design concrete edge resistance

$V_{Rd,c}=V^0_{Rd,c}*f_B*f_\beta*f_h*f_4*f_{hef}*f_c$		
$V_{Rd,c}=$	5,86	kN
$V_{Rk,c}=$	8,79	kN
$\gamma_{Mc}=$	1,5	
$V^0_{Rd,c}=$	8,2	kN

Influence of concrete strength (C25/30)

$f_B=$	1,1

Influence of angle between load applied and the direction perpendicular to the free edge

$f_\beta=$	1	0°

Influence of base material thickness

$f_h=\{h/(1,5*c)\}^{1,2}\leq 1$		1
$h/c=$	$5>1,5$	

Influence of anchor spacing and edge distance for concrete edge resistance

$f_4=(c/h_{ef})^{1,5}*(1+s/[3*c])*0,5$		0,27
$c/h_{ef}=$	0,42	
$s/h_{ef}=$	0,69	

Influence of edge distance

$f_{hef}=0,05*(h_{ef}/d)^{1,68}$		3,25
$h_{ef}/d=$	12	
$f_c=(d/c)^{0,19}$		0,74
$c/d=$	5	

b)

Fig. 6.3-3 – Resistance of the anchor M12 to shear loads in concrete: a) verification; b) calculation sheets. Source: Author

From the results, the anchor M12 was verified. The resistance value to tension loads, which corresponded to the splitting resistance, was equal to 14.98 kN, the lowest among all. Instead, the resistance value to shear loads was 5.86 kN, corresponding to the edge resistance. The anchorage length, equivalent to the value of h_{ef} measured 144 mm. The effective anchoring length considered was 150 mm, thus 200 mm long threaded bars have been ordered to ensure fixation by means of the washer and bolt.

At the same way, the calculation was performed for the anchors in the brick wall, taking in account the brick type in table 4.6-3. The anchor M8 was chosen in accordance with

the Table 4.6-2 of the methodology and the design resistance calculation at tension and shear loads was verified as illustrated in Figure 6.3-4a,b and Figure 6.3-5 a,b.

VERIFICATION			
$N_{Sd}=$	0,608 kN		
$\delta=$	15,00 mm		
$N_{Rd,s}=$	$N_{Rk,s}/\gamma_{Ms}=$	12,00 kN	TRUE
$N_{Rd,p}=$	$N_{Rk,p}/\gamma_{Mm}=$	1,00 kN	TRUE
$N_{Rd,p}=$	$N_{Rk,p}/\gamma_{Mm}=$	1,00 kN	TRUE
$N_{Rd,pb}=$	$N_{Rk,pb}/\gamma_{Mm}=$	3,32 kN	TRUE
$N_{Rd,p}=$	$\alpha_j*N_{Rk,p}/\gamma_{Mm}=$	0,75 kN	TRUE
$N_{Rd,b}=$	$\alpha_j*N_{Rk,b}/\gamma_{Mm}=$	0,75 kN	TRUE

a)

Design steel resistance

E_s	210000	MPa
ε_y	0,19%	

$N_{Rk,s}=A_s*f_{uk}$

$N_{Rd,s}=$	12,00 kN	
$N_{Rk,s}=$	18,30 kN	
$\gamma_{Ms}=$	1,25	
$A_s=$	36,6 mm^2	M8
$f_{yk}=$	400 MPa	
$f_{uk}=$	500 MPa	5.8
$f_{yk}/f_{tk}=$	0,80	

Design pull-out resistance of the anchor and brick breakout failure

$N_{Rd,p}=$	$N_{Rd,b}=$	1 kN
$N_{Rk,p}=$	$N_{Rk,b}=$	2,50 kN
$\gamma_{Mm}=$	2,5	
$h_{ef}=$	80 mm	$\geq$50mm
$f_b=$	27 MPa	
$c=$	80 mm	$\geq$50mm

Pull out of one brick

$N_{Rd,pb}=2*l_{brick}*b_{brick}\,(0,5*f_{vko}+0,4*\sigma_d)/(2,5*1000)$

$N_{Rd,pb}=$	3,32 kN	
$l_{brick}=$	285 mm	
$b_{brick}=$	135 mm	
$f_{vko}=$	0,2 MPa	
$\sigma_d=$	0,02 MPa	
$N_{Rk,pb}=$	8,31 kN	
$\gamma_{Mm}=$	2,50	

Influence of joints		(vertical joints not filled)
$N_{Rk,p}=$	$N_{Rk,b}=$	1,88 kN
	$\alpha_j=$	0,75
$N_{Rd,p}=$	$N_{Rd,b}=$	0,75 kN
	$\gamma_{Mm}=$	2,50

b)

Fig. 6.3-4 – Resistance of the anchor M8 to tension loads in bricks: a) verification; b) calculation sheets. Source: Author

VERIFICATION			
	$V_{Sd}=$	0,71 kN	
$V_{Rd,s}=$	$V_{Rk,s}/\gamma_{Ms}=$	7,32 kN	TRUE
$V_{Rd,b}=$	$V_{Rk,b}/\gamma_{Mm}=$	3,6 kN	TRUE
$V_{Rd,c}=$	$V_{Rk,c}/\gamma_{Mm}=$	1 kN	TRUE
$V_{Rd,pb}=$	$V_{Rk,pb}/\gamma_{Mm}=$	3,32 kN	TRUE
$V_{Rd,b}=$	$\alpha_j*V_{Rk,b}/\gamma_{Mm}=$	2,7 kN	TRUE
$V_{Rd,c}=$	$\alpha_j*V_{Rk,c}/\gamma_{Mm}=$	0,75 kN	TRUE

a)

Failure of the metal part, shear load without lever arm

$V_{Rk,s}=0,5*A_s*f_{uk}$

$V_{Rk,s}=$	9,15 kN
$V_{Rd,s}=$	7,32 kN
$\gamma_{Ms}=$	1,25
$A_s=$	36,6 mm
$f_{uk}=$	500 MPa

ETA-07/0260

Hollow or perfored brick edge failure

$V_{Rk,c}=k*\sqrt{(d_{nom})}*(h_{nom}/d_{nom})^{0,2}*\sqrt{(f_b)}*c_1^{1,5}$

$V_{Rk,c}=$	19,26 kN	
$V_{Rd,c}=$	1 kN	
$k=$	0,45	
$c_1\geq c_{min}=$	150 mm	
$d_{nom}=$	8 mm	diameter of the anchor
$h_{nom}=$	80 mm	overall anchor embedment
$f_b=$	27 Mpa	normalized mean compressive
$V_{Rk,c||}=$	2,5 kN	strength of masonry unit
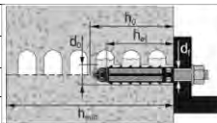
Influence of joints (vertical joints not filled)

$V_{Rd,c}=$	0,75 kN
$V_{Rd,b}=$	2,7 kN
$\alpha_j=$	0,75

Local brick failure

$V_{Rk,b}=$	1,44 kN
$V_{Rd,b}=$	3,6 kN
$c_1\geq c_{min}=$	150 mm
$h_{eff}=$	80 mm
$V_{Rk,b}=$	9 kN
$\gamma_{Mm}=$	2,50

Pushing out of one brick

$V_{Rd,pb}=2*l_{brick}*b_{brick}(0,5*f_{vko}+0,4*\sigma_d)/(2,5*1000)$

$V_{Rd,pb}=$	3,32 kN	
	$l_{brick}=$	285 mm
	$b_{brick}=$	135 mm
	$f_{vko}=$	0,2 MPa
	$\sigma_d=$	0,02 MPa
$V_{Rk,pb}=$	1,33 kN	
$\gamma_{Mm}=$	2,50	
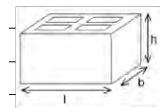
b)

Fig. 6.3-5 – Resistance of the anchor M8 to shear loads in bricks: a) verification; b) calculation sheets. Source: Author

Anchor M8 was verified too. The resistance to tension and shear loads were 0.75 kN, corresponding to the value of the hollow brick edge failure due to the vertical joints not filled. The resulting anchoring length (h_{ef}) was 80 mm, therefore threaded rods M8, 120 mm long were ordered.

After the calculation of the anchor diameters, the size and spacing of the holes in the mullions was defined. In correspondence of the anchors M12 the holes were Φ14, for anchors M8 the holes were Φ9. The spacing between the anchors for the connection in

concrete (s_1) was indicated in the calculation sheet in Figure 6.3-2 and was equal to 100 mm. In addition, it resulted that the minimal space from the edge of the concrete element (c) had to be at least 60 mm. To better understand these results, the production sheet related to the mullions is reported in the Figure 6.3-6. It also contains the indication about the hook, which standard dimensions have been already defined in the subsection 4.6.1.1. As the partner company was an Italian, the sheets are in Italian language.

MONTANTI A OMEGA CON GANCIO DI COLLEGAMENTO

ACCIAIO ZINCATO A CALDO Fe S235 JR S30/10

Qnt		6	unità
Altezza		330	cm
Larghezza complessiva		14	cm
Ali			
	larghezza	4	cm
Corpo			
	larghezza	6	cm
	profondità	4	cm
Asole per connessione strutturale			
	estremo superiore	6Φ14	
	estremo inferiore	6Φ14	
	c	6	cm
	s	9,5	cm
	s1	9	cm
Asole per collegamento di ritegno			
	ala sinistra	3Φ9	
	sp	26	cm
	sp2	100	cm
	sp3	56	cm
	ala destra	3Φ9	
	sp1	76	cm
	sp2	100	cm
	sp4	106	cm
Asole di collegamento gancio tramite bulloni			
	montanti 1° impalcato	3Φ13	
	d	76,5	cm
	d1	50	cm
	d2	53,5	cm

GANCIO DI COLLEGAMENTO AD L

ACCIAIO ZINCATO Fe S235 JR S20/10

qnt con piegatura a destra	9+2	unità
qnt con piegatura a sinistra	9+2	unità
l1	9,5	cm
a1	3.5	cm
a2	2	cm
a3	4	cm
a4	2	cm
a5	4	cm
l2	5	cm
l3	6	cm
b1	2,5	cm
b2	2,5	cm
asola	Φ13	

NOTE: piegatura a destra per montanti di sinistra;
piegatura a sinistra per montanti di destra

Fig. 6.3-6 – Production sheet about mullions and hooks: dimensions and quantities. Source: Author

The resins used for the chemical injections in concrete and brick wall, were chosen in function of the results obtained from the calculation. For the injection in the wall, the retinal capsules were also considered in order to avoid the loss of the resin into the empty cases of the brick.

The calculation of nuts and bolts to fix the hooks to the mullions has been carried out too applying the formulas (17-18) of the subsection 4.6.1.1 and considering the screw diameter of 12 mm (steel class 8.8 for structural use). However, the company preferred welded connection for convenience reasons. In Figure 6.3-7 the results are illustrated.

$\dfrac{F_{v,Ed}}{F_{v,Rd}} + \dfrac{F_{t,Ed}}{1.4F_{t,Rd}} \leq 1 \ \ con \ \dfrac{F_{t,Ed}}{F_{t,Rd}} \leq 1$		$\dfrac{F_{v,Ed}}{F_{v,Rd}} + \dfrac{F_{t,Ed}}{1.4F_{t,Rd}}$	0,033

$F_{v,Rd}$ (N)	32256	$\dfrac{F_{t,Ed}}{F_{t,Rd}}$	0,019
$F_{t,Rd}$ (N)	48384		
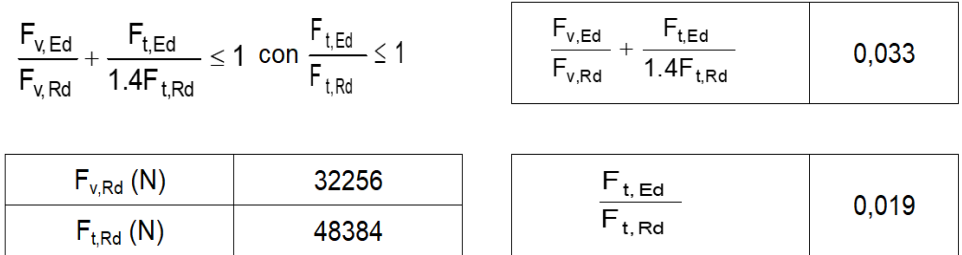
Fig. 6.3-7 – Bolted connections: calculation verification. Source: Author

It was widely verified. however, for safety reasons, the dimensions of the screw have not been modified. The hole in the hook should have been 9 mm in diameter and spaced at least 24 mm from the edge of the hook. The spacing considered in the hook design was 25 mm. Hence, also its sizes were verified.

Mullions and hooks have been supplied by Ferramati Italia that deals with iron works. For material availability reasons, the metallic sheet used for their forming was in black iron for which no galvanizing treatment has been realized as the prototype was finalized only to the system assembly verification and not to performance assessment. In Figure 6.3-8 are illustrated the mullions and hooks used for the system prototype. Further documentation is shown in the section 6.4.
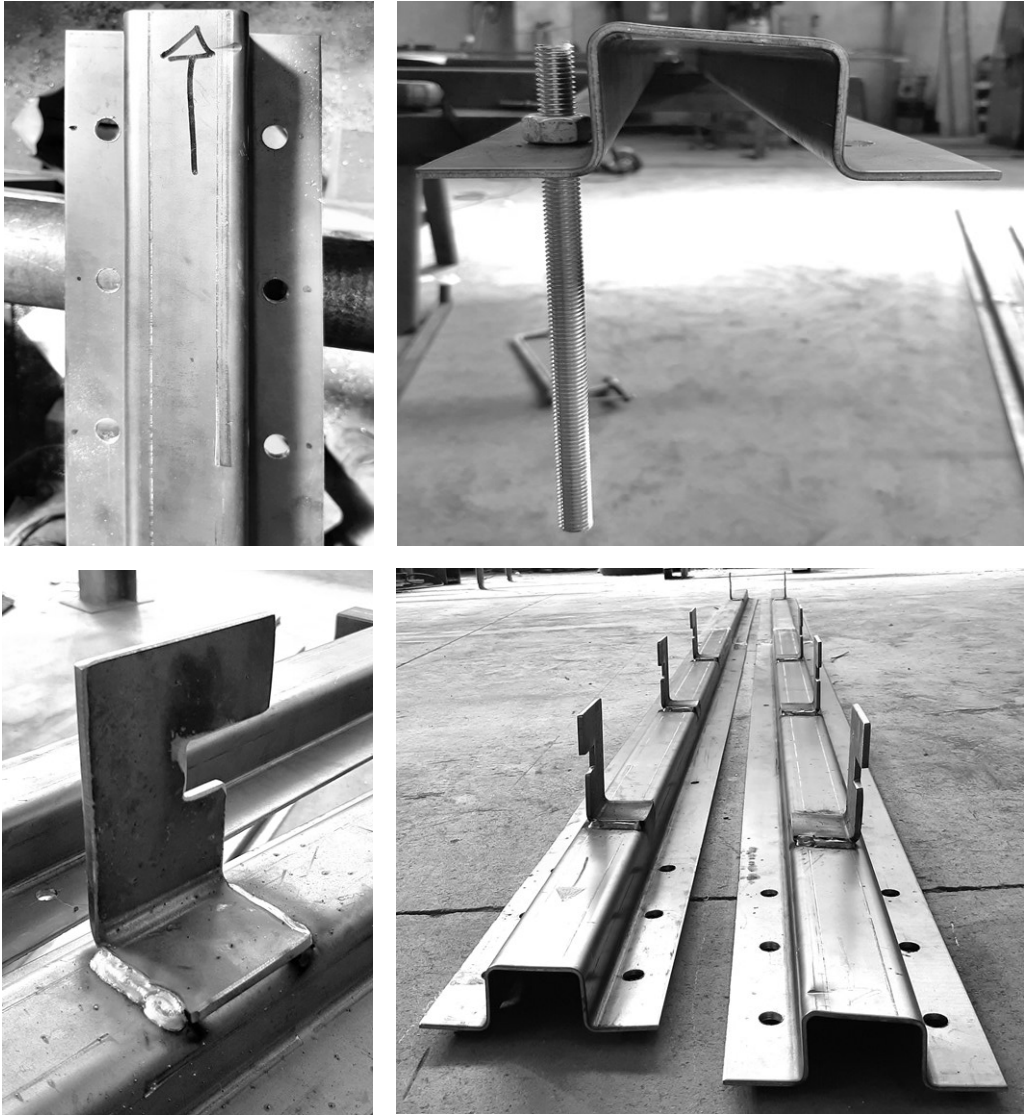
Fig. 6.3-8 – Mullions and hooks for panel anchoring. Source: Author

As regard the calculation of the post-installed rebar in concrete intended to connect the existing frame reinforcement with the new one, the procedure described in the section 4.6.1.1 was applied. In particular, using the formulas from (28) to (35), the results about anchor dimension for the connection in the different concrete elements (beams, pillars, foundation and shooting rods of the jet) were obtained and are illustrated in the production sheet in Figure 6.3-9. It has been assumed that the rebars had to be placed inside

the beam reinforcement cage, below the upper running bar. Since it had small dimensions (30 x 30 cm), the connectors have been designed to be placed at one third of the height of the beam from the upper edge (almost 10 cm). In Figure 6.3-10 are reported the photos about hooked post-installed rebars used for the prototype installation.
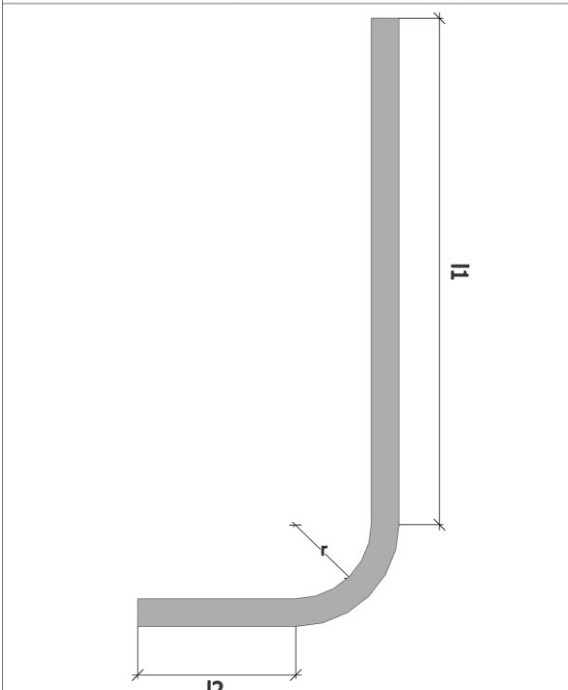
CARPENTERIA METALLICA			
TONDINI IN ACCIAIO Fe B450C AD ADERENZA MIGLIORATA			
	TRAVI E PILASTRI		
	Qnt	21	unità
	Diametro	Φ12	
	Dimensioni		
	l1	19	cm
	l2	6	cm
	r	3	cm
	FONDAZIONE		
	Qnt	9	unità
	Diametro	Φ12	
	Dimensioni		
	l1	40	cm
	l2	6	cm
	r	3	cm
	FERRI DI RIPRESA		
	Qnt	14	unità
	Diametro	Φ12	
	Dimensioni		
	l1	55	cm
	l2	6	cm
	r	3	cm

Fig. 6.3-9 – Production sheet about post-installed rebars: dimensions and quantities. Source: Author

Fig. 6.3-10 – Post-installed rebars. Source: Author

Since the resulting bar diameter was Φ12 and the drilling machine supplied by Ferramati was the hammer drill, the hole diameter in concrete was defined equal to Φ16 in accordance with the resin technical sheet supplied by the provider. The resin used for the chemical injection was the same employed for the mullion anchors in concrete.

The additional reinforcement of the system i.e., the rebars for the lightweight structural concrete (LWSC) casted in-situ, has been calculated following the requirements indicated in the subsection 4.6.1.1, coming from the Italian legislation LL.GG. 117/2011. The standard dimension of the rebar diameter has been considered equal to 10 mm (a tenth of the wall thickness). Hence, to perform the calculation, the area of the horizontal and vertical sections (A_{hc}, A_{vc}) of the LWSC wall were measured and divided per the area of the vertical and horizontal bars (A_{va}, A_{ha}), respectively, to calculate the geometric percentage of vertical and horizontal reinforcement (ρ_v, ρ_h). The results of the calculation are reported in the Table 6.3-1 below.

Table 6.3-1. Addition reinforcement calculation

$\sum A_{va}$	$\sum A_{ha}$	A_{vc}	A_{hc}	ρ_v	ρ_h	$\Phi_{v,h}$
mm²	mm²	mm²	mm²	%	%	mm
704	834	300000	337800	0,21%	0,3%	8

The values of ρ_v and ρ_h found, exceeded the minimum required by legislation, thus the calculation was validated. The rebar diameter was 8 mm spaced 25 cm from the next.

As regards the foundations of the new wall configured as a regular beam (30 x 40 cm), the steel rebar has been calculated in the hypothesis of double-joint beam with uniformly distributed load. The calculation has been executed in accordance with the Italian technical code (Ministero delle Infrastrutture e dei Trasporti, 2018). The resulting armour is reported in the production sheet in the Figure 6.3-11.

FERRAMATI

INTERNATIONAL

DISTINTA DI PRODUZIONE				DATA		PAG.
IMPRESA DOTTORATO				SIGLA		
CAR FERRO	Colore	CANTIERE BARI		Dis. rif.		

POS.	S C H E M A	N.	DIAM.	LUNGH.	TOT. ML.	PESO KG.
A)	☐ 34 / 22	16	8	120		
B)	5 ⌐‾‾‾‾‾‾⌐ 5 / 354	4	12	364		
C)	5 ⌐‾‾140‾‾	4	14	145		
D)	‾‾‾180‾‾‾	2	14	180		

Fig. 6.3-11 – Production sheet of the new foundation reinforcement. Source: Author

After calculating all the components of the system, the installation process started. In particular, the assessment of the execution phases of the technological system installation was conducted after constructing the wall sample with the same technical characteristics of the existing building considered for the system design. At the same time, a 3D model was created thanks to the software SketchUp Pro 2018, in order to support, predict and control each installation phase before the real execution. Figure 6.3-12 illustrates the simulated wall on the 3D model (a), compared with the real sample.

a) b)
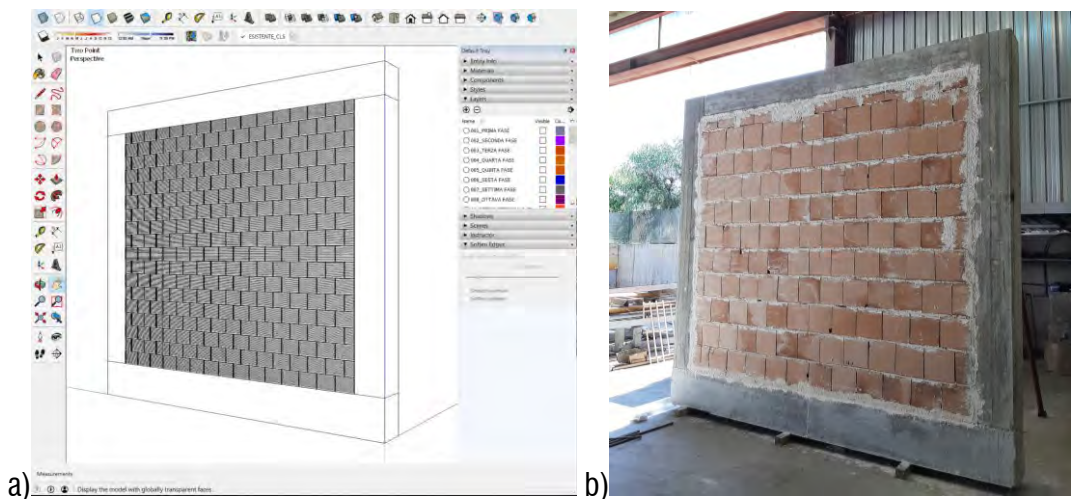
Fig. 6.3-12 – The existing façade sample: a) 3D simulated model; b) real wall. Source: Author

The disposition of the modules on the façade have been designed by rows. The first one contained the A modules, instead the overlapping row contained the B modules. Thanks to the property of modularity, the panels belonging to the same row could be associated with any module such that they could be distributed at will.

Thanks to the collaboration offered by the Ferramati's team, five macro installation phases have been programmed:

1) Preparation of the façade for receiving the modules;
2) New foundation;
3) Gluing EPS blocks to the brick wall and installation of the additional rebar;
4) Coupling of the first row of panels and LWSC casting according to the executive indications in the section 4.6.1.2;

5) Coupling of the second row of panels and LWSC completing casting.

The first phase was the longest one because it comprehended all the preliminary steps to execute directly on the façade. Using the 3D model, these phases has been visualized and optimized and validated before the real installation on the wall. Figure 6.3-13, 6.3-14, 6.3-15, 6.3-16, 6.3-17, 6.3-18 illustrate the steps for each macro-phase with the representation of the final effect extracted from the 3D model.
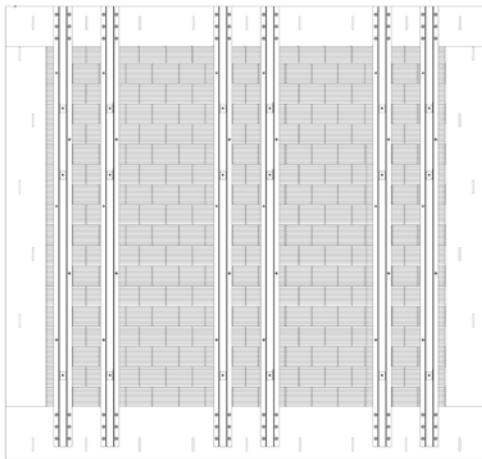
1.1 - Individuation, execution and air-cleaning of the drilling holes for connecting the mullion and the post-installed rebars along the column height, the base and upper beam length as well as in the bricks;

1.2 - Chemical injections of the resin for concrete into the holes and for bricks into the retinal capsule inserted in the bricks and subsequent incorporation of anchors up to anchor length;

1.3 - After the hardening of the resins, coupling of the mullions to the facade, making them coincide with the anchors and fixing through bolts and washers;

Fig. 6.3-13 - Programming of the executive steps through the 3D model: macro-phase 1. Source: Author
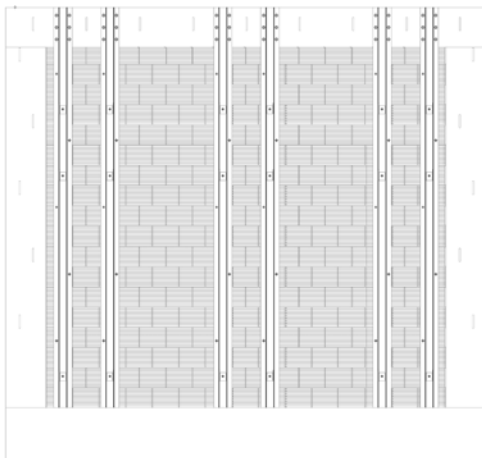
2.1 - Insertion of foundation reinforcement in the formworks

2.2 - Concrete casting

Fig. 6.3-14 - Programming of the executive steps through the 3D model: macro-phase 2. Source: Author
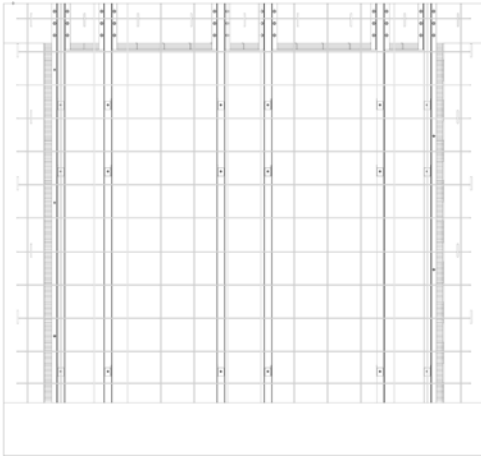
3.1 - Disposition and gluing of rEPS block betwen the mullions by means of adhesive foam insulation;

3.2 - binding of the additional reinforcement to the post-installed irons and to the waiting irons of the foundation;

3.3 - Insertion of spacers for the respect of the iron cover (2,5 cm)

Fig. 6.3-15 - Programming of the executive steps through the 3D model: macro-phase 3. Source: Author
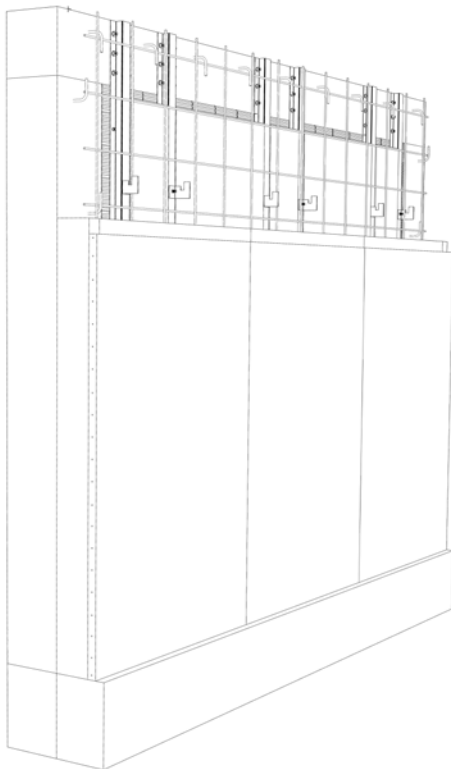
4.1 - Coupling of the first row of modules (A);

4.2 - Approach of rEPS blocks to the sides of the system to prepare for the jet;

4.3 - LWSC casting with low speed and per next layers
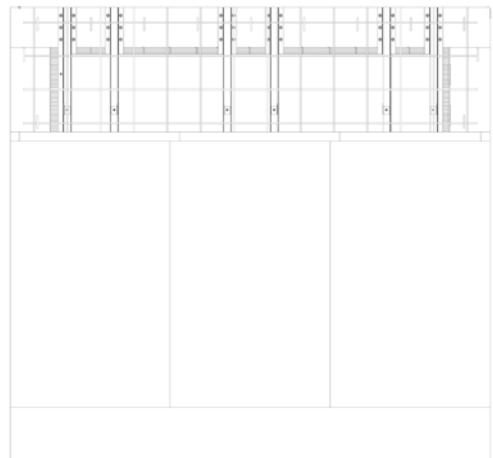
Fig. 6.3-16 - Programming of the executive steps through the 3D model: macro-phase 4. Source: Author
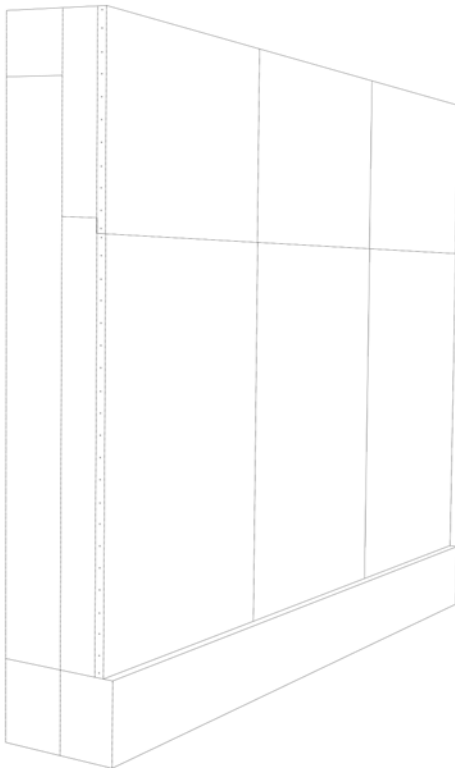
5.1 - Coupling of the second row of modules (B);

5.2 - Approach of blocks in rEPS to the sides of the system to prepare for the jet;

5.3 - LWSC casting with low speed and per next layers
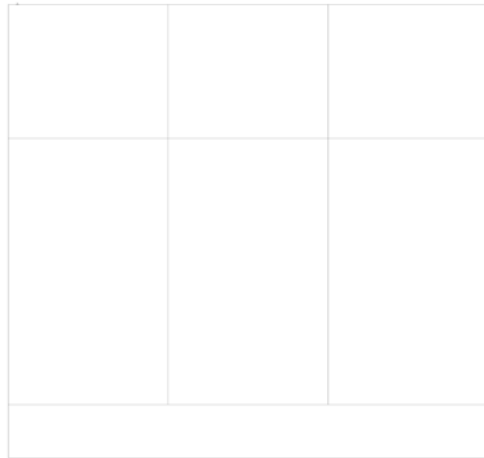
Fig. 6.3-17 - Programming of the executive steps through the 3D model: macro-phase 5. Source: Author

Therefore, the installation was executed according to the five macro-phases and the related steps validated by the 3D model. However, some differences between these steps and the real execution phases were individuated. They were related to the mullion mounting operations which resulted complicated due to the requirement of extreme precision in concrete drilling according to calculated spacings. Since they arrived in the plant already drilled by the technical drawings, the problem was making the slots coincide with the anchors already installed on the wall, contemporarily for the foundation and the upper beam. Therefore, for this first sample, the drills have been realised maintaining the mullions coupled to the wall.

Another problem was associated to the macro-phases 4 and 5 i.e. the coupling of the modules to the façade. After the panel was wedged into the hooks, it did not appear in the regular vertical position. This was due to the size of the hook, in particular the length

a2 too large to allow the lattices slipping towards the façade. However, the following concrete casting into the empty cavity between the panels and the façade, allowed pushing the panels outwards, bringing them back in vertical position and in line with the lateral modules. During the casting phase no phenomena of misalignment of the mullions from the façade, brick failures or hooks breakage occurred. No props were effectively used for the containment of concrete forces as the hooks worked according to forecasts. These results validated experimentally the calculations executed.

As regard the panel size verification, the use of the reduced modules (B) facilitated the installation operations since they allowed a greater visibility of the anchor hooks in the coupling step as well as better handling. Also the arrangement of the panels was validated since the male-female junctions matched without any problem of overlapping or material lacking (Figure 6.3-18). In general, the test which aimed to verify the installation phases, the safety in panel handling and mounting as well as the suitability of the proposed calculation approaches was declared valid. Figure 6.3-19, 6.3-20, 6.3-21, 6.3-22 show the real executing stages according to the five macro-phases explained before. A deepen documentation is inserted in the Annex.

Fig. 6.3-18 – Panel layer matching: a) front view; b) two modules joint (top view); c) lateral closing of the system (top view). Source: Author
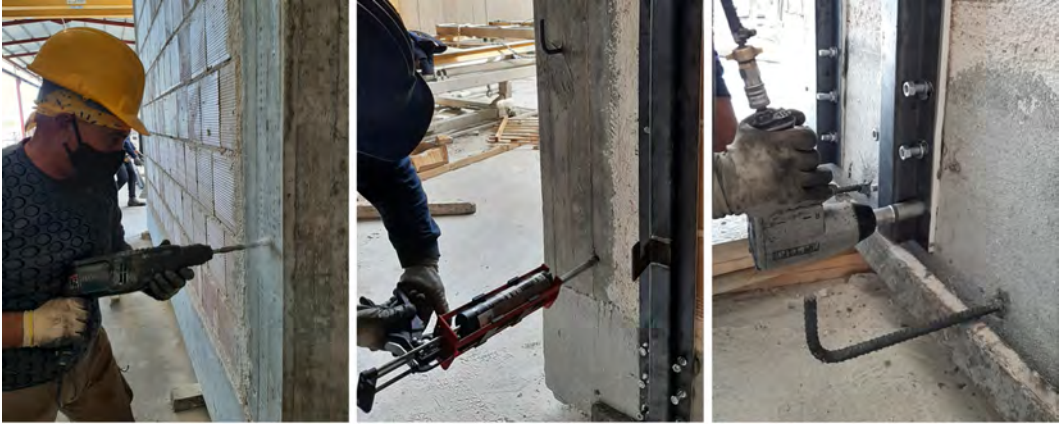
Fig. 6.3-19 – Prototype Phase: Macro-phase 1. Source: Author

Fig. 6.3-20 – Prototype Phase: Macro-phase 2. Source: Author

Fig. 6.3-21 – Prototype Phase: Macro-phase 3. Source: Author

Fig. 6.3-22 – Prototype Phase: Macro-phase 4. Source: Author

Fig. 6.3-23 – Prototype Phase: Macro-phase 2. Source: Author

7 FINAL REMARKS AND FUTURE DEVELOPMENTS

The **retrofit of the existing buildings** in reinforced concrete is a challenge felt at European level with the aim to mitigate the consequences due to the recent environmental events linked to climate change and seismic activity. The common policy of the Member States of the European Union on the definition of long-term strategies, intends to support the sustainable development of cities by placing the health of citizens first, starting from the protection of the places where they live. The great number of inefficient buildings constructed throughout the 20th century, in particular in the **second post World War**, involves at increasing the risk of greenhouse gas emissions and suffering significant damages due to the earthquakes. In reinforced concrete buildings, this hazard is mainly linked to the presence of the brick masonry covered by the rigid frame in concrete. The incapacity to react at temperature changes as well as to support the increasing of loads, may generates discomfort in the indoor environment, heat dispersions as well as damages and collapse of the structures. The three main problems are the inadequate **thermal protection**, deficient **technical details**, and lack of **maintenance**. The refurbishment of the elements belonging to the **building envelope** and the definition of **performance monitoring** approaches can lead to improve the building safety.

Academics and professionals have been experimenting with retrofit by implementing prefabricated modules for the benefits they provide in terms of speed, quality certification, safety, standardization, performance control, times, and costs optimization. The results they obtained were encouraging, although their proposals were dedicated only to energy or structural improvements due to the difficulty in considering many variables linked to the **adaptability** to the existing buildings.

The purpose of the doctoral study has been addressed to design a new building component in precast concrete (PC) to be applied to the existing RC buildings through an intelligent system. It aimed to optimize the thermal and structural performance of the external walls and prepare the building for the insertion of performance monitoring devices.

The methodology proposed was consistent with the "Sprint Execution" creative model of the "Design Thinking" approach for industrial projects. Based on the knowledge of the industrial scenario, the actual market as well as the academic results, it intended to define the characteristics of the innovative industrial proposal to arrive at prototyping and patenting of its technology in the shortest possible time.

Therefore, three main investigation phases were identified addressing to the definition of the conditions in which developing the project, of the strategical design approach for the geometric characterization of the component as well as to the industrial validation of the proposal. In detail, the critical review of the literature, the observation of the industrial prefabrication processes, and the analysis of the existing RC buildings in Europe, Italy and Spain performed in the first phase, conduced individuating the project specific goals and defining its conditions and criteria. From those assumptions, the design phase started from organizing the study according to three scales of detail, aiming at charactering the materials, designing the components, and combining the elements for the system composition. Since the project has been developed in collaboration with the Italian company of prefabricated elements, Ferramati International, every design step was subjected to the approval by its technical team, in particular with regard to the production phases, with the view to the future inclusion of the new component in its production chain. Therefore, the conceptual idea of the system, redefining the characteristics of the current products, has been configured as an innovative double-slab wall for existing buildings where the external slab was the prefabricated component i.e. the novel PC module, instead the internal one the existing façade. Their connection was ensured by steel elements anchored to the façade which remained embedded in the completion concrete casting intended to strength the

whole building. Shaped with omega profile, these elements also served as accommodation for monitoring devices.

The system was named "Intelligent PC panel system" (IPCS).

Its characterization started from the scale of detail of the materials, in particular from the experimentally study of the PC module insulating layer. Designed to overcome the problem of insulation linked to the actual prefabricated products, it consisted in a cement mortar with light aggregates in recycled extruded sintered polystyrene. The laboratory investigation and the industrial validation have led to individuate the best mortar in terms of thermal-insulating performance, also with characteristics better than the mixtures reviewed in the literature, such to initiate the patent request.

The next step was the design of the PC module in terms of steel reinforcement and layers configuration, considering the function for which was intended. With the aim to reduce the thermal bridges, the connecting junctions between the panels were staggered to create the male-female disposition. The assumption was validated by some preliminary simulations performed in the finite element model (FEM) environment of the software COMSOL Multiphysics. It showed that despite the presence of the steel reinforcement that deviated the heat flux, no thermal bridges occurred in the junctions.

Between the benefits provided by the novel module, the possibility to integrate the cladding already during its prefabrication was underlined. The study of six coating materials in terms of aesthetic aspects, realization complexity and thermal performance has led to the definition of an approach based on the analytic hierarchy process (AHP) to choose the best cladding type since many qualitative and quantitative criteria had to be considered. It has been practically applied to a case study for which the best cladding type was resulted the most consistent with the context in which the building was located.

Assuming that the sum of more panels created the external layer of the retrofitting system, the technological proposal has been defined and illustrated by several significant technical drawings. The detailed calculation methods to design and characterize the system components were proposed by deepening the European codes.

Since the main goal of the research was the technological design of the innovative system, only preliminary methods to assess the performance in terms of thermo-hygrometric insulation and seismic behaviour have been proposed. They were based on 3D simulations by FEM models and numerical attempts. Unfortunately, no experimental studies have been carried out.

At the same way, the monitoring technology based on an information system integrating a performance detecting platform and sensor devices remained at the proposal state.

Nevertheless, these preliminary approaches have been applied to a pilot case study having the same characteristics of the building typology chosen for the design of the technological system. The results showed that the application of the IPCS allowed reducing the thermal emissions more than 70%, reducing the risk of thermal bridges creation. Although, from the visual survey of the results concerning the distribution of the thermal flux emerged that some details required to be better investigated, especially in the assumption of integrating the novel system with traditional retrofitting methods.

The software SAP2000 has been employed for the preliminary assessment of the retrofitted building structural behaviour. In particular, a fiber approach was applied assuming two different configurations of retrofit: of the whole building and the only entire wall strips. From the pushover analyses emerged that only slight differences between the two configurations occurred and that both the solutions increased the whole structural stiffness and strength. On the other hand, the deformation capacity and the related ductility were strongly reduced, such that the retrofitting building assumed an elastic or low-ductile structural behaviour. In general, considering the seismic demand corresponding to the building location, the proposed retrofitting method allowed to obtain strongly higher safety levels for the entire structural system than the normal configuration.

The final stage of the doctoral investigation was the industrial validation in Ferramati's plants, of the designed elements through the realization of six prototypes of the PC panel in two different size categories with the aim to apply the retrofitting technique to

a real scale wall. The mathematical method proposed for the system elements dimensioning was applied with the aim to provide to the plant technicians, suitable production sheets useful to give the realization dispositions. In parallel, thanks to the collaboration of the technical team, the realization phases were defined and simulated on a 3D model in the SketchUp Pro virtual environment to predict possible problems related to the safety.

Five macro-phases were individuated with several subsequent steps. The installation testing of the retrofitting system was effectively conduced according to the defined sequences, despite some problems related to the geometric adaptability of the steel elements to the wall occurred. The work ended successfully without major problems, use of props or other safety measures. Therefore, this test which aimed to verify the installation phases, the safety in the handling and assembly of the panel as well as the suitability of the proposed calculation approaches was declared valid.

Of course, the system prototyping was useful to suggest several optimization measures in terms of production and arrangement of the panel layers or geometric improvements of the steel elements. They will be the subject of the future development of the project in addition to the necessary experimental characterization of the proposal for a deeper understanding of the thermal and structural behaviour of the system and to make technological improvements.

In the light of these studies, it is possible to draw the following conclusions:
- The innovative PC module is the first prefabricated panel composed of novel materials from industrial waste, devoted to cover the existing buildings.
- Thanks to its composition, the PC module can be easily combined with steel elements to generate an innovative double-slab wall with the façade of the existing buildings to provide thermal and structural improvements. It is named *"INTELLIGENT PC PANEL SYSTEM"*
- The technology is devoted to retrofit reinforced concrete buildings and infill walls in brick (type 25 x 25 x1 2 cm) of the South of Italy.

- Thanks to the properties of the PC modules the system reduces the risk of formation of thermal bridges in the most delicate points of the structure. It can also be adapted to buildings with a pilotis ground floor.
- In the climatic severity for which it has been studied, the system brings benefits in terms of reduced heat flow and energy savings due to the use of insulating materials and the inertial mass that it adds to the structure.
- From the structural point of view, it gives rigidity to the building at the expense of ductility. However, in the medium-low seismic area it has safety benefits (Apulia region, where the project was developed).
- The system prepares the building with the necessary technology to be equipped with monitoring sensors.

Concerning the future developments, the research will continue with the experimental technical definition of the solution characteristics as well as with the study and the choice of optimal data acquisition devices equipped with the technology of remote sensing and data transmission to be integrated into the system with the subsequent design and calibration of the data reading and processing platform. The technological proposal of the telescopic rail that can be removed from the mullions will also be verified through a deeper design and prototype.

Moreover, the analysis of feasibility and economic return of the investment will be carried out to confirm the objective of economic sustainability in accordance with Ferramati interest to invest in the solution improvements and future production.

At the actual state, for its innovation in intending mitigating contemporarily the two main problems that affected the existing buildings i.e., thermal and structural deficiencies, the "*INTELLIGENT PC PANEL SYSTEM*" is under patenting request.

ACRONYMS

AB	Apartment Blocks
AB*	Basic values of the ground horizontal acceleration
AG	Values of peak acceleration on hard ground
AHP	Analytical Hierarchy Process
AIPE	Associazione Italiana Polistirene Espanso, Italian Association Expanded Polystyrene
BF	Bare Frame
BFRP	Basalt Fiber-Reinforced Polymer
BR	Brindisi, Puglia, Italy
C/D	Capacity Demand ratio
CTE	Spanish technical code for construction
DD	Degree-Days
DOF	Degree of Freedom
EC	Eurocode
ECBCS	Energy Conservation in Buildings and Community Systems
EED	Energy efficiency Directive
EPB	Economic-Popular Building
EPBD	Energy Performance of Buildings Directive
EPS	Extruded Sintered Polystyrene
EPS200	EPS with density equal to 30 kg/m^3
EPS30	EPS with density equal to 10 kg/m^3
ETICS	External Thermal Insulation Cladding System
EU	European Union
EU27	27 Member States of European Union
F	Seismic Action
FEM	Finite Element Model
FRP	Fiber-Reinforced Polymer
g	Gravity Acceleration
GFRP	Glass Fiber-Reinforced Polymer
GHG	Greenhouse Gas
IEA	International Energy Agency
IF	infill with masonry panel
IO	Immediate Occupancy
IP	In-Plan
IP	In-plane
IPCS	Intelligent PC panel system

IS	Information System
LS	Life-Safety
LWM	Lightweight Mortar
LWSC	Lightweight Structural Concrete
MFH	Multi-Family Houses
NC	Near Collapse
NTC18	Italian technical code for construction 2018
NZEB	Near Zero-Energy Building
OOP	Out-of-Plane
PC	Precast Concrete
PDP	Performance Detecting Platform
PS	Polystyrene
RC	Reinforced Concrete
rEPS	recycled Extruded Sintered Polystyrene
rEPSa	recycled Extruded Sintered Polystyrene with high density
rEPSb	recycled Extruded Sintered Polystyrene with low density
RF1, RF2	Retrofit Configurations
SCI	Winter weather severity
SCV	Summer weather severity
SDG	Sustainable Development Goal
SEM	Scanning Electronic Microscope
SFH	Single-Family Houses
TH	Terraced Houses
U-value	Thermal Transmittance value [W/(m^{2}K)]
vEPS	virgin Extruded Sintered Polystyrene
vEPSb	virgin Extruded Sintered Polystyrene with low density
w/c	Water cement ratio
WW2	World War II

SIMBOLS

ρ	Density	[Kg/m³]
T	Temperature	[K]
RH	Relative Humidity	[%]
λ	Thermal conductivity	[W/mK]
λ_{int}	Intended thermal conductivity	[W/mK]
α_{dry}	Thermal diffusivity	[m²/s]
$c\rho$	Volumetric thermal capacity	[J/m³K]
c_p	Specific heat	[J/kgK]
G	Change of Mass	[mg/h]
g	Water vapour transmission rate	[mg/m²h]
Δp	Water vapour pressure difference	[Pa]
W	Water vapour permanence	[mg/m²hPa]
Z	Water vapour resistance	[m²hPa/mg]
δ	Water vapour permeability	[kg/msPa]
μ	Resistance to vapour diffusion	[-]
s_d	Water vapour diffusion air layer thickness	[m]
U	Thermal transmittance	[W/m²K]
Y_{ie}	Periodic thermal transmittance	[W/m²K]
k_1	Periodic internal thermal capacity	[kJ/m²K]
m_s	The specific wall heat and the surface thermal mass	[kg/m³]
ϕ	Time shift coefficient	[h]
f_d	Attenuation factor	[-]
F_f	Flexural Load	[N]
F_c	Compressive Load	[N]
S_d	Design action	[N]
R_d	Design resistance	[N]
$F_{v,Ed}$	Design shear force	[N]
$F_{t,Ed}$	Design tensile force	[N]
$F_{v,Rd}$	Resistance to shear loads	[N]
$F_{t,Rd}$	Resistance to tension loads	[N]
N_{Sd}	Design tension load	[kN]
$N_{Rd,s}$	Steel failure under tension loads	[kN]
$N_{Rd,p}$	Combined pull-out and concrete cone failure	[kN]
$N_{Rd,c}$	Concrete cone failure	[kN]
$N_{Rd,sp}$	Splitting failure	[kN]
$N_{Rd,b}$	Brick breakout failure	[kN]

$N_{Rd,pb}$	Pull out of one brick	[kN]
V_{Sd}	Design shear load	[kN]
$V_{Rd,s}$	Steel failure under shear loads	[kN]
$V_{Rd,cp}$	Concrete pry-out failure	[kN]
$V_{Rd,c}$	Concrete edge failure	[kN]
$V_{Rd,c\parallel}$ $V_{Rd,c\perp}$	Hollow brick edge failure	[kN]
$V_{Rd,pb}$	Pushing out of one brick failure	[kN]
γ_{Ms}	The steel partial safety factor	[-]
γ_{Msp}	The partial safety factor for splitting failure	[-]
γ_{Mc}	The partial safety factor for concrete	[-]
γ_{Mm}	The partial safety factor for masonry	[-]
l_{bd}	Anchor length	[mm]
l_0	Required overlapping length	[mm]
c_1	Iron cover	[mm]
$l_{b,rqd}$	The basic required anchorage length	[mm]
A_{hc}	The area of the concrete horizontal section	[mm]
A_{ha}	The area of the horizontal reinforcement bars	[mm]
A_{vc}	The area of the concrete vertical section	[mm]
A_{va}	The area of the vertical reinforcement bars	[mm]
ρ_v	The geometric percentage of vertical reinforcement	[%]
ρ_h	The geometric percentage of horizontal reinforcement	[%]
R_f	Flexural Resistance	[MPa]
R_c	Compressive Strength	[MPa]
f_{yk}	The characteristic yield strength	[MPa]
f_{tk}	The characteristic tension strength	[MPa]
f_{yd}	The design strength	[MPa]
f_{ub}	The nominal value of the ultimate tensile strength for bolts	[MPa]
f_{uk}	The characteristic nominal ultimate strength	[MPa]
E_s	The modulus of elasticity of reinforcement steel	[MPa]
G	The transverse modulus of elasticity	[MPa]
ν	The Poisson's ratio	[-]
ε_y	The characteristic deformation	[%]
σ_{hd}	Theoretical pressure	[kN/m^3]
$\sigma_{hk,max}$	Maximum lateral pressure of the concrete	[kN/m^3]
$\sigma_{hd,max}$	The design fresh concrete pressure	[kN/m^3]
v	The casting rate	[m/h]
γ_c	The specific concrete weight	kN/m^3
t_E	The setting time	[h]
F_n	The concrete consistency class	[-]

K1	The stiffening and setting concrete factors	[-]
K2	The factor for specific weight	[-]
H	The casting height	[m]
h_s	Hydrostatic concrete pressure	[m]
y	The height of the concrete hydrostatic behaviour	[m]
V_b	Base shear	[kN]
δ_R	Roof displacement	[m]
f'_{cm}	Mean compressive strength of in situ concrete	[MPa]
f'_{ym}	Mean tensile strength of steel rebars	[MPa]
E_c	Elastic modulus of concrete	[MPa]
E_w	Vertical Elastic modulus	[MPa]
$E_{w\theta}$	Diagonal Elastic modulus	[MPa]
G_w	Shear Elastic modulus	[MPa]
σ_m	Compression strength	[MPa]
f_{tp}	Tensile strength	[MPa]
G_1, G_2, Q	Gravity loads	[kN/m^2]
Lat, Lon	Coordinates	[°]
N_L	Normal life	[years]
U_C	Usage class	[-]
Φ, d_0	Diameter	[mm]
c_{min}	Recommended value of minimum concrete cover	[mm]
c_{nom}	Nominal value of the concrete cover	[mm]
c_0	Minimal cover value	[mm]
Δc_{dev}	Execution tolerance	[mm]
t	Thickness	[mm]
A_s	Nominal stress area	[mm^2]

REFERENCES

1 THE PROBLEMS OF THE EXISTING RC BUILDINGS

- Asteris, P. G. *et al.* (2011) 'Mathematical Macromodeling of Infilled Frames: State of the Art', *Journal of Structural Engineering*. doi: 10.1061/(asce)st.1943-541x.0000384.

- Corrado, V., Ballarini, I. and Corgnati, S. P. (2014) 'Building Typology Brochure – Italy Fascicolo sulla Tipologia Edilizia Italiana', p. 130.

- Dell'era, C. (2018) *Sprint Execution: il valore aggiunto del Design Thinking*, *www.osservatori.net-digital innovation*. Available at: https://blog.osservatori.net/it_it/sprint-execution-design-thinking?hsCtaTracking=0b7aef03-cab6-4e02-a71c-e6842ac5164b%7C2ec7ad37-37b0-4f74-b677-5da7365829eb (Accessed: 29 November 2020).

- Dolšek, M. and Fajfar, P. (2001) 'Soft storey effects in uniformly infilled reinforced concrete frames', *Journal of Earthquake Engineering*. doi: 10.1080/13632460109350383.

- El-Dakhakhni, W. W., Elgaaly, M. and Hamid, A. A. (2003) 'Three-Strut Model for Concrete Masonry-Infilled Steel Frames', *Journal of Structural Engineering*. doi: 10.1061/(asce)0733-9445(2003)129:2(177).

- EN ISO 10211 (2018) *Thermal bridges in building construction - Heat flows and surface temperatures - Detailed calculations*. Available at: http://store.uni.com/catalogo/uni-en-iso-10211-2008 (Accessed: 19 January 2020).

- EN ISO 13788 (2013) *Hygrothermal performance of building components and building elements - Internal surface temperature to avoid critical surface humidity and interstitial condensation - Calculation methods*. Available at: http://store.uni.com/catalogo/index.php/uni-en-iso-13788-2013.html (Accessed: 12 April 2019).

- EPISCOPE (2016) *Monitor Progress Towards Climate Targets in European*

Housing Stocks Main Results of the EPISCOPE Project - Final Project Report - (Deliverable D1.2). Available at: http://episcope.eu/fileadmin/episcope/public/docs/reports/EPISCOPE_FinalReport.pdf.

- European Union (2020) *Sustainable Development in the European Union*, *Luxemburg: Publications Office of the European Union.* doi: 10.2785/555257.

- Furtado, A. and De Risi, M. T. (2020) 'Recent Findings and Open Issues concerning the Seismic Behaviour of Masonry Infill Walls in RC Buildings', *Advances in Civil Engineering*, 2020. doi: 10.1155/2020/9261716.

- García-Prieto Ruiz, A., Serrano Lanzarote, B. and Ortega Madrigal, L. (2016) *Catálogo de tipología edificatoria residencial Ámbito: España*, *Instituto Valenciano de la Edificación*.

- Martiradonna, S., Fatiguso, F. and Lombillo, I. (2020a) 'Precast Concrete Module for Structural and Energy Rehabilitation of Reinforced Concrete Buildings', in *REHABEND 2020*, pp. 1618–1626.

- Martiradonna, S., Fatiguso, F. and Lombillo, I. (2020b) 'Thermal improvements of existing reinforced concrete buildings by an Innovative Precast Concrete Panel system', in *Colloqui.AT.e 2020*, pp. 511–522.

- Negro, P. and Colombo, A. (1997) 'Irregularities induced by nonstructural masonry panels in framed buildings', *Engineering Structures*. doi: 10.1016/S0141-0296(96)00115-0.

- Pagliai, C. (2018) *Piani di Ricostruzione del Dopoguerra*, *Conformità Urbanistica*. Available at: https://www.studiotecnicopagliai.it/piani-di-ricostruzione-dopoguerra/ (Accessed: 27 November 2020).

- Pasca, M. and Liberatore, L. (2015) 'Predicting models for the evaluation of out-of-plane ultimate load carrying capacity of masonry infill walls', in *Earthquake Resistant Engineering Structures X*. doi: 10.2495/eres150071.

- Ruggieri, S. (2018) *Advanced strategies for the seismic assessment of existing RC moment-frame buildings: appraisal of modelling assumptions and development of parsimonious PBEE-based methods of analysis*.

- Zanchini, E. *et al.* (2014) 'TUTTI IN CLASSE A', 2014, pp. 1–187.

3 STATE OF THE ART

- Abramski, M. (2017) 'Improving Thermal Insulation Properties for Prefabricated Wall Components Made of Lightweight Aggregate Concrete with Open Structure'. doi: 10.1088/1757-899X/245/2/022034.

- *ACI 318-14* (2005).

- Aciu, C. *et al.* (2015) 'Recycling of Polystyrene Waste in the Composition of Ecological Mortars', *Procedia Technology*, 19(September), pp. 498–505. doi: 10.1016/j.protcy.2015.02.071.

- AIPE (2017) *PRODURRE L 'EPS*.

- Akhoundi, F., Vasconcelos, G. and Lourenço, P. (2018) 'In-Plane Behavior of Infills using Glass Fiber Shear Connectors in Textile Reinforced Mortar (TRM) Technique', *International Journal of Structural Glass and Advanced Materials Research*, 2(1), pp. 1–14. doi: 10.3844/sgamrsp.2018.1.14.

- Akin, A. and Sezer, R. (2016) 'A study on strengthening of reinforced concrete frames using precast concrete panels', *KSCE Journal of Civil Engineering*, 20(6), pp. 2439–2446. doi: 10.1007/s12205-016-0188-z.

- Aksoylu, C. and Kara, N. (2020) 'Strengthening of RC frames by using high strength diagonal precast panels', *Journal of Building Engineering*. Elsevier Ltd, 31. doi: 10.1016/j.jobe.2020.101338.

- Aksoylu, C. and Sezer, R. (2018) 'Investigation of precast new diagonal concrete panels in strengthened the infilled reinforced concrete frames', *KSCE Journal of Civil Engineering*, 22(1), pp. 236–246. doi: 10.1007/s12205-017-1290-6.

- Al-Rubaye, S. *et al.* (2018) 'Evaluating Elastic Behavior for Partially Composite Precast Concrete Sandwich Wall Panels', *PCI Journal*, 63(5), pp. 71–88. doi: 10.15554/pcij63.5-04.

- Altin, S., Anil, Ö. and Kara, M. E. (2008) 'Strengthening of RC nonductile frames with RC infills: An experimental study', *Cement and Concrete Composites*, 30(7),

pp. 612–621. doi: 10.1016/j.cemconcomp.2007.07.003.

- American Concrete Institute (2013) 'ACI Concrete Terminology - An ACI Standard', p. 32. Available at: www.concrete.org.

- Azcarate-aguerre, J., Guerra-santin, O. and Silvester, S. (2017) 'Investigating the business case for a zero- energy refurbishment of residential buildings by applying a prefabricated façade module', *ECEEE 2017 SUMMER STUDY*, (June), pp. 1113–1122.

- Babu, K. G. and Babu, D. S. (2003) 'Behaviour of lightweight expanded polystyrene concrete containing silica fume', *Cement and Concrete Research*. doi: 10.1016/S0008-8846(02)01055-4.

- Ballarini, I. *et al.* (2011) 'Definition of building typologies for energy investigations on residential sector by Tabula Iee-Project: Application to Italian case studies', in *Roomvent*, pp. 19–22.

- Baran, M. and Tankut, T. (2011) 'Retrofit of non-ductile RC frames with precast concrete (PC) wall panels', *Advances in Structural Engineering*, 14(6), pp. 1149–1166. doi: 10.1260/1369-4332.14.6.1149.

- Bedeković, G. *et al.* (2019) 'Recovery of waste expanded polystyrene in lightweight concrete production', *Rudarsko Geolosko Naftni Zbornik*, 34(3), pp. 73–80. doi: 10.17794/rgn.2019.3.8.

- Bida, S. M. *et al.* (2018) 'Advances in Precast Concrete Sandwich Panels toward Energy Efficient Structural Buildings', *Preprints*, (October), p. 2018100147. doi: 10.20944/preprints201810.0147.v1.

- Binici, B. and Ozcebe, G. (2006) 'Seismic evaluation of infilled reinforced concrete frames strengthened with FRPS', *8th US National Conference on Earthquake Engineering 2006*, 1(1717), pp. 92–101.

- Borodinecs, A. *et al.* (2017) 'Development of Prefabricated Modular Retrofitting Solution for Post-World War II Buildings', (April), pp. 27–28. doi: 10.3846/enviro.2017.252.

- Borodinecs, A. *et al.* (2018) '3D scanning data use for modular building renovation based on BIM model', *MATEC Web of Conferences*, 251(January). doi:

10.1051/matecconf/201825103004.

- Bravinski, L. G. (2006) '3-D CONSTRUCTION MODULES'. United States.

- Cavaleri, L. and Di Trapani, F. (2014) 'Cyclic response of masonry infilled RC frames: Experimental results and simplified modeling', *Soil Dynamics and Earthquake Engineering*, 65, pp. 224–242. doi: 10.1016/j.soildyn.2014.06.016.

- CEN (2004) *Eurocode 2: Design of concrete structures - Part 1-1 : General rules and rules for buildings Eurocode*, *British Standards Institution*. doi: [Authority: The European Union Per Regulation 305/2011, Directive 98/34/EC, Directive 2004/18/EC].

- Chen, B. and Liu, N. (2013) 'A novel lightweight concrete-fabrication and its thermal and mechanical properties', *Construction and Building Materials*. Elsevier Ltd, 44, pp. 691–698. doi: 10.1016/j.conbuildmat.2013.03.091.

- Choi, S. H. *et al.* (2020) 'Seismic performance assessments of RC frame structures strengthened by external precast wall panel', *Applied Sciences (Switzerland)*. MDPI AG, 10(5). doi: 10.3390/app10051749.

- Consiglio dei Ministri (2006) *Criteri generali per l'individuazione delle zone sismiche e per la formazione e l'aggiornamento degli elenchi delle medesime zone*.

- Corrado, V., Ballarini, I. and Corgnati, S. P. (2014) 'Building Typology Brochure – Italy Fascicolo sulla Tipologia Edilizia Italiana', p. 130.

- Dixit, A. *et al.* (2019) 'Lightweight structural cement composites with expanded polystyrene (EPS) for enhanced thermal insulation', *Cement and Concrete Composites*. Elsevier, 102(December 2018), pp. 185–197. doi: 10.1016/j.cemconcomp.2019.04.023.

- Dobelis, M., Kalinka, M. and Borodinecs, A. (2016) 'The Capture of BIM Compatible 3D Building Model from Laser Scanner Data', *The 17th International Conference on Geometry and Graphics*, China, Bei(August), pp. 4–8.

- Dolce, M. and Manfredi, G. (2011) *Linee Guida per riparazione e rafforzamento di elementi strutturali, tamponature e partizioni*, *Reluiss*.

- Durand, P. (1991) 'PREFABRICATED FORMS FOR CONCRETE WALLS'. United States.

- Emin, M. and Altin, K. (2006) 'Behavior of reinforced concrete frames with reinforced concrete partial infills', *Aci Structural Journal*, 103(5), pp. 701–709. Available at: https://www.researchgate.net/publication/292002099_Behavior_of_reinforced_concrete_frames_with_reinforced_concrete_partial_infills (Accessed: 17 October 2020).

- EPISCOPE (2016) *Monitor Progress Towards Climate Targets in European Housing Stocks Main Results of the EPISCOPE Project - Final Project Report - (Deliverable D1.2)*. Available at: http://episcope.eu/fileadmin/episcope/public/docs/reports/EPISCOPE_FinalReport.pdf.

- Ferrándiz-Mas, V. *et al.* (2014) 'Lightweight mortars containing expanded polystyrene and paper sludge ash', *Construction and Building Materials*, 61, pp. 285–292. doi: 10.1016/j.conbuildmat.2014.03.028.

- Ferrándiz-Mas, V. and García-Alcocel, E. (2012) 'Caracterización física y mecánica de morteros de cemento Portland fabricados con adición de partículas de poliestireno expandido (EPS)', *Materiales de Construccion*, 62(308), pp. 547–566. doi: 10.3989/mc.2012.04611.

- Ferrándiz-Mas, V. and García-Alcocel, E. (2013) 'Durability of expanded polystyrene mortars', *Construction and Building Materials*, 46, pp. 175–182. doi: 10.1016/j.conbuildmat.2013.04.029.

- Ferrándiz, V., Huesca, J. a and García, E. (2011) 'Normalized cement mortar with expanded polystyrene', *13th International Congress on the Chemistry of Cement.*, (October), pp. 1–6. doi: 10.13140/2.1.5013.2484.

- Frankl, B. A. *et al.* (2011) 'Behavior of precast, prestressed concrete sandwich wall panels reinforced with CFRP shear grid', *PCI Journal*. Precast/Prestressed Concrete Institute, 56(2), pp. 42–54. doi: 10.15554/pcij.03012011.42.54.

- Furtado, A. *et al.* (2020) 'Effect of the Panel Width Support and Columns Axial Load on the Infill Masonry Walls Out-Of-Plane Behavior', *Journal of Earthquake*

Engineering. Taylor and Francis Ltd., 24(4), pp. 653–681. doi: 10.1080/13632469.2018.1453400.

- G. de Moraes, E. *et al.* (2019) 'Innovative thermal and acoustic insulation foam by using recycled ceramic shell and expandable styrofoam (EPS) wastes', *Waste Management*. Elsevier Ltd, 89, pp. 336–344. doi: 10.1016/j.wasman.2019.04.019.

- Gara, F. *et al.* (2012) 'Experimental tests and numerical modelling of wall sandwich panels', *Engineering Structures*, 37, pp. 193–204. doi: 10.1016/j.engstruct.2011.12.027.

- Garay, R., Arregi, B. and Elguezabal, P. (2017) 'Experimental Thermal Performance Assessment of a Prefabricated External Insulation System for Building Retrofitting', *Procedia Environmental Sciences*. The Author(s), 38, pp. 155–161. doi: 10.1016/j.proenv.2017.03.097.

- García-Prieto Ruiz, A., Serrano Lanzarote, B. and Ortega Madrigal, L. (2016) *Catálogo de tipología edificatoria residencial Ámbito: España*, *Instituto Valenciano de la Edificación*.

- Gomes, M. G. *et al.* (2018) 'Thermal conductivity measurement of thermal insulating mortars with EPS and silica aerogel by steady-state and transient methods', *Construction and Building Materials*, 172, pp. 696–705. doi: 10.1016/j.conbuildmat.2018.03.162.

- Ha, S. K., Yu, S. Y. and Kim, J. S. (2018) 'Experimental Study on Existing Reinforced Concrete Frames Strengthened by L-type Precast Concrete Wall Panels to Earthquake-Proof Buildings', 22, pp. 3579–3591. doi: 10.1007/s12205-018-1197-x.

- Hodicky, K. *et al.* (2015) 'Experimental and numerical investigation of the FRP shear mechanism for concrete sandwich panels', *Journal of Composites for Construction*, 19((5)), p. 04014083. doi: 10.1061/(ASCE)CC.1943-5614.0000554.

- IDAE (2016) *Analysis of the Energetic Consumption of the Residential Sector in Spain (Proyecto Sech-Spahousec, Análisis del consumo energético del sector residencial en España)*, *Idae*. Available at: www.idae.es.

- Italian Decree (1993) *DPR 412/93: Norme per la progettazione, l'installazione, l'esercizio e la manutenzione degli impianti termici degli edifici ai fini del contenimento dei consumi di energia.* Available at: https://www.mendeley.com/catalogue/7d0b7847-da0f-3010-8e94-2b7a93119808/?utm_source=desktop&utm_medium=1.19.4&utm_campaign=open_catalog&userDocumentId=%7Bcf241085-ad8f-3b38-a16f-a61f241c60cb%7D (Accessed: 7 November 2020).

- IVE (2011) *Use of Building Typologies for Energy Performance Assessment of National Building Stock.* Available at: http://episcope.eu/fileadmin/tabula/public/docs/scientific/ES_TABULA_Report_IVE.pdf

- Kamanli, M. *et al.* (2015) 'Seismic improvement of infilled nonductile RC frames with external mesh reinforcement and plaster composite', *Earthquake and Structures*. Techno Press, 8(3), pp. 761–778. doi: 10.12989/eas.2015.8.3.761.

- Kang, J. (2015) 'Composite and non-composite behaviors of foam-insulated concrete sandwich panels', *Composites Part B: Engineering*, 68, pp. 153–161. doi: 10.1016/j.compositesb.2014.08.034.

- Kaplan, H. and Ylmaz, S. (2012) 'Seismic Strengthening of Reinforced Concrete Buildings', in *Earthquake-Resistant Structures - Design, Assessment and Rehabilitation*. InTech. doi: 10.5772/28854.

- Kargin, I. (2011) 'Ready wall for noise and heat insulation'.

- Kekanović, M. *et al.* (2014) 'Lightweight concrete with recycled ground expanded polystyrene aggregate', *Tehnicki Vjesnik*, 21(2), pp. 309–315.

- Kim, C. T. (1995) 'CONCRETE STRUCTURES AND METHODS FOR THEIR MANUFACTURE'. United States.

- Kim, S. Y. (1996) 'FORM-FILL CONCRETE WALL'.

- Kinnane, O., West, R. and Hegarty, R. O. (2020) 'Structural shear performance of insulated precast concrete sandwich panels with steel plate connectors', *Engineering Structures*. Elsevier Ltd, 215. doi: 10.1016/j.engstruct.2020.110691.

- Klõšeiko, P. *et al.* (2020) 'Thermal bridge effect of vertical diagonal tie connectors

in precast concrete sandwich panels : an experimental and computational study', 8001, pp. 1–7.

- Kobler, R. L. *et al.* (2011) *IEA ECBCS Annex 50 Prefabricated Systems for Low Energy Renovation of Residential Buildings Retrofit Module Design Guide This report documents results of cooperative work performed under the IEA Programme for Energy Conservation in Buildings and Community*. Available at: http://www.ecbcs.org.

- Konstantinou, T. *et al.* (2017) 'A zero-energy refurbishment solution for residential apartment buildings by applying an integrated, prefabricated façade module', *Powerskin Conference*, (January), pp. 231–240.

- Li, Y., Liu, N. and Chen, B. (2015) 'Properties of lightweight concrete composed of magnesia phosphate cement and expanded polystyrene aggregates', *Materials and Structures*, 48(1–2), pp. 269–276. doi: 10.1617/s11527-013-0182-6.

- Lu, S.-Y. (1995) 'WALL STRUCTURE FOR BUILDINGS'.

- Maaroufi, M. *et al.* (2018) 'Characterization of EPS lightweight concrete microstructure by X-ray tomography with consideration of thermal variations', *Construction and Building Materials*. Elsevier Ltd, 178, pp. 339–348. doi: 10.1016/j.conbuildmat.2018.05.142.

- Madandoust, R., Ranjbar, M. M. and Yasin Mousavi, S. (2011) 'An investigation on the fresh properties of self-compacted lightweight concrete containing expanded polystyrene', *Construction and Building Materials*. Elsevier Ltd, 25(9), pp. 3721–3731. doi: 10.1016/j.conbuildmat.2011.04.018.

- Martiradonna, S., Fatiguso, F. and Lombillo, I. (2020) 'Thermal improvements of existing reinforced concrete buildings by an Innovative Precast Concrete Panel system', in *Colloqui.AT.e 2020*, pp. 511–522.

- Masera, G. *et al.* (2017) 'Prefabrication as Large-scale Efficient Strategy for the Energy Retrofit of the Housing Stock : An Italian Case Study', *Procedia Engineering*. The Author(s), 180(May), pp. 1160–1169. doi: 10.1016/j.proeng.2017.04.276.

- Matsubara, H. (2001) 'APPARATUS AND METHOD FOR FORMING PRECAST

MODULAR UNITS AND METHOD FOR CONSTRUCTING PRECAST MODULAR STRUCTURE'. United States.

- Mercader-Moyano, P., Yajnes, M. E. and Caruso, S. I. (2016) 'Experimental characterisation of a cement-based compound with recycled aggregates and EPS from rehabilitation work', *Revista de la Construccion*, 15(3), pp. 97–106. doi: 10.4067/s0718-915x2016000300010.

- Messiqua, P. (2007) 'CONCRETE FORMWORK WALL SERVING ALSO AS REINFORCEMENT'. United States.

- Messiqua, P. and Messiqua, R. (2009) 'HIGH-STRENGTH CONCRETE WALL FORMWORK'. United States.

- Miloni, R. *et al.* (2011) *Building Renovation Case Studies IEA ECBCS Annex 50*.

- Ministerial Decree (2015) *Application of calculation methods for energy performance and definition of minimum building requirements*, *Official Gazzette of Italian Republic n°39 of 15th July 2015*. Available at: https://www.mise.gov.it/images/stories/normativa/DM_requisiti_minimi.pdf.

- Ministerio de Fomento (2009) *Norma de Construcción Sismorresistente: Parte general y edificación (NSCE-02)*.

- Ministerio de Fomento (2019) *Documento Básico HE Ahorro de Energía 2019*, *Código Técnico de la Edificacion*. Available at: http://www.arquitectura-tecnica.com/hit/Hit2016-2/DBHE.pdf.

- Norris, T. G. and Chen, A. (2016) 'Development of insulated FRP-confined Precast Concrete Sandwich panel with side and top confining plates and dry bond', *Composite Structures*, 152, pp. 444–454. doi: 10.1016/j.compstruct.2016.05.053.

- O'Hegarty, R. and Kinnane, O. (2020) 'Review of precast concrete sandwich panels and their innovations', *Construction and Building Materials*. Elsevier Ltd, 233, p. 117145. doi: 10.1016/j.conbuildmat.2019.117145.

- Petrella, A. *et al.* (2014) 'Recycled EPS in the production of cement mortars for the construction industry', *ISTEA*, (4), pp. 477–492.

- Petrella, A., Di Mundo, R. and Notarnicola, M. (2020) 'Recycled Expanded Polystyrene as Lightweight Aggregate for Environmentally Sustainable Cement Conglomerates', *Materials*, 13(4), p. 988. doi: 10.3390/ma13040988.

- Pihelo, P., Kalamees, T. and Kuusk, K. (2017) 'NZEB Renovation with Prefabricated Modular Panels', *Energy Procedia*. Elsevier B.V., 132, pp. 1006–1011. doi: 10.1016/j.egypro.2017.09.708.

- Porco, F. *et al.* (2015) 'The influence of infilled panels in retrofitting interventions of existing reinforced concrete buildings: a case study', *Structure and Infrastructure Engineering*, 11(2), pp. 162–175. doi: 10.1080/15732479.2013.862726.

- da Porto, F. *et al.* (2015) 'Effectiveness of plasters and textile reinforced mortars for strengthening clay masonry infill walls subjected to combined in-plane/out-of-plane actions / Wirksamkeit von Putz und textilbewehrtem Mörtel bei der Verstärkung von Ausfachungswänden aus Ziegel', *Mauerwerk*. Wiley, 19(5), pp. 334–354. doi: 10.1002/dama.201500673.

- *Precast Concrete Market Size, Share, Global Industry Forecast Till 2023* (no date). Available at: https://www.marketresearchfuture.com/reports/precast-concrete-market-4850 (Accessed: 5 October 2020).

- Qun, X., Shuai, W. and Chun, L. (2018) 'Axial Compression Behavior of a New Type of Prefabricated Concrete Sandwich Wall Panel', in *IOP Conference Series: Materials Science and Engineering*. doi: 10.1088/1757-899X/317/1/012063.

- Ramli Sulong, N. H., Mustapa, S. A. S. and Abdul Rashid, M. K. (2019) 'Application of expanded polystyrene (EPS) in buildings and constructions: A review', *Journal of Applied Polymer Science*, 136(20), p. 47529. doi: 10.1002/app.47529.

- Record, G. C. (1999) 'INSULATED BUILDING PANEL WITH A UNITARY SHEAR RESISTANCE CONNECTOR ARRAY'. doi: 10.1197/jamia.M1139.Adar.

- Ricci, P., Di Domenico, M. and Verderame, G. M. (2018) 'Experimental assessment of the in-plane/out-of-plane interaction in unreinforced masonry infill walls', *Engineering Structures*. Elsevier, 173(August 2017), pp. 960–978. doi: 10.1016/j.engstruct.2018.07.033.

- De Risi, M. T. *et al.* (2020) 'Experimental analysis of strengthening solutions for the out-of-plane collapse of masonry infills in RC structures through textile reinforced mortars', *Engineering Structures*. Elsevier, 207(June 2019), p. 110203. doi: 10.1016/j.engstruct.2020.110203.

- Sancho, R. *et al.* (2014) 'Changes of mechanical properties of lightweight cement mortar mixed with recycled expanded polystyrene and subjected to high temperatures', *Advanced Materials Research*, 1051, pp. 752–756. doi: 10.4028/www.scientific.net/AMR.1051.752.

- Sayadi, A. A. *et al.* (2016) 'Effects of expanded polystyrene (EPS) particles on fire resistance, thermal conductivity and compressive strength of foamed concrete', *Construction and Building Materials*. Elsevier Ltd, 112, pp. 716–724. doi: 10.1016/j.conbuildmat.2016.02.218.

- Schwehr, P., Fischer, R. and Geier, S. (2011) *Retrofit Strategies Design Guide: Advanced Retrofit Strategies & 10 Steps to a Prefab Module*, *IEA Annex 50 – Prefabricated Systems for Low Energy Renovation of Residential Buildings*. Available at: http://www.empa-ren.ch/A50/Annex 50 Final Publications for Internet/DesignGuide_ECBCS_A50.pdf.

- Scioti, A. (2015) 'Pre-cast concrete walls : techniques and technologies for performance optimization', 1, pp. 83–88. doi: https://doi.org/10.17410/tema.v1i1.6.

- Seghezzi, E. and Masera, G. (2015) 'Building Retrofit through Prefabricated Panels: an Overview of the State of the Art', *ISTEA*.

- Sharpe, D. P. and Sharpe, P. R. (2010) 'Stud frame and formwork panel constructed therefrom'.

- Sharpe, D. P. and Sharpe, P. R. (2011) 'STUD FRAME AND FORMWORK PANEL CONSTRUC TED THEREFROM'.

- Silva, P. C. P. *et al.* (2013) 'Development of prefabricated retrofit module towards nearly zero energy buildings', *Energy and Buildings*, 56, pp. 115–125. doi: 10.1016/j.enbuild.2012.09.034.

- Smith, W. H. (2002) 'REINFORCED CONCRETE PANELAND METHOD OF

MANUFACTURE'. United States.

- Sohns, U. (2006) 'REINFORCED CONCRETE PART FOR PRODUCING FOUNDATIONS OF BUILDINGS'. doi: 10.1126/science.Liquids.

- Tamborelli, S. and Furno, E. (2014) *EPS : Impatto Ambientale e ciclo di vita*, *Aipe*.

- Teixeira, N., Tomlinson, D. G. and Fam, A. (2016) 'Precast concrete sandwich wall panels with bolted angle connections tested in flexure under simulated wind pressure and suction', *PCI Journal*, 61(4), pp. 65–83.

- Terkl, H.-U. (1988) 'LARGE-PANEL COMPONENT FoR BUILDINGS'.

- The European Commission (2019) 'Recomendations on building renovation', *Official Journal of the European Union.*, 6(L127/34), pp. 34–79. Available at: https://eur-lex.europa.eu/legal-content/EN/TXT/?qid=1442476465850&uri=CELEX:32019H0786.

- The European Commission (2020a) *EU Building Stock Observatory | Energy*. Available at: https://ec.europa.eu/energy/topics/energy-efficiency/energy-efficient-buildings/eu-bso_en#the-datamapper (Accessed: 6 November 2020).

- The European Commission (2020b) *EU Buildings Database | Energy*. Available at: https://ec.europa.eu/energy/eu-buildings-database_en (Accessed: 6 November 2020).

- Tittarelli, F. *et al.* (2016) 'Effect of Using Recycled Instead of Virgin EPS in Lightweight Mortars', *Procedia Engineering*, 161, pp. 660–665. doi: 10.1016/j.proeng.2016.08.728.

- Turk, A. M., Ersoy, U. and Ozcebe, G. (2006) 'Effect of introducing RC infill on seismic performance of damaged RC frames', *Structural Engineering and Mechanics*. Techno Press, 23(5), pp. 469–486. doi: 10.12989/sem.2006.23.5.469.

- Valluzzi, M. R. *et al.* (2014) 'Out-of-plane behaviour of infill masonry panels strengthened with composite materials', *Materials and Structures/Materiaux et Constructions*. Kluwer Academic Publishers, 47(12), pp. 2131–2145. doi: 10.1617/s11527-014-0384-6.

- Van de Voorde, S., Bertels, I. and Wouters, I. (2015) 'Post-War Building Materials in Housing in Brussels 1945-1975', *Construction History*, 31(1), p. 437.

- Wang, J., Hu, B. and Soon, J. H. (2019) 'Physical and Mechanical Properties of a Bulk Lightweight Concrete with Expanded Polystyrene (EPS) Beads and Soft Marine Clay', *Materials*, 12(10), p. 1662. doi: 10.3390/ma12101662.

- Williams Portal, N. *et al.* (2017) 'Bending behaviour of novel Textile Reinforced Concrete-foamed concrete (TRC-FC) sandwich elements', *Composite Structures*. Elsevier Ltd, 177, pp. 104–118. doi: 10.1016/j.compstruct.2017.06.051.

- Wilson, S. D. (2001) 'PREFABRICATED CONCRETE WALL FORM SYSTEM'. United States. doi: US6319203B1.

- Woltman, G. D., Tomlinson, D. G. and Fam, A. (2011) 'A comparative study of various FRP shear connectors for sandwich concrete walls', in *Advances in FRP Composites in Civil Engineering - Proceedings of the 5th International Conference on FRP Composites in Civil Engineering, CICE 2010*, pp. 237–240. doi: 10.1007/978-3-642-17487-2_50.

- Woningbouw, B. *et al.* (2016) *2 nd SKIN zero energy apartment renovation via an integrated façade approach*. Available at: https://projecten.topsectorenergie.nl/storage/app/uploads/public/5a0/c14/5dc/5a0c145dc79f1846323269.pdf.

- You, Q. *et al.* (2019) 'Experimental study on preventing expanded polystyrene concrete segregation', *Advances in Cement Research*, 31(10), pp. 457–471. doi: 10.1680/jadcr.17.00226.

- Young, D. A. (1987) 'PERMANENT NON-REMOVABLE INSULATING TYPE CONCRETE WALL FORMING STRUCTURE'.

- Zimmermann, M. (2012) 'Prefabricated Systems for Low Energy Renovation of Residential Buildings', *EBC Annex 50 Prefabricated Systems for Low Energy Renovation of Residential Buildings*, p. 24. Available at: http://www.iea-ebc.org/projects/completed-projects/ebc-annex-50/.

4   STRATEGICAL DESIGN PROCESS

- American Concrete Institute (2013) 'ACI Concrete Terminology - An ACI Standard', p. 32. Available at: www.concrete.org.

- Babu, K. G. and Babu, D. S. (2003) 'Behaviour of lightweight expanded polystyrene concrete containing silica fume', *Cement and Concrete Research*. doi: 10.1016/S0008-8846(02)01055-4.

- DM n. 495 (1992) *Regolamento di esecuzione e di attuazione del nuovo codice della strada*, *Gazzetta Ufficiale*. Available at: https://www.gazzettaufficiale.it/eli/id/1992/12/28/092G0531/sg (Accessed: 20 November 2020).

- EN 16025-1 (2013) *Thermal and/or sound insulation products in building construction - Bound EPS ballastings - Part 1: Requirements for factory premixed EPS dry mortar*.

- Ferrándiz-Mas, V. and García-Alcocel, E. (2012) 'Caracterización física y mecánica de morteros de cemento Portland fabricados con adición de partículas de poliestireno expandido (EPS)', *Materiales de Construccion*, 62(308), pp. 547–566. doi: 10.3989/mc.2012.04611.

- Ferrándiz-Mas, V. and García-Alcocel, E. (2013) 'Durability of expanded polystyrene mortars', *Construction and Building Materials*, 46, pp. 175–182. doi: 10.1016/j.conbuildmat.2013.04.029.

- Petrella, A., Di Mundo, R. and Notarnicola, M. (2020) 'Recycled Expanded Polystyrene as Lightweight Aggregate for Environmentally Sustainable Cement Conglomerates', *Materials*, 13(4), p. 988. doi: 10.3390/ma13040988.

- Ali, H. H. and Al Nsairat, S. F. (2009) 'Developing a green building assessment tool for developing countries - Case of Jordan', *Building and Environment*. doi: 10.1016/j.buildenv.2008.07.015.

- Amati, L. *et al.* (2015) 'LIGHTWEIGHT CEMENT BASED MORTAR WITH HIGH

THERMAL PERFORMANCES FOR STRUCTURAL APPLICATIONS'. Italy.

- Barzilai, J., Cook, W. D. and Golany, B. (1992) 'The Analytic Hierarchy Process: Structure of the Problem and Its Solutions', in *Systems and Management Science by Extremal Methods*. Springer US, pp. 361–371. doi: 10.1007/978-1-4615-3600-0_23.

- Bobylev, N. (2011) 'Comparative analysis of environmental impacts of selected underground construction technologies using the analytic network process', *Automation in Construction*. doi: 10.1016/j.autcon.2011.04.004.

- CEN (2004) *Eurocode 3: Design of steel structures - Part 1-8: Design of joints*.

- CSI (2016) 'SAP2000. Analysis Reference Manual', *CSI: Berkeley (CA, USA): Computers and Structures INC*.

- EN ISO 13786 (2018) *Thermal performance of building components - Dynamic thermal characteristics - Calculation methods*. Available at: http://store.uni.com/catalogo/uni-en-iso-13786-2018 (Accessed: 29 November 2020).

- EN ISO 13788 (2013) *Hygrothermal performance of building components and building elements - Internal surface temperature to avoid critical surface humidity and interstitial condensation - Calculation methods*. Available at: http://store.uni.com/catalogo/index.php/uni-en-iso-13788-2013.html (Accessed: 12 April 2019).

- EN ISO 6946 (2018) *Building components and building elements - Thermal resistance and thermal transmittance - Calculation methods*. Available at: http://store.uni.com/catalogo/index.php/uni-en-iso-6946-2018.html (Accessed: 12 April 2019).

- EOTA TR 029 (2007) *Design of Bonded Anchors*.

- ETA-07/0260 (2017) *Injection System Hilti HIT-RE 500-SD for cracked concrete*.

- ETA-13/1036 (2017) *Sistema a iniezione per l'utilizzo in muratura*.

- ETAG 001-ANNEX C (2010) *Metal Anchors for Use in Concrete*.

- ETAG 001 (2013) *GUIDELINE FOR EUROPEAN TECHNICAL APPROVAL OF METAL ANCHORS FOR USE IN CONCRETE*.

- ETAG 029-ANNEX C (2013) *Metal injection anchors for use in masonry*.

- Garay, R., Arregi, B. and Elguezabal, P. (2017) 'Experimental Thermal Performance Assessment of a Prefabricated External Insulation System for Building Retrofitting', *Procedia Environmental Sciences*. The Author(s), 38, pp. 155–161. doi: 10.1016/j.proenv.2017.03.097.

- Gigliarelli, E., Cessari, L. and Cerqua, A. (2011) 'Application of the Analytic Hierarchy Process (Ahp) for Energetic Rehabilitation of Historical Buildings', *International Symposium on the Analytic Hierarchy Process*.

- Graubner, C. A., Motzko, C. and Proske, T. (2009) 'Anforderungen an Schalungssysteme bei Verwendung fließfähiger Hochleistungsbetone', *Betonwerk und Fertigteil-Technik/Concrete Plant and Precast Technology*, 75(2), pp. 162–164.

- Guzmán-Sánchez, S. *et al.* (2018) 'Assessment of the contributions of different flat roof types to achieving sustainable development', *Building and Environment*. doi: 10.1016/j.buildenv.2018.05.063.

- Ho, W. (2008) 'Integrated analytic hierarchy process and its applications - A literature review', *European Journal of Operational Research*, 186(1), pp. 211–228. doi: 10.1016/j.ejor.2007.01.004.

- Kaushik, H. B., Rai, D. C. and Jain, S. K. (2007) 'Stress-Strain Characteristics of Clay Brick Masonry under Uniaxial Compression', *Journal of Materials in Civil Engineering*. doi: 10.1061/(asce)0899-1561(2007)19:9(728).

- Kwon, S. *et al.* (2014) 'A Modified-AHP Method of Productivity Analysis for

Deployment of Innovative Construction Tools on Construction Site', *Journal of Construction Engineering and Project Management*. doi: 10.6106/jcepm.2014.4.1.045.

- Kwon, S. H. *et al.* (2010) 'Intrinsic model to predict formwork pressure', *ACI Materials Journal*, 107(1), pp. 20–26. doi: 10.14359/51663460.

- Lesecq, S. *et al.* (2017) 'TOPAs, an IoT Driven Framework for Energy Efficiency in Buildings', *Proceedings*, 1(10), p. 685. doi: 10.3390/proceedings1070685.

- Mander, J. B., Priestley, M. J. N. and Park, R. (1988) 'Theoretical Stress-Strain Model for Confined Concrete', *Journal of Structural Engineering*. doi: 10.1061/(asce)0733-9445(1988)114:8(1804).

- Martiradonna, S., Ruggieri, S., Fatiguso, F., Uva, G. (no date) 'Explorative analyses for the thermal and structural behaviour evaluation of the Innovative System of Precast Concrete panels for the existing building retrofit', under drafting.

- Martiradonna, S., Fatiguso, F. and Lombillo, I. (2020) 'Thermal improvements of existing reinforced concrete buildings by an Innovative Precast Concrete Panel system', in *Colloqui.AT.e 2020*, pp. 511–522.

- Martiradonna, S., Lombillo, I. and Fatiguso, F. (2019) 'Performance monitoring of refurbished buildings through innovative precast concrete modules', in *Conference Proceedings - IEEE International Conference on Systems, Man and Cybernetics*, pp. 953–957. doi: 10.1109/SMC.2019.8914472.

- Ministerial Decree (2015) *Application of calculation methods for energy performance and definition of minimum building requirements*, *Official Gazzette of Italian Republic n°39 of 15th July 2015*. Available at: https://www.mise.gov.it/images/stories/normativa/DM_requisiti_minimi.pdf.

- Mondal, G. and Jain, S. K. (2008) 'Lateral stiffness of masonry infilled reinforced concrete (RC) frames with central opening', *Earthquake Spectra*. doi: 10.1193/1.2942376.

- Nassar, K., Thabet, W. and Beliveau, Y. (2003) 'A procedure for multi-criteria selection of building assemblies', *Automation in Construction*. doi: 10.1016/S0926-5805(03)00007-4.

- Ozturkoglu, O., Ucar, T. and Yesilce, Y. (2017) 'Effect of masonry infill walls with openings on nonlinear response of reinforced concrete frames', *Earthquake and Structures*. doi: 10.12989/eas.2017.12.3.333.

- Perna, C. Di *et al.* (2009) 'Massa e comfort : necessità di una adeguata interna periodica', *MuratureOggi*, Marzo, pp. 52–59.

- Perrot, A. *et al.* (2015) 'Prediction of lateral form pressure exerted by concrete at low casting rates', *Materials and Structures/Materiaux et Constructions*. Kluwer Academic Publishers, 48(7), pp. 2315–2322. doi: 10.1617/s11527-014-0313-8.

- Pittau, F. *et al.* (2017) 'Prefabrication as Large-scale Efficient Strategy for the Energy Retrofit of the Housing Stock: An Italian Case Study', in *Procedia Engineering*, pp. 1160–1169. doi: 10.1016/j.proeng.2017.04.276.

- Proske, T. *et al.* (2014) 'Form pressure generated by fresh concrete: A review about practice in formwork design', *Materials and Structures/Materiaux et Constructions*, 47(7), pp. 1099–1113. doi: 10.1617/s11527-014-0274-y.

- Saaty, T. L. (2002) 'Decision making with the Analytic Hierarchy Process', *Scientia Iranica*. doi: 10.1504/ijssci.2008.017590.

- Sangiorgio, V. *et al.* (2017) 'An information system for masonry building monitoring', in *2017 IEEE International Conference on Service Operations and Logistics, and Informatics (SOLI)*. IEEE, pp. 230–235. doi: 10.1109/SOLI.2017.8120999.

- Sangiorgio, V. *et al.* (2019) 'Structural degradation measurement and diagnostics of historical masonry buildings.', in *2019 IMEKO TC4 International Conference on Metrology for Archaeology and Cultural Heritage, MetroArchaeo 2019*. IMEKO-International Measurement Federation Secretariat, pp. 125–130.

- Sangiorgio, V. *et al.* (2021) 'Augmented reality based - decision making (AR-DM) to support multi-criteria analysis in constructions', *Automation in Construction*. Elsevier B.V., 124(November 2020), p. 103567. doi: 10.1016/j.autcon.2021.103567.

- Sangiorgio, V., Uva, G. and Fatiguso, F. (2018) 'Optimized AHP to Overcome Limits in Weight Calculation: Building Performance Application', *Journal of Construction Engineering and Management*. doi: 10.1061/(asce)co.1943-7862.0001418.

- Scuro, C. *et al.* (2018) 'IoT for structural health monitoring', *IEEE Instrumentation and Measurement Magazine*, 21(6), pp. 4–14. doi: 10.1109/MIM.2018.8573586.

- Shapira, A. and Goldenberg, M. (2005) 'AHP-Based Equipment Selection Model for Construction Projects', *Journal of Construction Engineering and Management*. doi: 10.1061/(asce)0733-9364(2005)131:12(1263).

- Shing, P. B. and Mehrabi, A. B. (2002) 'Behaviour and analysis of masonry-infilled frames', *Progress in Structural Engineering and Materials*. doi: 10.1002/pse.122.

- Silva, P. C. P. *et al.* (2013) 'Development of prefabricated retrofit module towards nearly zero energy buildings', *Energy and Buildings*, 56, pp. 115–125. doi: 10.1016/j.enbuild.2012.09.034.

- The European Union (2005) 'Eurocodice 2 - Progettazione delle strutture di calcestruzzo Parte 1-1 : Regole generali e regole per gli edifici ENV 1992-1-1', *Design*, (1), pp. 1–12.

- Ursini Casalena, A. (2018) *Trasmittanza Termica Periodica: Foglio di Calcolo Excel UNI 13786 per Calcolare le Proprietà Termiche Dinamiche di un Componente Edilizio*, *www.mygreenbuildings.org*. Available at: https://www.mygreenbuildings.org/2009/07/27/trasmittanza-termica-periodica-foglio-di-calcolo-excel-per-calcolare-le-proprieta-termiche-dinamiche-di-un-componente-edilizio.html (Accessed: 29 November 2020).

- Uva, G. *et al.* (2012) 'On the role of equivalent strut models in the seismic assessment of infilled RC buildings', *Engineering Structures*. doi: 10.1016/j.engstruct.2012.04.005.

- Viana Vargas, R. (2010) 'Using the Anaytic Hierarchy Process (AHP) To Select and Prioritize Projects in a Portfolio', in *PMI Global Congress*.

- Wang, E. and Shen, Z. (2013) 'A hybrid Data Quality Indicator and statistical method for improving uncertainty analysis in LCA of complex system-application to the whole-building embodied energy analysis', *Journal of Cleaner Production*. doi: 10.1016/j.jclepro.2012.12.010.

- Wang, M. *et al.* (2017) 'Design an IoT-based Building Management Cloud Platform for Green Buildings'. doi: 10.1109/CAC.2017.8243793.

- Zaglio, V. *et al.* (2018) 'Manini Connect: prefabbricati e capannoni più sicuri con l'IoT', *https://www.manini.it/manini-connect/tecnologia-predittiva/*. Available at: www.zerounoweb.it.

- Zhong, R. Y. *et al.* (2017) 'Prefabricated construction enabled by the Internet-of-Things Ray', *Automation in Construction*. Elsevier B.V., 76, pp. 59–70. doi: 10.1016/j.autcon.2017.01.006.

5   PILOT CASE STUDY

- CEN (2004) *Eurocode 3: Design of steel structures - Part 1-8: Design of joints*.

- Martiradonna, S., Ruggieri, S., Fatiguso, F., Uva, G. (no date) 'Explorative analyses for the thermal and structural behaviour evaluation of the Innovative System of Precast Concrete panels for the existing building retrofit', under drafting.

- Ruggieri, S. and Uva, G. (2020) 'Accounting for the Spatial Variability of Seismic Motion in the Pushover Analysis of Regular and Irregular RC Buildings in the New Italian Building Code', *Buildings*, 10(10), p. 177. doi: 10.3390/buildings10100177.

- Saaty, T. L. (2008) 'Decision making with the analytic hierarchy process', *Int. J. Services Sciences*, 1.

- Sangiorgio, V. *et al.* (2021) 'Augmented reality based - decision making (AR-DM)

to support multi-criteria analysis in constructions', *Automation in Construction*. Elsevier B.V., 124(November 2020), p. 103567. doi: 10.1016/j.autcon.2021.103567.

- Sangiorgio, V., Martiradonna, S. and Fatiguso, F. (2020) 'Augmented Reality to Support Multi-Criteria Decision Making in Building Retrofitting', in *2020 IEEE International Conference on Systems, Man, and Cybernetics (SMC)*. IEEE, pp. 760–765. doi: 10.1109/SMC42975.2020.9283420.

6   PROTOTYPE STAGE

- Ministero delle Infrastrutture e dei Trasporti (2018) NORME TECNICHE PER LE COSTRUZIONI, Gazzetta Ufficiale della repubblica italiana.

LIST OF FIGURES

4 STRATEGICAL DESIGN PROCESS

5 PILOT CASE STUDY

6 PROTOTYPE STAGE

LIST OF TABLES

5 PILOT CASE STUDY

6 PROTOTYPE STAGE

ACKNOWLEDGEMENTS

al's team with which I spent six months of the PhD route. To the director Luigi Amati who gave me the possibility to discover the exciting world of prefabrication and let me work with his team of technicians and workers. A great recognition is directed to Ing. Francesco Carparelli who guided me for the structural definition of the system and to Ing. Cosimina Acquaviva, my reference in the company who took on the commitment to manage all phases of project development despite her already hard work. I extend my appreciation for the collaboration with geom. Massimo Paolillo, Leo Vinci, Paolo Ippolito, Davide Brizi and all the workers.

I am grateful with my family which supported me during the hardest periods but also rejoiced with me in the moments of satisfaction. Beyond my parents, a special thanks goes to my sister Stefania, my uncles Maria and Pino and my grandmother for their constant support.

Friends are the family that you choose, so I believe to have a very big family. A greatful thanks goes to my dear Diana who, despite recently appears in my life, is present in every moment, knowing how support me. Thanks to Valentina, Enza, Jacopo, Marco, Davide, Ramona, Corrado, Mariagilda, Katia, Andrea, Michele and Valentino to always be there for me; to my adventure companions in Santander and beyond, Rosa, César, Denise, Marco, Salva, Sonia and Betta.

A sweet memory for my PhD collegues, Antonella, Rosella, Silvana, Giulia, Vincenzo, Claudia, Giuseppe, Valeria, Andrea, Pierluigi, Luigi and Aleksandra with which I spent very enjoyable time, beyond the work commitments.

ANNEX: PHOTOGRAPHIC DOCUMENTATION

A Large scale production of the novel LWM

B Standardized production of the innovative PC modules

C Wall sample construction

D Metal components

E "The Intelligent PC panel system" (IPCS) installation test

A. Large scale production of the novel LWM

Figure A.1: rEPS additivation in the mixing machine

Figure A.2: resting time for the additive absorption

Figure A.3: not additivated aspect of the rEPS

Figure A.4: additivated aspect of the rEPS

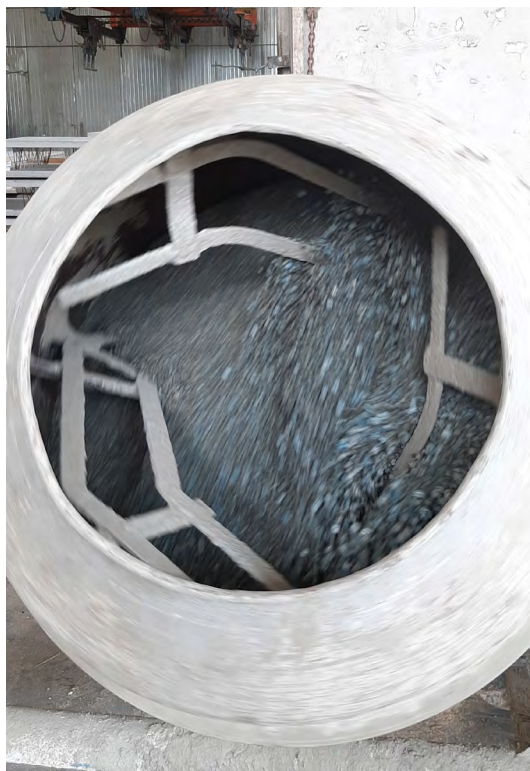**Figure A.5:** Cement addition to the additivated rEPS to execute the pre-mixing phase

Figure A.6: Pre-mixing phase

Figure A.7: Addition of water to the premixed compound

Figure A.8: Mixing phase

B. Standardized production of the innovative PC modules

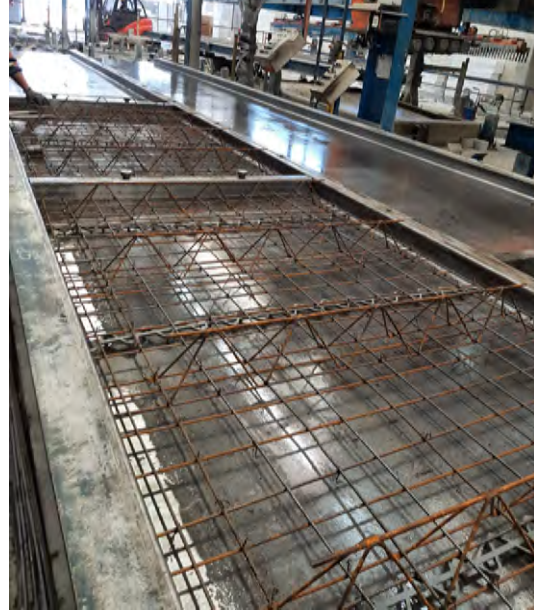**Figure B.1:** Labour assembling of the panel reinforcement.

Figure B.2: Placing of the spacers and arrangement of the reinforcement.

Figure B.3-4: Details of the reinforcement arrangement

Figure B.5: The reinforcement arrangement on the formworks of the modules type A

Figure B.6: The reinforcement arrangement on the formworks of the series of modules type B
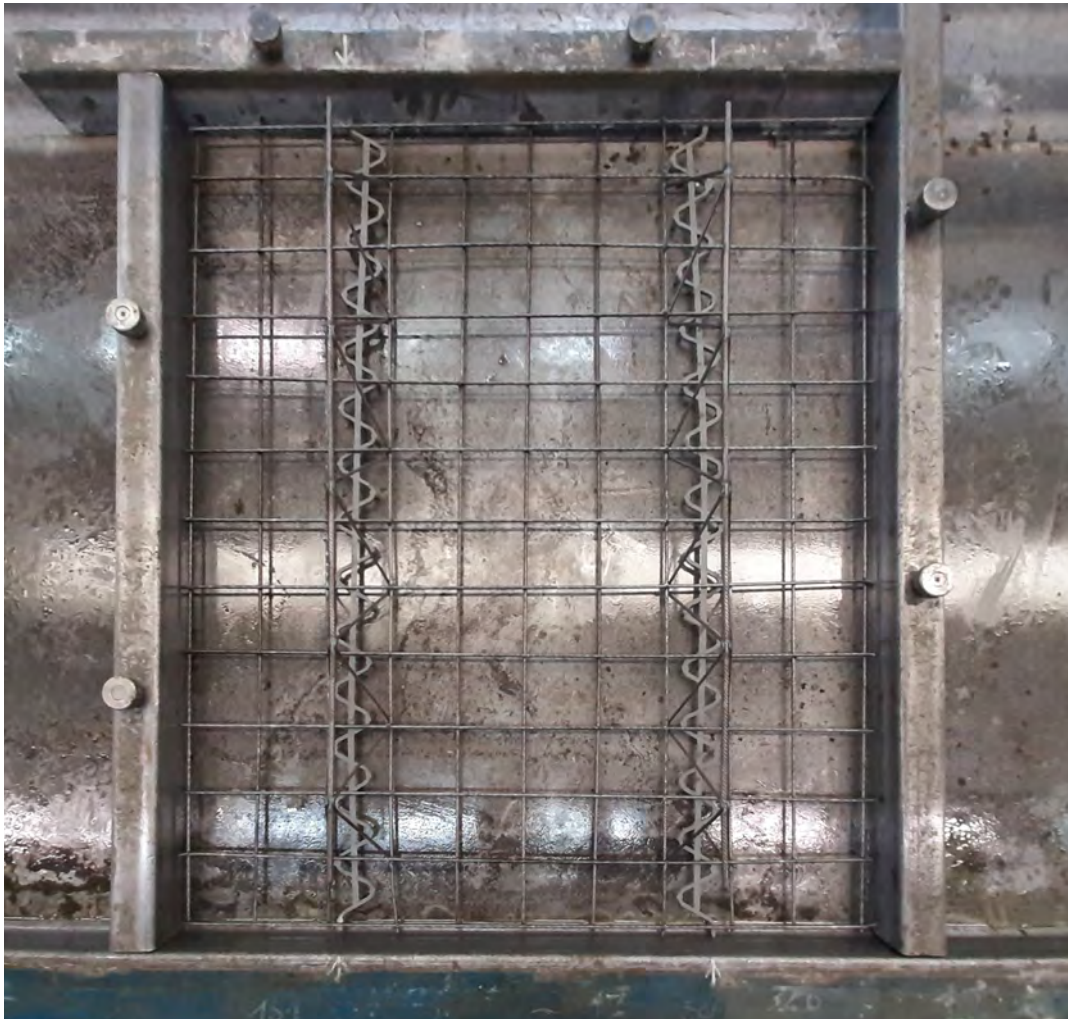
Figure B.7: The reinforcement arrangement on the formworks of the modules type B: top view

Figure B.8: The arrangement on the formworks of the modules type B: perspective view

Figure B.9: Formwork moving to the concrete casting station of the carousel system

Figure B.10: Concrete casting until the custom thickness

Figure B.11-12: Automatic concrete casting by means of the bridge crane

Figure B.13: Mechanical vibration of the formwork

Figure B.14: Form stripping of the base modules
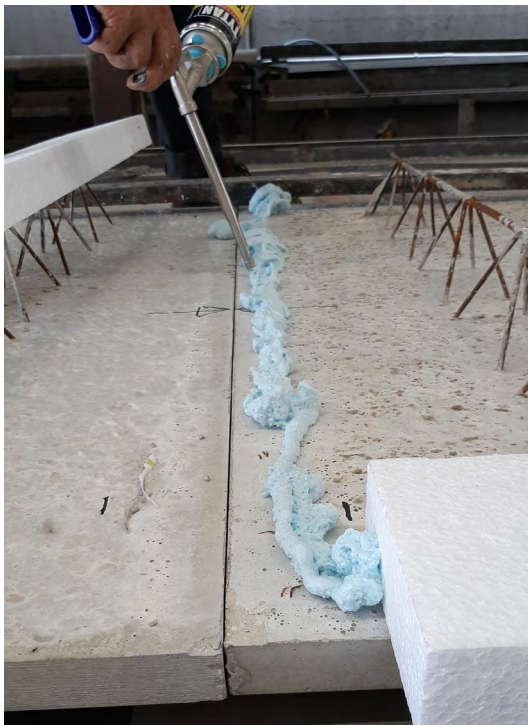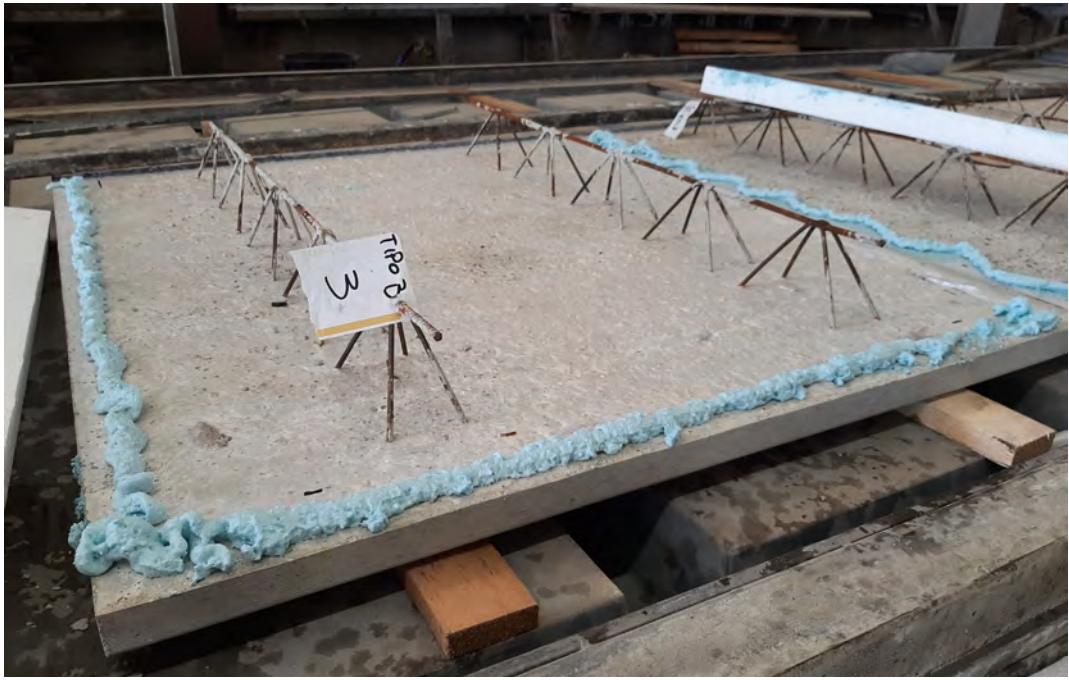
Figure B.15-16-17: Disposition of the rEPS blocks on the base modules to generate the male-female joints

Figure B.18-19: Preparation to the novel lightweight mortar (LWM) casting

Figure B.20: LWM casting on the inner face of the base modules up to 5 cm

Figure B.21-22: Spreading of the fresh LWM on the inner surface of the base module

Figure B.23: Surface leveling of the fresh LWM

Figure B.24: PC panel type A

Figure B.25-26: PC panel type B: dried aspect

Figure B.27: Junction between the LWM layer and the rEPS block

Figure B.28: Inner surface of the LWM

Figure B.29-30-31: Lifting and handling tests of PC modules using a bridge crane

C. Wall sample construction

Figure C.1: Wall foundation: construction of the formwork and reinforcement assembling

Figure C.2: Construction of the pillars

Figure C.3: Concrete frame of the wall sample

Figure C.4: Concrete frame of the wall sample

D. Metal components

Figure D.1: Precision cut of the connecting hooks to the pantograph
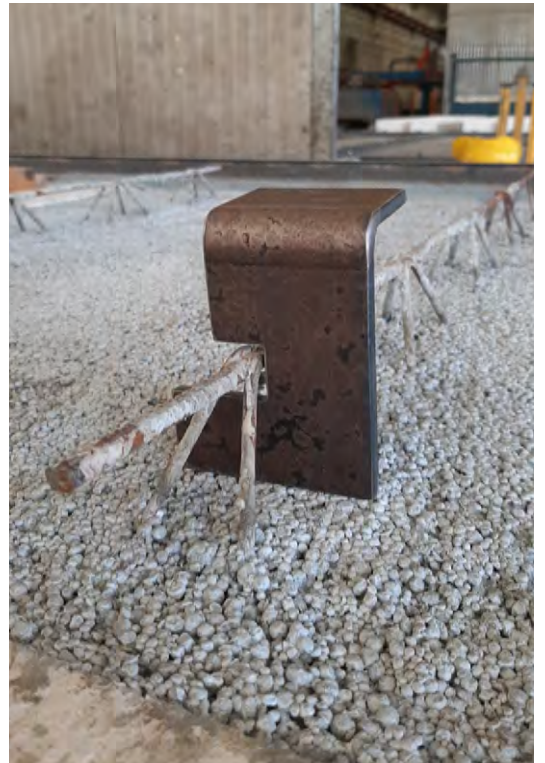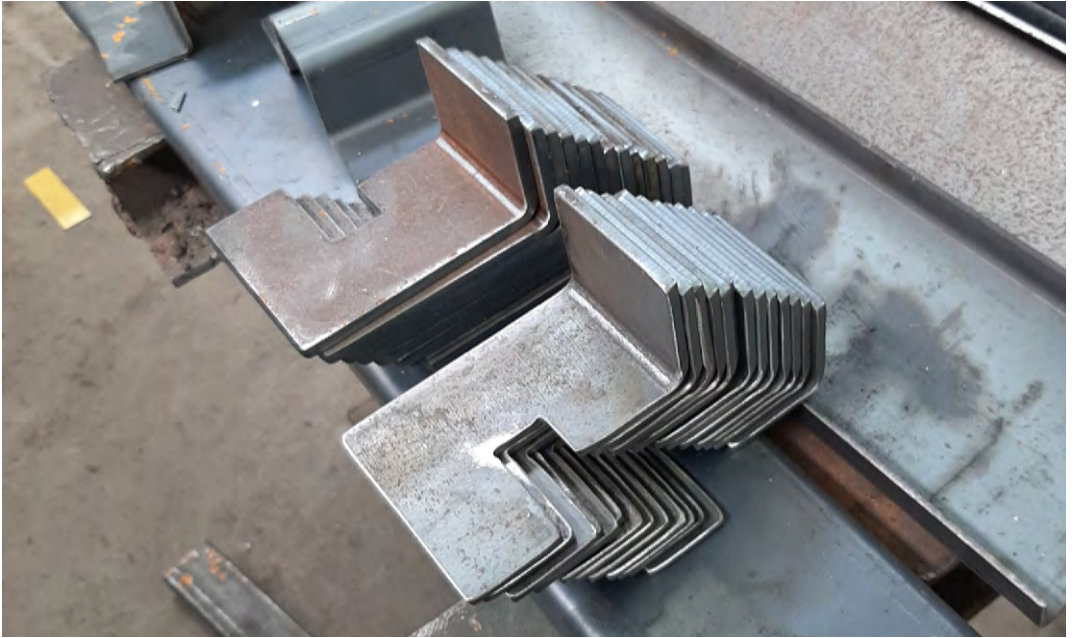
Figure D.2-3-4: Connecting hook details

Figure D.5: The three pairs of mullions

Figure D.6-7-8: Slotting of the mullions according to calculations and design drawings

Figure D.9: Hook welding with left folding

Figure D.10: Hook welding with right folding

Figure D.11: The couple of mullions for the vertical anchoring of the PC modules

Figure D.12: The three pairs of mullions ready to be anchored on the sample for the system installation

Figure D.13: The three pairs of mullions ready to be anchored on the sample for the system installation

Figure D.14: The reinforcement of the system foundation

E. "The Intelligent PC panel system" (IPCS) installation test

Figure E.1-2-3: Drilling of the concrete frame up to the calculated depth for chemical injection and anchoring of post-installed reinforcing bars and connectors

Figure E.4-5-6: Chemical injenction for the fixing of the anchoris and the hooked post-installed rebars

Figure E.7-8-9: Post-installed rebars insertion into the chemical injected holes

Figure E.10-11-12: Insertion and tightening of washers and bolts

Figure E.13-14: Aspect of the sample at the end of the first macro-phase of system installation
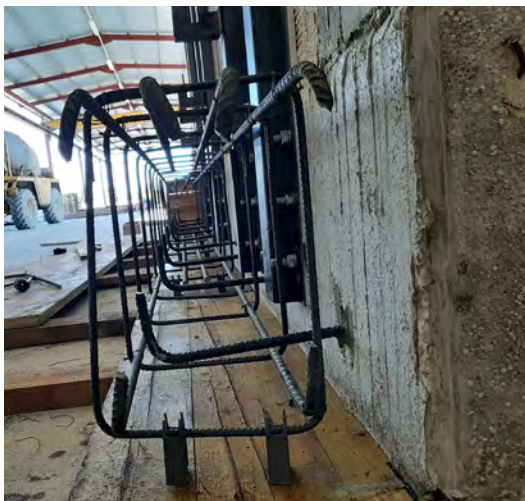
Figure E.15-16-17: Assembling of the foundation rebars of the system

Figure E.18: Gluing of the thermal insulation panels in rEPS

Figure E.19: Insertion of the connecting bars between the foundation and the next reinforcement mesh

Figure E.20: Work status: perspective view

Figure E.21: Concrete casting of the system foundation

Figure E.22: Installation of the reinforcement net of the internal concrete layer of the system

Figure E.23: Binding of the connecting bars with the reinforcement mesh

Figure E.24-25: Binding of the post-installed bars with the reinforcement mesh

Figure E.26: Insertion of the spacers to assure the concrete cover as the calculating drawings

Figure E.27: Preparation for the coupling of the first PC module A to the armed wall using the bridge crane

Figure E.28: Coupling of the PC module A to the wall

Figure E.29-30: The PC module accousted to the wall: lateral view

Figure E.31: Installation of the second PC module

Figure E.32: Coupling the first row of panels with the wall

Figure E.33-34: Anchoring details (lateral view): upper and lower connection

Figure E.35-36: Resulting space between the wall and the PC modules for the next concrete casting

Figure E.37: The concrete cover according to the design drawings

Figure E.38-39: Anchoring details (top view)

Figure E.40: Junction between two PC modules (top view)

Figure E.41: Installation of the second row of PC modules (type B)

Figure E.42: Detail of junction among the two different rows of modules (front view)

Figure E.43: Detail of the omega profile of the empty mullion (top view)

Figure E.44: Detail of the empty mullion (perspective view)

Figure E.45: Detail of the empty mullion and lateral closing of the system (top view)

Figure E.46: Lightweight structural concrete casting in the cavity between the wall and the modules

Figure E.47-48-49: LWSC casting through successive layers and with low velocity

Figure E.50-51: Closing surface of the IPCS after LWSC casting: fresh state (left); dry state (right).

Figure E.52: Retrofitted wall thickness

Figure E.53: The model of the "Intelligent PC panel system": front view

Figure E.54-55-56: The model of the "Intelligent PC panel system": perspective views

Figure E.57: Part of the Ferramati's team

CURRICULUM VITAE

PERSONAL INFORMATION

Scientific Publications

Martiradonna Silvia

📍 Via Ugo Foscolo 8, 70010 Capurso (BA)

📱 (+39) 342 56 31 410

✉ sil.martiradonna@gmail.com
✉ silvia.martiradonna@ingpec.eu

🌐 https://www.researchgate.net/profile/Silvia_Martiradonna

🆔 https://orcid.org/0000-0002-5944-0700

Sex Female | **Birthday** 11/26/1992 | **Nationality** Italian

- V. Sangiorgio, S. Martiradonna, F. Fatiguso, I. Lombillo "Augmented reality based - decision making (AR-DM) to support multi-criteria analysis in constructions", Automation in Construction. Elsevier B.V., 124 (November 2020), p. 103567, 2021.

- V. Sangiorgio, S. Martiradonna, F. Fatiguso "Augmented Reality to Support Multi-Criteria Decision Making in Building Retrofitting", in 2020 IEEE International Conference on Systems, Man, and Cybernetics (SMC). IEEE, pp. 760–765.

- S. Martiradonna, F. Fatiguso, I. Lombillo, "Thermal improvements of existing reinforced concrete buildings by an Innovative Precast Concrete Panel system", in Colloqui.AT.e 2020, New Horizons for Sustainable Architecture, Catania, Italy, June 17-20, 2020. (in press)

- S. Martiradonna, F. Fatiguso, I. Lombillo, "Precast concrete module for structural and energy rehabilitation of reinforced concrete buildings", in REHABEND 2020: Euro-American Congress: Construction pathology, rehabilitation technology and heritage management, 2020, pp. 1618-1626.

- V. Sangiorgio, S. Martiradonna, F. Fatiguso, G. Uva, "AHP-Based methodology integrating modern information technologies for historical masonry churches diagnosis", Archeologia e Calcolatori, 31.2, pp. 257-268, 2020.

- V. Sangiorgio, S. Martiradonna, F. Fatiguso, G. Uva, "Historical masonry churches diagnosis supported by an AHP-based Decision Support System", Acta IMEKO, 2019. (in press)

- V. Sangiorgio, S. Martiradonna, F. Fatiguso, G. Uva, "Structural degradation measurement and diagnostics of historical masonry buildings", in 2019 IMEKO TC-4 International Conference on Metrology for Archaeology and Cultural Heritage, MetroArchaeo 2019, pp. 125–130, 2019.

- S. Martiradonna, I. Lombillo, F. Fatiguso, "Performance Monitoring of Refurbished Building through Innovative Precast Concrete Modules" in Proceedings 2019 IEEE International Conference on Systems, Man and Cybernetics, SMC 2019, pp. 953–957, 2019.

- V. Sangiorgio, S. Martiradonna, G. Uva, F. Fatiguso, "An information system for masonry building monitoring", in 2017 IEEE International Conference on Service Operations and Logistics, and Informatics, SOLI 2017, pp. 230–235, 2017.

11/01/2017 – 03/18/2021	**Industrial PhD "PON RI 2014-2020" in Double Supervision (XXXIII ciclo)**

- **(ITALY) Polytechnic University of Bari; Department of Civil, Environmental, Building Engineering and Chemistry**
  PhD Program in *"Environmental and Building Risk and Development"*
  Partnership with: *"FERRAMATI INTERNATIONAL S.r.l"*
  (https://www.ferramati.it/web)

- **(SPAIN) Universidad de Cantabria, Santander; Departamento de Ingeniería Estructural y Mecánica**
  PhD Program in *"Patrimonio Arquitectónico, Civil, Urbanístico y Rehabilitación de Construcciones Existentes"*

PhD Thesis: "Intelligent Precast Construction Systems: project, realization, maintenance and control for the optimization of the environment and economic sustainability"

09/15/2019 – 03/18/2021	**Member of the research group for the project: "PRIN BE S2ECURe: Built Environment Safer in Slow and Emergency Conditions through behavioUral assessed/designed Resilient solutions"**

    National coordinator: Prof. Enrico Quagliarini (UNIVPM)

    Local Coordinators: Prof. Fabio Fatiguso (POLIBA); Prof. Graziano Salvalai (POLIMI); Prof. Giovanni Mochi (UNIPG); Prof. Edoardo Currà (UNIROMA1)

07/25/2019 – 03/18/2021	**Member of the research group for the project: "Analisi prestazionale di tecnologie di involucro adattive per la mitigazione degli effetti dell'isola di calore urbana"**

    Coordinator: Prof. Francesco Fiorito

2019 – 2020	**Architectural design of a rural villa for civil dwelling, Capurso (BA)**

10/01/2018 – 12/20/2018	**Professional collaboration with "Mauro Sàito Architetti" for the project "Bari Costa Sud"**

12/07/2017 – 30/09/2017	**Stage at "EMR - ESTUDIOS MÉTODOS DE LA RESTAURACIÓN", Valencia (ES)**

    Coordinator: Arch. Mercedes Ortì

    Restoration and conservation of historical/cultural architectural heritage

10/2016 – 01/2017	**Stage at "Universidad Politècnica de València", Valencia (ES)**

    Coordinator: Arch. López González, María Concepción

    Application of innovative techniques for geometric and pathological detection of traditional architectures

06/2016	**Proposal for "Parco sul sito ex Gasometro ed aree connesse"**
	Design of public green spaces and aggregation

09/2011 – 05/07/2017	**Master's Degree in Building Engineering Architecture (110 cum laude)**
	<u>**Polytechnic University of Bari, Bari (IT)**</u>
	Thesis Director: prof. FABIO FATIGUSO
	Title: "Innovative Approach for the large scale monitoring of churches"
09/01/2016 – 02/01/2017	**Erasmus+ SMS (Student Mobility for Study)**
	Universitat Politècnica de València, Ingeniería de Edificación, Valencia (ES)
09/2006 – 07/2011	**High school Diploma (98/100)**
	High school "Enrico Fermi", Bari (IT)

Native Language	**Italian**
Other languages	**English (B2)**
	Spanish (C1)
Professional skills	▪ Problem solving; Public speaking; Team work; Leadership; Versatility; Resilience; Organization; Patience, Will; Punctuality.
Digital skills	▪ excellent command of office suite (**Word, Excel, PowerPoint, Publisher**)
	▪ excellent command of photo editing software (**Photoshop, InDesign, Illustrator**)
	▪ excellent command of drawing, modelling and rendering software (**AutoCad, SketchUp, Rhinoceros, Artlantis Studio)**
	▪ good command of project by BIM Software (**Revit**)
	▪ good command of analysis software (**Ecotect, ArcGis, COMSOL Multiphysics**)
	▪ good command of various software and web platforms (**Movie Maker, Web Mail, Outlook, One Drive, SharePoint, Microsoft Teams. Google Drive, DropBox**), Browsers (**Chrome, Firefox, Internet Explorer**)
	▪ good command of operating system (**Updates, drivers, backup, firewall**)
	▪ Remote support with **TeamViewer**
Driver License	B

UNIONE EUROPEA
Fondo Sociale Europeo

Ministero dell'Università e della Ricerca

PON
RICERCA
E INNOVAZIONE